Work Order No. 582-19-95350-07
Contract No. 582-19-90500
Tracking No. 2019-28

Prepared for:

Texas Commission on Environmental Quality
12100 Park 35 Circle MC 164
Austin, TX 78753

Prepared by:

Ramboll US Corporation
7250 Redwood Blvd., Suite 105
Novato, California 94945

August 1, 2019

Houston 2018 Exceptional Event Analysis - Final Report

PREPARED UNDER A CONTRACT FROM THE
TEXAS COMMISSION ON ENVIRONMENTAL QUALITY

The preparation of this document was financed through a contract from the State of Texas through the Texas Commission on Environmental Quality.
The content, findings, opinions and conclusions are the work of the author(s) and do not necessarily represent findings, opinions or conclusions of the TCEQ.

Houston 2018 Exceptional Event Analysis - Final Report

Ramboll
7250 Redwood Boulevard
Suite 105
Novato, CA 94945
USA

T +1 415 899 0700
https://ramboll.com

Contents

APPENDICES

TABLES

FIGURES

LIST OF ACRONYMS AND ABBREVIATIONS

AERONET	Aerosol Robotics Network
AGL	Above ground layer
AIRS	Atmospheric Infrared Sounder
AOD	Aerosol optical depth
BCs	Boundary Conditions
CALIPSO	Cloud-Aerosol Lidar and Infrared Pathfinder Satellite Observation
CAMS	Continuous Air Monitoring Station
CAMx	Comprehensive Air quality Model with extensions
CASTNET	Clean Air Status and Trends Network
CO	Carbon Monoxide
CST	Central Standard Time
DFW	Dallas-Fort Worth Area
EDAS	Eta Data Assimilation System
EER	Exceptional Events Rule
EPA	Environmental Protection Agency
EPS3	Emissions Processing System version 3
FIM	Fire Impact Modeling
FINN	Fire INventory from NCAR
GEOS	Goddard Earth Observing System
GDAS	GFS Data Assimilation System
GFS	Global Forecasting System
GOES	Geostationary Operational Environmental Satellite
HGB	Houston-Galveston-Brazoria Area
HMS	Hazard Mapping System
HRRR	High Resolution Rapid Refresh Model
HRVOC	Highly Reactive Volatile Organic Compound
HYSPLIT	Hybrid Single-Particle Lagrangian Integrated Trajectory Model
ICs	Initial Conditions
mb	millibars
MDA1	daily maximum 1-hour average
MDA8	daily maximum 8-hour average
MODIS	Moderate Resolution Imaging Spectroradiometer
MOZART	Model for OZone and Related chemical Tracers
m	meter
NAAQS	National Ambient Air Quality Standard
NAM	North American Model
NARR	North American Regional Reanalysis
NASA	National Aeronautics and Space Administration
NCAR	National Center for Atmospheric Research
NCDC	National Climatic Data Center
NCEP	National Centers for Environment Prediction
NCL	NCAR Command Language
NDAS	NAM Data Assimilation System
Nm	nanometers
NMB	Normalized Mean Bias
NME	Normalized Mean Error
NO	Nitric Oxide

NOAA	National Oceanic and Atmospheric Administration
NOx	Oxides of Nitrogen
NRT	Near Real-Time
NRTEEM	Near Real-Time Exceptional Events Model
NWS	National Weather Service
PBL	Planetary Boundary Layer
PM	Particulate Matter
$PM_{2.5}$	Particulate Matter < 2.5 ug m^{-3}
ppb	parts per billion
PPM	Piecewise Parabolic Method
Q-Q	Quantile-Quantile
RMSE	Root Mean Squared Error
SIP	State Implementation Plan (for the ozone NAAQS)
TCEQ	Texas Commission on Environmental Quality
ug	micrograms
UH	University of Houston
US	United States
VOC	Volatile Organic Compound
WRF	Weather Research and Forecast model

1.0 EXECUTIVE SUMMARY

The Texas Commission on Environmental Quality (TCEQ) is evaluating whether a clear, causal relationship exists between upwind wildfires and monitored air quality in the Houston area on July 26-28, 2018 and August 23-24, 2018. The US Environmental Protection Agency (EPA) has adopted a weight-of-evidence approach to evaluating exceptional event demonstrations. Therefore, the TCEQ has prepared observational analyses to evaluate whether a causal relationship exists between wildfire emissions and high values of monitored ozone at the Bayland Park and Aldine Continuous Air Monitoring Stations (CAMS) in Houston. Ramboll has prepared additional analyses to supplement the body of evidence prepared by the TCEQ. In this Report, we summarize the results of analyses evaluating the possibility of a causal relationship between the emissions of a series of wildfires outside of Texas and ozone air quality at measured at the following Houston-Galveston-Brazoria (HGB) area monitoring sites:

- Aldine (CAMS 8) on July 27, 2018, July 28, 2018 and August 24, 2018
- Bayland Park (CAMS 53) on July 26, 2018 and August 23, 2018.

The narrative conceptual model of the July 27-28 and August 23-24 high ozone events is outlined below.

1.1 July 26-28, 2018 Houston Ozone Episode

During July 2018, wildfires in Ontario, Canada and Louisiana generated ozone precursors that may have contributed to unusually high ozone concentrations at Bayland Park CAMS 53 on July 26 and at Aldine CAMS 8 on July 27 and July 28.

During the last week of July 2018, the Houston area and the surrounding region of East Texas experienced a multi-day period of high ozone. Houston ozone values rose between July 24-27 and then fell from July 27-July 30. Ozone monitors located in rural areas outside Houston show rising and falling trends similar to Aldine CAMS 8 and Bayland Park CAMS 53, consistent with a regional ozone episode influenced by the arrival of polluted continental air with high levels of background ozone.

July 27 had the highest value of the daily maximum 8-hour average (MDA8) ozone measured at Aldine CAMS 8 during the previous five years. MDA8 values for July 27 exceeded the 99th percentile of values for April-October for the 2014-2018 period, while July 26 and July 28 were above the 98th percentile for Bayland Park CAMS 53 and Aldine CAMS 8, respectively. When the full year is considered, all three days exceeded the 99th percentile for their monitors for the 2014-2018 period, indicating that MDA8 ozone values during July 26-28 were among the very highest values measured at CAMS 8 and CAMS 53 during the preceding five years.

Meteorological conditions during the July episode were generally consistent with TCEQ's conceptual model for non-event high ozone days in Houston. However, July 26 and 27 were unusual in that they had northeasterly afternoon winds that were favorable for transport of ozone and precursors from upwind fires in Louisiana and from more distant fires.

HYSPLIT trajectories using three different meteorological analyses are consistent in showing a source-receptor relationship between the North Bay Wildfire Complex in eastern Ontario and the Houston area for emissions occurring through a deep layer of the lower atmosphere and at multiple times. Of the other large fire complexes burning during the week prior to July 26-28, only the Garner Complex and

South Umpqua Complex in Oregon had forward trajectories that reached Houston, and this was only true for a small number of hours for a single meteorological analysis with trajectories initialized at an altitude of 3,000 m. Therefore, evidence from the HYSPLIT trajectory analysis for transport from distant fires to Houston is strongest for the North Bay Complex. HYSPLIT trajectories using all three meteorological analyses also showed a source-receptor relationship between Louisiana fires occurring July 25-26 and the Houston area.

Satellite imagery from multiple platforms shows that the smoke plume from the North Bay Complex fires moved southward across the Midwest and Southeast US toward Louisiana between July 22-25. Between July 24 and July 25, the Canadian wildfire plume signal grew more diffuse and less intense until it merged with a broad area of smoke over Louisiana on July 25. By July 26, the National Oceanographic and Atmospheric Administration (NOAA) Hazard Mapping System (HMS) smoke field no longer covered a broad swath of Texas and Louisiana, as it had on July 25. By July 26, the area of dense, regional smoke was north of Oklahoma and Arkansas and the only smoke diagnosed by HMS over East Texas and Louisiana came from smaller fires, whose individual plumes were visible in the vicinity of the fires. During July 26-28, the HMS product shows only small smoke plumes from fires in Louisiana and Texas.

Although the NOAA HMS smoke product suggests transport of smoke from western wildfires to Houston was possible, we were not able to trace the plume from western wildfires across the US to southeast Texas using satellite products that track aerosols, carbon monoxide (CO) or visible smoke plumes.

Multiple lines of evidence from surface and satellite-based monitoring systems indicate the presence of smoke in the Houston area aloft and at the surface during July 26-28. The widespread presence of smoke in the Houston area as well as the detection of the biomass burning marker levoglucosan at two Houston monitors provide support for the hypothesis that wildfires influenced ground level ozone during July 26-28.

Photochemical modeling indicated small (<1 ppb) MDA8 ozone impacts from wildfire emissions at Bayland Park CAMS 53 and Aldine CAMS 8 during the July 26-28 episode. However, both matching day and statistical regression analyses that examined the relationship between Houston ozone and weather conditions suggest that an atypical process or processes had a larger impact on Houston ozone during July 26-28. In this context "atypical" means that ozone was higher than expected given the weather conditions on the episode days. The matching day analysis and the statistical regression analysis do not provide information on the nature of the process or processes making an atypical contribution to high ozone in Houston on July 26-28.

1.2 August 23-24, 2018 Houston Ozone Episode

During August 2018, very large wildfires were burning in California, Oregon, Washington and in the Canadian Province of British Columbia. Wildfires in California, Oregon, Nevada and Louisiana generated ozone precursors that may have contributed to unusually high ozone concentrations at Bayland Park CAMS 53 on August 23 and at Aldine CAMS 8 on August 24.

During late August 2018, the Houston area experienced a multi-day period of high ozone. Ozone values rose between August 21-24 and then fell from August 24-29. Ozone monitors located in rural areas outside Houston show rising and falling trends similar to Aldine CAMS 8 and Bayland Park CAMS 53, consistent with a regional ozone episode influenced by the arrival of polluted continental air with high levels of background ozone. Meteorological conditions August episode were generally consistent with TCEQ's conceptual model for non-event high ozone days in Houston.

On August 23, Bayland Park CAMS 53 monitored an MDA8 ozone value of 82 ppb and reached a peak 1-hour ozone value of 112 ppb. On August 24, the MDA8 at Aldine CAMS 8 was 91 ppb. This was the highest value of the MDA8 in the Houston area on August 24 and the peak 1-hour average ozone at Aldine was 106 ppb. August 23 and 24 exceeded the 99th percentile of values for CAMS 53 and CAMS 8, respectively, for 2014-2018 for both the full year and April-October periods.

HYSPLIT trajectories using three different meteorological analyses are consistent in showing source-receptor relationships between the Houston area and the Mendocino Complex (CA) the Carr Fire (CA) the South Sugarloaf Complex (NV) and the Klondike, Taylor Creek and Miles Fire Complexes (OR). HYSPLIT trajectories using all three meteorological analyses also showed a source-receptor relationship between Louisiana fires occurring August 22-23 and the Houston area.

Satellite imagery from multiple platforms shows extensive, thick plumes of smoke across Canada and the northern and central US emanating from fires in British Columbia and the western US during the week before the August 23-24 Houston ozone episode. During the week leading up to August 23-24, the smoke plumes moved from California and Oregon southward and eastward toward Texas behind an advancing cold front associated with a low-pressure system moving eastward across the Midwest. The southeast movement of the smoke-influenced air is apparent in satellite visible light images and in satellite aerosol and CO products. The evolution of the photochemical model smoke tracer plume emanating from the fire locations is consistent with the evolution of satellite-retrieved regions of high CO and aerosols associated with the fire plumes as well as with the smoke plumes emanating from the western US/Canada fires simulated by NOAA's smoke model surface and vertically integrated smoke analyses.

As the cold front advanced southward across East Texas on August 20, new fires began burning in central and western Louisiana. The number of Louisiana fires grew with each passing day between August 20 and August 23. On August 22 and 23, the satellite products, the photochemical modeling smoke tracer and NOAA smoke product animations all show that smoke from the plumes of the Louisiana fires merged with the smoke from the distant wildfires and was advected toward Houston as high pressure built over the southeast US and low-level winds developed an easterly component.

Multiple lines of evidence from surface and satellite-based monitoring systems indicate the presence of smoke in the Houston area aloft and at the surface. The widespread presence of smoke in the Houston area as well as the detection of the biomass burning marker levoglucosan at two Houston monitors provide support for the hypothesis that wildfires influenced ground level ozone during August 23-24.

Photochemical modeling indicated MDA8 ozone impacts less than 3 ppb from wildfire emissions at Bayland Park CAMS 53 and Aldine CAMS 8 during the August 23-24 episode. However, both matching day and statistical regression analyses that examined the relationship between Houston ozone and weather conditions suggest that an atypical process or processes had a larger impact on Houston ozone during July 26-28. In this context "atypical" means that ozone was higher than expected given the weather conditions on the episode days. The matching day analysis and the statistical regression analysis do not provide information on the nature of the process or processes making an atypical contribution to high ozone in Houston on August 23-24.

2.0 INTRODUCTION

Wildfires can emit large quantities of trace gases and aerosols into the atmosphere. These emissions undergo chemical and physical changes as they are transported away from the active fire region. Primary emitted species are depleted as they are deposited and chemically processed, while secondary species such as ozone and secondary organic aerosols form within the fire plume. Research shows that both primary and secondary species can influence air quality at local and regional scales (e.g. Jaffe and Wigder, 2012). Ozone and particulates formed in wildfire plumes can be transported to populated regions and can influence measured concentrations at air quality monitors.

The U.S. EPA allows the exclusion of monitoring data influenced by exceptional events such as wildfires or dust transport when making regulatory determinations based on design values of criteria pollutants relating to the National Ambient Air Quality Standards (NAAQS). States must demonstrate to the U.S. EPA that a wildfire event satisfies Exceptional Events Rule (EER) requirements.

The EER states that an exceptional event and its resulting emissions affect air quality in such a way that there exists a clear causal relationship between the specific event(s) and the monitored exceedance(s) or violation(s), is not reasonably controllable or preventable, is an event(s) caused by human activity that is unlikely to recur at a particular location or a natural event(s), and is determined by the EPA Administrator in accordance with 40 CFR 50.14 to be an exceptional event.

The TCEQ is evaluating whether a clear, causal relationship exists between upwind wildfires and monitored air quality in the Houston area on July 26-28, 2018 and August 23-24, 2018. The EPA has adopted a weight-of-evidence approach to evaluating exceptional event demonstrations. Therefore, the TCEQ has prepared observational analyses to evaluate whether a causal relationship exists between wildfire emissions and high values of monitored ozone at the Bayland Park and Aldine Continuous Air Monitoring Stations (CAMS) in Houston. Ramboll has prepared additional analyses to supplement the body of evidence prepared by the TCEQ. The purpose of this Report is to:

- Summarize the results of analyses evaluating the possibility of a causal relationship between the emissions of a series of wildfires outside of Texas and ozone air quality at measured at the following Houston-Galveston-Brazoria (HGB) area monitoring sites:
    Aldine (CAMS 8) on July 27, 2018, July 28, 2018 and August 24, 2018
    - Bayland Park (CAMS 53) on July 26, 2018 and August 23, 2018.

- Develop a narrative conceptual model of the high ozone events.

Section 3.0 outlines the conceptual model in narrative format and summarizes evidence that fire emissions were transported to the monitors and then affected the monitors. We also present additional analysis of the relationship between wildfire emissions and the Houston high ozone episodes from photochemical modeling, statistical regression analysis and matching day analysis. Section 4.0 presents evidence supporting the conceptual model and Section 5.0 presents evidence supporting the existence of a clear causal connection between wildfire emissions and high ozone at Bayland Park CAMS 53 and Aldine CAMS 8. Finally, Section 6.0 summarizes the analysis.

3.0 NARRATIVE CONCEPTUAL MODEL

3.1 July 26-28, 2018 Houston Ozone Episode

During the last week of July 2018, the Houston area and the surrounding region of East Texas experienced a multi-day period of high ozone. Houston ozone values rose between July 24-27 and then fell from July 27-July 30. Ozone monitors located in rural areas outside Houston show rising and falling trends similar to Aldine CAMS 8 and Bayland Park CAMS 53, consistent with a regional ozone episode influenced by the arrival of polluted continental air with high levels of background ozone.

On July 26, Bayland Park CAMS 53 monitored daily maximum 8-hour average (MDA8) ozone value of 77 ppb and reached a peak 1-hour ozone value of 93 ppb. On July 27, the MDA8 ozone value at Aldine CAMS 8 was 109 ppb. This was the highest value of MDA8 ozone in the Houston area on July 27 and peak 1-hour average ozone at CAMS 8 was 144 ppb. By July 28, the ozone episode began to subside and MDA8 ozone at Aldine CAMS 8 was 86 ppb and the peak 1-hour ozone was 97 ppb. The MDA8 at Aldine CAMS 8 was again the highest value monitored in Houston on July 28.

July 27 had the highest value of MDA8 ozone measured at Aldine CAMS 8 during the previous five years. MDA8 values for July 27 exceeded the 99th percentile of values for the April-October for 2014-2018 period, while July 26 and July 28 were above the 98th percentile for Bayland Park CAMS 53 and Aldine CAMS 8, respectively. When the full year is considered, all three days exceeded the 99th percentile for their monitors for the 2014-2018 period.

Weather conditions during the July episode were generally consistent with TCEQ's conceptual model for non-event high ozone days in Houston. However, July 26 and 27 were unusual in that they had northeasterly afternoon winds that were favorable for transport of ozone and precursors from upwind fires in Louisiana and from more distant fires.

3.1.1 Evidence that the Fire Emissions were Transported to the Monitors

During the latter half of July 2018, large wildfires were burning in California and southwestern Oregon and in the Canadian provinces of Manitoba and Ontario. The Fire INventory from NCAR (FINN; Wiedinmyer et al, 2011) fire emission inventory shows emissions of ozone precursors from wildfire complexes burning in California, Oregon and along the Ontario/Manitoba and Ontario/Quebec borders during the days leading up to the July 26-28 high ozone episode in Houston. The fires with the largest emissions during the week before the Houston ozone episode were the North Bay Complex in eastern Ontario, fire complexes on the border of Ontario and Manitoba, the Garner Complex and South Umpqua Complex in southeast Oregon and the Ferguson Complex in California.

5-day HYSPLIT[1] back trajectories using the NAM 12 km, EDAS 40 km and NARR 36 km meteorological analyses are consistent in showing that air arriving at 500 m and 1000 m above ground level at Bayland Park and Aldine on July 26 and 27 travelled southward from the Midwest and southern Ontario through the Mississippi Valley and Louisiana before arriving in Houston. For air parcels arriving at 2,500 m above Houston on July 26-27, the back trajectories for the three analyses indicate different origins. The NAM and EDAS analysis 5-day back trajectories extend northwest from Houston toward California, Oregon and British Columbia, while the back trajectories for the NARR analysis are consistent with the lower level back trajectories and extend northward from Houston toward the

[1] The National Oceanographic and Atmospheric Administration's (NOAA's) Hybrid Single-Particle Lagrangian Integrated Trajectory (HYSPLIT) model.

central US and southern Canada. HYSPLIT forward trajectories from the North Bay Complex in eastern Ontario showed that a source-receptor relationship existed between the fires and the Houston area for emissions occurring through a deep layer of the lower atmosphere and at multiple times. HYSPLIT produced similar forward trajectories using EDAS, NAM and NARR analyses. Of the other large fire complexes, only the Garner Complex and South Umpqua Complex had forward trajectories that reached Houston, and this was only true for a small number of hours for NARR analysis trajectories initialized at 3,000 m. Therefore, evidence from the HYSPLIT trajectory analysis for transport from distant fires to Houston is strongest for the North Bay Complex.

During the week leading up to the July 26-28 Houston high ozone episode, smoke plumes from the western US and Canadian fire complexes are visible in the Moderate Resolution Imaging Spectroradiometer (MODIS) true color (visible) satellite images as well as in the Atmospheric Infrared Sounder (AIRS) satellite carbon monoxide (CO) and MODIS aerosol optical depth (AOD) retrievals and in the National Oceanographic and Atmospheric Administration (NOAA) Hazard Mapping System (HMS) smoke product. The satellite products show that the smoke plume from the North Bay Complex fires moved southward across the Midwest and Southeast US toward Louisiana between July 22-25.

The NOAA NESDIS Descriptive Text Narrative for Smoke/Dust Observed in Satellite Imagery for July 25 notes, "*The smoke over the Western and Central US was likely attributed to wildfire activity over the Western US. The mass of thin to moderately dense smoke stretching from the Great Lakes region to the Gulf Coast was more likely being transported southward from Canada with the source potentially from wildfires in Canada and even now possibly from the longer range transport from Europe/Asia.*"

The NOAA HMS smoke product shows the movement of this plume of smoke from Ontario southward into Louisiana and Texas, including the Houston area, by July 25. The MODIS and GOES 16 AOD retrievals are generally consistent with the NOAA HMS product, but have data gaps due to the presence of clouds. During July 22-24, the plume from the Canadian wildfires in North Bay, Ontario can be identified in the MODIS AOD and GOES 16 AOD retrievals as it travels southward across the Midwest and Southeast. Between July 24 and July 25, the Canadian wildfire AOD signal grows more diffuse and less intense until it merges with an area of enhanced AOD over Louisiana on July 25. By July 26, the NOAA HMS smoke field no longer covers a broad swath of Texas and Louisiana, as it did on July 25. The area of dense, regional smoke has retreated north of Oklahoma and Arkansas and the only smoke diagnosed by HMS over East Texas and Louisiana comes from smaller fires, whose individual plumes are visible in the vicinity of the fires. During July 26-28, the HMS product shows only small smoke plumes from fires in Louisiana and Texas. During July 26-28, the GOES 16 and MODIS AOD retrievals show the presence of aerosol consistent with smoke over Houston.

Although the NOAA HMS product suggests transport of smoke from western wildfires to Houston was possible, we were not able to trace an AOD or CO signal from western wildfires across the US to southeast Texas.

The FINN fire emission inventory shows wildfires burning in Louisiana and Texas immediately preceding and during the July 26-27 Houston high ozone days. Smoke plumes from the Louisiana and Texas fire complexes are visible in the MODIS true color (visible) satellite images for July 26 as well as in the MODIS AOD retrievals and the NOAA HMS smoke product.

The TCEQ's ozone forecast for July 26 notes the influence of smoke: "*Additionally, transported light smoke from isolated fires (particularly those in the lower Mississippi Valley and southeast United*

States) may intermittently and locally increase $PM_{2.5}$ levels at locations in the vicinity and immediately downwind of the fires, adding to the already elevated particulates associated with African dust. Overall, the daily $PM_{2.5}$ AQI is forecast to reach "Moderate" in parts of the Austin, Beaumont-Port Arthur, Brownsville-McAllen, Corpus Christi, Dallas-Fort Worth, Houston, Laredo, San Antonio, Tyler-Longview, and Victoria areas and the upper end of the "Good" range throughout Waco-Killeen area."

Animations of the NOAA High-Resolution Rapid Refresh (HRRR) Model's surface smoke analysis and vertically integrated smoke analysis are consistent with the MODIS AOD retrieval and the NOAA HMS smoke product in showing that smoke from fires in Canada arrived in southern Louisiana by July 25. On July 26, the HRRR modeling shows plumes from these distant fires merged with plumes from fires in Louisiana and moved into the Houston area. On July 26, the HRRR-modeled smoke plumes from the fires in Louisiana were more intense than the smoke from the distant fires in Canada and the western US.

Photochemical modeling of July-August 2018 was conducted using the Near-Real Time Exceptional Event Modeling (NRTEEM) System (Johnson et al., 2018). The NRTEEM model's smoke tracer results were consistent with the NOAA HRRR smoke modeling in suggesting that fires in Louisiana played a more important role than distant fires in Canada and the western US in determining the concentrations of smoke over Houston on July 26-28. HYSPLIT back trajectory and forward trajectory analysis indicates that fires in Louisiana were upwind of Houston during July 25-27.

The orientation of fire plumes in the HMS smoke product for July 26 suggests that plumes from wildfires in Texas and Louisiana may have influenced Houston. Ramboll performed a Q/D (emissions/distance) analysis consistent with EPA Guidance[2] for all fires present in the FINN emission inventory on July 26 and determined that no fire present on July 26 met EPA's 100 tpd/km criterion for a Tier II exceptional event. Ramboll performed a forward trajectory analysis for the fires burning north of Houston near Livingston, TX on July 26-27. The forward trajectory analysis showed that these fires were not upwind of Houston during this period.

3.1.2 Evidence that the Fire Emissions Affected the Monitors

Multiple lines of evidence from surface and satellite-based monitoring systems indicate the presence of smoke in the Houston area aloft and at the surface. The widespread presence of smoke in the Houston area provides support for the hypothesis that wildfires influenced ground level ozone during July 26-28.

Speciated PM measurements provided by the University of Houston (UH) for two Houston monitors (Clinton CAMS 403 and UH West Liberty CAMS 699) indicate the presence of the biomass burning marker levoglucosan at ground level on July 26 and 27 as well as the presence of soluble potassium during July 26-28. Soluble potassium is associated with biomass burning plumes. PM concentrations of organic and elemental carbon and measured attenuation from black carbon were also enhanced during July 26-27 relative to July 29-30 and September 16-18, the two non-event periods for which speciated PM data were available. Measured attenuation from brown carbon was lower during July 26-28 than during the July 29-30 and September 16-18 periods.

Ground-based AOD measurements made at the University of Houston Aerosol Robotic Network (AERONET) site show enhanced levels of particles in the atmosphere over Houston during July 26-28 and measurements of the ratio of the fine and coarse aerosol modes and of the aerosol Angstrom

[2] https://www.epa.gov/sites/production/files/2018-10/documents/exceptional_events_guidance_9-16-16_final.pdf

parameter indicate the size of the particles was consistent with smoke. On July 26 and July 27, the 500 nm fine mode AOD met or exceeded the 99th percentile for this quantity for the years 2014-2018 and on July 28, it exceeded the 90th percentile.

$PM_{2.5}$ measurements from multiple CAMS and Houston Regional Monitoring (HRM) network monitors in Houston showed enhanced levels of CO and $PM_{2.5}$ at ground level during July 26-28. CO and $PM_{2.5}$ levels remained enhanced throughout the period, consistent with a regional transport event of polluted continental air. Monitors in rural areas near the northern and eastern borders of Texas also showed elevated levels of $PM_{2.5}$ during this period, and this is also consistent with a regional transport event and the arrival of an air mass influenced by biomass burning.

MODIS AOD retrievals show areas of enhanced AOD over the greater Houston area and across coastal southeast Texas and southern Louisiana during July 26-28. The value of the MODIS Deep Blue Aerosol Angstrom Exponent is greater than one across much of the areas of enhanced AOD in southern Louisiana and southeast Texas during July 26-28, indicating the presence of fine particles consistent with smoke from nearby and/or distant wildfires. This is consistent with the AERONET measurements of the Angstrom aerosol exponent. CO retrievals from the AIRS sounder show enhanced CO over southeast Texas and southern Louisiana during July 26-28 consistent with the influence of biomass burning in distant and/or nearby wildfires.

3.1.3 Additional Evidence that Wildfire Emissions Caused the Ozone Exceedances at Bayland Park CAMS 53 and Aldine CAMS 8

EPA Guidance on Exceptional Event Demonstrations (EPA, 2016) notes that air agencies may develop supporting evidence for a clear, causal relationship between wildfire(s) and ozone exceedance(s) using photochemical modeling, matching day analyses and statistical regressions. All three of these analyses were performed and we summarize the methods and results below.

NRTEEM photochemical modeling shows that the impact of wildfire emissions on the daily maximum 8-hour average (MDA8) ozone at the Bayland Park and Aldine CAMS was less than 1 ppb during July 26-28. The NRTEEM modeling results indicate large amounts of ozone (hourly ozone impacts from fire exceeding 15 ppb) immediately downwind of the California and Ontario fires, and do show a transport path between the Canadian fires and the Houston area. However, ozone impacts are small by the time the plume from the Canadian fires arrives in Texas due to plume dispersion and ozone removal by deposition. The NRTEEM smoke tracer indicates that several fires in Louisiana and Texas influenced the Houston area, but the most intense parts of the modeled fire plumes travelled north of Houston. On July 26, a fire plume with wildfire MDA8 ozone enhancements exceeding 10 ppb passed north of Houston. In the NRTEEM modeling, fires in Louisiana and Texas had larger impacts in Texas than the more distant fires in Canada and the western US and impacts to MDA8 ozone from all fire emissions taken together were less than 3 ppb at Aldine CAMS 8 and Bayland Park CAMS 53.

NRTEEM model performance for 1-hour ozone was good[3] at Bayland Park during July 26-28, but the model greatly underestimated peak ozone at Aldine on July 26 (observed: 144 ppb, modeled: 62 ppb) and July 27 (observed: 92 ppb, modeled: 69 ppb). The model reproduced July 26-28 ozone at UH West Liberty CAMS 699 reasonably well[4], which suggests that the model did not have large biases in simulating the regional background ozone entering Houston. UH West Liberty CAMS 699 is located northeast of downtown Houston and is upwind of Houston during periods of northeasterly flow. The

[3] Daily mean normalized bias of 1% on July 26, 6% on July 27 and 20% on July 28

[4] Daily mean normalized bias ≤10% on July 25-27 and 22% on July 28

NRTEEM model was run with the TCEQ's 2017 "future year" anthropogenic emission inventory and does not capture impacts from atypical anthropogenic emissions.

Ramboll performed a matching day analysis for July 26, 27 and 28 following EPA (2016) guidance. The purpose of this analysis is to use a set of weather-related criteria to find days that have meteorological conditions similar to the exceedance days but were not influenced by wildfires. By comparing ozone on the non-fire influenced days to the exceedance days, the ozone contribution of unusual processes (including wildfires) on the exceedance days can be estimated. The August 14, 2015 and August 15, 2015 matching days had MDA8 ozone 16-21 ppb lower than on July 26, 2018 at Bayland Park CAMS 53. The August 14, 2015 and August 15, 2015 matching days had MDA8 ozone 45-47 ppb lower than on July 27, 2018 at Aldine CAMS 8 and had MDA8 ozone 22-24 ppb lower than on July 26, 2018 at Aldine CAMS 8.

Dr. Dan Jaffe performed a generalized additive model (GAM) statistical regression analysis of weather- and air quality-related parameters and MDA8 ozone at Houston monitors and provided his analysis to the TCEQ. Because the regression equations were developed with ten years of data, they represent the relationship between air quality and meteorology under typical emission patterns.

Dr. Jaffe explains the method: "*In brief, the method develops a statistical prediction scheme for the MDA8 using meteorological predictors such as daily max temperature, wind speed, relative humidity, trajectory distance, etc. The model uses a training dataset to predict MDA8 ozone based on past years relationships. The residual (the unexplained portion of the variance) can identify days with unusual ozone levels, if the residual is sufficiently large* ". The GAM analysis quantified residuals suggesting that atypical conditions contributed ozone to the Aldine Park MDA8 on July 27. Dr. Jaffe concludes that evidence for unusual enhancement of the MDA8 ozone was weaker for July 26. July 28 was not analyzed. Using analyses complementary to the GAM analysis, Dr. Jaffe infers that wildfire emissions contributed to the ozone residuals found by the GAM and therefore to the Houston ozone exceedances on July 27. The complementary analyses considered that enhanced levels of $PM_{2.5}$ occurred in Houston during this period and that hourly ground level $PM_{2.5}$ and ozone were correlated at Houston CAMS during the hours 10 am – 6 pm.

In summary, photochemical modeling provides evidence of small (< 1 ppb) ozone impacts from wildfires at Bayland Park CAMS 53 and Aldine CAMS 8. However, matching day and GAM analyses suggest that an atypical process or processes had a larger impact on Houston ozone during July 26-28. The matching day analysis does not provide information on whether wildfires are among the atypical processes contributing to high ozone on July 26-28. The GAM analysis also does not provide information on the nature of the process or processes contributing to the ozone residuals on July 26-27. Dr. Jaffe infers that wildfires are the cause of the residuals based on his analysis of $PM_{2.5}$ and ozone for a subset of Houston CAMS on July 26-27.

3.2 August 23-24, 2018 Houston Ozone Episode

During late August 2018, the Houston area experienced a multi-day period of high ozone. Ozone values rose between August 21-24 and then fell from August 24-29. Ozone monitors located in rural areas outside Houston show rising and falling trends similar to Aldine CAMS 8 and Bayland Park CAMS 53, consistent with a regional ozone episode influenced by the arrival of polluted continental air with high levels of background ozone.

On August 23, Bayland Park CAMS 53 monitored an MDA8 ozone value of 82 ppb and reached a peak 1-hour ozone value of 112 ppb. Higher values of MDA8 ozone were measured elsewhere in Houston on

August 23. UH Moody Tower CAMS 695 had an MDA8 ozone of 100 ppb on August 23. On August 24, the MDA8 at Aldine CAMS 8 was 91 ppb. This was the highest value of the MDA8 in the Houston area on August 24 and the peak 1-hour average ozone at Aldine was 106 ppb. August 23 and 24 exceeded the 99th percentile of values for CAMS 53 and CAMS 8, respectively for 2014-2018 for both the full year and April-October periods. By August 25, the Houston ozone episode had begun to subside.

Weather conditions during the July and August episodes were generally consistent with TCEQ's conceptual model for non-event high ozone days in Houston.

3.2.1 Evidence that the Fire Emissions were Transported to the Monitors

During August 2018, large wildfires were burning in the western US and British Columbia. The FINN fire emission inventory shows large wildfire complexes burning in California, Oregon, Washington, Nevada and British Columbia during the week before the August 23-24 high ozone days in Houston.

HYSPLIT 5-day back trajectories using the NAM, EDAS 40 km and NARR meteorological analyses are consistent in showing that air arriving at 500 m above ground level at Bayland Park on August 23 and Aldine on August 24 travelled northwest across the Gulf of Mexico before arriving in Houston. Although low-level parcels arriving in Houston had a maritime influence, there is significant vertical wind shear on both days, and air farther aloft originated over the continental US. For air parcels arriving at 2,500 m above Bayland Park on August 23, the back trajectories for the EDAS, NAM and NARR analyses extend from Houston northwest toward California, Nevada and Oregon. The NAM and EDAS analysis 5-day 1,000 m back trajectories are similar to the 500 m back trajectory, extending southeast over the Gulf of Mexico, while the back trajectories for the NARR analysis extend northward from Houston toward the central US and southern Canada.

The HMS smoke product is consistent with the MODIS and GOES AOD retrievals in showing extensive, thick plumes of smoke across Canada and the northern and central US emanating from fires in British Columbia and the western US during the week before the August 23-24 Houston ozone episode. The NOAA NESDIS Descriptive Text Narrative for Smoke/Dust Observed in Satellite Imagery for August 20 notes, "*The ongoing wildfire activity in the western U.S. and western Canada continues to produce enormous amounts of smoke of varying density that covers most of southern Canada and the northern United States. The densest smoke within this area extended from the Texas Panhandle north to eastern Montana and also extending offshore the Pacific Northwest to western British Columbia*."

During the week leading up to August 23-24, the smoke plumes moved from California and Oregon southward and eastward toward Texas behind an advancing cold front associated with a low-pressure system moving eastward across the Midwest. The southeast movement of the smoke-influenced air is apparent in MODIS AOD and AIRS CO retrievals as well as the true color (visible) satellite images. The evolution of the NRTEEM photochemical model smoke tracer plume emanating from the FINN fire locations is consistent with the evolution of satellite-retrieved regions of high CO and AOD associated with the fire plumes as well as with the smoke plumes emanating from the western US/Canada fires simulated by the NOAA HRRR surface and vertically integrated smoke analyses.

As the cold front advanced southward across East Texas on August 20, new fires began burning in central and western Louisiana. The number of Louisiana fires grew with each passing day between August 20 and August 23. On August 22 and 23, the MODIS and GOES 16 AOD retrievals, the NRTEEM modeling smoke tracer and NOAA HRRR smoke product animations show that smoke from the plumes of the Louisiana fires merged with the smoke from the distant wildfires and was advected toward

Houston as high pressure built over the southeast US and low-level winds developed an easterly component.

On August 22, the Terra/MODIS corrected true reflectance image for 11:25 CDT shows the presence of smoke across East Texas, including Houston and Beaumont. The enhanced AOD over the Houston area and the value of the aerosol Angstrom exponent (> 1) across this region indicates the presence of fine particles aloft consistent with smoke.

Similar to the GOES and MODIS AOD, the NOAA HMS smoke product shows the movement of this plume of smoke southward into Texas behind an advancing front and reaching Houston by August 22.

3.2.2 Evidence that the Fire Emissions Affected the Monitors

Multiple lines of evidence from surface and satellite-based monitoring systems indicate the presence of smoke in the Houston area aloft and at the surface. The presence of smoke in the Houston area provides support for the hypothesis that wildfire emissions contributed to high values of Houston ozone on August 23-24.

Speciated PM measurements for two Houston monitors provided by UH indicate the presence of the biomass burning marker levoglucosan at ground level in Houston on August 23-24 as well as the presence of soluble potassium during these two days. Concentrations of organic and elemental carbon and measured attenuation from black carbon were generally slightly larger during August 23-24 relative to July 29-30 and September 16-18, the two non-event periods for which data were available. Measured attenuation from brown carbon was lower during August 23-24 than during the July 29-30 and September 16-18 periods.

AERONET ground-based AOD measurements show enhanced levels of particles in the atmosphere over Houston during August 23-24 and measurements of the ratio of the fine and coarse aerosol modes and of the aerosol Angstrom parameter indicate the size of the particles was consistent with smoke. On August 23-24, the 500 nm fine mode AOD met or exceeded the 99^{th} percentile for this quantity for the years 2014-2018.

$PM_{2.5}$ measurements from multiple CAMS and HRM monitors in Houston show enhanced levels of CO and $PM_{2.5}$ at ground level during August 23-24. CO and $PM_{2.5}$ levels remained enhanced throughout the period, consistent with a regional transport event of polluted continental air. Monitors in rural areas of Texas also showed elevated levels of $PM_{2.5}$ during this period, and this is also consistent with a regional transport event with the arrival of an air mass influenced by biomass burning.

$PM_{2.5}$ measurements from CAMS and HRM monitors in Houston show enhanced levels of $PM_{2.5}$ at ground level during August 22-24. MODIS AOD retrievals show areas of enhanced AOD over the cloud-free areas of Houston and across east Texas and Louisiana during August 23-24. AOD retrieval cannot be performed for cloud-covered regions. The value of the MODIS Deep Blue Aerosol Angstrom Exponent is greater than one across nearly all of the area of enhanced AOD in Houston and regionally across East Texas and Louisiana, indicating the presence of fine particles consistent with smoke.

CO retrievals from the AIRS sounder show enhanced CO over Houston on August 23 consistent with wildfire influence. CO levels over Houston declined by August 24 but are still higher than the values found over the cleaner air offshore over the Gulf of Mexico.

3.2.3 Additional Evidence that Wildfire Emissions Caused the Ozone Exceedances at Bayland Park CAMS 53 and Aldine CAMS 8

NRTEEM photochemical modeling shows wildfire impacts on MDA8 ozone at the Bayland Park and Aldine CAMS were approximately 2 ppb on August 23-24. The NRTEEM modeling simulated large amounts of ozone (hourly ozone impacts from fires exceeding 100 ppb) downwind of the California and Oregon fires, and show a transport path between the large western wildfires and the Houston area. The NRTEEM model smoke tracer clearly shows transport of fine PM from wildfires in British Columbia, California, Oregon, Washington, Colorado, Nevada and to Houston and the evolution of the NRTEEM smoke tracer is consistent with the evolution of wildfire plumes as shown by satellite retrievals of AOD and CO as well as in true color visible images and the NOAA HRRR surface smoke product. The NRTEEM model smoke tracer also shows that fires in Louisiana contributed smoke to the Houston area.

The NRTEEM model underestimated peak 1-hour ozone at Aldine by 25-30 ppb on August 23-24. At Bayland Park, peak 1-hour ozone on August 23 was 10 ppb low and occurred 3 hours earlier than the observed peak. On August 24, peak 1-hour ozone was underestimated by about 6 ppb. As in the July episode, the NRTEEM model's performance at the UH West Liberty monitor had smaller biases than at the Aldine and Bayland Park monitors.

Ramboll performed a matching day analysis for August 23-24. The purpose of this analysis is to use a set of weather-related criteria to find days that have weather similar to the exceedance days but were not influenced by wildfires. By comparing ozone on the non-fire influenced days to the exceedance days, the ozone contribution of unusual processes (including wildfires) on the exceedance days can be estimated. The August 14, 2015 and August 15, 2015 matching days had MDA8 ozone 21-26 ppb lower than on August 23, 2018 at Bayland Park CAMS 53. The matching days had MDA8 ozone 27-29 ppb lower than on August 24, 2018 at Aldine CAMS 8 and had MDA8 ozone 22-24 ppb lower than on July 26, 2018 at Aldine CAMS 8.

Dr. Dan Jaffe performed a generalized additive model (GAM) statistical regression analysis of weather- and air quality-related parameters and MDA8 ozone at Houston monitors and provided his analysis to the TCEQ. Because the regression equations were developed with ten years of data, they represent the relationship between air quality and meteorology under typical emission patterns.

The GAM analysis quantified residuals suggesting that atypical conditions contributed ozone to the Bayland Park MDA8 on August 23 and to the Aldine Park MDA8 on August 24. Dr. Jaffe concludes that his analysis provides strong evidence that wildfire emissions contributed to Houston exceedances on August 23-24 based on the GAM residuals and on his analysis of the enhanced levels of $PM_{2.5}$ in Houston during this period and the correlation of hourly ground level $PM_{2.5}$ and ozone at Houston CAMS during the hours 10 am – 6 pm.

In summary, photochemical modeling simulations indicate small ozone impacts from wildfires at Bayland Park CAMS 53 and Aldine CAMS 8 during August 23-24. However, the matching day analysis and the GAM analysis suggest that an atypical process or processes had a larger effect on Houston ozone during August 23-24. The GAM and matching day analyses do not provide information on the nature of the process or processes contributing to the atypically high ozone in Houston. Dr. Jaffe infers that wildfires are the cause of the residuals based on his analysis of $PM_{2.5}$ and ozone for a subset of Houston monitors on August 23-24.

4.0 CONCEPTUAL MODEL OF WILDFIRE IMPACTS ON HOUSTON AIR QUALITY DURING JULY 26-28 AND AUGUST 23-24

EPA's "Guidance on the Preparation of Exceptional Events for Demonstrations for Wildfire Events that May Influence Ozone Concentrations" (EPA, 2016) requires that a conceptual model describe the interaction of emissions, meteorology, and chemistry of event and non-event ozone formation in the area. In this section, we describe a conceptual model of the impact of wildfire emissions on ozone concentrations for the July 26-28 and August 23-24 Houston ozone episodes.

4.1 July 26-28, 2018 Episode Conceptual Model

During July 2018, large wildfires were burning in California and southwestern Oregon and in the Canadian Provinces of Manitoba and Ontario. The Fire INventory from NCAR (FINN) fire emission inventory shows large emissions of ozone precursors from wildfire complexes burning in California, Oregon and along the Ontario/Manitoba and Ontario/Quebec borders during the days leading up to the July 26-28 high ozone days in Houston (Figure 4-1 and Figure 4-2).

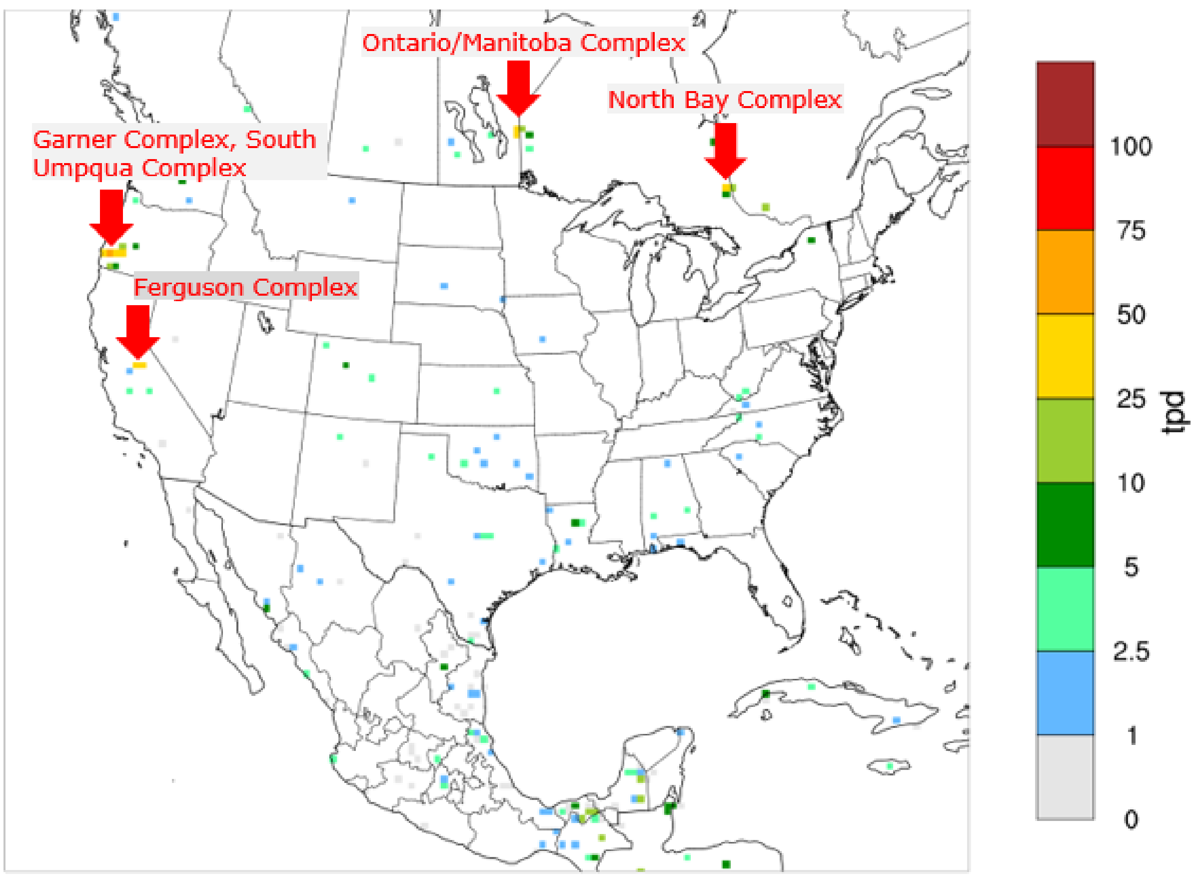

Figure 4-1. FINN fire NOx emissions (tpd) for July 21, 2018. Red arrows indicate large fire complexes potentially upwind of Houston based on HYSPLIT back trajectory analysis.

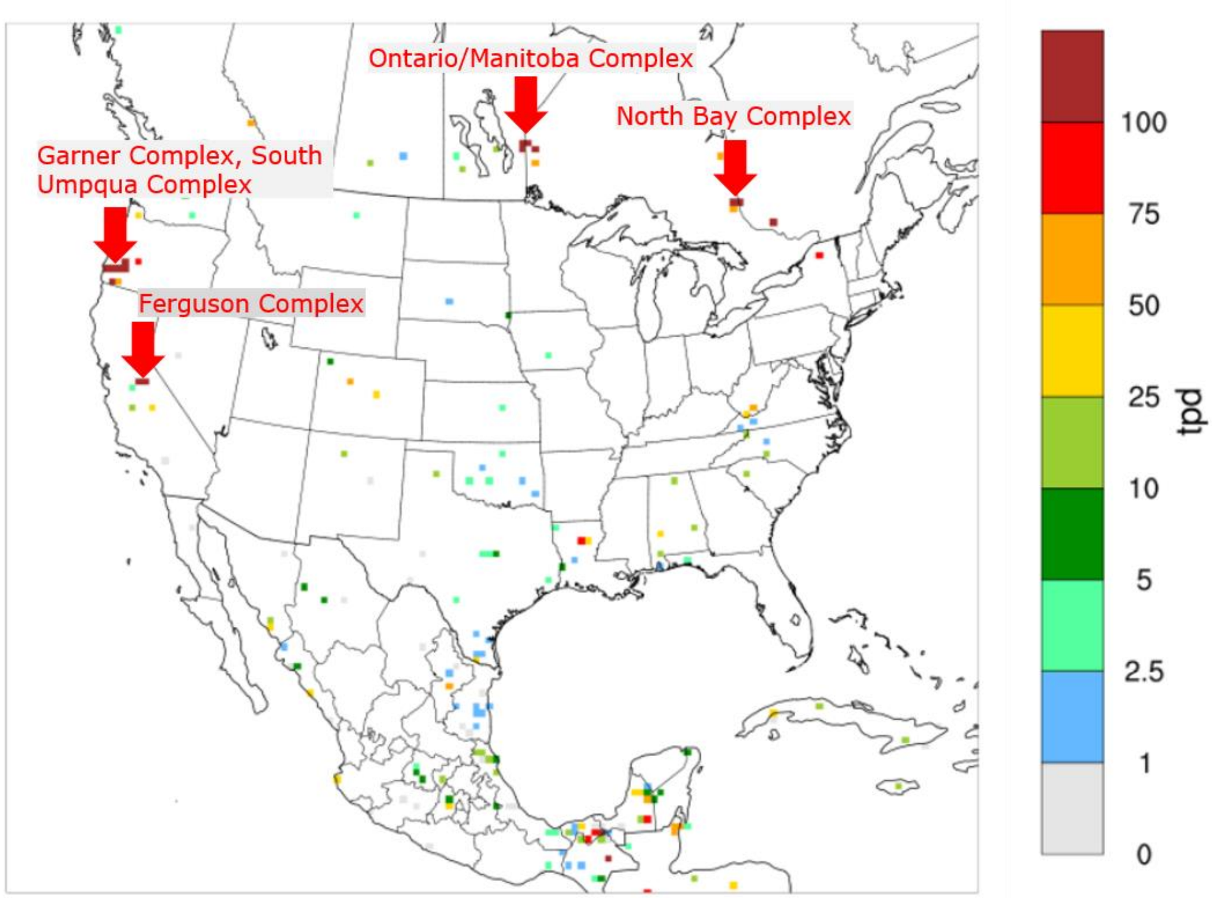

Figure 4-2. FINN fire VOC emissions (tpd) for July 21, 2018. Red arrows indicate large fire complexes potentially upwind of Houston based on HYSPLIT back trajectory analysis.

The fires with the largest emissions during the week before the Houston ozone episode were the North Bay Complex in eastern Ontario, fire complexes on the border of Ontario and Manitoba, the Garner Complex and South Umpqua Complex in southeast Oregon and the Ferguson Complex in California. We evaluated the potential for emissions to be transported from each of these fire complexes to Houston and found evidence to support transport from the North Bay Complex only (see Section 5.3.1).

4.1.1 North Bay Wildfire Complex, Ontario, Canada

In July 2018, dry conditions in Ontario created conditions favorable for wildfire (Figure 4-3). The Canadian Drought Monitor assessment map showed that Southeast Ontario was unusually dry during July 2018 (Figure 4-4). Lightning touched off a series of wildfires in southeast Ontario that were exacerbated by high winds.

On July 10, the Toronto Star reported, "*A massive swath of the province outside of North Bay continues to burn after lightning from storms triggered fires that are raging out of control due to high winds. At least 3,000 hectares are in flames in the North Bay district, which stretches from north of North Bay to Temagami. Further to the north, another 12,000 hectares are burning in Lady Evelyn-Smoothwater Provincial Park. Numerous other fires are being held or brought under control while still* *others, in less populated areas, are being monitored — part of a trend in the province that already has seen 537 fires this year, compared to the 10-year annual average (360)"*[5].

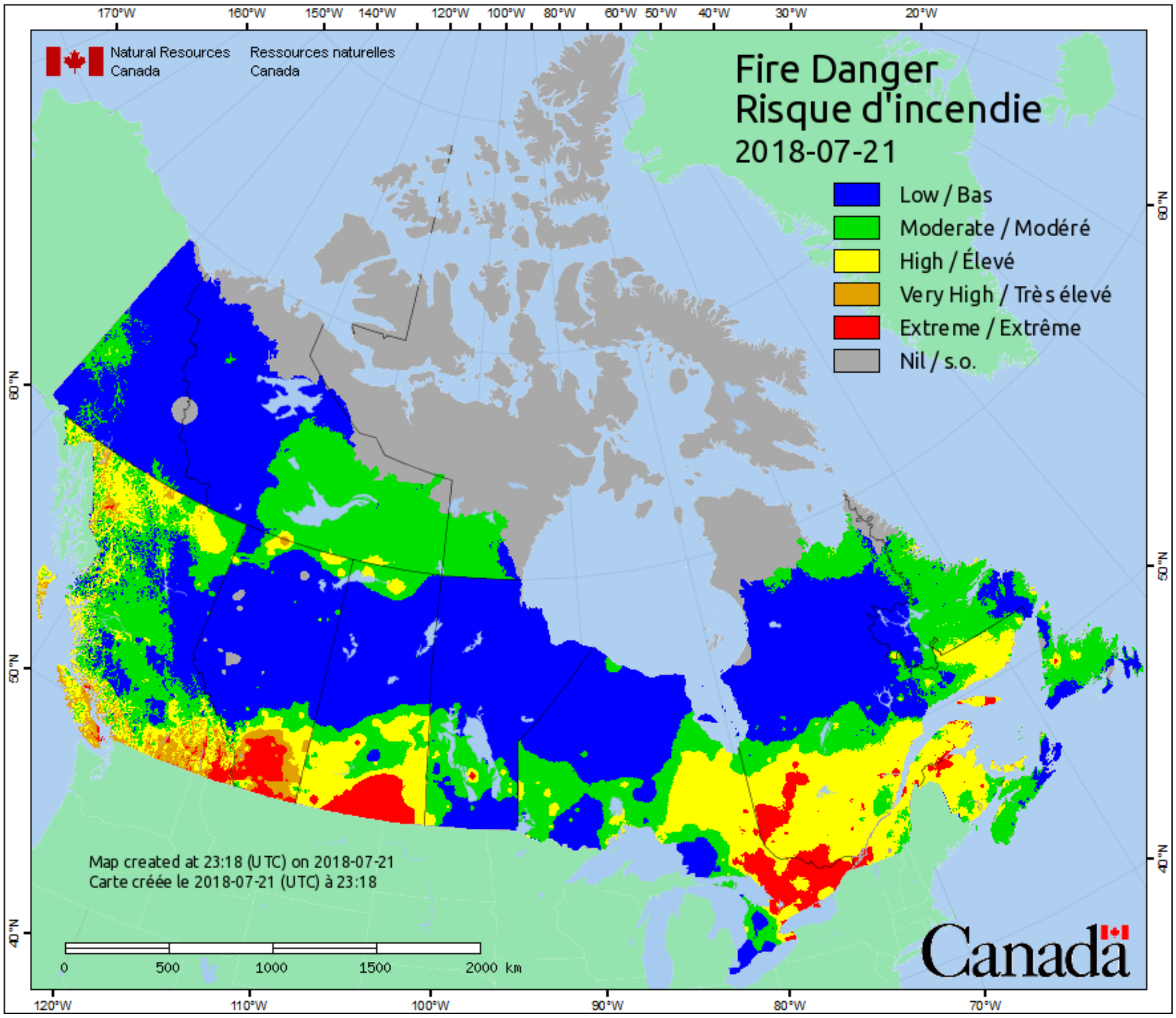

Figure 4-3. Natural Resources Canada's map of fire danger in Canada for July 21, 2018[6].

[5] https://blogs.mprnews.org/updraft/2018/07/smoky-skies-63-canadian-wildfires-mean-periodic-smoke-invasions-in-minnesota/

[6] https://cwfis.cfs.nrcan.gc.ca/maps/fw?type=fdr&year=2018&month=7&day=21

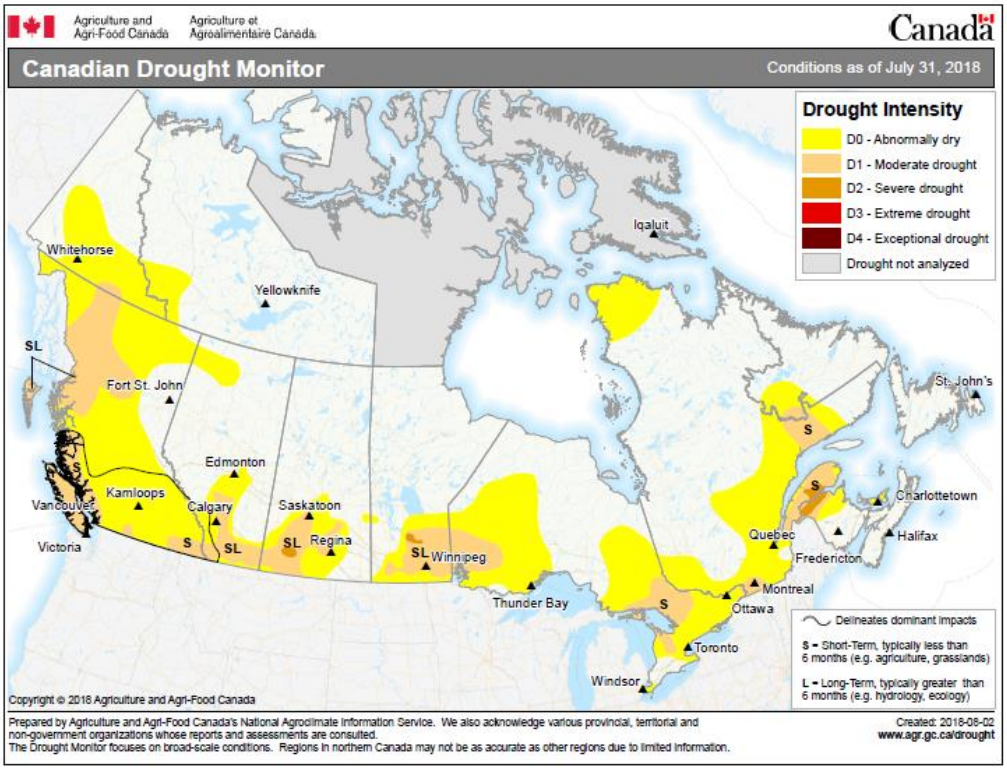

Figure 4-4. Canadian Drought Monitor map of drought intensity in Canada in July 2018.

The July 18 Natural Resources Canada Wildfire Situation Report[7] reads, "*CIFFC Priority Fires Ontario currently has six priority fires at various stages of control. NOR 069 southwest of Tamagami has an Incident Management Team in place. Fire is approximately 221 ha in size and is listed as not under control. NOR 072 approximately 30km west of Temiskaming Shores and has an Incident Management Team on site. The fire is approximately 10,755 ha in size and currently listed as not under control. The River Valley Fire Cluster includes NOR 062 approximately 2,500 ha in size, listed as not yet under control. NIP 030 Southwest of Winisk Provincial Park has an Ignition Team in place for values protection is approximately 23,150 ha in size. RED 070 Southwest of Pikangikum Lake has an Ignition Team in place for values protection is approximately 1,400 ha in size... In Ontario, pursuant to the Emergency Area Order signed July 12, 2018 prohibited access has been issued to portions of North Bay, Sudbury and Kirkland Lake Districts where there are public safety hazards as a result of increased fire activity*." The location of the fires is shown in Figure 4-5 and a photo of the impact of the fires on local air quality is shown in Figure 4-6.Minnesota Public Radio noted air quality impacts were occurring in Minnesota as smoke from the fires was blown south into the US and reported the potential for further impacts: "*Our prevailing winds this week will be from the northwest overall. A cold front diving south Wednesday could severe as a focus that may bring smoke down to ground level in Minnesota. Northerly flow from Canada Thursday may also blow smoke south into Minnesota*."[8]

[7] https://cwfis.cfs.nrcan.gc.ca/report/archives?year=2018&month=07&day=18&process=Submit

[8] https://blogs.mprnews.org/updraft/2018/07/smoky-skies-63-canadian-wildfires-mean-periodic-smoke-invasions-in-minnesota/

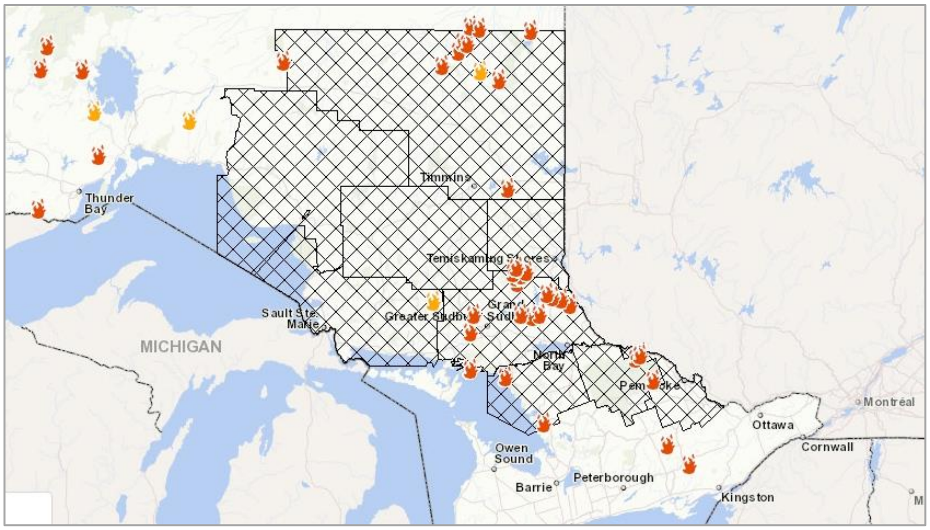

Figure 4-5. Map of fires in North Bay Complex on July 23, 2018 from the Province of Ontario[9].

Figure 4-6. CBC News tweet on Ontario wildfires, with image of wildfire smoke from the fires.

[9] https://www.ontario.ca/page/forest-fires

4.1.2 Affected Monitors

During July 26-28, 2018, Aldine CAMS 8 and Bayland Park CAMS 53 monitored high values of ozone. Aldine CAMS 8 is located north of downtown Houston and Bayland Park CAMS 53 is west of downtown Houston (Table 4-1, Figure 4-7).

Table 4-1. Monitor locations and identification numbers.

Aldine CAMS 8	
EPA ID	482010024
County	Harris
Latitude	29.901036 ºN
Longitude	95.326137 ºW
Elevation	24
Bayland Park CAMS 53	
EPA ID	482010055
County	Harris
Latitude	29.6957294 ºN
Longitude	95.4992190 ºW
Elevation	19.5 m

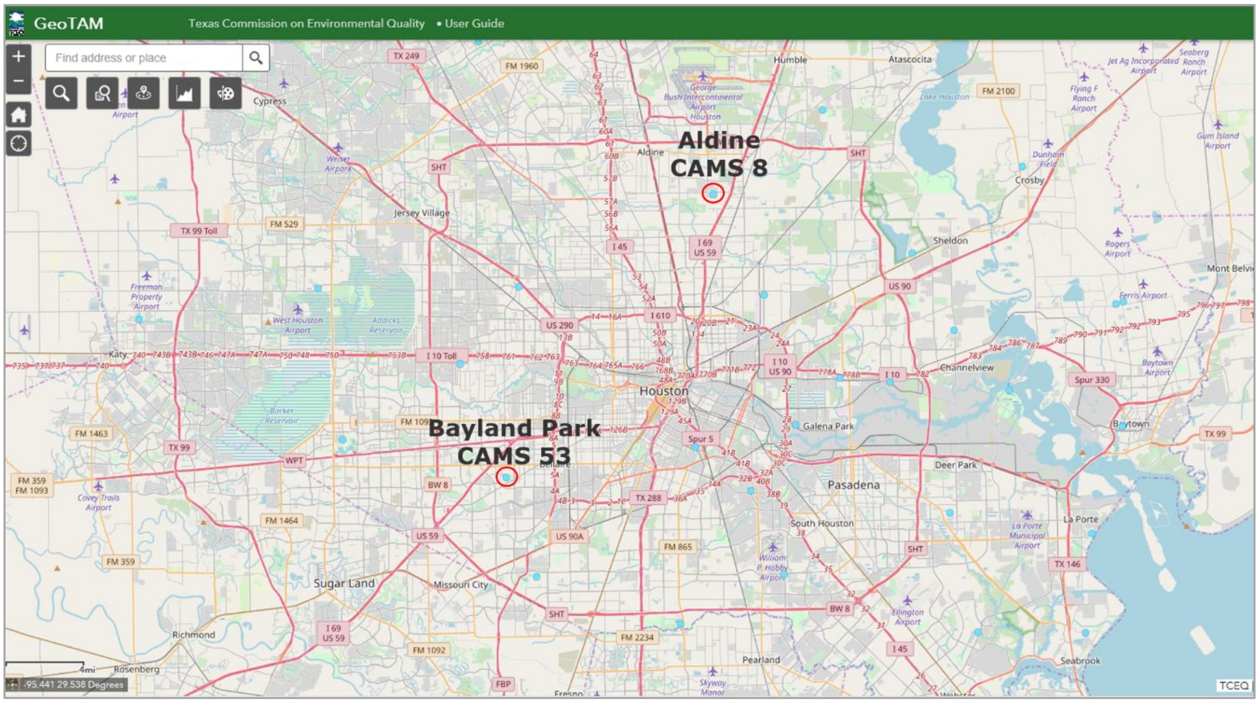

Figure 4-7. Location of affected monitors Aldine CAMS 8 and Bayland Park CAMS 53. Map adapted from TCEQ GeoTAM map viewer[10].

During the last week of July 2018, the Houston area and the surrounding region of East Texas experienced a multi-day period of high ozone. Ozone values rose between July 24-27 and then fell from July 27-July 30. Figure 4-8 and Figure 4-9 show 1-hour average ozone time series for Bayland Park CAMS 53 and Aldine CAMS 8 that show the diurnal cycle of ozone superposed on lower frequency rise and fall consistent with an episode of continental air arriving in Texas. Figure 4-10 and Figure 4-11 are similar time series for West Liberty CAMS 699 and the Alabama Coushatta CASTNET site, which are located outside Houston and serve as upwind background monitors for air travelling south from the continental US into the Houston area. These monitors show rising and falling trends similar to Aldine CAMS 8 and Bayland Park CAMS 53, consistent with a regional ozone episode influenced by the arrival of polluted continental air with high levels of background ozone.

On July 26, Bayland Park CAMS 53 monitored an MDA8 ozone value of 77 ppb and reached a peak 1-hour ozone value of 93 ppb at 13:00 CST (Figure 4-8). On July 27, the MDA8 at Aldine CAMS 8 was 109 ppb. This was the highest value of the MDA8 in the Houston area on July 27 (Figure 4-13) and peak 1-hour average ozone was 144 ppb at 15:00 CST (Figure 4-9). July 27 had the highest value of MDA8 ozone measured at Aldine CAMS 8 during the previous five years. MDA8 values for July 27 exceeded the 99th percentile of values for the April-October for 2014-2018 period, while July 26 and July 28 were above the 98th percentile for Bayland Park CAMS 53 and Aldine CAMS 8, respectively. When the full year is considered, all three days exceeded the 99th percentile for their monitors for the 2014-2018 period. By July 28, the ozone episode had begun to subside and MDA8 ozone at Aldine was 86 ppb and the peak 1-hour ozone was 97 ppb at 16:00 CST. The MDA8 at Aldine CAMS 8 was again the highest value monitored in Houston on July 28 (Figure 4-14).

[10] https://tceq.maps.arcgis.com/apps/webappviewer/index.html?id=ab6f85198bda483a997a6956a8486539

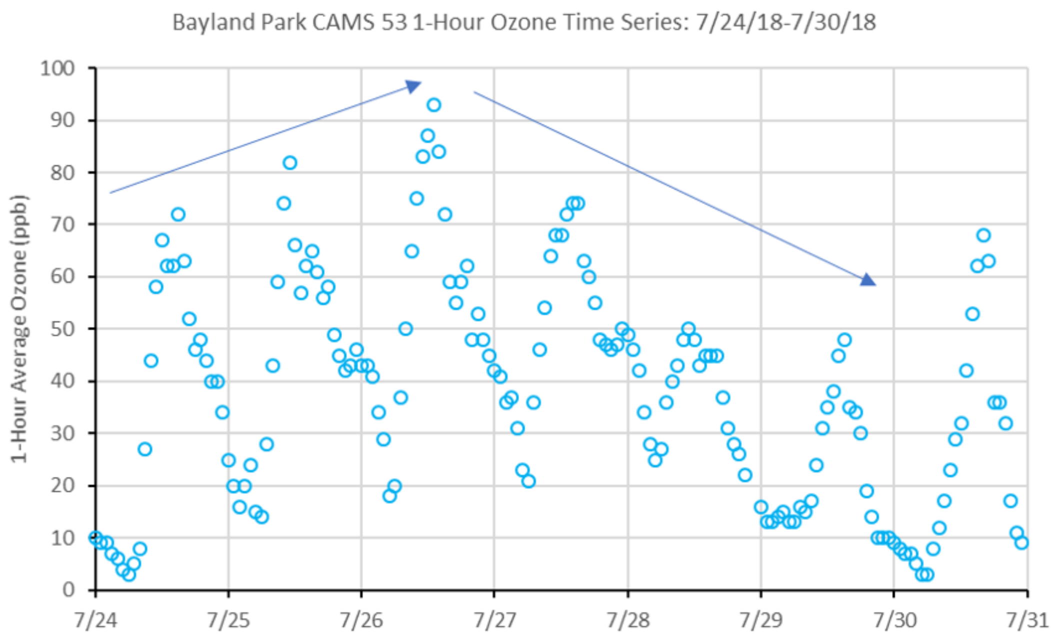

Figure 4-8. 1-hour ozone time series for Bayland Park CAMS 53 for July 24-31, 2018.

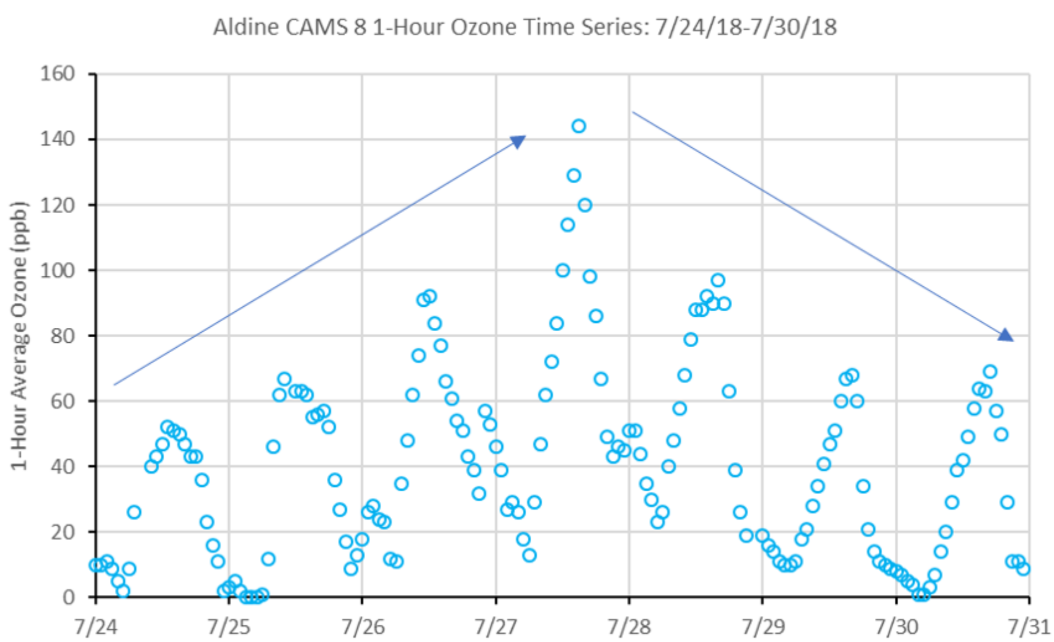

Figure 4-9. 1-hour ozone time series for Aldine CAMS 8 for July 24-31, 2018.

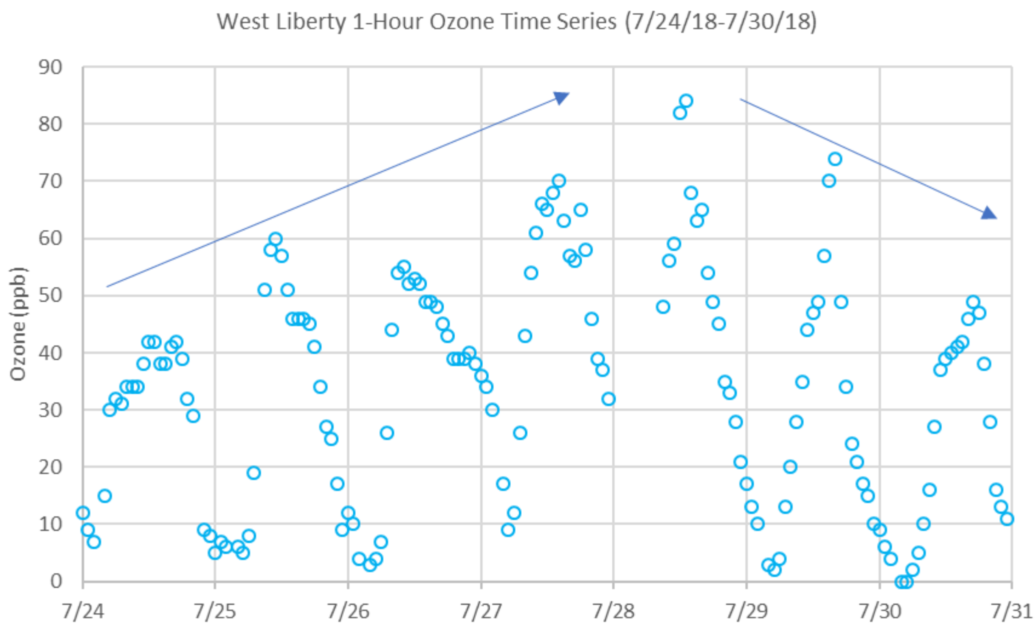

Figure 4-10. 1-hour ozone time series for West Liberty CAMS 699 for July 24-31, 2018.

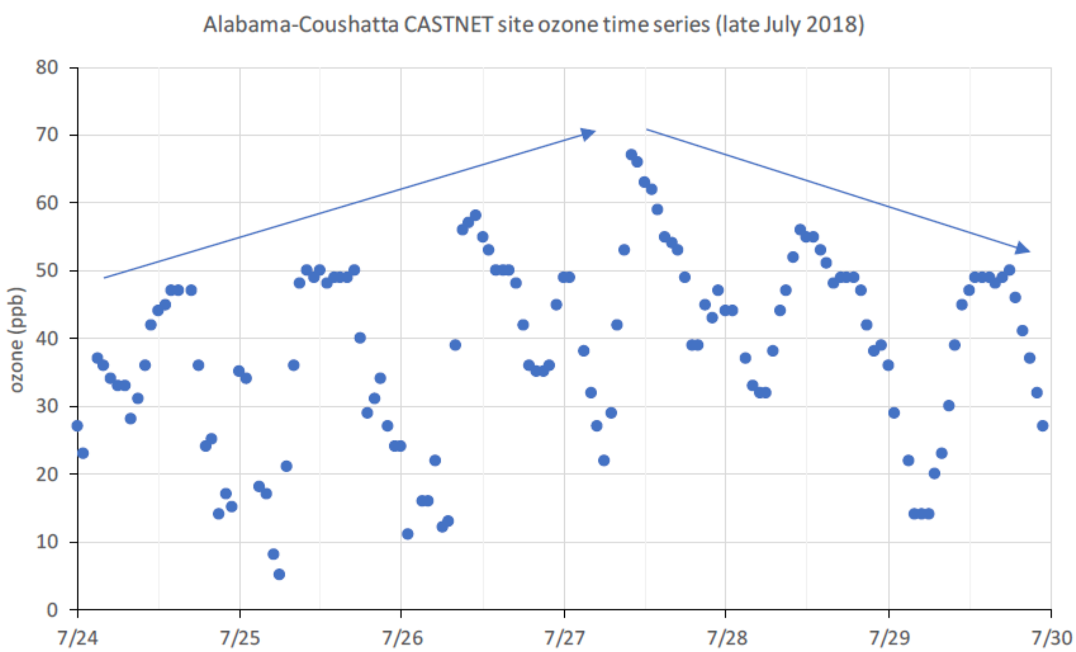

Figure 4-11. 1-hour ozone time series for the Alabama-Coushatta CASTNET site for July 24-30, 2018.

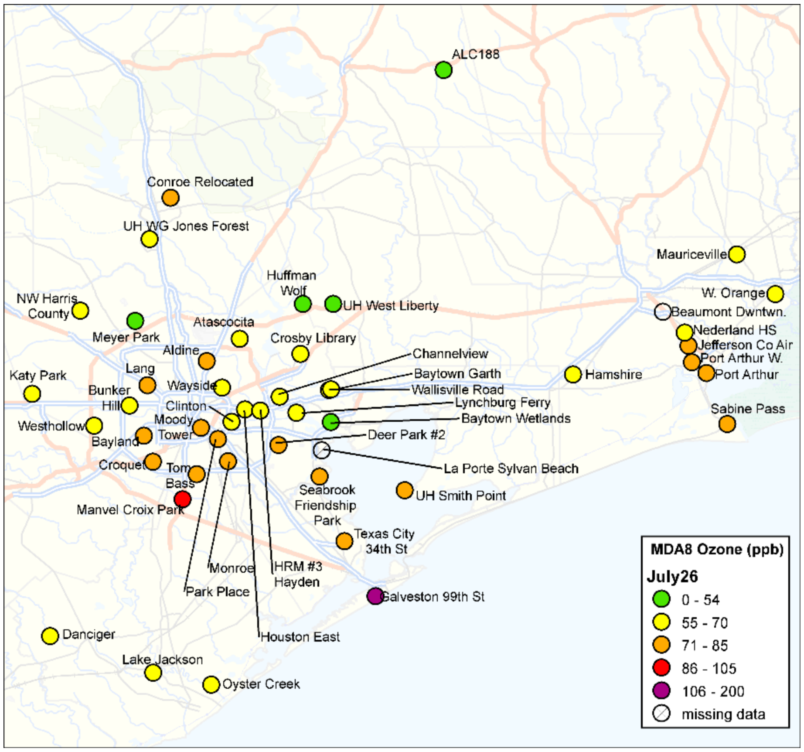

Figure 4-12. July 26, 2018 MDA8 ozone for Houston CAMS and the Alabama-Coushatta CASTNET site (ALC188).

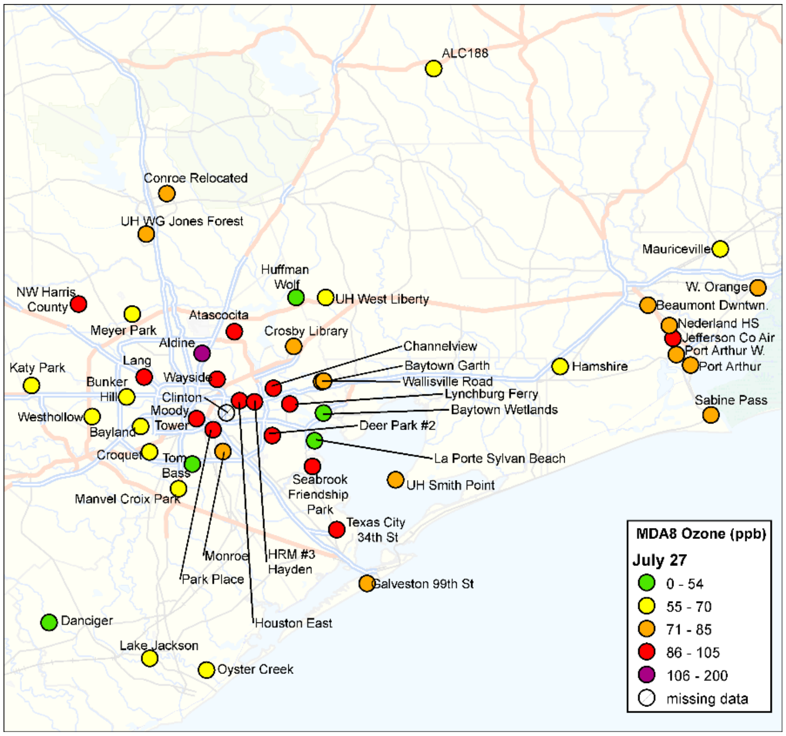

Figure 4-13. July 27, 2018 MDA8 ozone for Houston CAMS and the Alabama-Coushatta CASTNET site (ALC188).

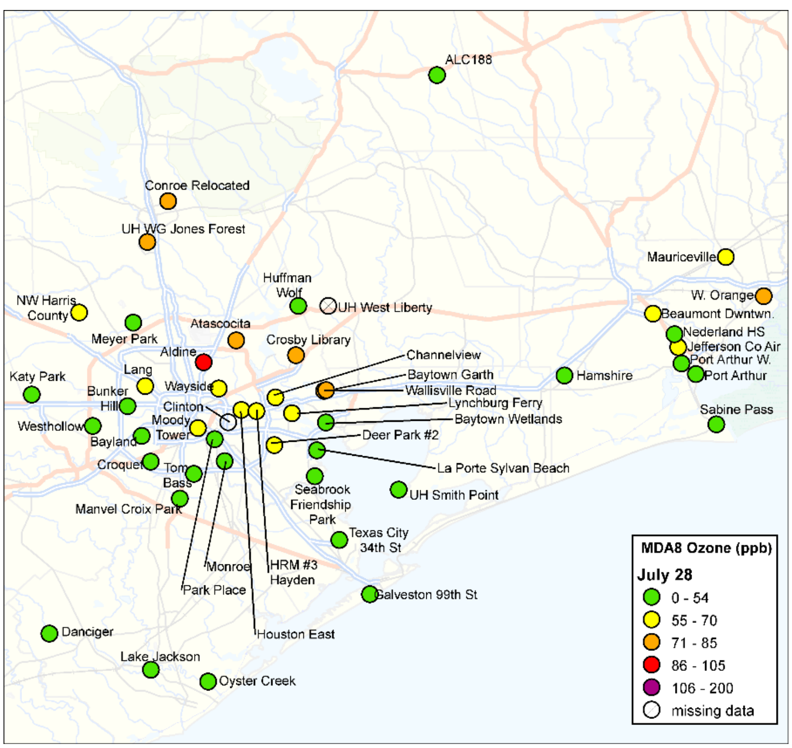

Figure 4-14. July 28, 2018 MDA8 ozone for Houston CAMS and the Alabama-Coushatta CASTNET site (ALC188).

4.1.3 Transport from Wildfires to Affected Monitors

A detailed evaluation of the potential for transport of ozone and precursors from the wildfires to Bayland Park CAMS 53 and Aldine CAMS 8 in Houston may be found in Section 5.3. Section 5.3 describes synoptic meteorological conditions relevant to transport and the route of the wildfire emissions to the Houston.

4.2 August 23-24, 2018 Conceptual Model

During August 2018, large wildfires were burning in California, Oregon, Washington and in the Canadian Provinces of British Columbia. A NASA press release noted: "*Fires have been breaking out all over the western United States due to weather conditions which favor fire outbreak and copious amounts of very dry fire fuel in timber, grasses, and underbrush. In Oregon there are 15 large ongoing fires and 231,278 acres have been burned*.

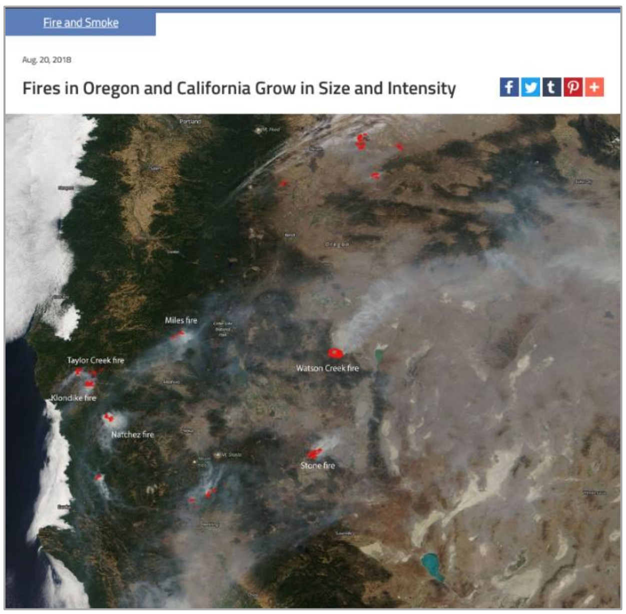

Figure 4-15. NASA satellite image of Oregon and California wildfires on August 20.

The satellite image above shows several of the larger fires in both Oregon as well as California. California has 10 large fires including the two largest to date, the Ferguson fire and the Mendocino Complex. California has seen 716,276 acres burned this year. In Oregon, the Taylor Creek and Klondike Fires are burning in the Rogue River-Siskiyou National Forest. Both fires were started by lightning on July 15. These two fires were split into zones on Saturday, Aug. 18. The fires are now referred to as "Taylor Creek and Klondike East Fires," …. As of the morning of Aug. 20, the Taylor Creek Fire is estimated 52,588 acres and is 79 percent contained. The Klondike Fire is estimated at 72,074 acres and is 28 percent contained. The Miles Fire is the new name for the fire previously named the Sugar Pine. The Miles Fire and Sugar Pine fire have merged. On Sunday July 15, lightning started hundreds of fires across Southwest Oregon. The Miles fire has currently affected 47,015 and is 38% contained at present. Today some instability will swing into the area with the threat of some isolated showers or a thunderstorm. Continued smoke in the valleys will moderate daytime temperatures but will also continue to affect air quality for local communities."[11]

The FINN fire emission inventory shows large emissions of ozone precursors from wildfire complexes burning in California, Oregon, Nevada and British Columbia during the days leading up to the August 23-24 high ozone days in Houston (Figure 4-16 and Figure 4-17). The regions of California, Oregon and Nevada where the fires occurred were experiencing abnormally or drought conditions in July, when the fires began (Figure 4-18).

[11] https://www.nasa.gov/image-feature/goddard/2018/fires-in-oregon-and-california-grow-in-size-and-intensity

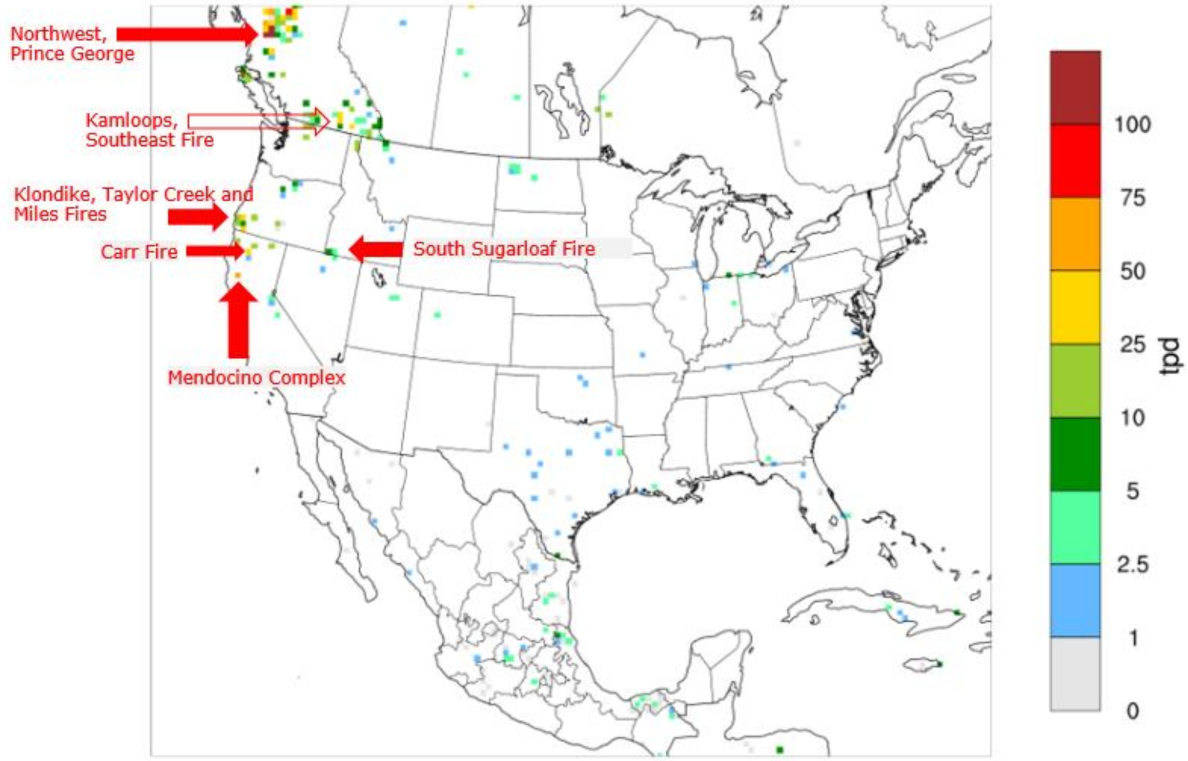

Figure 4-16. FINN fire NOx emissions (tpd) for August 18, 2018. Red arrows indicate large fire complexes determined to be upwind of Houston based on HYSPLIT back trajectory analysis.

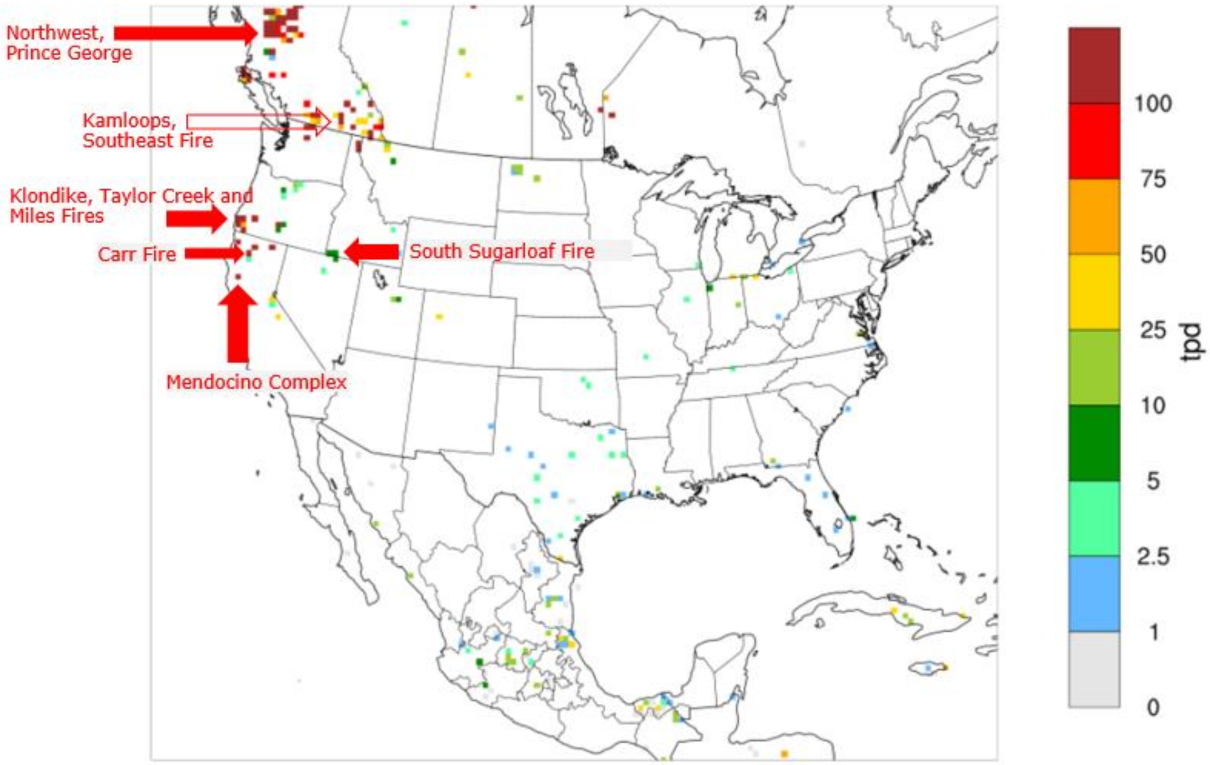

Figure 4-17. FINN fire VOC emissions (tpd) for August 18, 2018. Red arrows indicate large fire complexes determined to be upwind of Houston based on HYSPLIT back trajectory analysis.

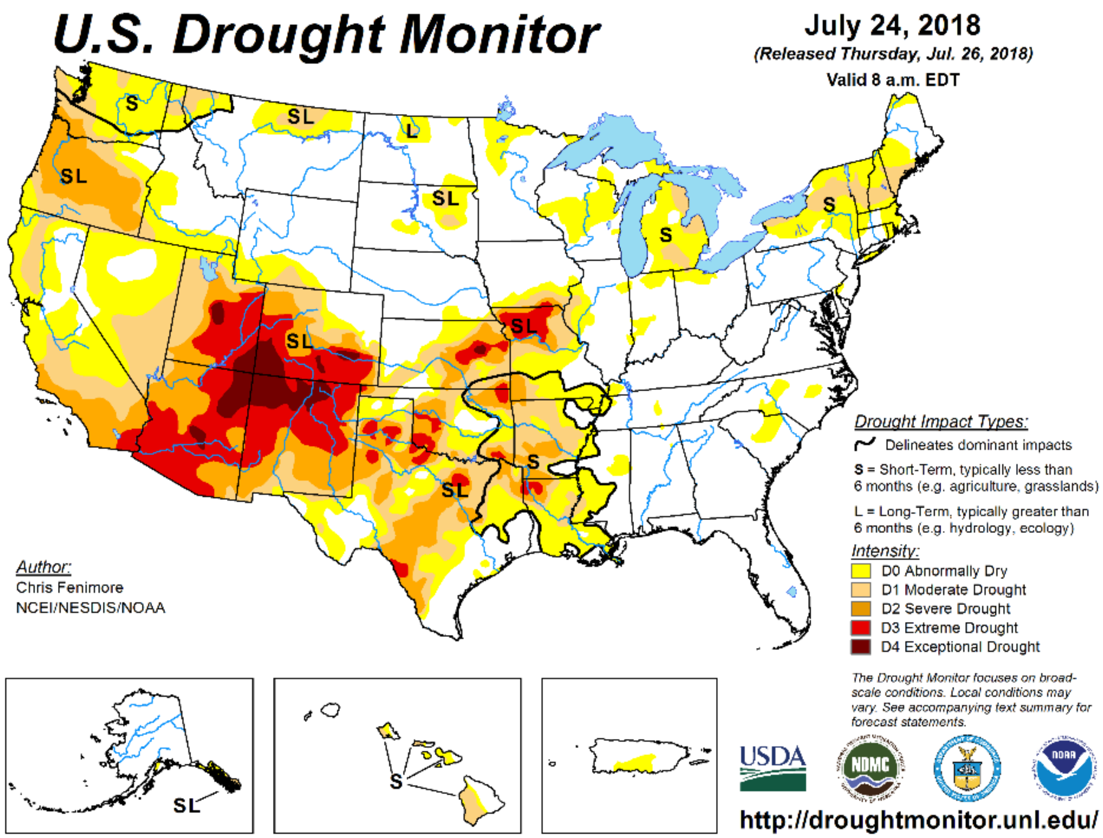

Figure 4-18. US Drought Monitor drought intensity plot for July 24, 2018.

Below, we describe the larger fires that were determined to be upwind of Houston during the week before the August 23-24 high ozone episode through the HYSPLIT back trajectory analysis described in Section 5.3.1. All burned area estimates and information on fire origins are taken from the InciWeb website (https://inciweb.nwcg.gov/).

4.2.1 Mendocino Complex, California

The Mendocino Complex started Friday July 27th, 2018. By the time it was 100% contained, the Mendocino Complex fires had burned 459,123 acres, making it the largest fire complex ever recorded in California. The Mendocino Complex consisted of two wildfires, the River Fire and Ranch Fire. The Ranch Fire was located about eight miles northeast of Ukiah, and the River Fire burned six miles north of Hopland, south of the larger Ranch Fire. Figure 4-19 shows a NASA press release describing the Mendocino Complex and a satellite image showing the fire plume.

Fire and Smoke

Aug. 21, 2018

California's Mendocino Complex Fire Still Ongoing

California's Mendocino Complex fire is still ongoing and recently turned the 400,000 (404,532) mark for acres burned. Huge columns of smoke still rise from the fire complex and the smoke that has risen and drifted now clouds the skies above the state. The fire is 74% contained.

Inciweb reports that the fire is now burning through portions of grass, timber litter, brush patches and dense timber stands. Fire activity is expected to increase in the afternoon hours after smoke clears the area. The fire growth has been moving north/northeast and east for the past several days. As westerly winds increase in the day, the fire will increase rate of spread to the east as it enters east/west aligned drainages. Fire activity will remain active into the evenings. Over 9 miles of firing occurred last night on the northern portion of the Ranch Fire. Firing operations will continue as weather conditions permit. The southern portion of the fire remains in patrol status as crews continue with suppression repair and mop up.

Figure 4-19. NASA press release on the Mendocino Complex fire[12].

4.2.2 Carr Fire, California

The Carr Fire started on Monday July 23rd, 2018 and burned in Shasta and Trinity Counties in California. By the time it was 100% contained, the Carr Fire had burned more than 229,651 acres. The fire was caused by the mechanical failure of a vehicle. Figure 4-20 is a USDA Forest Service Twitter post on the Carr Fire.

[12] https://www.nasa.gov/image-feature/goddard/2018/californias-mendocino-complex-fire-still-ongoing

https://twitter.com/forestservice/status/1029848987153653762

Figure 4-20. USDA Forest Service Twitter post on the Carr Fire.

4.2.3 Klondike, Taylor Creek and Miles Fires, Oregon

On Sunday July 15, lightning started hundreds of fires across Southwest Oregon. The Taylor Creek and Klondike Fires burned in the Rogue River-Siskiyou National Forest. Both fires were started by lightning on July 15, 2018 about 10 miles west of Grant's Pass. By the time the two fires were 100% contained, they had burned more than 52,839 acres.

The Miles Fire was originally known as the Sugar Pine. The Miles Fire and Sugar Pine fires merged and collectively burned more than 54,000 acres before 100% containment was achieved.

4.2.4 South Sugarloaf Complex, Nevada

The South Sugarloaf Complex started Friday August 17th, 2018, 20 miles Southwest of Owyhee, Nevada. The fire was ignited by lightning. By the time it was 100% contained, the South Sugarloaf Complex fires had burned 233,462 acres.

Figure 4-21 shows a NOAA smoke forecast from August 20. The modeled smoke plume extends from the region of the western US containing the fires described above and stretches southeast across the US toward Texas. By August 21, smoke from the fires was visible over Texas in satellite imagery as seen in a Twitter post from the Austin/San Antonio National Weather Service Office (Figure 4-22).

Figure 4-21. NOAA HRRR-smoke forecast for August 20, 2018 showing a smoke plume extending from western wildfires southeast toward Texas[13].

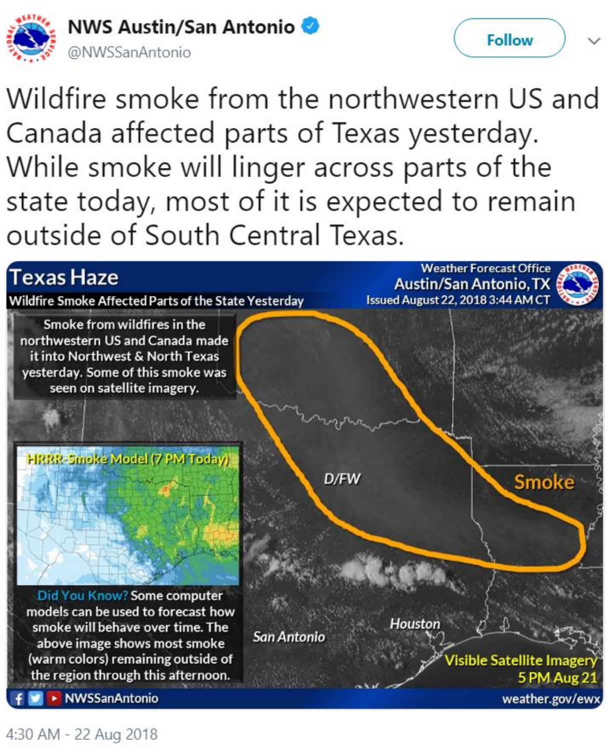

Figure 4-22. National Weather Service discussion of smoke transported from distant wildfires in western US arriving in Texas on August 21, 2018.

[13] https://www.nasa.gov/sites/default/files/thumbnails/image/hrrsmoke-map.jpg

4.2.5 Affected Monitors

During late August 2018, the Houston area experienced a multi-day period of high ozone. Ozone values rose between August 21-24 and then fell from August 24-29. Figure 4-24 and Figure 4-23 display 1-hour average ozone time series for Aldine CAMS 8 and Bayland Park CAMS 53 that show the diurnal cycle of ozone superposed on the multi-day rise and fall consistent with an episode of polluted continental air arriving in Texas and then dissipating. Figure 4-25 and Figure 4-26 are similar time series for West Liberty CAMS 699 and the Alabama Coushatta CASTNET site, which are located outside Houston and serve as upwind background monitors for air travelling south from the continental US into the Houston area. These monitors show rising and falling trends similar to Aldine CAMS 8 and Bayland Park CAMS 53, consistent with a regional ozone episode influenced by the arrival of polluted continental air with high levels of background ozone.

On August 23, Bayland Park CAMS 53 monitored an MDA8 ozone value of 82 ppb and reached a peak 1-hour ozone value of 112 ppb at 15:00 CST (Figure 4-23). Higher values of MDA8 ozone were measured elsewhere in Houston on August 23 (Figure 4-27). UH Moody Tower CAMS 695 had an MDA8 ozone of 100 ppb on August 23. On August 24, the MDA8 at Aldine CAMS 8 was 91 ppb. This was the highest value of the MDA8 in the Houston area on August 24 (Figure 4-28) and peak 1-hour average ozone was 106 ppb at 15:00 CST (Figure 4-24). August 23 and 24 exceeded the 99th percentile of values for CAMS 53 and CAMS 8, respectively for 2014-2018 for both the full year and April-October periods. By August 25, the ozone episode had begun to subside and MDA8 ozone at Aldine was 86 ppb and the peak 1-hour ozone was 97 ppb at 16:00 CST.

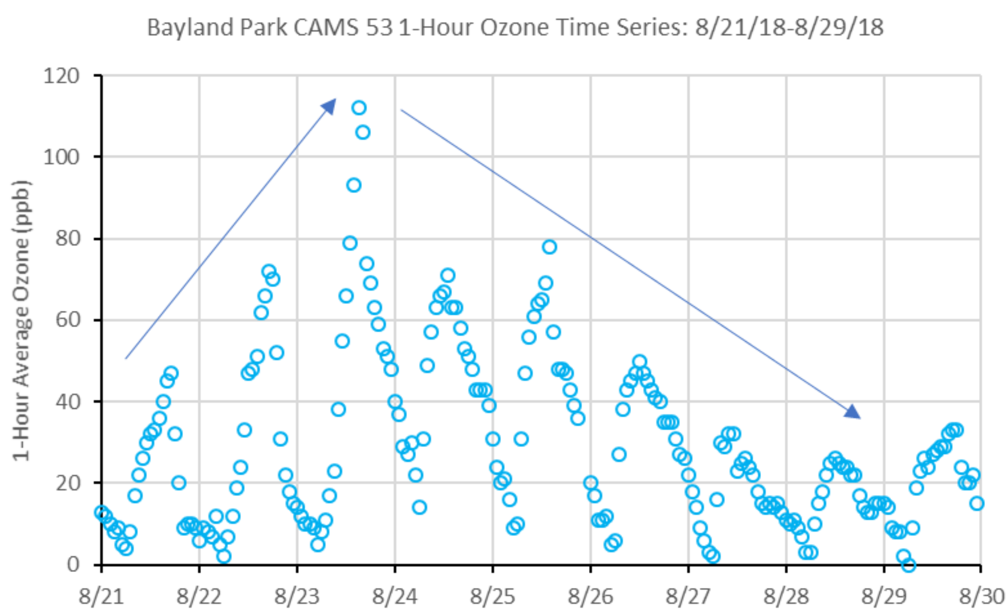

Figure 4-23. 1-hour ozone time series for Bayland Park CAMS 53 for August 21-30, 2018.

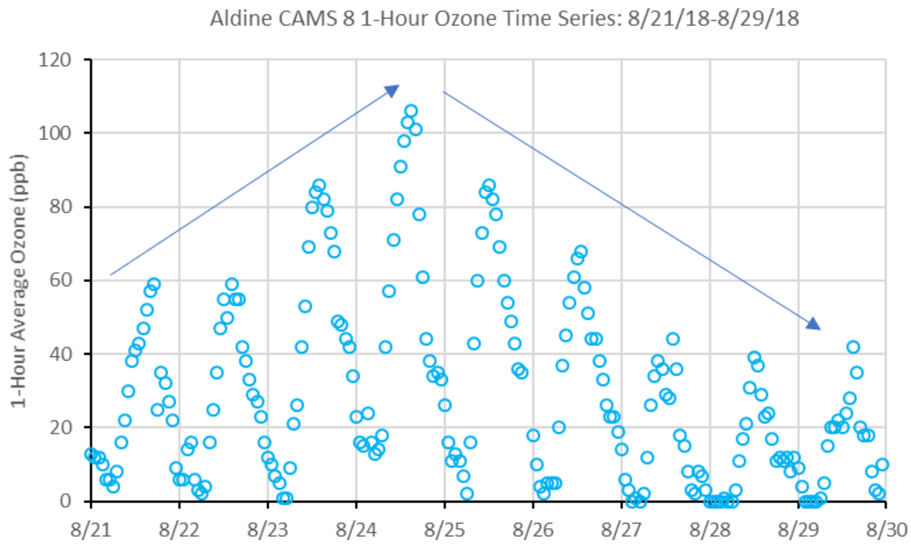

Figure 4-24. 1-hour ozone time series for Aldine CAMS 8 for August 21-30, 2018.

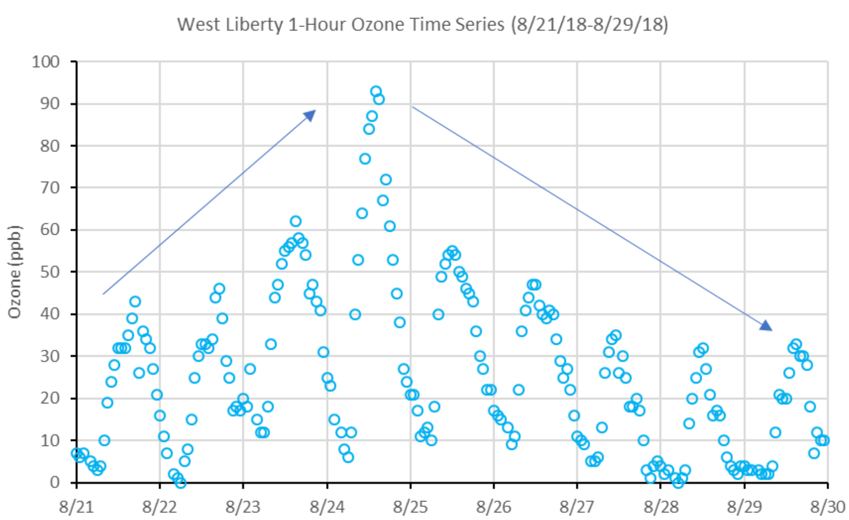

Figure 4-25. 1-hour ozone time series for West Liberty CAMS 699 for August 21-30, 2018.

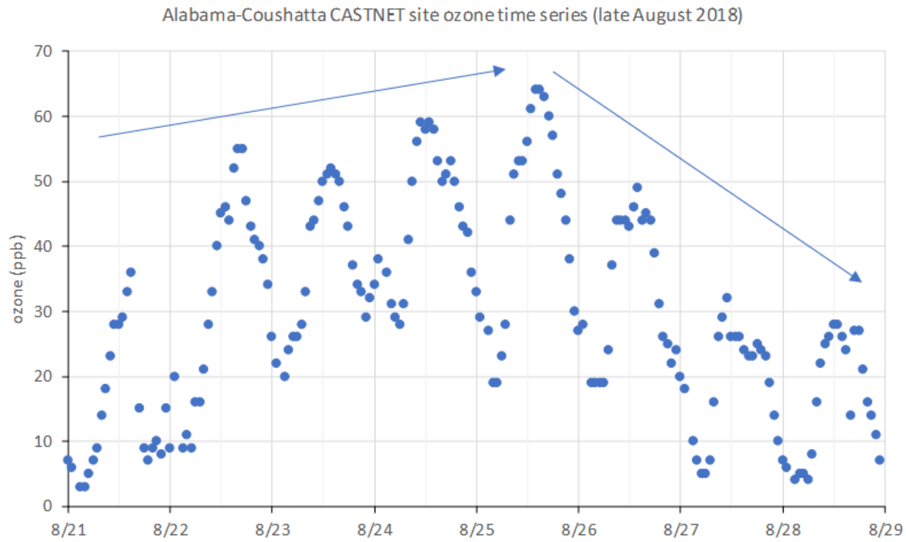

Figure 4-26. 1-hour ozone time series for the Alabama-Coushatta CASTNET site for August 21-29, 2018.

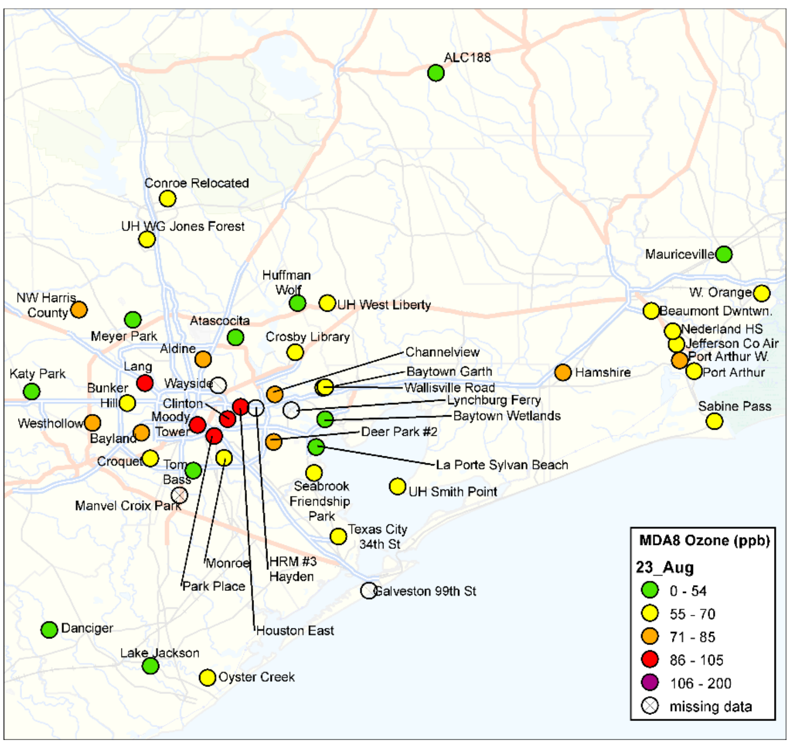

Figure 4-27. August 23, 2018 MDA8 ozone for Houston CAMS and the Alabama-Coushatta CASTNET site (ALC188).

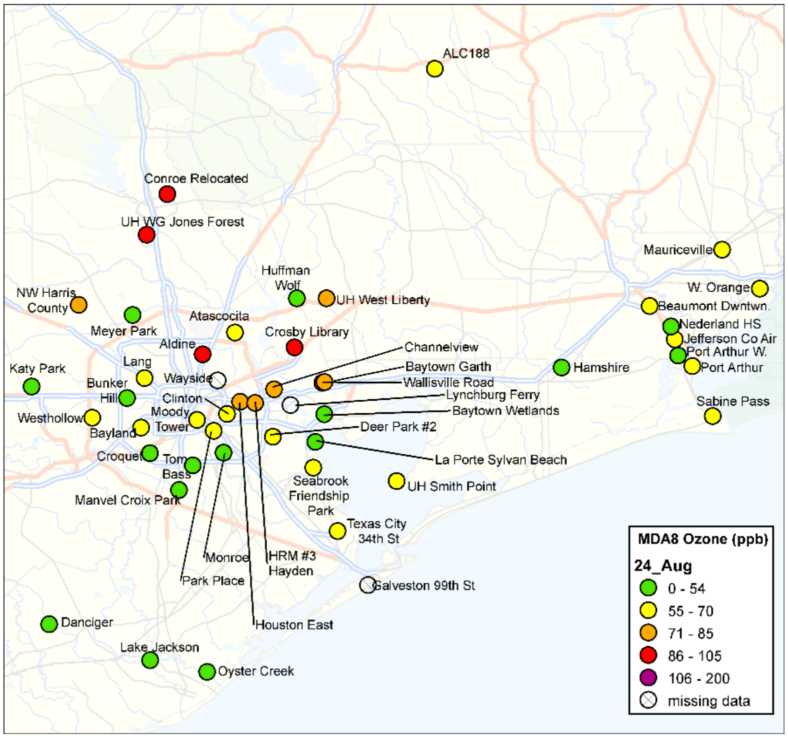

Figure 4-28. August 24, 2018 MDA8 ozone for Houston CAMS and the Alabama-Coushatta CASTNET site (ALC188).

4.2.6 Transport from Wildfires to Affected Monitors

A detailed evaluation of the potential for transport of ozone and precursors from the wildfires to Bayland Park CAMS 53 and Aldine CAMS 8 in Houston may be found in Section 5.3. Section 5.3 describes synoptic meteorological conditions relevant to transport and the route of the wildfire emissions to the Houston.

4.3 Comparison of Conceptual Model of Ozone in Houston for Non-Event Days and the July and August Episodes

EPA (2016) recommends comparison of conditions during the wildfire-influenced event with the normal (non-event) [14] conceptual model that describes the key features of non-event high ozone episodes. If such a comparison shows that key air quality, meteorological, and emission features of the event differ in one or more significant ways from the non-event conceptional model, then the case for concluding that the event in question is exceptional is strengthened. In other words, if the high ozone concentrations observed during the event would not have been expected based on the conceptual understanding of the conditions usually associated with high ozone episodes at the location(s) of interest, then the event is more likely to have been caused by atypical conditions.

TCEQ (2009) provides a detailed description of the non-event conceptual model of high ozone episodes in the HGB nonattainment area. In this section, we evaluate conditions during the 2018 high

[14] EPA's guidance refers to the "non-event" conceptual model to distinguish it from the conceptual model advanced to explain the exceptional events being analyzed as required under the guidance.

ozone target days (July 26-28 and August 23-24) within the context of the TCEQ's conceptual model. According to the TCEQ's conceptual model, HGB ozone episodes typically feature:

1. Minimal or weak synoptic-scale surface pressure gradients with little or slow movement of surface or upper-air weather features
2. Subsidence aloft leading to low mixing heights and delayed onset of any convective activity until late afternoon
3. A diurnal land/sea breeze regime, frequently with a convergence zone (sea breeze front) located over Galveston Bay. Features of this diurnal wind regime include:
   (a) Flat synoptic-scale pressure gradients which allow local thermal (i.e., land/ocean surface temperature contrasts) and Coriolis (inertial) forcing to dominate the circulation
   (b) A clockwise circular flow pattern with light winds from the W early in the morning shifting to NW and N shortly after sunrise, then turning through NE to E by around noon, then SE with increasing speeds until shortly before sunset before turning further towards S and slowing around midnight and then completing the turn back to W by early morning (Figure 4-29).

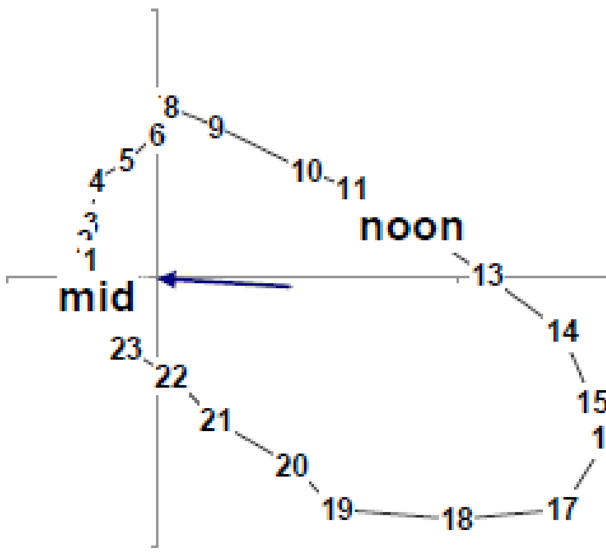

Figure 4-29. Idealized wind pattern on ozone episode days from the conceptual model (TCEQ, 2009). Hourly resultant wind direction and speeds: each hourly wind vector points to the axis origins from the blue dot plotted for each hour with time (CST) indicated by the blue numbers; speed (mph) is indicated by the distance from the origin to the hour marker.

4. Day-to-day variations in the relative strength of synoptic-scale and thermal forcing relative to the inertial forcing leads to three categories of surface diurnal wind patterns associated with ozone episodes ranging from a relatively abrupt mid-day reversal in direction from NW to SE (with an associated coastal convergence zone) to a more gradual clockwise turning of the wind direction as shown in Figure 4-30.
5. Under otherwise approximately similar conditions, high ozone days tend to have lighter afternoon SE sea breezes preceded by light morning winds first from the NW and then NE and E whereas low ozone days tend to have stronger afternoon SE sea breezes starting

earlier in the morning and lasting well into the evening, thus limiting the degree of recirculation of emissions and ozone within the HGB area.

6. Ozone formation within the HGB area is driven by numerous large and small NOx sources from stationary (industrial) and mobile sources combined with anthropogenic VOC emissions from petrochemical complexes which have been observed to include highly reactive VOCs (HRVOCs) such as ethene and propene. Some VOC and HRVOC emissions (e.g., those associated with startups, shutdowns, and upset events) can be highly intermittent leading to localized formation of very high ozone concentrations downwind of the releases.

Figure 4-30. Three categories of diurnal wind reversals (curved white arrows) and associated ozone and precursor emissions transport included in the HGB conceptual model (source: TCEQ, 2009).

Transport of ozone and precursors from upwind sources can contribute to ozone episodes in HGB. Sullivan (2009) presents an analysis of the relationship between HGB ozone concentrations and the directional patterns of 72-hour air parcel back trajectories 300 m AGL over central Houston at 12:00 CST calculated from the HYSPLIT model for all days 2000 – 2007 during the HGB ozone season (May – October). Sullivan applied a clustering algorithm to the trajectory patterns and derived six clusters (excluding a few outliers) as shown in Figure 4-31 and computed the average over days in each cluster of the MDA8 ozone concentration over all HGB monitoring sites (Figure 4-32). On average, the lowest ozone concentrations are associated with trajectories arriving from out over the Gulf of Mexico (ESE and SE trajectory clusters) while the highest are associated with short trajectories located over east Texas and southern Louisiana (indicative of stagnant, recirculating flows). A small number (12%) of trajectories were directed towards the northeast (NE), roughly along the Mississippi River Valley as far as Illinois and another small group (3%) were directed towards the north (N) extending as far as North Dakota. Mean MDA8 ozone concentrations are highest under the Short and NE trajectories and significantly lower under the N trajectories which differ from the NE trajectories by higher average transport distances and a path that lies further to the west with less of an easterly fetch near Houston. The N trajectories are most consistent with transport of wildfire emissions from the northwest U.S. and western Canada to Houston when fires are burning in those areas. Thus, trajectories that would be most likely to transport emissions from large western wildfires to Houston <u>when fires are present</u> are actually associated with lower ozone in Houston <u>on average</u>, suggesting that the occasional high ozone events in Houston associated with N type trajectories may be due to transport of emissions from major western wildfires. Of course, wildfires may also contribute to high ozone events under the Short or NE trajectories, but such events would be harder to identify given the relatively high average ozone concentrations observed in connection with these two trajectory patterns.

Comparison of 5-day back trajectories on the July and August 2018 episode days (Figure 4-33; Figure 4-34) with the 3-day back trajectory pattern clusters in Figure 4-31 and the mean trajectory paths within each cluster (see Sullivan, 2009 Figure 6.15) indicates that July 26 and July 27 are most similar to the NE cluster. July 28 is between the Short cluster pattern and the NE cluster patter. August 23 is similar to the NE cluster for the lowest (200 m) trajectory (which is closest to the 300 m starting height used in Sullivan's trajectory cluster) but hard to classify due to the widely divergent trajectory paths from the three different starting heights, and August 24 is most similar to the Short pattern over the first three days, after which it recurves further back to the northwest similar to the N trajectory cluster. Both July 28 and August 24 back trajectories loop southeast over the Gulf near Houston which is not an obvious feature of the NE or N clusters but is consistent with the Short cluster. Thus, none of the episode days can be clearly associated with the N cluster pattern, thus making it more difficult to conclude that the high ozone values on these days are atypical relative to the overall low ozone characteristic of N cluster events.

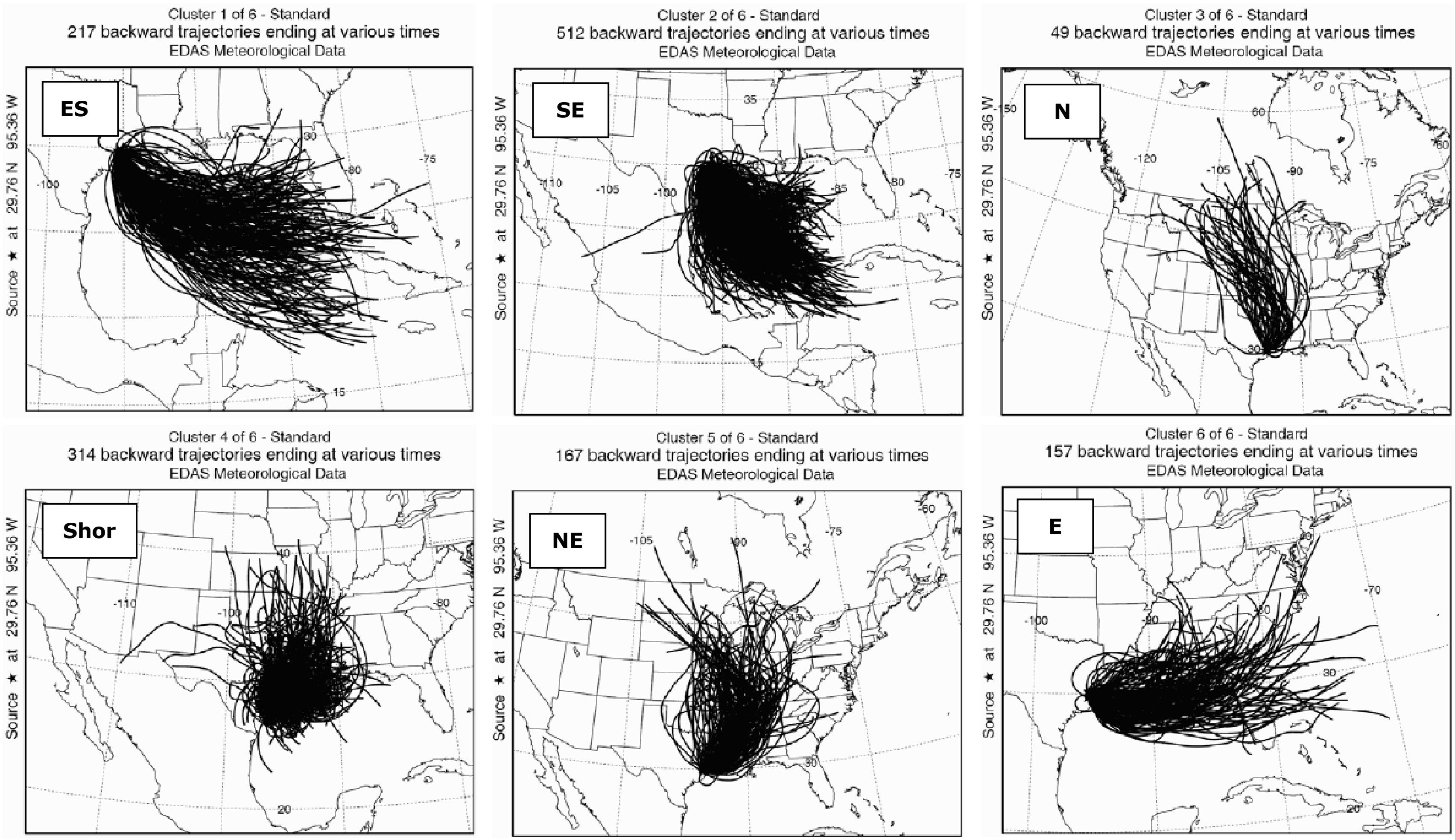

Figure 4-31. Results of cluster analysis of patterns of 72-hour HYSPLIT back trajectories starting 12:00 CST at 300 m AGL over central Houston for all days May – October 2000 – 2007 (Sullivan, 2009; figure adapted from TCEQ, 2009).

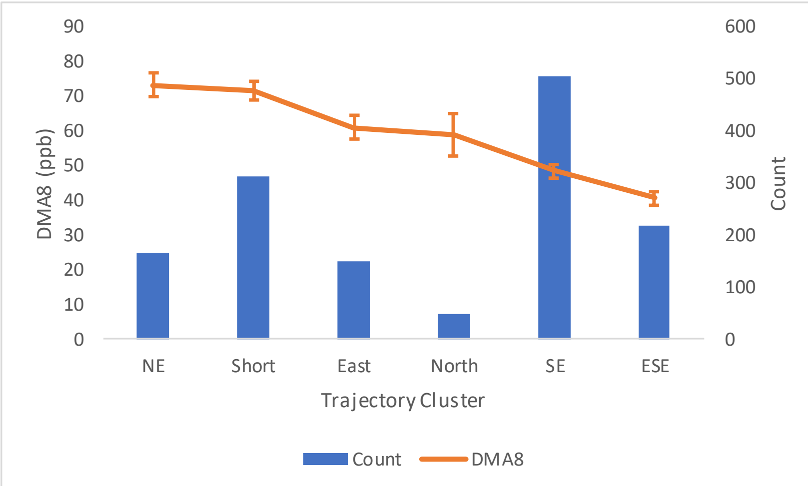

Figure 4-32. Average of daily maximum 8-hour average (MDA8) ozone concentrations over HGB monitoring sites by trajectory clusters shown in Figure 4-31 with 95% confidence intervals; blue bars show number of trajectories in each cluster.

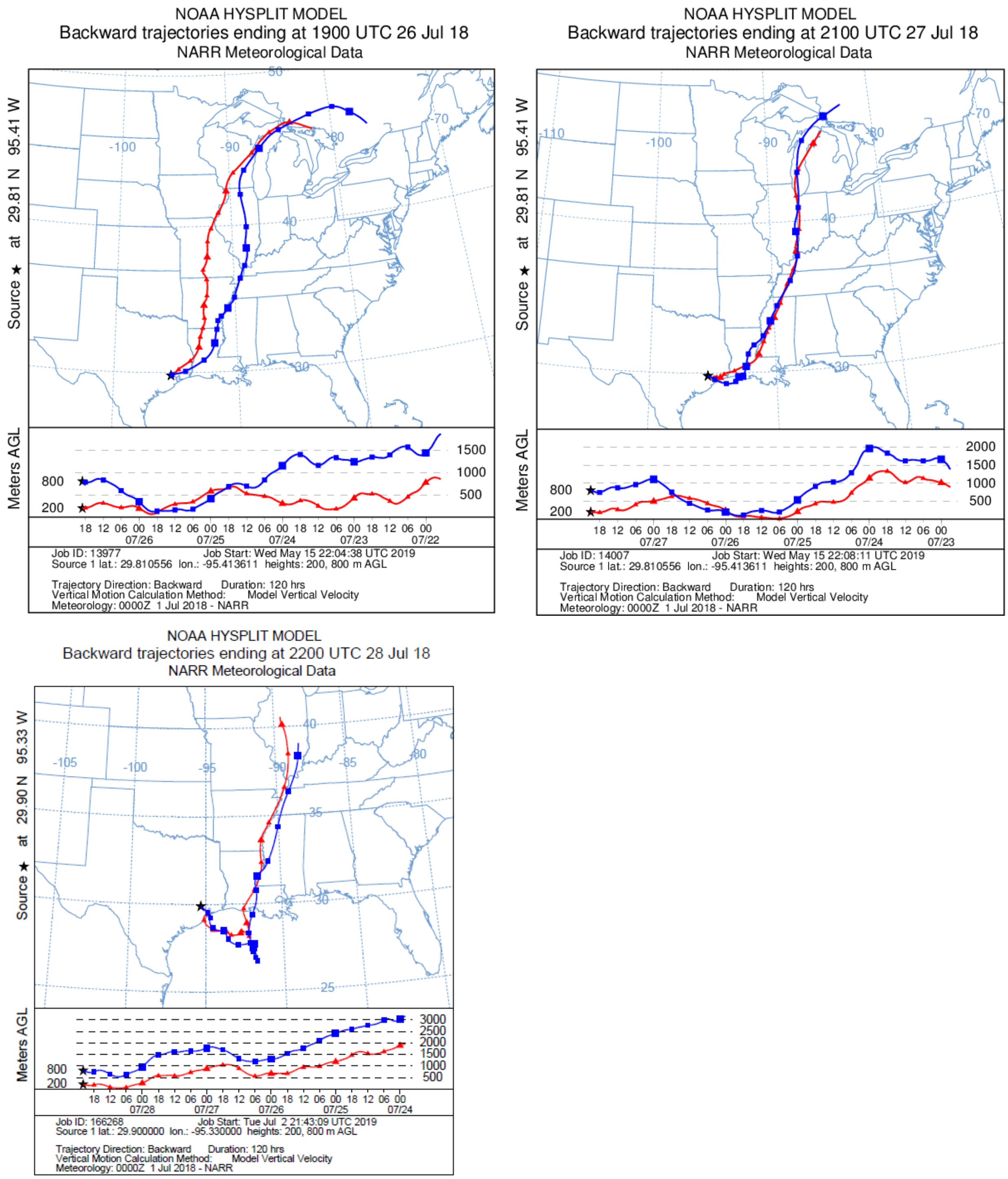

Figure 4-33. HYSPLIT 5-day back trajectories from Houston starting at 22:00 UTC for 26 and 27 July 2018 (top row) and starting at 22:00 UTC on 28 July 2018 (bottom row).

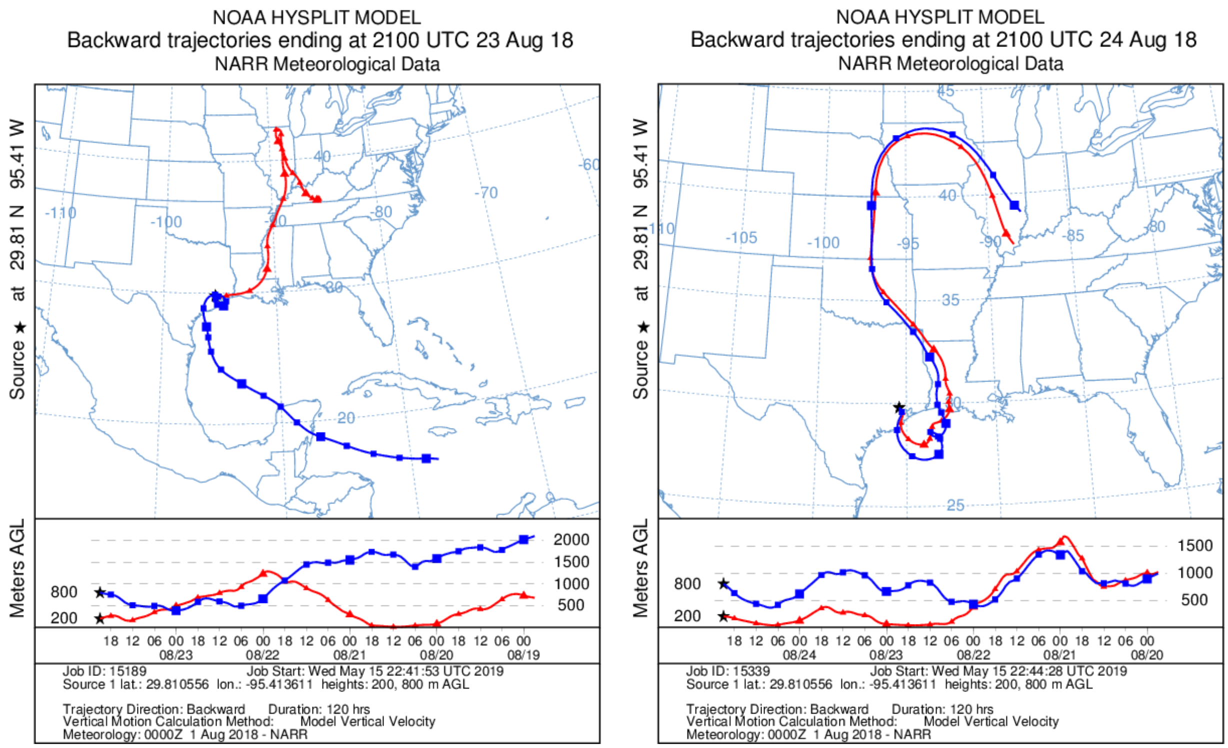

Figure 4-34. HYSPLIT 5-day back trajectories for 23 (top) and 24 (bottom) August starting at 19:00 UTC and 21:00 UTC.

4.4 Synoptic-Scale Weather Conditions on July and August 2018 Episode Days

Synoptic conditions on the five high ozone days are presented in Figure 5-155 through Figure 5-159. Surface and upper air conditions during these days are consistent with the HGB conceptual model with generally stagnant conditions due to weak pressure gradients at the surface and aloft, weakly anti-cyclonic flow aloft, little morning cloud cover, and no measurable precipitation. True color satellite images show virtually no convective cloud cover at ~11:00 CST (Terra satellite overpasses) and relatively little mid-afternoon (~14:00 CST) cloud cover over most of HGB on 26 – 28 July, but much more extensive convective cloud cover on 23 – 24 August. Consistent with this, Houston area relative humidities were lower (57 – 67%) on the July days as compared to the August days (69 – 70%).

As the average relative humidity on the 27 days with MDA8 greater than 75[15] ppb at Aldine between 2014 – 2018 is 63% (also 63% for days with MDA8 greater than 75 ppb at Bayland Park), the August days are relatively humid for a high ozone day (89 – 95th percentile based on Aldine and 84 – 87th percentile based on Bayland Park), making them somewhat unusual in this respect. Similarly, daily average wind speeds at Aldine on the episode days range from 2.1 – 2.2 m/s corresponding to the 76 – 93d percentile of the 17 days with MDA8 > 75 ppb while for Bayland Park the corresponding

[15] 75 ppb was used as the threshold for a high 8-hour average ozone value in this analysis. On November 14, 2018, EPA published Federal Register notice that Houston-Galveston-Brazoria failed to attain the 2008 ozone NAAQS (75 ppb) making HGB a Serious nonattainment area for the 2008 standard. Therefore 75 is still an applicable design value in HGB and is the most recent standard that was in effect for most of the 2015 – 2018 period analyzed here (HGB's designation for the 70 ppb 2015 NAAQS occurred on August 3, 2018).

percentile range was 74 – 87th percentile, indicating that the episode days were also somewhat unusual for high ozone days in terms of wind speed.

4.5 Wind Patterns on July and August 2018 High Ozone Episode Days

Diurnal wind patterns for the five episode days in 2018 are shown in Figure 4-35 together with the idealized ozone episode wind pattern from the HGB conceptual model (TCEQ, 2009). Winds on the episode days generally follow the idealized clockwise inertial cycle from the conceptual model but with some variations. Bayland Park on July 26 and Aldine on July 27 differ from the other days and the conceptual model pattern in that northeast winds occurred during the afternoon hours (especially at Bayland Park on July 26). This wind direction is consistent with transport of wildfire-influenced air from Louisiana and the southeast. Of the 17 days with MDA8 greater than 75 ppb at Bayland Park between 2014 – 2018, July 26 is the only day with resultant afternoon (14:00 – 20:00 CST) wind from the northeast.

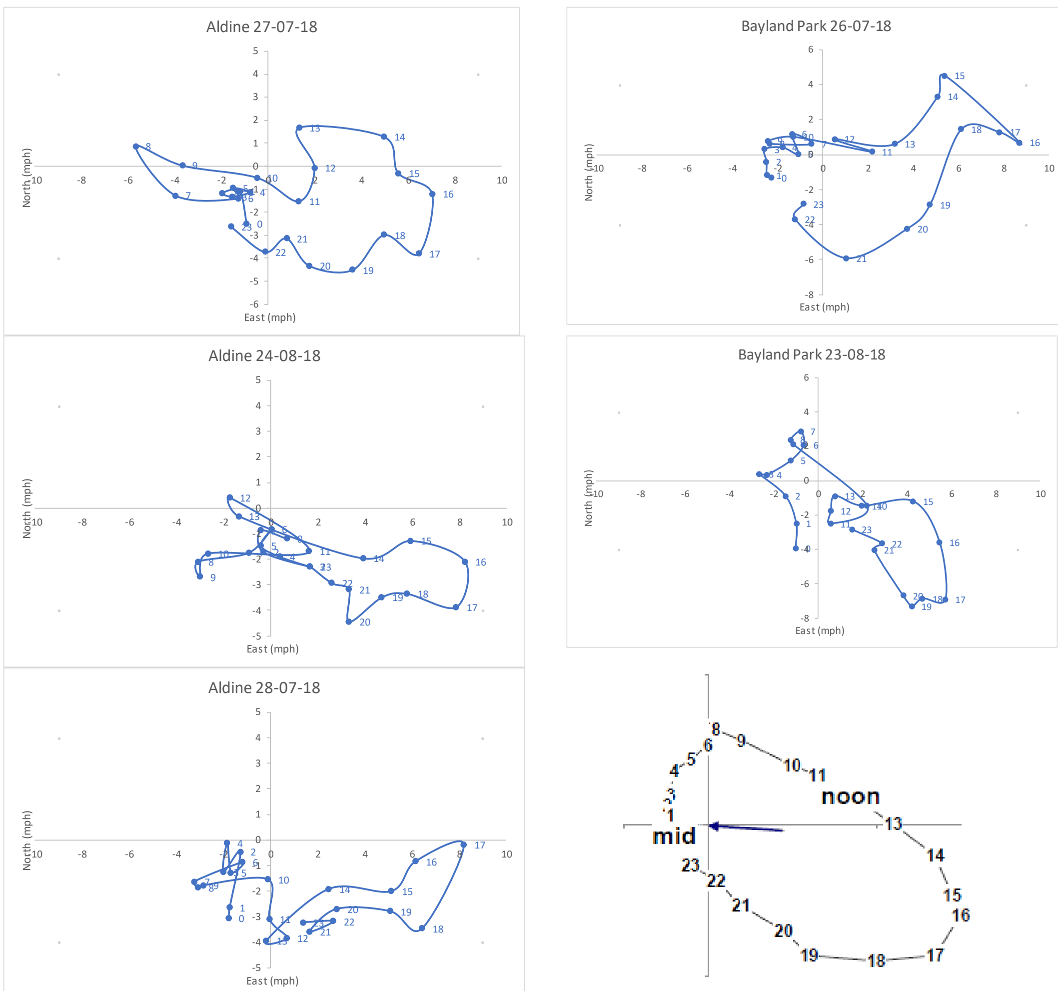

Figure 4-35. Hourly resultant wind direction and speeds: each hourly wind vector points to the axis origins from the blue dot plotted for each hour with time (CST) indicated by the blue numbers; speed (mph) is indicated by the distance from the origin to the hour marker. Idealized wind pattern on ozone episode days from the conceptual model (TCEQ, 2009) is shown at bottom right.

4.6 Diurnal Patterns

The diurnal pattern of ozone concentrations is strongly driven by sunlight, resulting in peak concentrations during the afternoon; therefore, significant departures from the usual pattern on non-event days would suggest an abnormal condition which might be indicative of an exceptional event.

In Figure 4-36, diurnal patterns of hourly average ozone at Aldine CAMS 8 on the episode days are compared with concentrations averaged over all June-August days with MDA8 greater than 75 ppb during 2010 – 2018. July 27 stands out as having an unusually sharp and high afternoon peak. The afternoon peak on July 28 does not fall outside the hourly +/- 1 standard deviation (SD) limits but has a later-than-average peak at 16:00 CST. Early morning (0:00 – 5:00 CST) concentrations on both July event days were unusually high. In contrast, ozone on August 24 was very close to the average throughout the day.

Diurnal patterns of hourly average ozone at Bayland Park CAMS 53 on the episode days are compared with concentrations averaged over all June-August days with MDA8 greater than 75 ppb during 2014 – 2018 in Figure 4-39. The diurnal pattern on July 26 differs from the average with higher concentrations before sunrise followed by a typical morning production rate which lessens at 13:00 when the wind speed picks up and shifts around to the NE (Figure 4-35). Morning concentrations are low on August 23 but increase through 15:00, resulting in a peak value at the high end of the range.

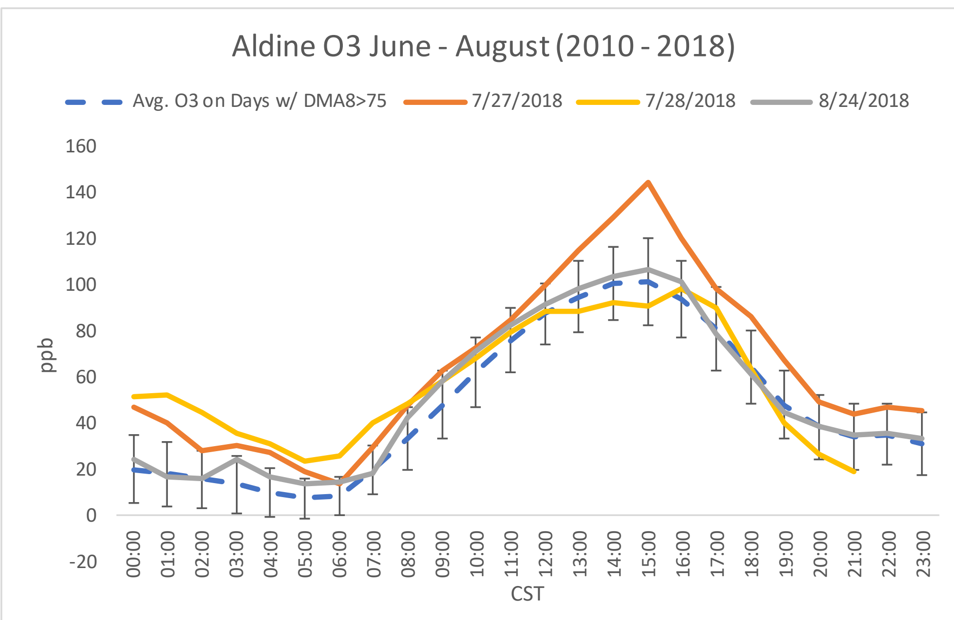

Figure 4-36. Hourly average ozone at Aldine on episode days and average over all days with MDA8 greater than 75 ppb during June – August 2010 – 2018 (error bars are +/- 1 SD).

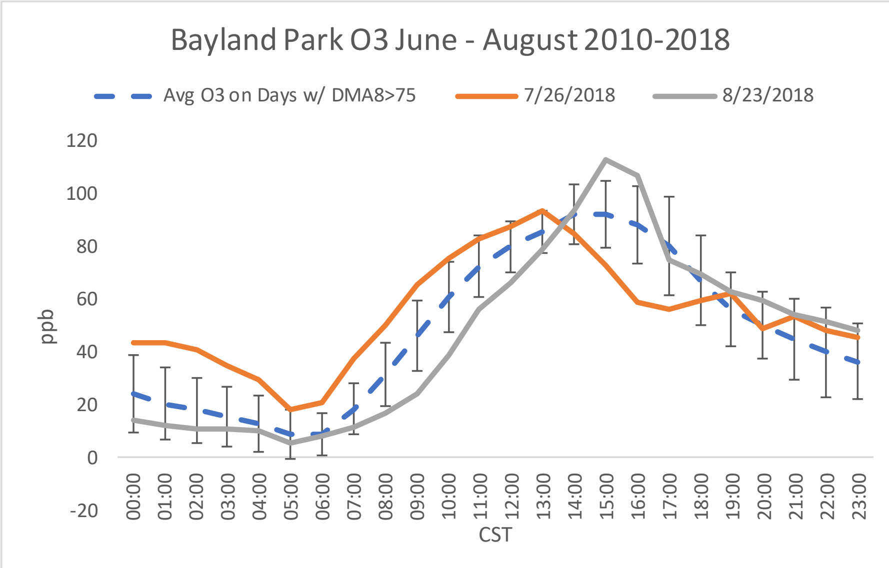

Figure 4-37. Hourly average ozone at Bayland Park on target days and average over all days with MDA8 greater than 75 ppb during June – August 2010 – 2018 (error bars are +/- 1 SD).

4.7 Spatial Patterns

Examination of MDA8 values on the episode days (Figure 4-12 through Figure 4-28) shows that August 24 had high concentrations northwest and well north of downtown Houston and low concentrations in the eastern, southern, and western areas. The spatial pattern on July 28 is similar to August 24. High values were also seen in some of the same locations on July 27 (Figure 4-13) but also occurred to the east and southeast of downtown Houston.

A more detailed look at site-to-site differences in MDA8 values on the episode days as compared to all days on which one or more HGB monitors exceeded 75 ppb (HGB exceedance days) is provided in Figure 4-38 and Figure 4-39. These figures show the rank percentile (quantile) of the MDA8 ozone value on each episode day within the distribution of all MDA8 values at that site on HGB exceedance days. Thus, a quantile close to 1 indicates that the MDA8 value on the target day was unusually high at that monitoring site compared to all days when MDA8 exceeded 75 ppb somewhere in the HGB area. Conversely, a value close to 0 indicates that the MDA8 value was unusually low for an HGB exceedance day. Very high or very low quantiles are a measure of how unusual conditions on the target day were compared to most HGB exceedance days. These results are based on all days during 2014 – 2018 on which one or more HGB monitors recorded an MDA8 ozone value greater than 75 ppb (a total of 106 days). Monitoring sites with more than 11 missing MDA8 values (i.e., about 10% of the 106 days) were excluded from the analysis. The spatial distribution of quantiles for HGB CAMS is shown in Figure 4-40.

Figure 4-38 shows that July 27 is characterized by unusually high ozone at many sites in addition to Aldine CAMS 8. In fact, MDA8 values were above the median at all but one site, with 16 of 27 sites above the 90th percentile. MDA8 values on the Aldine July 28 high ozone day exhibited a wide range with three sites above the 90th percentile (WG Jones Forest CAMS 698, Conroe CAMS 78, Atascocita

CAMS 560) and seven below the 10th percentile and the rest in between. The defining feature of the August 24, 2018 is that five sites including Aldine CAMS 8 had MDA8 values in the 90th percentile; the other sites are: WG Jones Forest CAMS 698, Baytown Garth CAMS 1017, Wallisville Road CAMS 617, and Conroe CAMS 78, all located north and east of downtown Houston. Thus, while MDA8 values on July 27 do not seem to have any obvious unusual spatial features, July 28 was unusual in that sites to the north of downtown Houston had unusually high values (and Aldine CAMS 8 was at the 86th percentile) whereas many others were unusually low. August 24 was unusual in that sites to the north and east of Houston had unusually high values whereas many other sites (13 in all) had values below the median.

Figure 4-39 shows that MDA8 values on July 26 (high ozone at Bayland Park) were above the median at all but two sites (Houston North Wayside and Meyer Park) with values above the 90th percentile at seven sites (but not at Bayland Park). MDA8 values on August 23 days were above the 90th percentile at six sites (including Bayland Park) with the highest quantiles at Moody Tower, Park Place, and Clinton. Based on these results, neither July 26 or August 23 appear to have any significantly unusual spatial features.

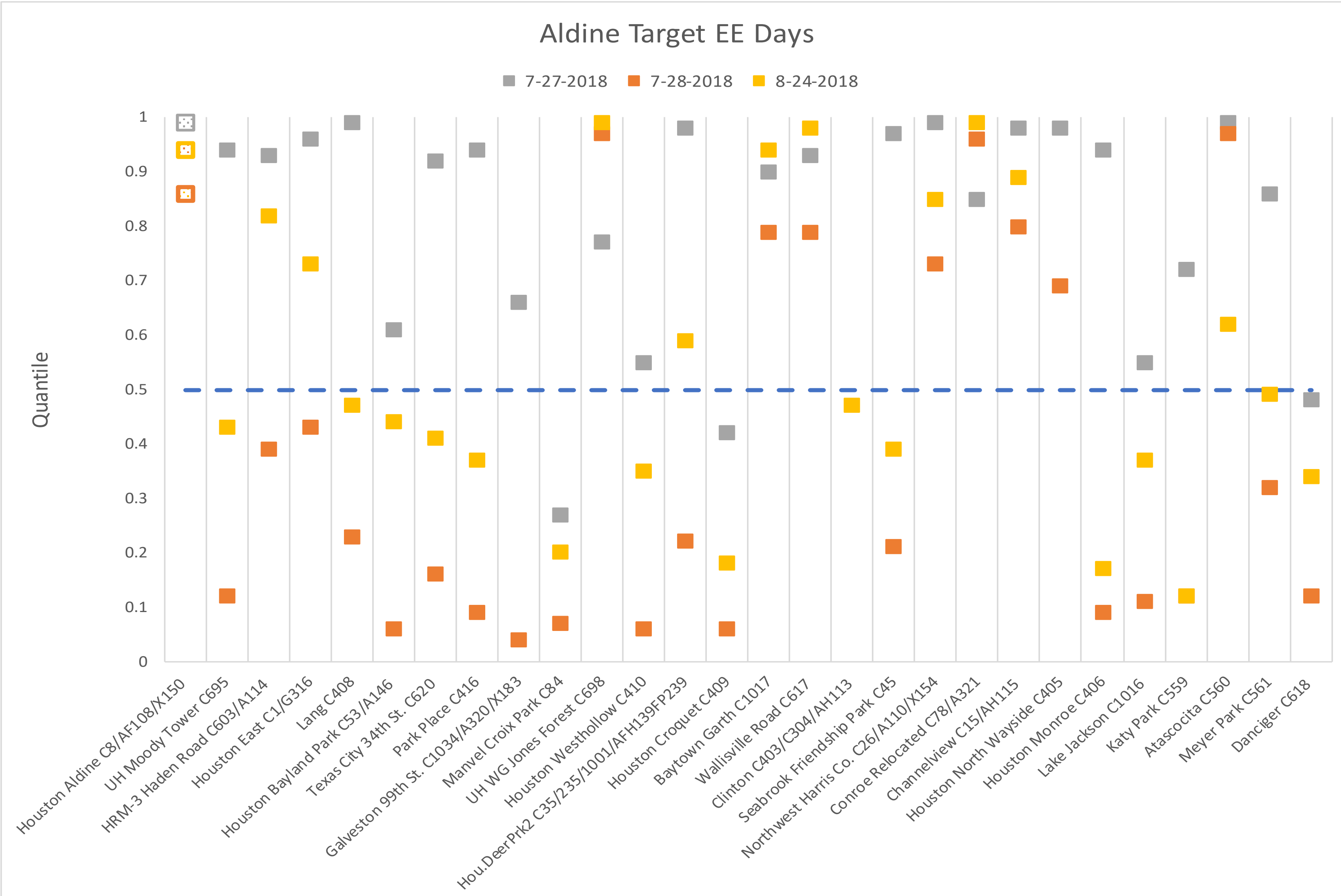

Figure 4-38. Quantiles of MDA8 ozone on high ozone episode days at Aldine relative to all days (May-October 2014-2018) with MDA8 greater than 75 ppb at any HGB monitoring site.

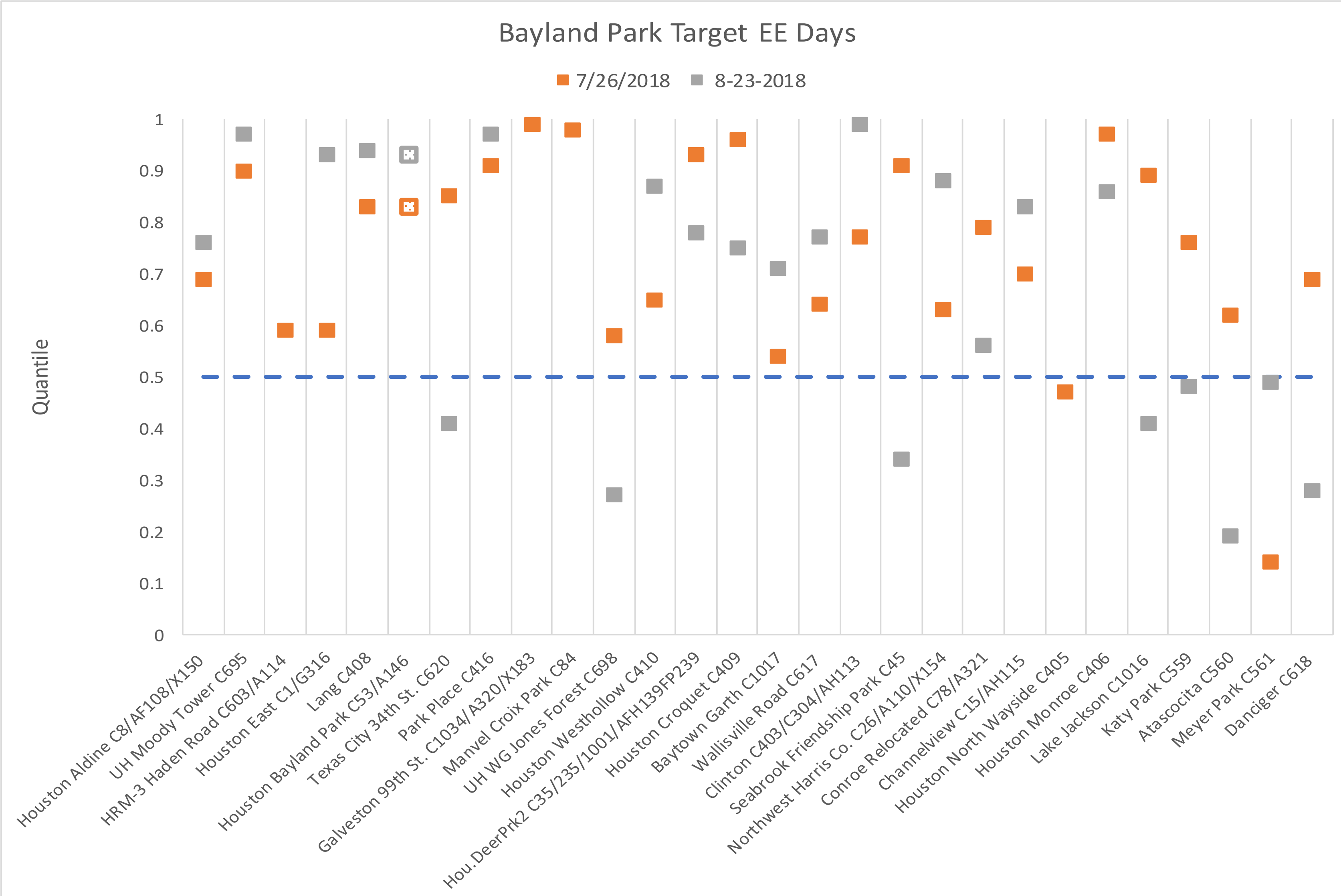

Figure 4-39. Quantiles of MDA8 ozone on episode days at Bayland Park relative to all days (May- October 2014-2018) with MDA8 greater than 75 ppb at any HGB monitoring site.

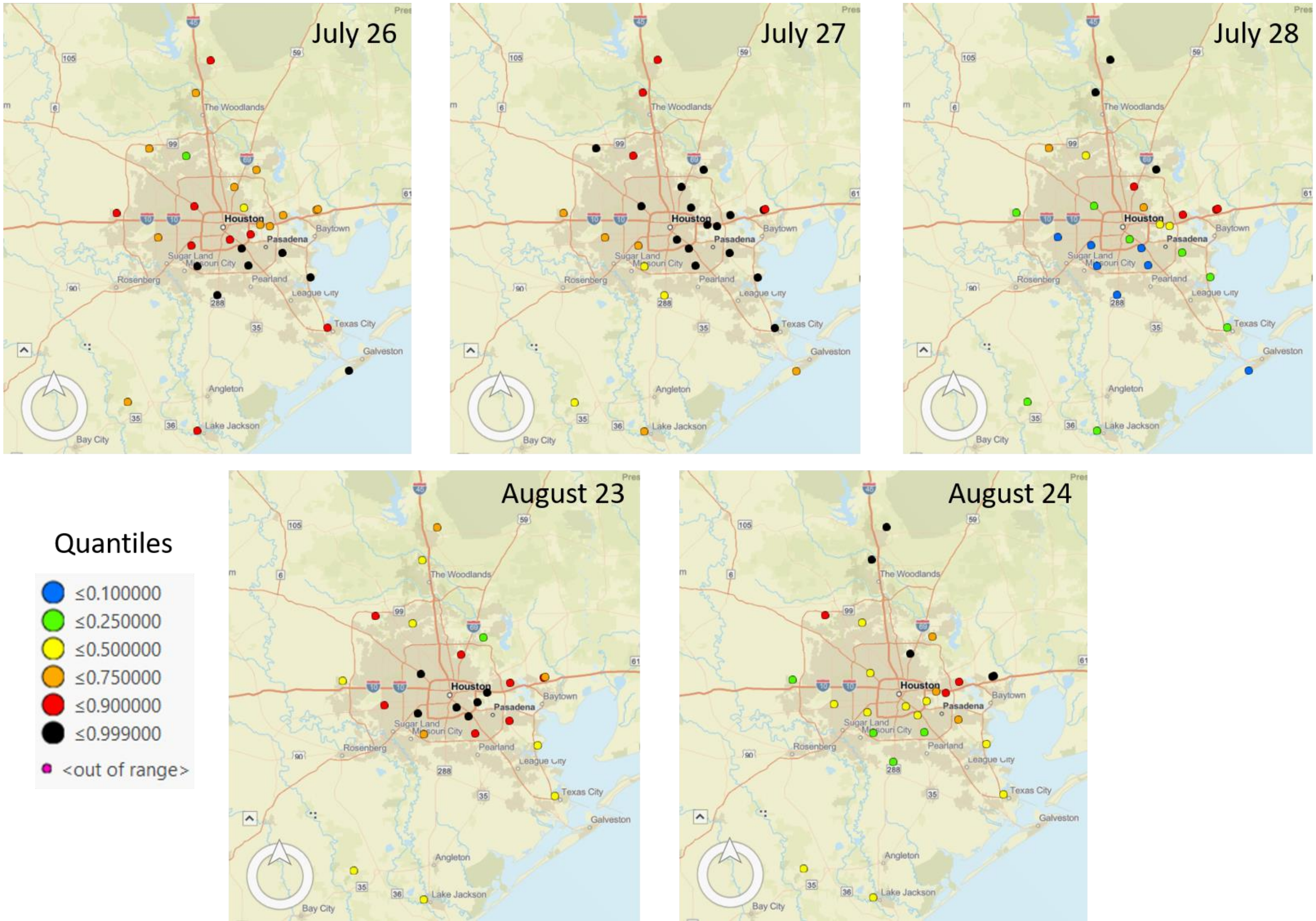

Figure 4-40. Spatial distribution of quantiles of MDA8 ozone on July-August 2018 high ozone episode days relative to all days (May- October 2014-2018) with MDA8 greater than 75 ppb at any HGB monitoring site

5.0 CLEAR CAUSAL RELATIONSHIP

EPA (2016) matches the type of analysis required for an exceptional event demonstration to the nature and severity of the ozone exceedance.

- Tier 1 analyses are used for wildfire events that cause ozone concentrations that are clearly higher than non-event related concentrations for the monitor or occur outside of the area's normal ozone season.
- Tier 2 analyses are used when the fire-related ozone concentrations are higher than non-event related concentrations, and the ratio of fire emissions to the distance between the wildfire and the affected monitor exceeds a threshold set by EPA. Tier 2 analyses require more supporting evidence than Tier 1 analyses.
- Tier 3 analyses are used for events in which the wildfire does not fall into the specific scenarios that qualify for Tier 1 or Tier 2, but the clear causal relationship criterion can still be satisfied by a weight of evidence showing. Tier 3 analyses require the most documentation and can include, in addition to Tier 2 analyses, photochemical modeling, statistical regression modeling and matching day analysis.

The July and August 2018 episodes occurred during Houston's ozone season, defined to be March-November. Concentrations on some days are the highest or among the highest in the last 5 years (e.g. July 27 at Aldine). Given the distance of the wildfires from Houston and the fact that local sources can cause very high ozone readings in Houston during the ozone season, a Tier 3 analysis was performed for the July and August episodes to establish a clear causal relationship between wildfires and high ozone in Houston. In Section 4, we present evidence supporting a clear causal relationship.

5.1 Comparison of the Ozone Data Requested for Exclusion with Historical Concentrations at the Air Quality Monitor

In this section, we review the event-related ozone concentrations at Aldine CAMS 8 and Bayland Park CAMS 53 In the context of historical ozone concentrations at each monitor. Figure 5-1 and Figure 5-2 show MDA8 ozone concentrations at the Aldine CAMS 8 monitor for the 5-year period 2014-2018 for the months of April-October and the full year, respectively. July 27 has the highest value of MDA8 ozone at Aldine CAMS 8 during the period 2014-2018. For the April-October period, MDA8 values for July 27 and August 24 exceed the 99th percentile while July 28 has MDA8 ozone at the 98.7th percentile. When the full year is considered, all three days exceed the 99th percentile.

For Bayland Park CAMS 53, MDA8 values for July 26 and August 23 exceed the 98th percentile when compared against April-October 2014-2018 MDA8 values (Figure 5-3) and exceed the 99th percentile when the full year is considered (Figure 5-4). This analysis shows that ozone was unusually high at Aldine CAMS 8 and Bayland Park CAMS 53 during the July and August episodes and that MDA8 values were among the very highest values measured at these monitors during the preceding 5 years.

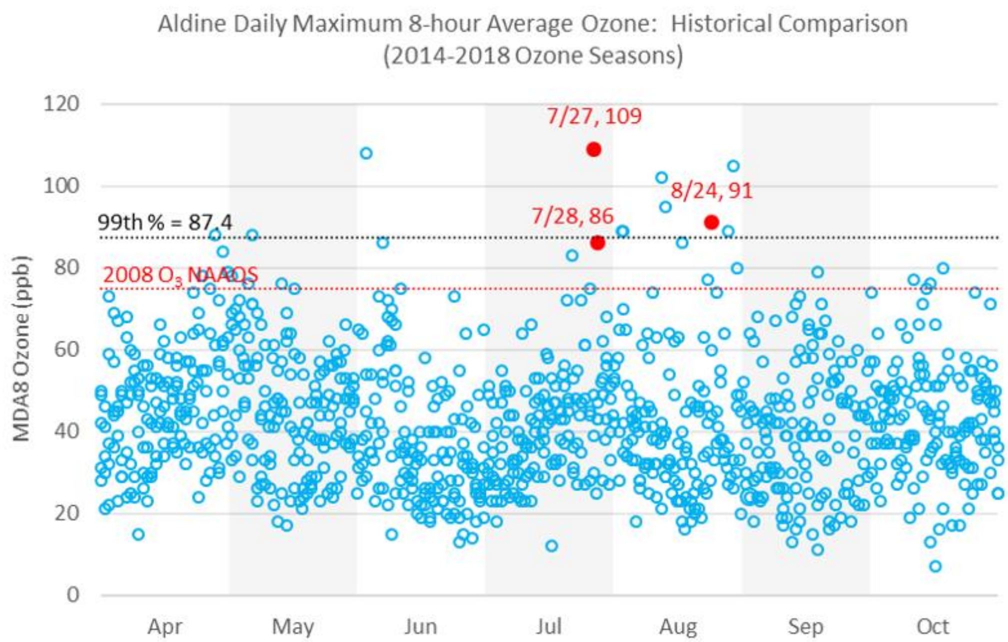

Figure 5-1. Historical comparisons for MDA8 ozone for Aldine CAMS 8 for the months April-October 2014-2018. High ozone days and the MDA8 ozone (in ppb) are shown in red.

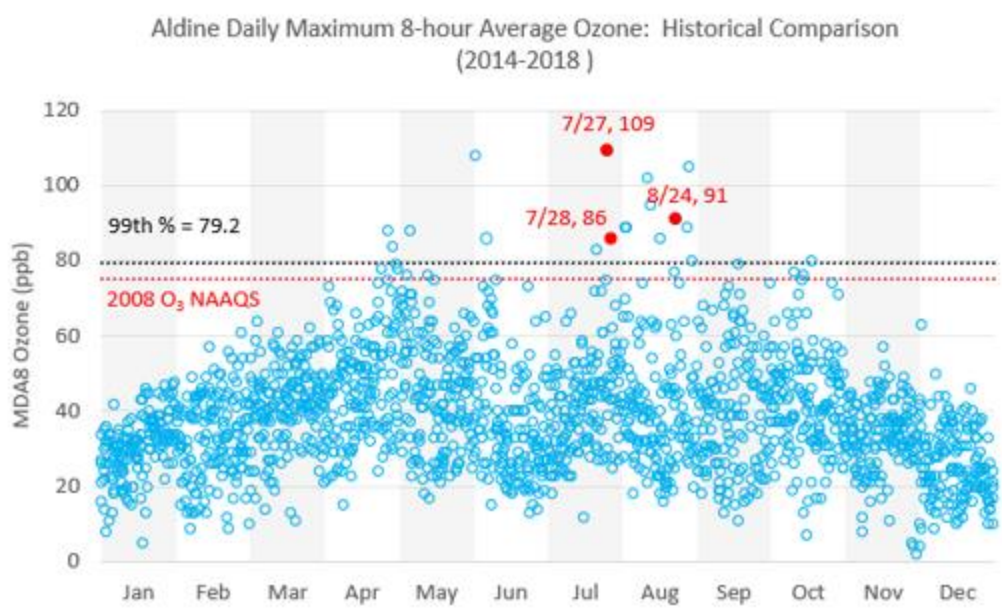

Figure 5-2. Historical comparisons for MDA8 ozone for Aldine CAMS 8 for the full year for the years 2014-2018. High ozone days and the MDA8 ozone (in ppb) are shown in red.

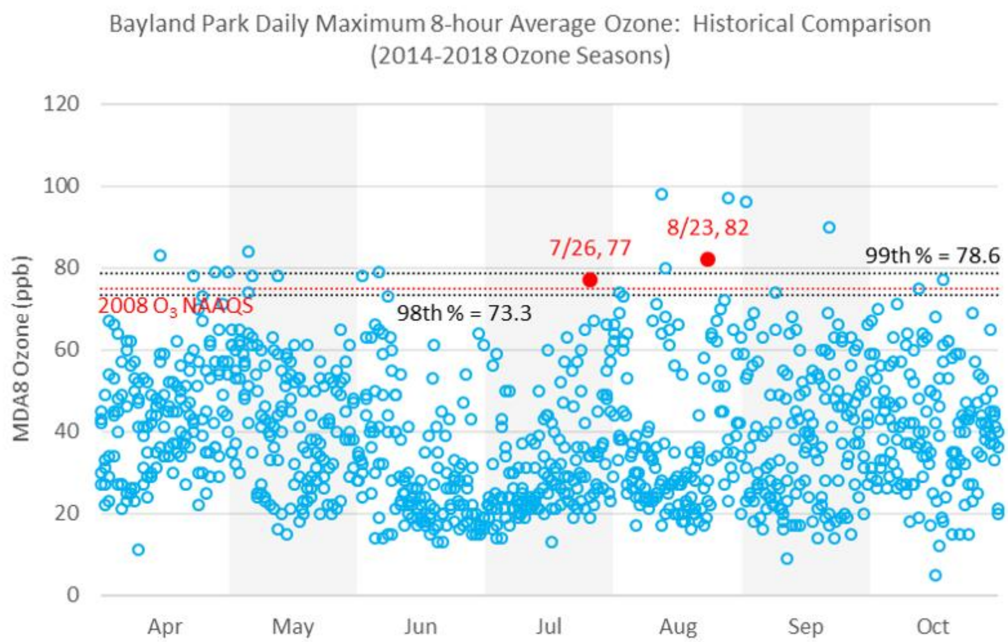

Figure 5-3. Historical comparisons for MDA8 ozone for Bayland Park CAMS 53 for the months April-October 2014-2018. High ozone days and the MDA8 ozone (in ppb) are shown in red.

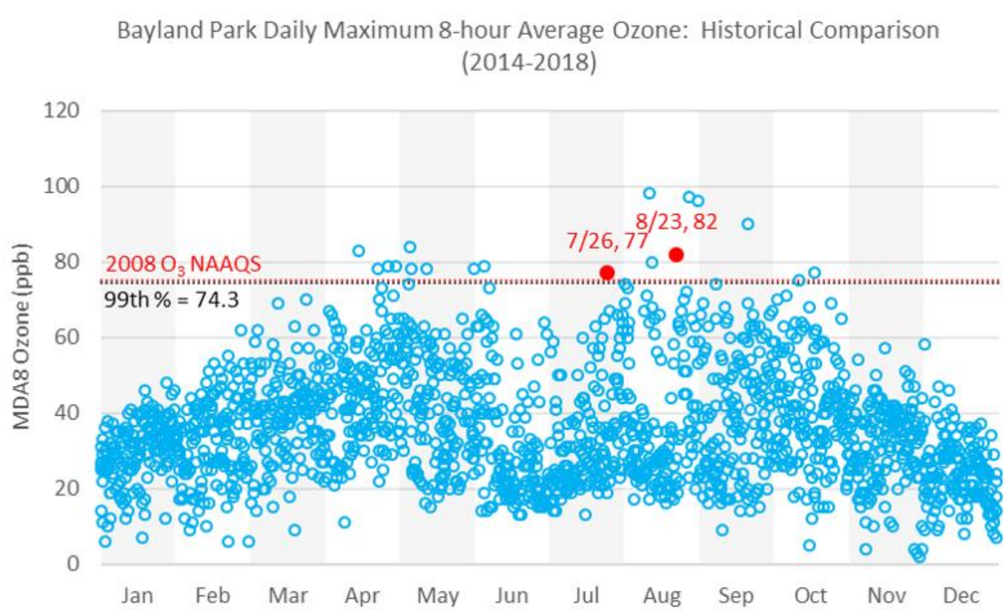

Figure 5-4. Historical comparisons for MDA8 ozone for Bayland Park CAMS 53 for the full year for the years 2014-2018. High ozone days and the MDA8 ozone (in ppb) are shown in red.

EPA recommends evaluating the rank of the episode days in case design value trends obscure the fact that they are exceptional. Design values in Houston are declining with time (Figure 5-5), but these trends do not obscure the fact that the July and August 2018 values measured at Aldine CAMS 8 and Bayland Park CAMS 53 were exceptionally high. Table 5-1 shows that the high ozone days at Aldine and Bayland Park during July and August 2018 event days rank among the values of MDA8 in 2018. During the July 26-28 and August 23-24 period, both Aldine and Bayland Park measured their highest values of MDA8 during 2018 and all of the MDA8 values during these two periods fell within the top five values of the MDA8.

Table 5-1. Ranking of episode days by MDA8 within the year 2018. Days identified as potential exceptional events are highlighted in yellow.

Rank	Aldine CAMS 8		Bayland Park CAMS 53	
	Date	MDA8 Ozone (ppb)	Date	MDA8 Ozone (ppb)
1	7/27/2018	109	8/23/2018	82
2	8/24/2018	91	4/28/2018	79
3	4/28/2018	88	5/7/2018	78
4	5/7/2018	88	7/26/2018	77
5	7/28/2018	86	8/2/2018	74
6	9/18/2018	79	4/25/2018	73
7	4/25/2018	78	8/3/2018	73
8	8/23/2018	77	4/24/2018	70
9	5/17/2018	75	3/14/2018	69
10	7/26/2018	75	7/27/2018	67

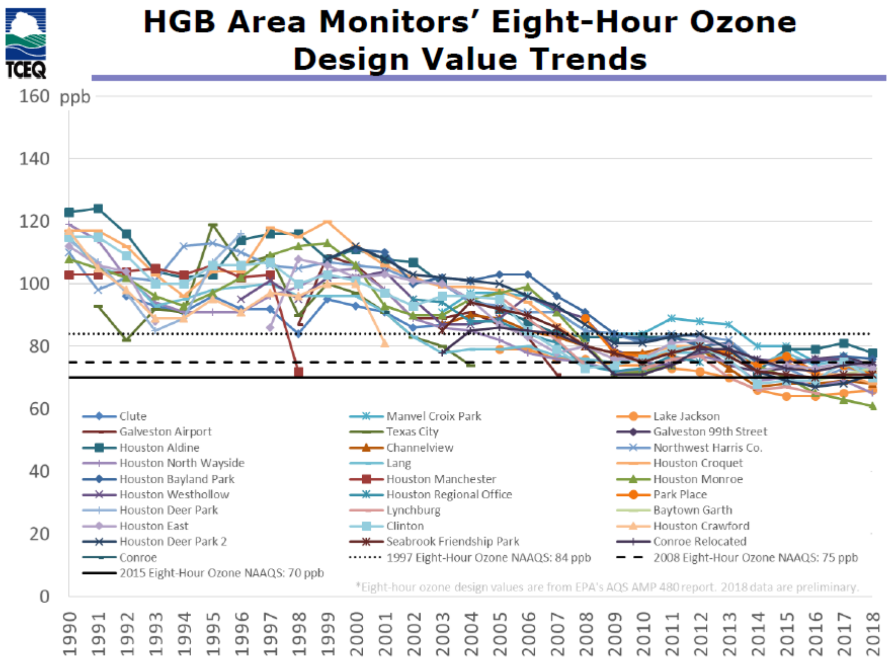

Figure 5-5. 8-hour ozone design values for monitors in the Houston-Galveston-Brazoria area. TCEQ figure.

5.2 Evidence that the Fire Emissions Affected the Monitor

Combustion of biomass in a wildfire produces emissions of PM, CO, VOC and NOx (e.g. Wiedinmyer et al., 2011; Jaffe and Wigder, 2012). The impact of a fire plume can change the typical concentrations of ozone and its precursors in a region and can affect levels of CO, NOx and $PM_{2.5}$ as well as its speciation. Enhanced levels of these species that are widespread throughout a region or are upwind of an urban area may be due to impact of a fire plume. Peaks at locations and times different than those normally seen in an ozone episode can indicate fire plume impacts. EPA (2016) notes "Elevated levels of CO or PM (including pre-cursors) at an affected ozone monitor upwind of urban centers or occurring at non-commute times at a monitor within an urban area despite the lack of a surface inversion would be consistent with wildfire plume impact". Ceilometer data collected at LaPorte by the University Houston (Section 5.2.3) indicate that no daytime inversions were present during July 26-28, 2018 and August 23-24, 2018. In this section, we review measurements of monitored species that can be affected by wildfires. We review measurements in Houston and the surrounding region from surface based and satellite monitoring systems.

5.2.1 Ground level $PM_{2.5}$, NOx and CO Measurements

$PM_{2.5}$ and CO are monitored at the CAMS and HRM monitoring networks in the Houston are and at CAMS in the surrounding region of Texas. We begin by reviewing data for $PM_{2.5}$ at Aldine CAMS 8. $PM_{2.5}$ and CO are not monitored at Bayland Park CAMS 53, and CO is not monitored at Aldine CAMS 8. Figure 5-6 and Figure 5-7 show hourly $PM_{2.5}$ for the July and August 2018 episodes. $PM_{2.5}$ data are available through 8 am on July 26 and show a steadily rising trend superimposed on the diurnal cycle. Data after 8 am on July 26 were rejected by TCEQ validators who assigned an AQI data flag to the remaining data on July 26. The $PM_{2.5}$ time series for the August episode shows an overall rise in $PM_{2.5}$ from August 21 through August 24 and then declining $PM_{2.5}$ from August 25-28. The maximum values of hourly $PM_{2.5}$ are 27.9 μg/m³ at 7 pm on August 23 and 27.6 μg/m³ at 2 pm on August 24.

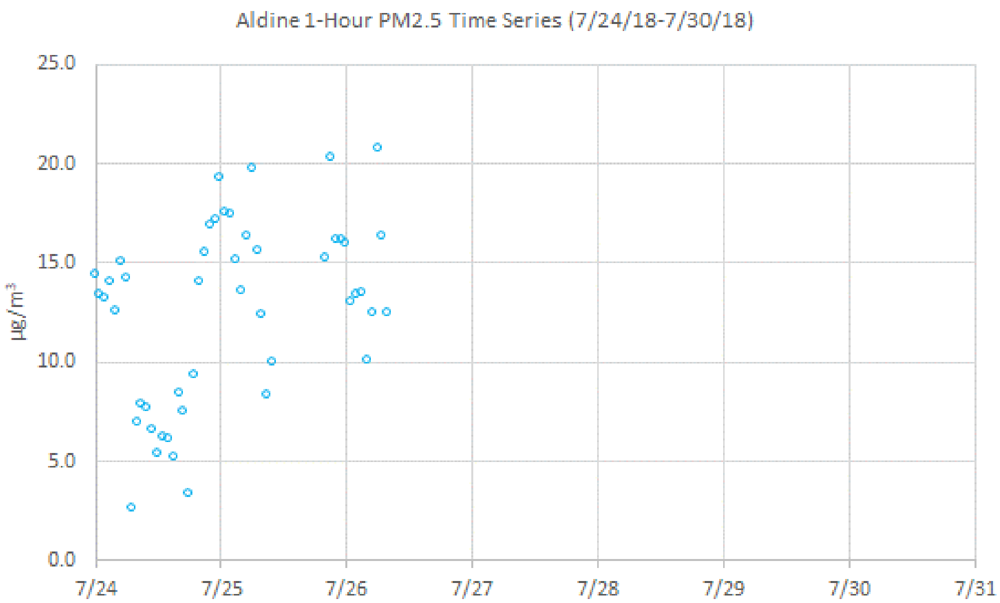

Figure 5-6. Time series of hourly $PM_{2.5}$ at Aldine CAMS 8 for July 24-31, 2018. Data are missing for July 26-31.

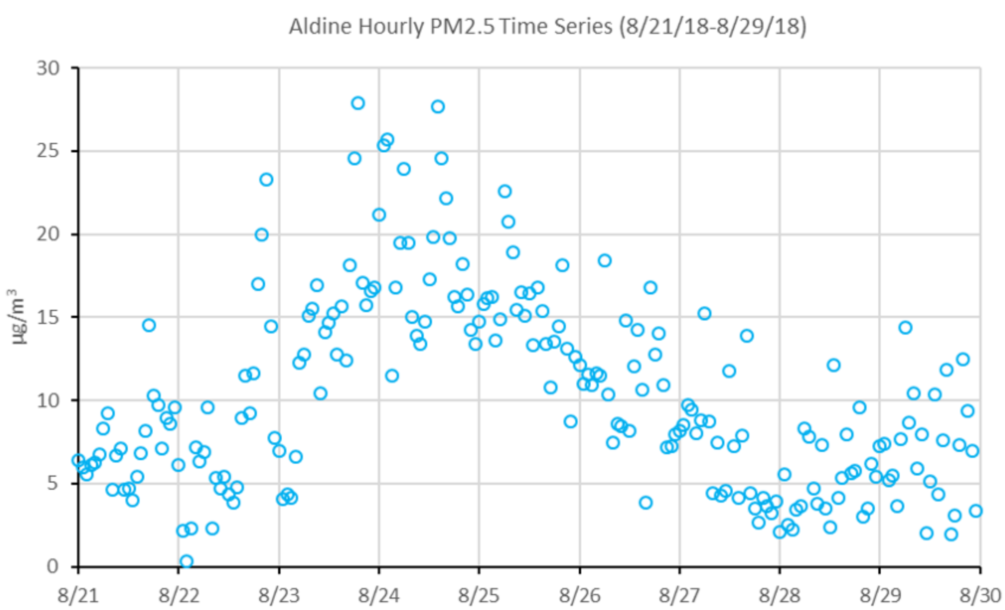

Figure 5-7. Time series of hourly $PM_{2.5}$ at Aldine CAMS 8 for August 21-August 30, 2018.

Figure 5-8 places August 23-24 $PM_{2.5}$ daily average values at Aldine CAMS 8 in context. The daily average $PM_{2.5}$ for August 24 (18.6 µg/m^3) is above the 95th percentile while the value for August 23 (13.8 µg/m^3) is just below the 90th percentile.

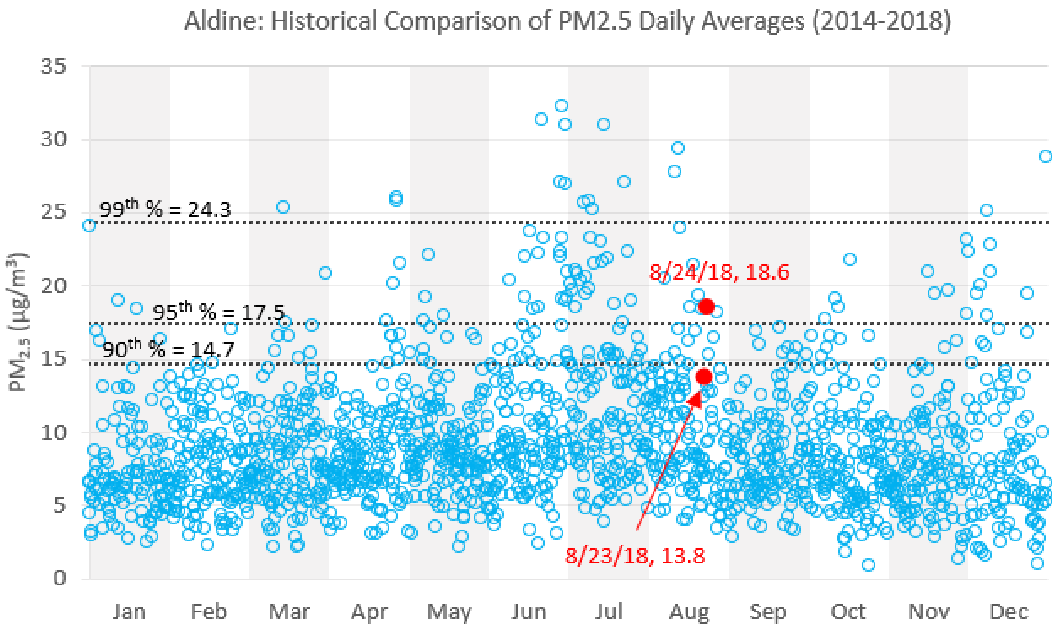

Figure 5-8. Historical comparisons for daily average $PM_{2.5}$ for Aldine CAMS 8 for the full year for the years 2014-2018. August episode high ozone days and the daily average $PM_{2.5}$ value (in µg/m³) are shown in red.

The daily maximum 1-hour average $PM_{2.5}$ occurred at 2 pm. Peak values of $PM_{2.5}$ in an urban area are often associated with rush hour traffic, and a peak at midday can be the signature of an unusual emissions source, such as a wildfire. Figure 5-9 shows that the values of $PM_{2.5}$ fall above the interquartile range for all hours of the day. For the hours of 0100-0200 and 1300-1600, the August 24 $PM_{2.5}$ are the highest value for that hour during the entire 2010-2014 period. PM2.5 monitoring at Aldine therefore shows unusually high levels of $PM_{2.5}$ during the August 23-24 period.

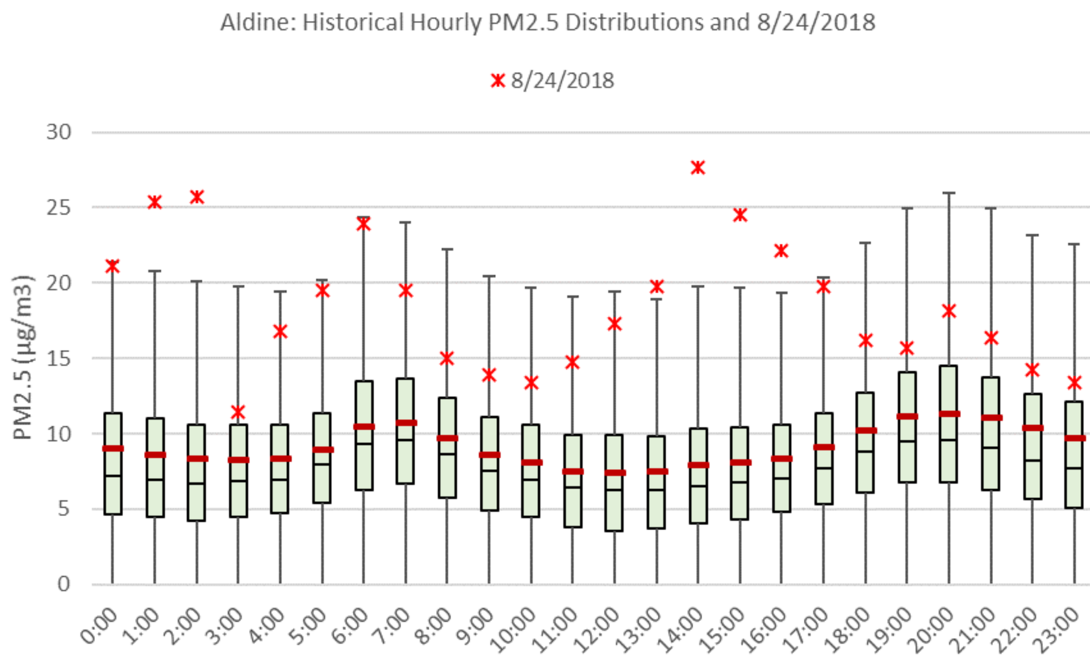

Figure 5-9. Aldine $PM_{2.5}$ comparison with 2010-2014 hourly data with boxplots. Aldine hourly $PM_{2.5}$ value is shown as a red X. The red horizontal bars within the box plots are the mean value.

Next, we review $PM_{2.5}$ measurements for other monitors in Houston and East Texas. $PM_{2.5}$ measurements for HRM network monitors are shown in Figure 5-10. $PM_{2.5}$ at all HRM monitors begins rising on July 24 and generally stays above 15 µg/m^3 through the afternoon of July 27, when $PM_{2.5}$ concentrations begin to fall. From August 5 through August 14, the HMS smoke product displayed in airnowtech.org shows no smoke over Houston (not shown). The behavior of the HRM monitor $PM_{2.5}$ time series is similar for the August ozone episode. $PM_{2.5}$ at all HRM monitors begins rising on August 22, stays high through August 24, and declines thereafter. The fact that all of the HRM monitor $PM_{2.5}$ time series behave in a similar manner suggests that the increased $PM_{2.5}$ is driven by a regional-scale phenomenon such as a transport event that brought polluted continental air to East Texas. A local plume impact, on the other hand, would tend to affect only a subset of the HRM monitors. For example, on August 11, HRM 11 measures a sharp peak in $PM_{2.5}$ which did not affect the other HRM monitors.

In Figure 5-10, the time series for Texarkana CAMS 1031 is shown together with the HRM monitors. CAMS 1031 is located in Northeast Texas approximately 2 miles from the Texas-Arkansas border. During the July 26-28 and August 23-24 episodes, the Texarkana CAMS 1031 $PM_{2.5}$ time series is similar to the HRM monitor time series. During the August episode, the CAMS 1031 $PM_{2.5}$ time series begins to rise before the HRM time series, which is consistent with the conceptual picture of a plume containing wildfire emissions that moves southeast into Texas. During the July episode, however, the HRM and CAMS 1031 $PM_{2.5}$ begin to rise at approximately the same time.

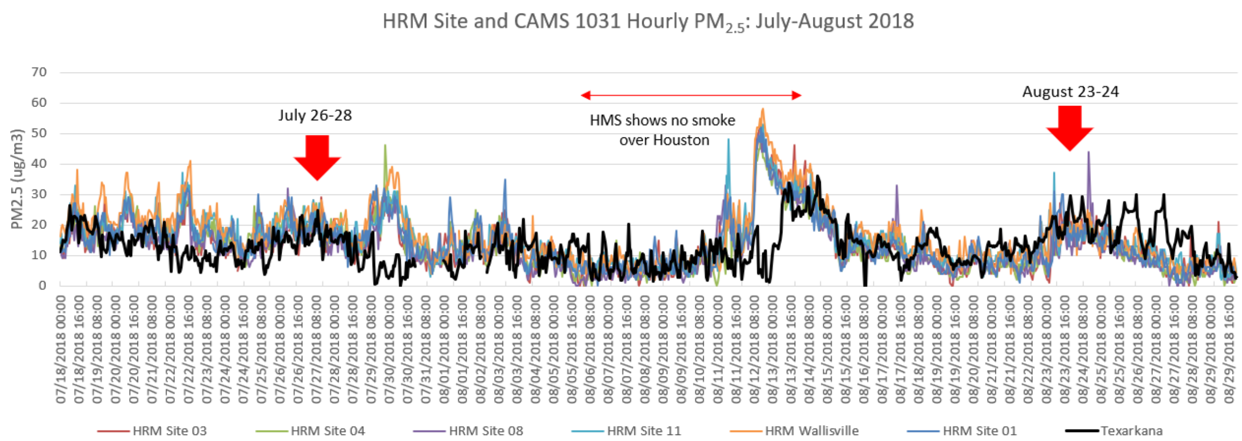

Figure 5-10. Time series of hourly $PM_{2.5}$ at Texarkana CAMS 1031 and HRM monitoring network sites in Houston during July 18-August 29, 2018.

Figure 5-11 shows daily maximum $PM_{2.5}$ time series for several monitors in East Texas that are not located in major metropolitan areas. For example, Karnack CAMS 85 is located in a rural area of northeast Texas and Conroe CAMS 78 is located outside of downtown Houston and under conditions of northerly flow samples air flowing into Houston. Neither the July 26-28 or August 23-24 period stand out as a time of unusually high $PM_{2.5}$ during July-August at these monitors. However, all five monitors do show a rise and fall in $PM_{2.5}$ that is consistent with the pattern of the HRM monitors shown in Figure 5-10.

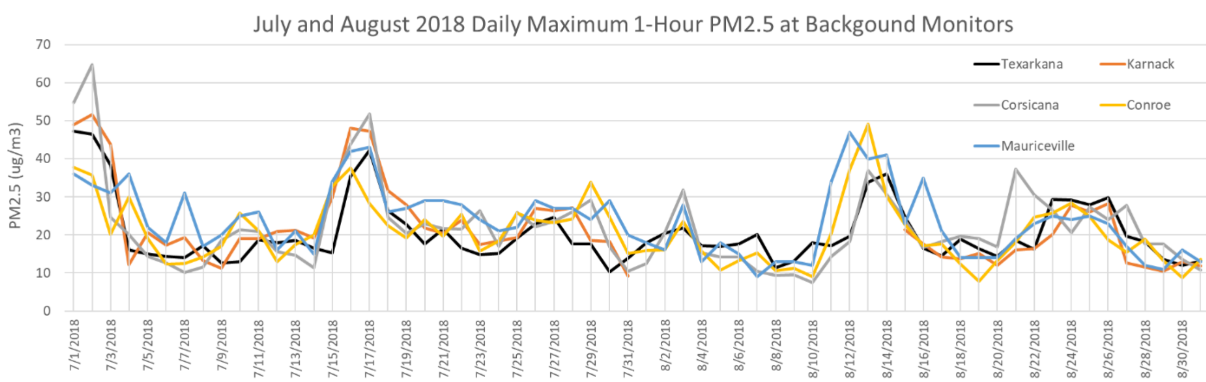

Figure 5-11. Time series of daily maximum 1-hour average $PM_{2.5}$ at CAMS monitors located in rural areas of East Texas July 1-August 31, 2018.

Next, we review CO measurements in the Houston area. Figure 5-12 shows 1-hour average CO time series for the West Liberty CAMS 699, Clinton CAMS 403 and Deer Park CAMS 35. Clinton CAMS 403 and Deer Park CAMS 35 are located in downtown Houston, while West Liberty CAMS 699 is located in a rural area northeast of Houston and samples the transported background on days when the winds are from the northeast. There is enhanced CO at several Houston monitors, consistent with a regional transport event. CO time series for all three monitors shows increases in CO starting on July 22 and also on August 22 that are consistent with a developing ozone episode. All three monitors have CO levels that are enhanced relative to the rest of the July-August period during the July 26-28 and

August 23-24 episodes. The Clinton CAMS 403 and Deer Park CAMS 35 time series have a series of sharp peaks superposed on the lower frequency increase that is consistent with a regional transport event. The rural West Liberty CAMS 699 monitor does not show spikes of such large amplitude consistent with its greater distance from urban sources of CO. The similar behavior of these three CO time series (aside from the sharp peaks at urban monitors) suggests a common influence on their behavior during July 26-28 and August 23-24.

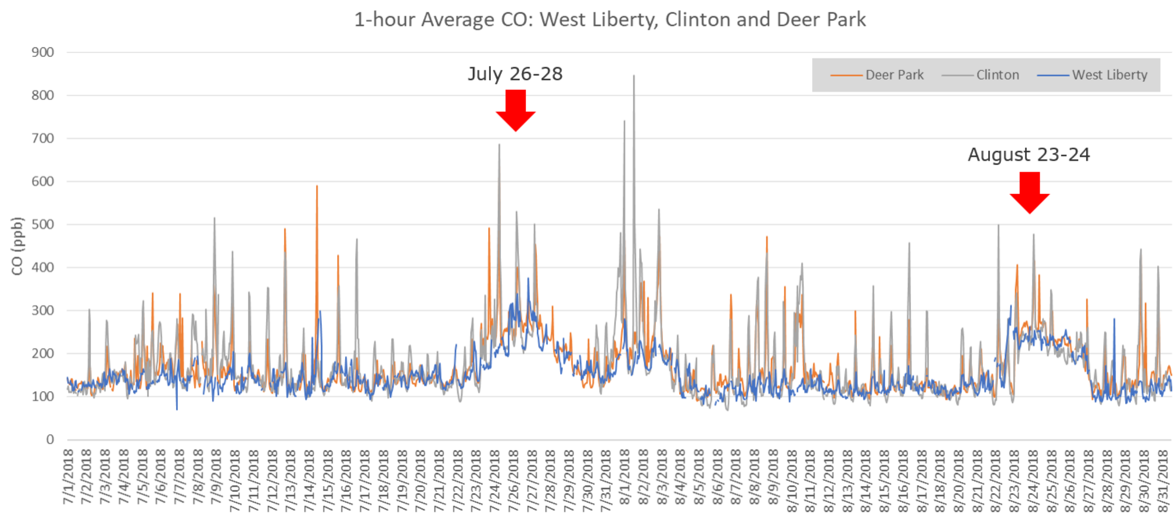

Figure 5-12. Time series of daily maximum 1-hour average CO at Houston area CAMS monitors for July 1-August 31, 2018.

Deer Park CAMS 35 and Clinton CAMS 403 are two sites in the Houston area that have hourly measurements of both CO and $PM_{2.5}$. The time series for these two species are plotted together in Figure 5-13 and Figure 5-14. At both Clinton CAMS 403 and Deer Park CAMS 35, $PM_{2.5}$ and CO show variability at short (< 1 day) time scales with CO peaks sometimes coinciding with peaks in $PM_{2.5}$. For example, at midnight on July 15, Deer Park CAMS 35 $PM_{2.5}$ reached a peak of 154 µg/m^3, and there is a peak in CO of 0.59 ppm at the same time. By 1 am, $PM_{2.5}$ dropped down to 18 µg/m^3 and CO to 0.20 ppm. Less frequently, peaks are visible in CO but are less evident in the $PM_{2.5}$ time series (e.g. August 30 at Clinton CAMS 403). During the July 24-28 and August 22-27 periods, CO and $PM_{2.5}$ rose together and remained high for several days, and then fell back together. This is consistent with the arrival of a polluted continental air mass in Houston that causes a multi-day episode of enhanced values of CO and $PM_{2.5}$.

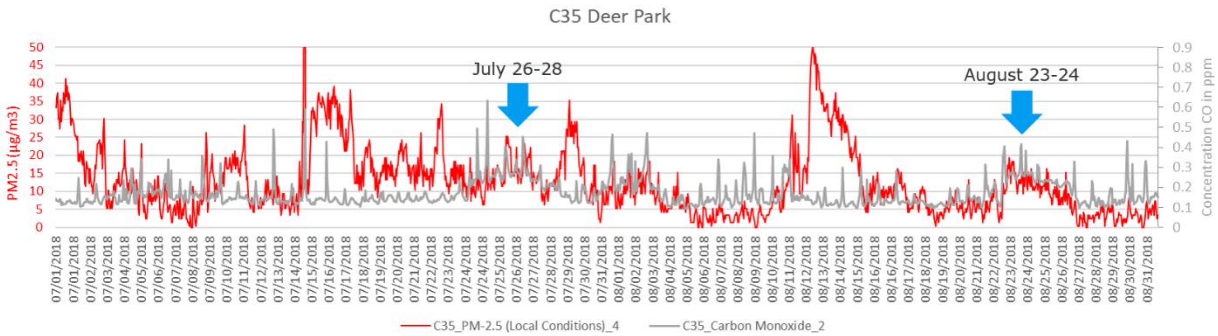

Figure 5-13. Time series of hourly CO and $PM_{2.5}$ at Deer Park CAMS 35 for July 1-August 31, 2018.

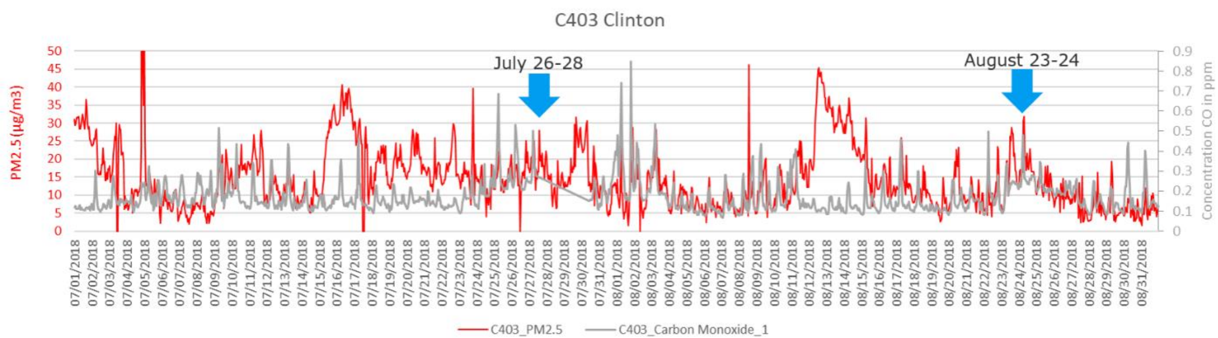

Figure 5-14. Time series of hourly CO and $PM_{2.5}$ at Clinton CAMS 403 for July 1-August 31, 2018.

The TCEQ evaluated the relationship between hourly ozone and $PM_{2.5}$ collected during the monitor's maximum eight-hour ozone average period. Table 5-2 shows the July episode daily correlation coefficients and confidence levels for Houston CAMS and HRM monitors. Confidence is based on results of regression F test. Aldine CAMS 8 was missing $PM_{2.5}$ data for July 26 and July 27. TCEQ's analysis finds evidence that ozone and $PM_{2.5}$ were correlated during the period June 26-27, with a higher level of confidence on July 27.

Table 5-2. TCEQ July correlation analysis for ozone and $PM_{2.5}$ at CAMS and HRM monitors in Houston.

Monitor	Coefficient	Adjusted R^2	Confidence?
July 26, 2018			
West Liberty CAMS 699	0.45	0.328	Yes (0.1)
HRM Wallisville	0.69	0.398	Yes (0.1)

Monitor	Coefficient	Adjusted R^2	Confidence?
July 27, 2018			
Deer Park CAMS 35	3.87	0.583	Yes (0.05)
Houston East CAMS 1	4.72	0.764	Yes (0.05)
HRM Wallisville	2.39	0.518	Yes (0.05)
HRM-01	3.83	0.607	Yes (0.05)
HRM-03	2.99	0.301	Yes (0.1)
HRM-11	0.89	0.324	Yes (0.1)

Figure 5-15 and Figure 5-16 show time series of ozone and NOx for Bayland Park CAMS 53 and Aldine CAMS 8, respectively. During the July 26-28 periods, there are no large peaks in NOx that coincide with daytime peaks in ozone that would be consistent with impacts from a nearby wildfire. The largest NOx peaks occur early and late in the day during times of rush hour traffic. $PM_{2.5}$ data are available for Aldine CAMS 8 for a portion of July 25-26 and the $PM_{2.5}$ peaks occur together with the NOx peaks during times of rush hour traffic. $PM_{2.5}$ data are not available for the July 26-28 high ozone periods, so variation of ozone with NOx cannot be evaluated for these times.

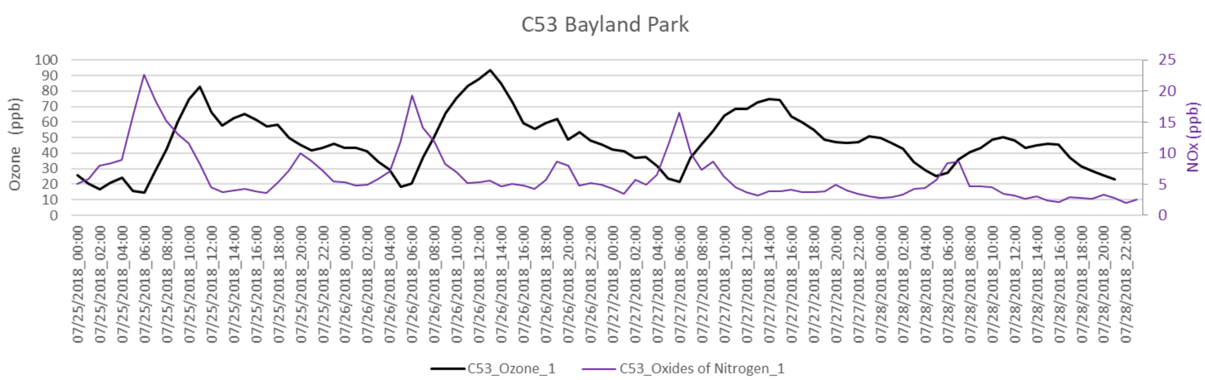

Figure 5-15. Time series of hourly NOx and ozone at Bayland Park CAMS 53 for July 25-28, 2018.

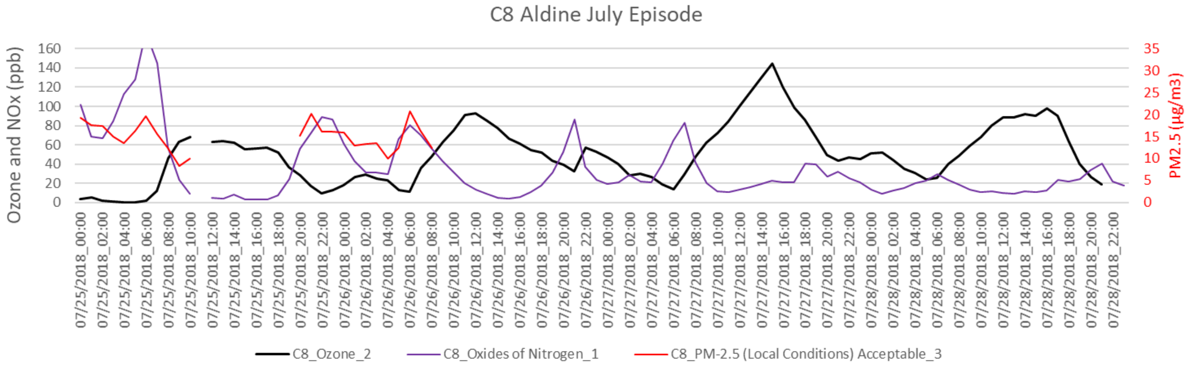

Figure 5-16. Time series of hourly NOx, $PM_{2.5}$ and ozone at Aldine CAMS 8 for July 25-28, 2018.

Figure 5-18 through Figure 5-21 show NOx, ozone and $PM_{2.5}$ for Houston CAMS that have measurements for all three species during July 26-28. Houston East CAMS 1, Deer Park CAMS 35 and Seabrook Friendship Park CAMS 45 show midday peaks of $PM_{2.5}$ that are well-correlated with ozone, consistent with the TCEQ analysis shown in Table 5-2. For Houston East CAMS 1, Deer Park CAMS 35, these peaks do not have coincident midday peaks in the NOx time series. On July 27, however Seabrook Friendship Park CAMS 45 has a 10 am peak in NOx that occurs at the same time as a peak in $PM_{2.5}$ and rising ozone that peaks 1-2 hours after the peaks in $PM_{2.5}$ and NOx. The 100 m HYSPLIT back trajectory for 10 am at Seabrook Friendship Park CAMS 45 extends back over downtown Houston during the morning hours, which suggest this late peak may be influenced by urban sources.

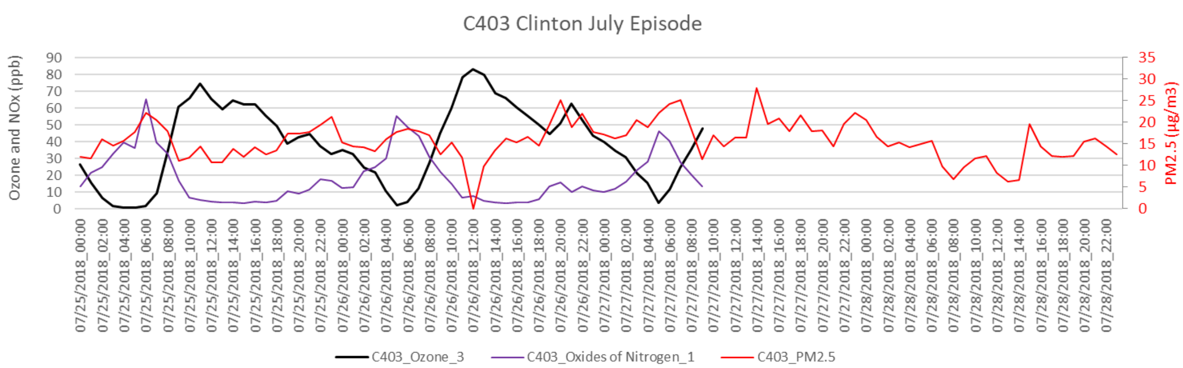

Figure 5-17. Time series of hourly NOx, $PM_{2.5}$ and ozone at Clinton CAMS 403 for July 25-28, 2018. NOx and ozone data are flagged LST (lost) for July 27-28.

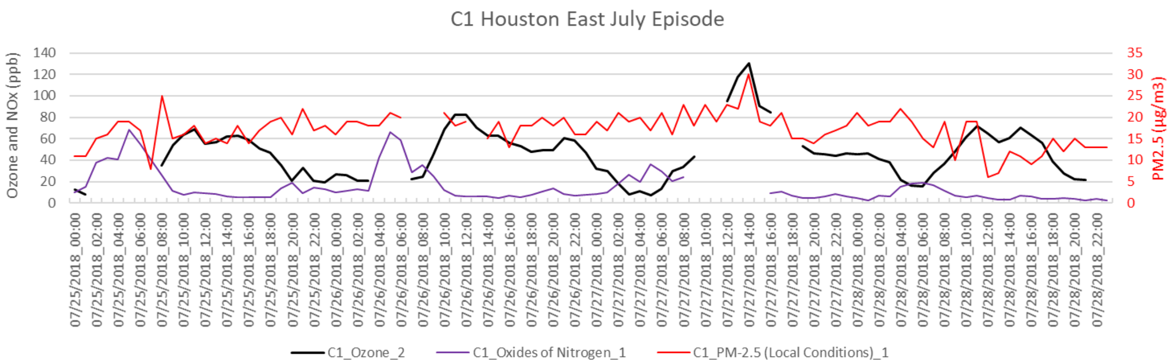

Figure 5-18. Time series of hourly NOx, $PM_{2.5}$ and ozone at Houston East CAMS 1 for July 1-August 31, 2018. NOx data for July 27 are flagged PMA (preventive maintenance) and CAL (calibration) during the period of no data.

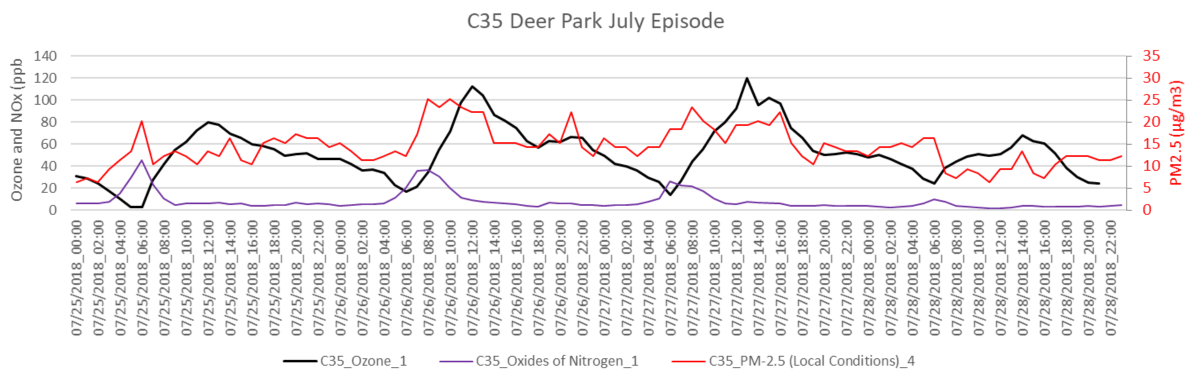

Figure 5-19. Time series of hourly NOx, $PM_{2.5}$ and ozone at Deer Park CAMS 35 for July 25-28, 2018.

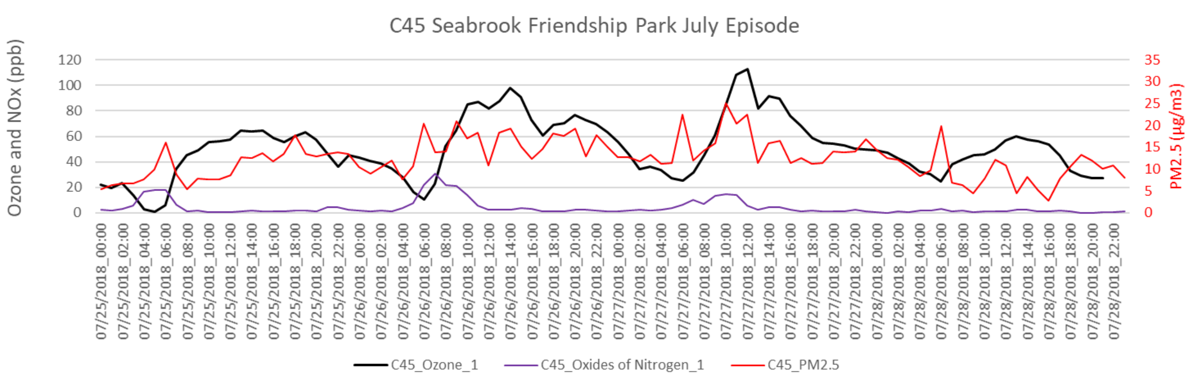

Figure 5-20. Time series of hourly NOx, $PM_{2.5}$ and ozone at Seabrook Friendship Park CAMS 45 for July 25-28, 2018.

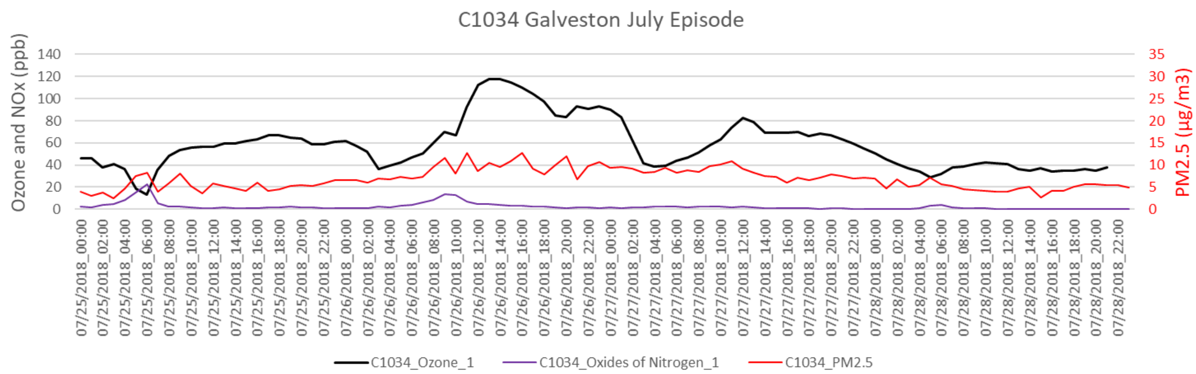

Figure 5-21. Time series of hourly NOx, $PM_{2.5}$ and ozone at Galveston CAMS 1034 for July 25-28, 2018.

The TCEQ evaluated the relationship between hourly ozone and $PM_{2.5}$ collected during the monitor's maximum eight-hour ozone average period. Table 5-2 shows the August episode daily correlation coefficients and confidence levels for Houston CAMS and HRM monitors. Confidence is based on results of regression F test. The TCEQ's analysis finds evidence that ozone and $PM_{2.5}$ were correlated during the period August 23-24. Time series of ozone and $PM_{2.5}$ (Figure 5-23 through Figure 5-28) illustrate the correlations, with enhanced $PM_{2.5}$ coinciding with ozone peaks for Aldine CAMS 8, Clinton CAMS 403, Houston East CAMS 1 and Deer Park CAMS 35. Several monitors show small enhancements of NOx during ozone peaks (e.g. Aldine CAMS 8 on August) but these NOx peaks are very small compared to the peaks due to rush hour traffic.

Table 5-3. TCEQ August correlation analysis for ozone and $PM_{2.5}$ at CAMS and HRM monitors in Houston.

Monitor	Coefficient	Adjusted R^2	Confidence?
August 23, 2018			
Clinton CAMS 403	5.80	0.643	Yes (0.05)
Houston East CAMS 1	2.94	0.428	Yes (0.05)
HRM-01	4.97	0.777	Yes (0.05)
HRM-03	4.39	0.315	Yes (0.1)
August 24, 2018			
Aldine CAMS 8	2.24	0.644	Yes (0.05)
Deer Park CAMS 35	1.10	0.483	Yes (0.05)
Houston East CAMS 1	2.70	0.644	Yes (0.05)
Conroe-Relocated CAMS 78	1.34	0.382	Yes (0.1)
HRM-03	4.70	0.875	Yes (0.05)
HRM-04	2.42	0.327	Yes (0.1)
HRM-11	1.57	0.478	Yes (0.05)

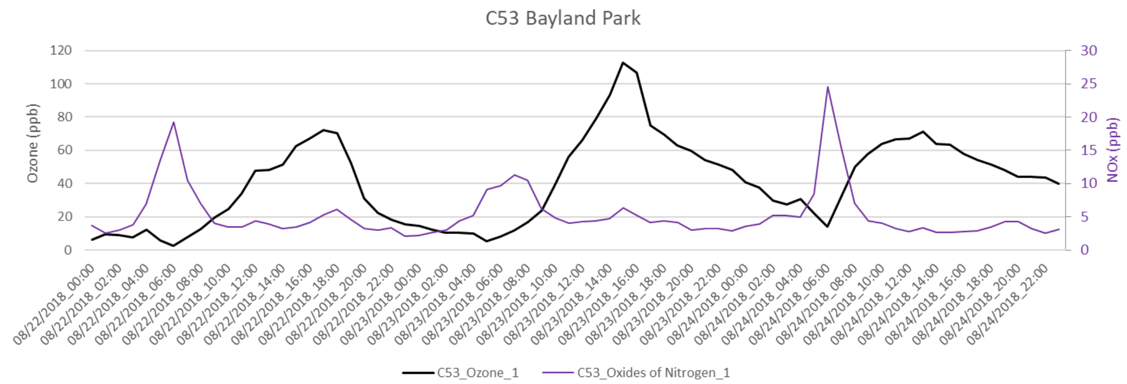

Figure 5-22. Time series of hourly NOx and ozone at Bayland Park CAMS 53 for August 22-24, 2018.

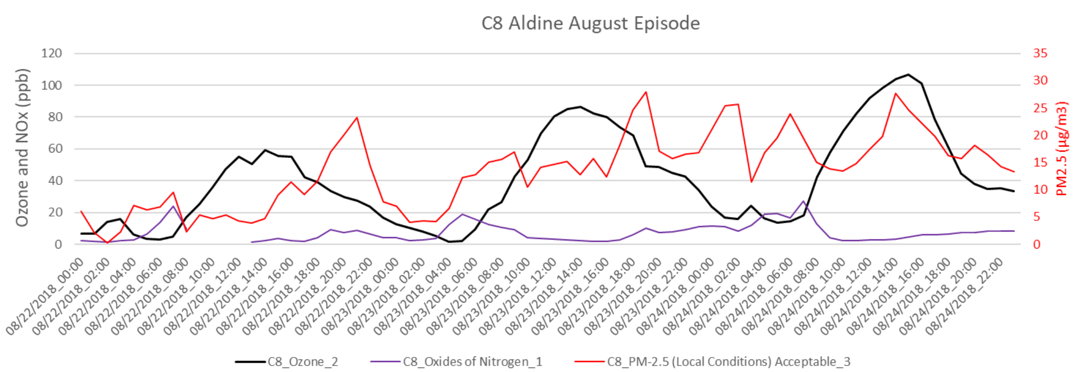

Figure 5-23. Time series of hourly NOx, $PM_{2.5}$ and ozone at Aldine CAMS 8 for August 22-24, 2018.

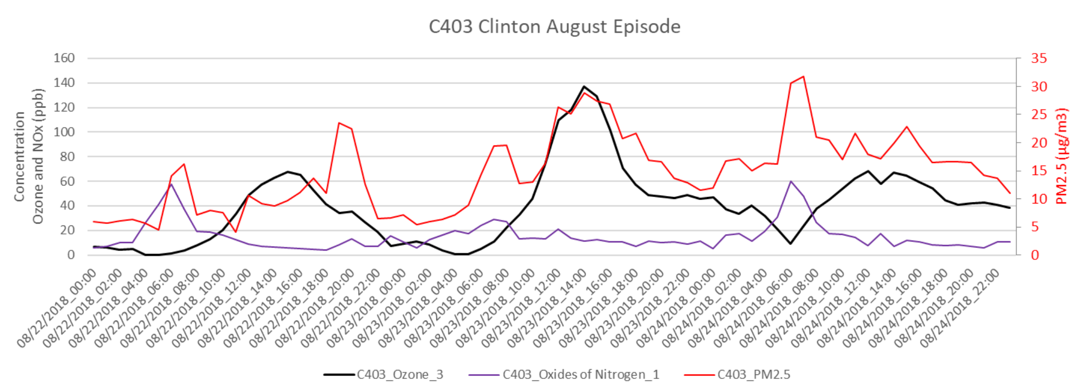

Figure 5-24. Time series of hourly NOx, $PM_{2.5}$ and ozone at Clinton CAMS 403 for August 22-24, 2018.

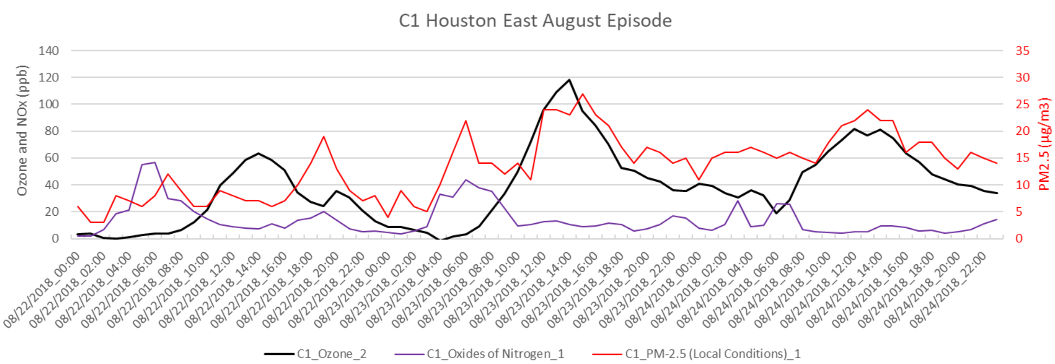

Figure 5-25. Time series of hourly NOx, $PM_{2.5}$ and ozone at Houston East CAMS 1 for August 22-24, 2018.

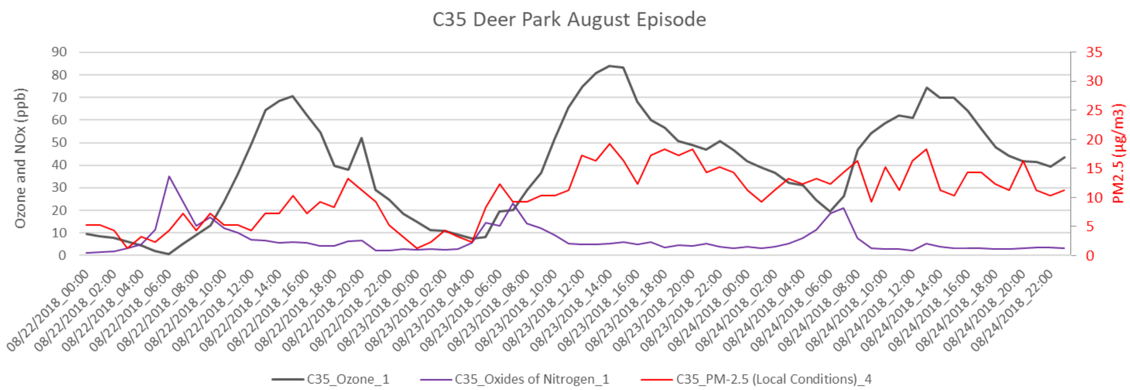

Figure 5-26. Time series of hourly NOx, $PM_{2.5}$ and ozone at Deer Park CAMS 35 for August 22-24, 2018.

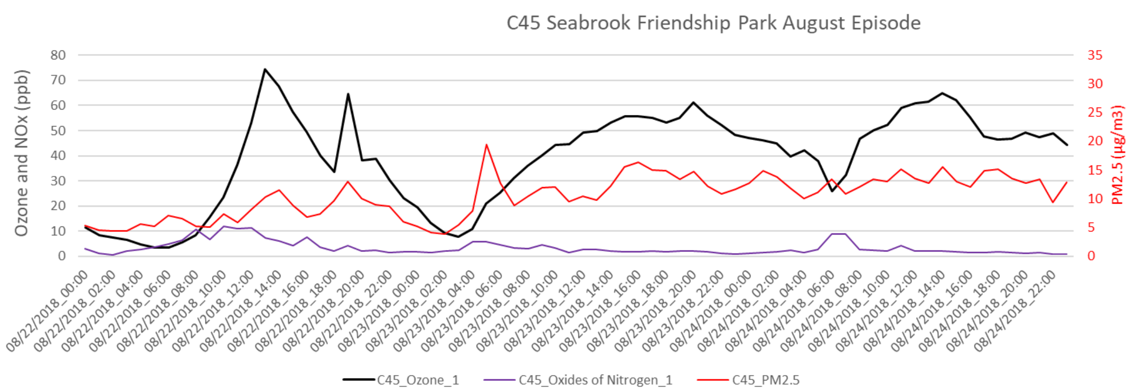

Figure 5-27. Time series of hourly NOx, $PM_{2.5}$ and ozone at Seabrook Friendship Park CAMS 45 for August 22-24, 2018.

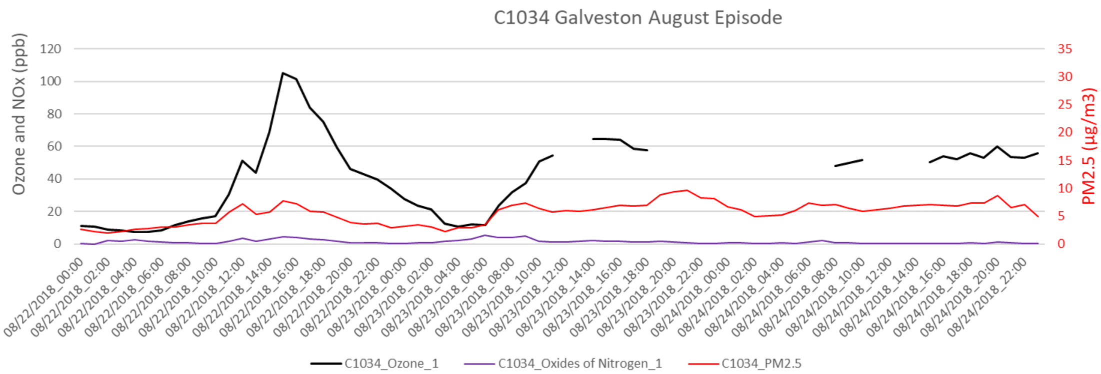

Figure 5-28. Time series of hourly NOx, $PM_{2.5}$ and ozone at Galveston CAMS 1034 for August 22-24, 2018.

5.2.2 AERONET Aerosol Measurements in Houston

The Aerosol Robotics Network (AERONET) is a global aerosol monitoring network administered by NASA and partner agencies and consists of approximately 400 sites in 50 countries on all seven continents. AERONET deploys near-ground level sun-sky radiometers to measure the intensity of light that penetrates the atmospheric column between the top of the atmosphere and the instrument. Aerosols in the atmospheric column scatter and/or absorb portions of the incoming light, and their size, shape, and chemical composition can be inferred from inversion of the photometer radiance measurements at multiple wavelengths by calculating aerosol characteristics such as size distribution, single scattering albedo, phase functions and complex index of refraction.

The University of Houston operates an AERONET site at UH Moody Tower in downtown Houston. The site is located at 29.71770° N, 95.34160° W and an elevation of 65 meters. UH provided AERONET measurements of aerosol optical depth and other optical properties to the TCEQ for the period 2014-2018. AERONET data are available at different stages of the quality control/quality assurance process. AOD data are computed for three data quality levels: Level 1.0 (unscreened), Level 1.5 (cloud-screened and quality controlled), and Level 2.0 (quality-assured). Data provided by UH for are Level 1.5.

Figure 5-29 is a time series of the total, fine and coarse AOD at 500 nm for the month of July. The month of July has several periods with relatively high values of AOD, and the period July 26-28 does not stand out among them. However, when all data from 2014-2018 are considered, the 500 nm fine mode AOD is among the highest values, near or exceeding the 99th percentile value on July 26-27 (Figure 5-30). The July 26-28 period is also notable for the high fraction of the total AOD attributed to the fine mode. Figure 5-31 shows the fine mode fraction of AOD at 500 nm for July 2018. During the period July 26-28, the fine mode fraction is higher than 0.8 except for a brief period during the afternoon of July 26 and a longer period during the evening of July 26. The Angstrom aerosol exponent is greater than one during most of the July 26-28 period (Figure 5-32), indicating the presence of fine particles consistent with smoke.

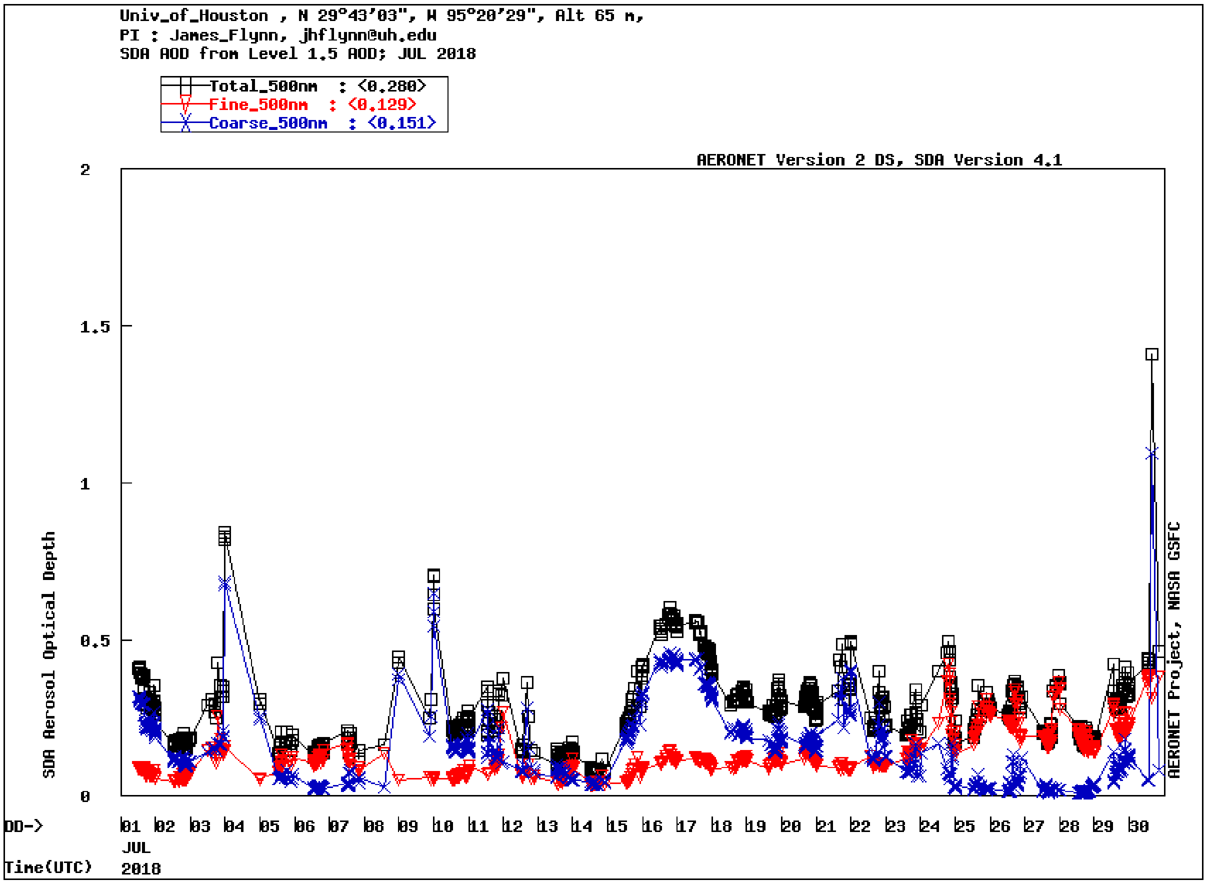

Figure 5-29. UH Moody Tower AERONET measurements of the 500 nm total, coarse and fine aerosol optical depths for July 2018.

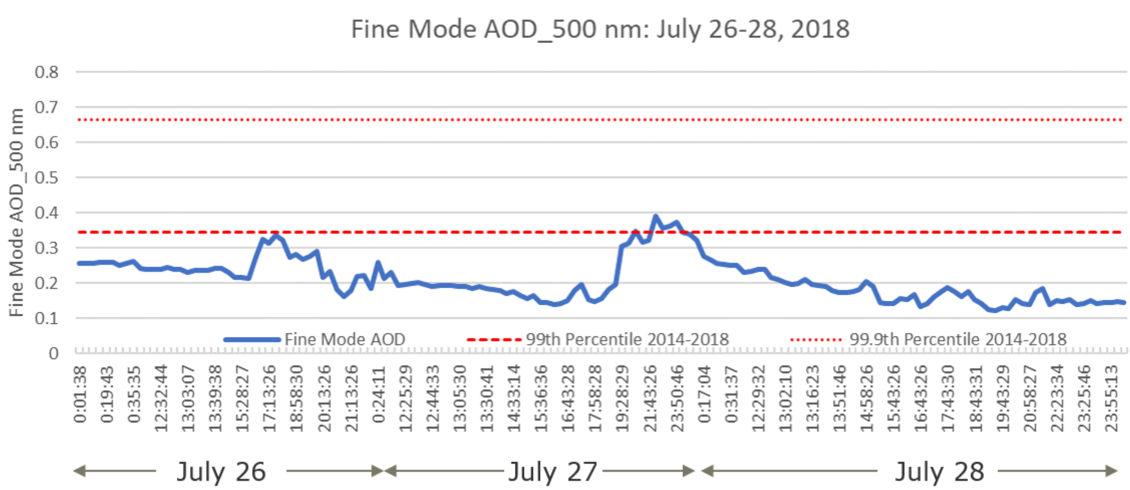

Figure 5-30. UH Moody Tower AERONET measurements of the 500 nm fine mode aerosol optical depth for July 26-28, 2018.

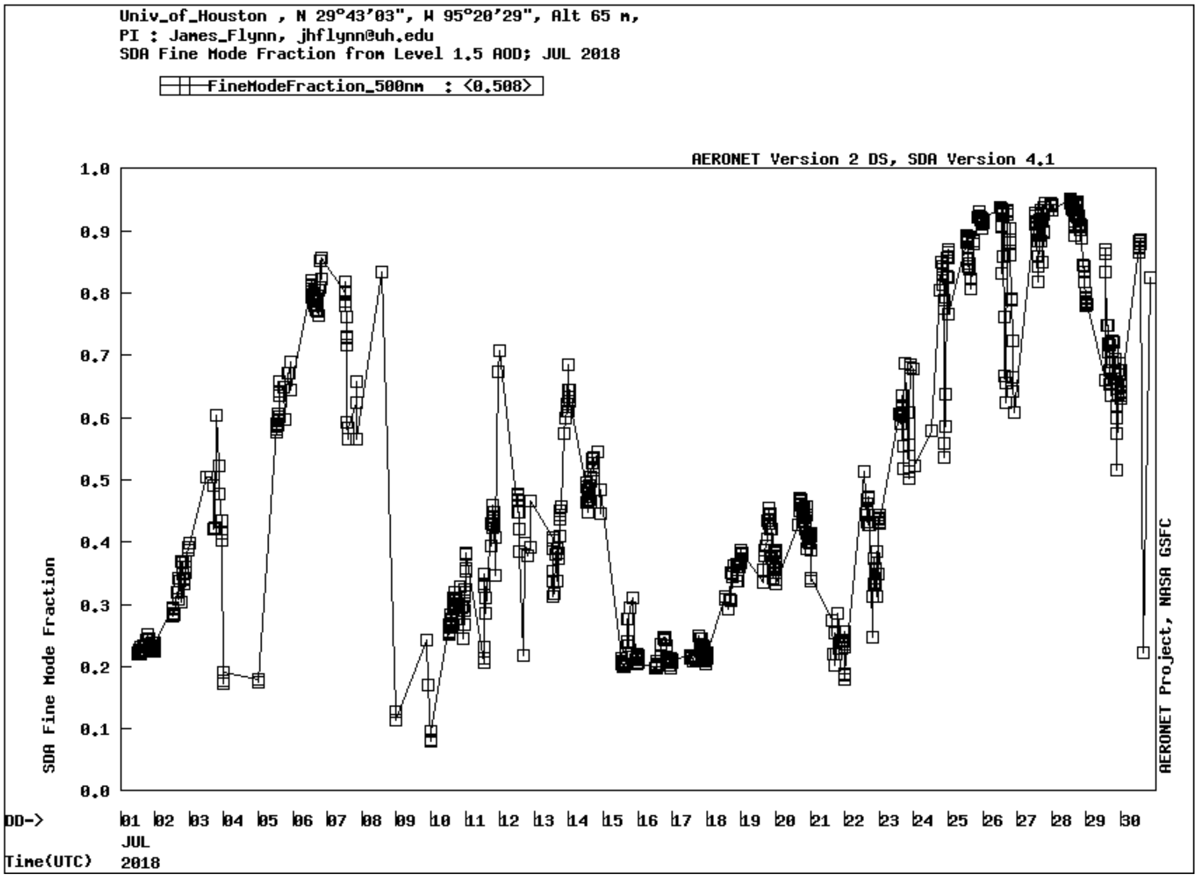

Figure 5-31. UH Moody Tower AERONET measurements of the 500 nm fine mode fraction for July 2018.

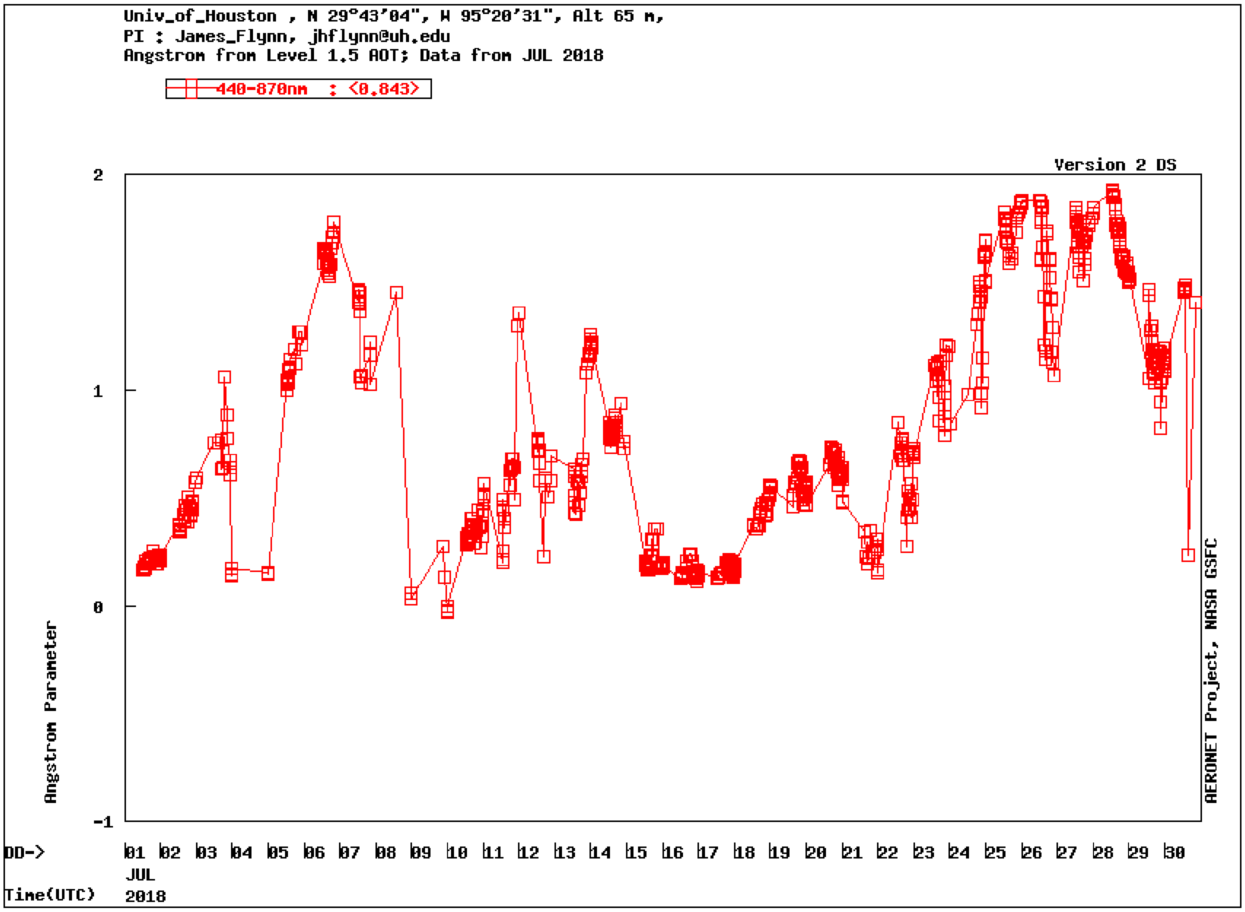

Figure 5-32. UH Moody Tower AERONET measurements of the Angstrom aerosol exponent for July 2018.

Figure 5-33 shows the time series of the total, fine and coarse AOD at 500 nm for the month of August. There is a large spike in the coarse mode AOD on August 13 and then, during the period August 22-25, there is a lower, broader peak driven by enhanced fine mode aerosol. During much of August 23-24, the 500 nm fine mode AOD exceeded the 99th percentile value (Figure 5-34). A high fraction of the total AOD is attributed the fine mode during August 23-24 (Figure 5-35). shows the fine mode fraction of AOD at 500 nm for August 2018. During August 23-24, the fine mode fraction is higher than 0.8. The Angstrom aerosol exponent is greater than one during the August 23-24 period (Figure 5-36), consistent with fine particles and the presence of smoke.

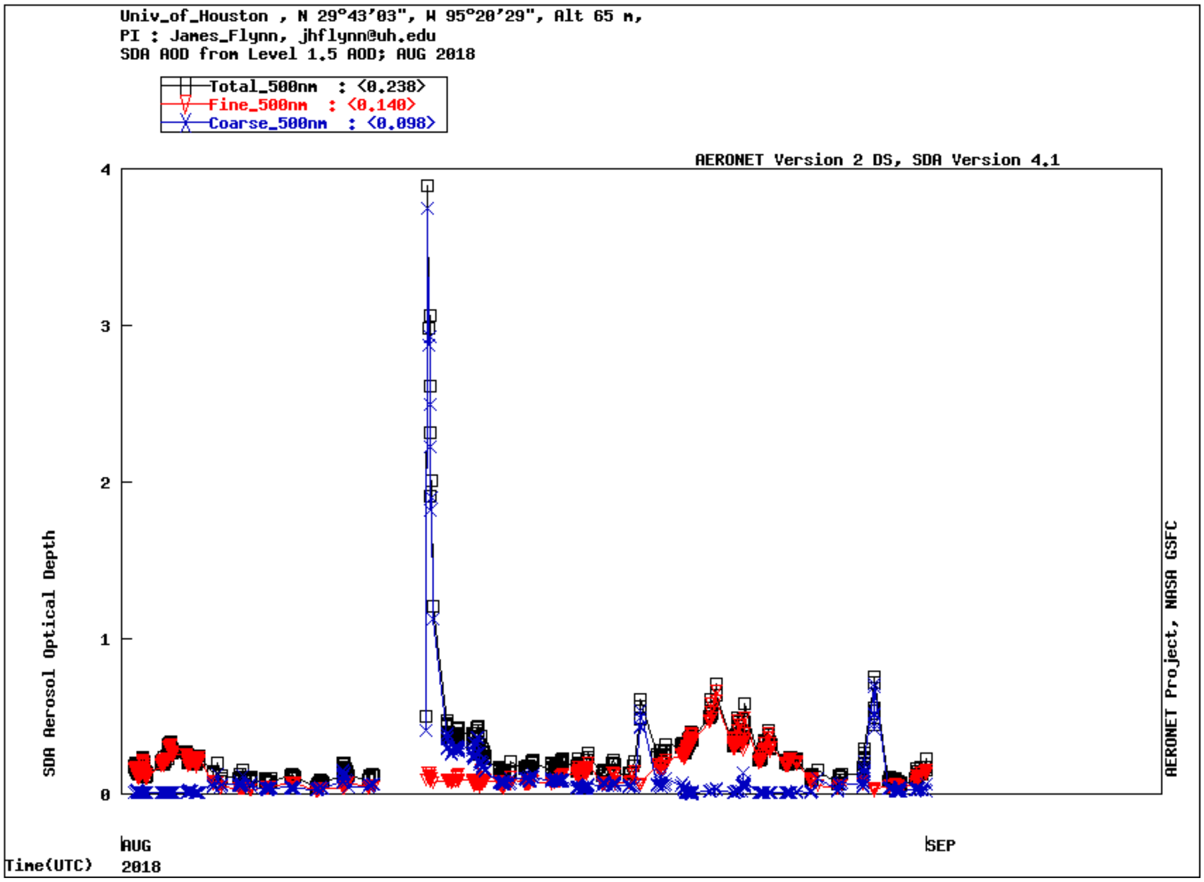

Figure 5-33. UH Moody Tower AERONET measurements of the 500 nm total, coarse and fine aerosol optical depths for August 2018.

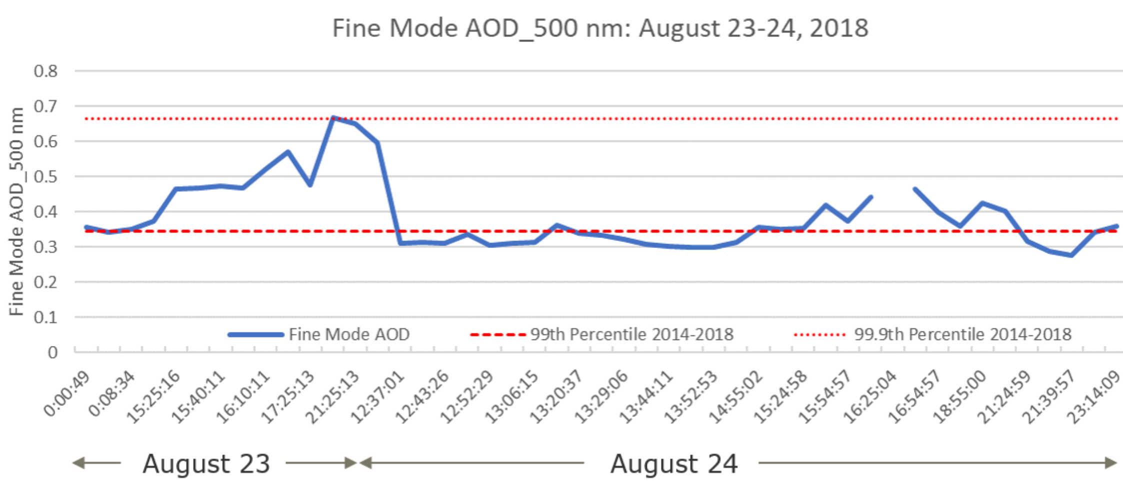

Figure 5-34. UH Moody Tower AERONET measurements of the 500 nm fine mode aerosol optical depth for August 23-24, 2018.

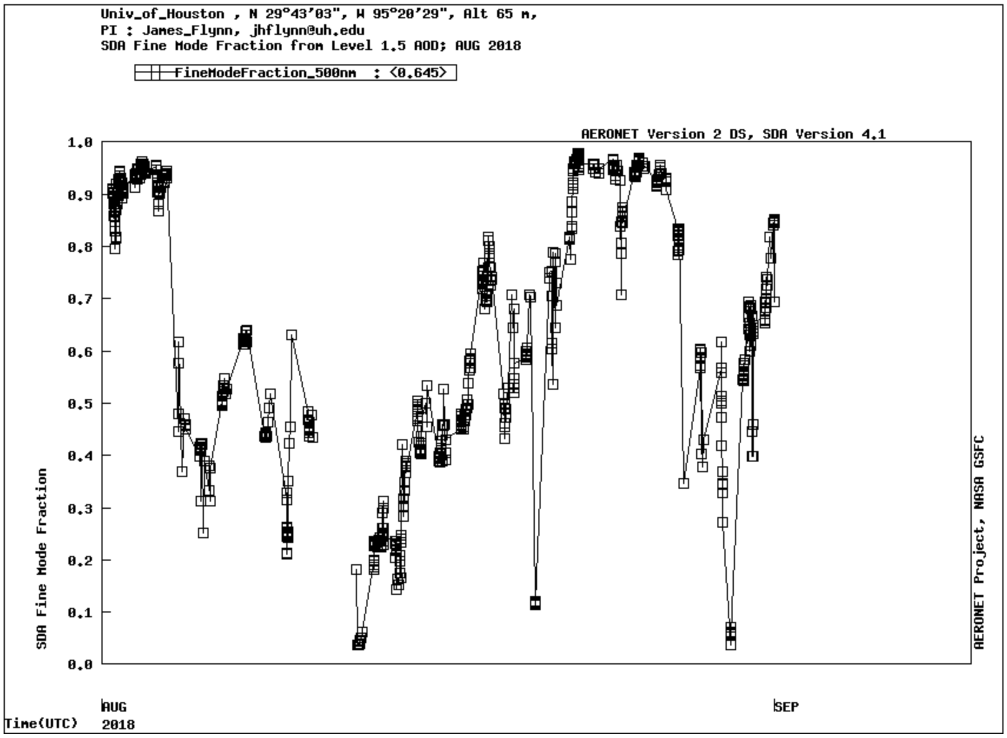

Figure 5-35. UH Moody Tower AERONET measurements of the 500 nm fine mode fraction for August 2018.

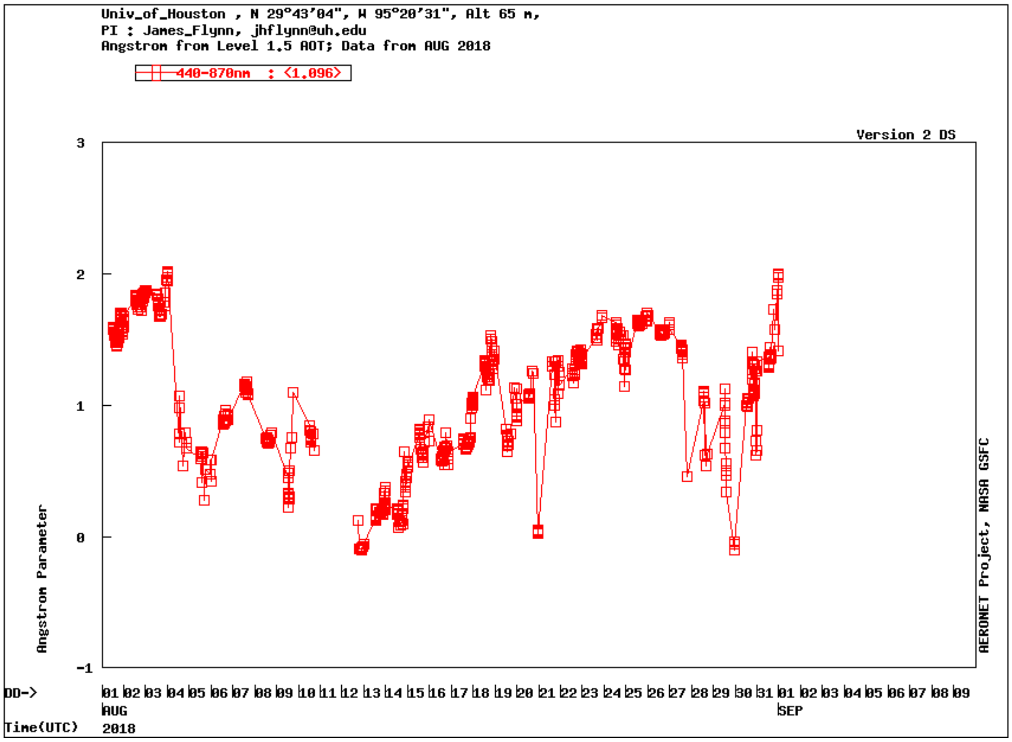

Figure 5-36. UH Moody Tower AERONET measurements of the Angstrom aerosol exponent for August 2018.

5.2.3 LaPorte Ceilometer Data

The University of Houston operates a ceilometer at LaPorte in the greater Houston area. The ceilometer uses LIDAR (light detection and ranging) to detect the presence of clouds and aerosols in the atmosphere. By transmitting a beam of light upward into the atmosphere and measuring the backscattered radiation a ceilometer maps the distribution of aerosols in the atmosphere and this information can be used to estimate the mixed layer height. The mixed layer height is diagnosed by evaluating regions of large gradients in the attenuated backscatter density. EPA (2016) notes that elevated light extinction measurements at or near an ozone monitoring site that cannot be explained by emissions from other sources may indicate wildfire impacts. Attenuated backscatter density time series from the Laporte ceilometer are shown in Figure 5-37 through Figure 5-39. Figure 5-40 shows time series of the July 26-28 convective boundary layer height diagnosed from the ceilometer data by the University of Houston. All three days show strong backscatter consistent with the presence of enhanced levels of aerosols, with the deepest layer of higher values coming on July 26. The convective boundary layer height exceeded 3,000 m on all three days and no daytime inversion is present. The LaPorte ceilometer was offline from 7 pm (CST) on August 22 through August 28 so that no data are available for the August 23-24 period.

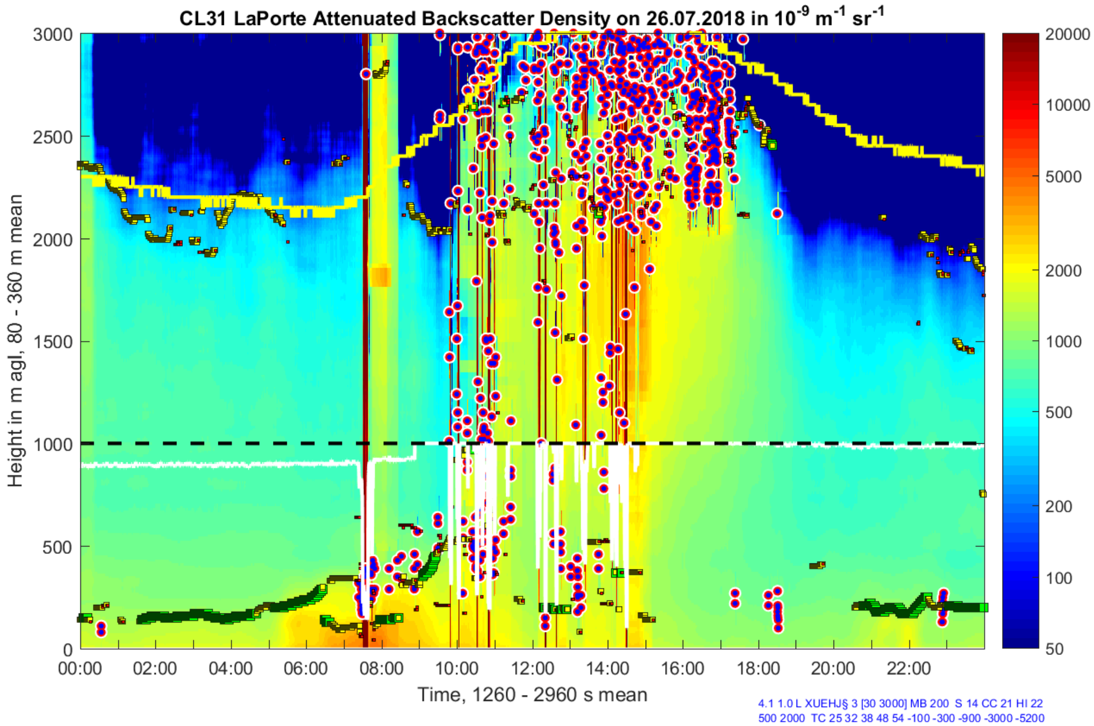

Figure 5-37. LaPorte ceilometer attenuated backscatter density for July 26. Blue filled circles indicate the presence of cloud and yellow squares indicate regions of strong vertical gradients in backscatter.

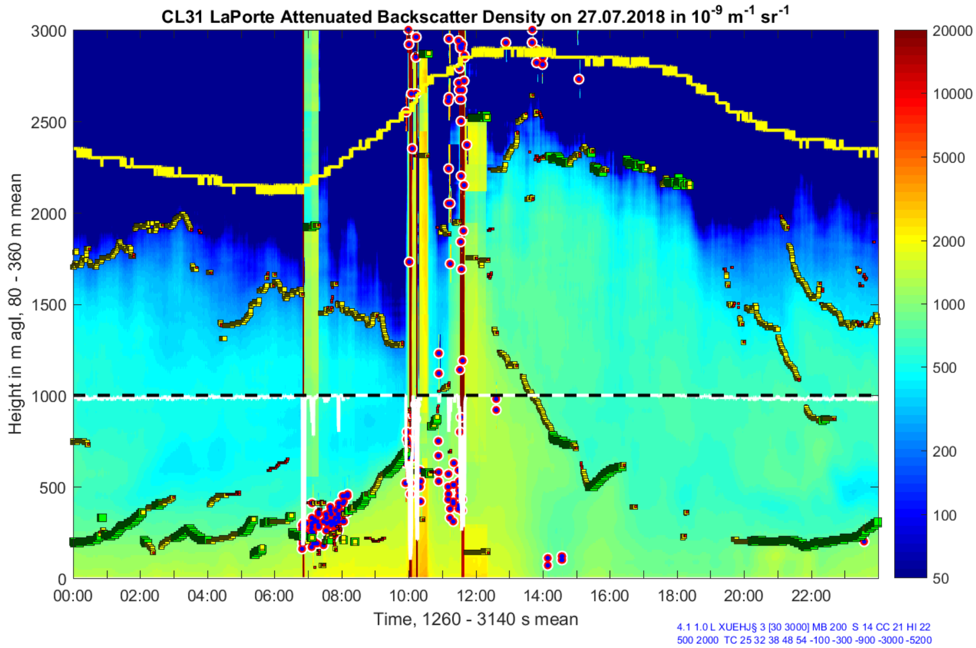

Figure 5-38. LaPorte ceilometer attenuated backscatter density for July 27. Blue filled circles indicate the presence of cloud and yellow squares indicate regions of strong vertical gradients in backscatter.

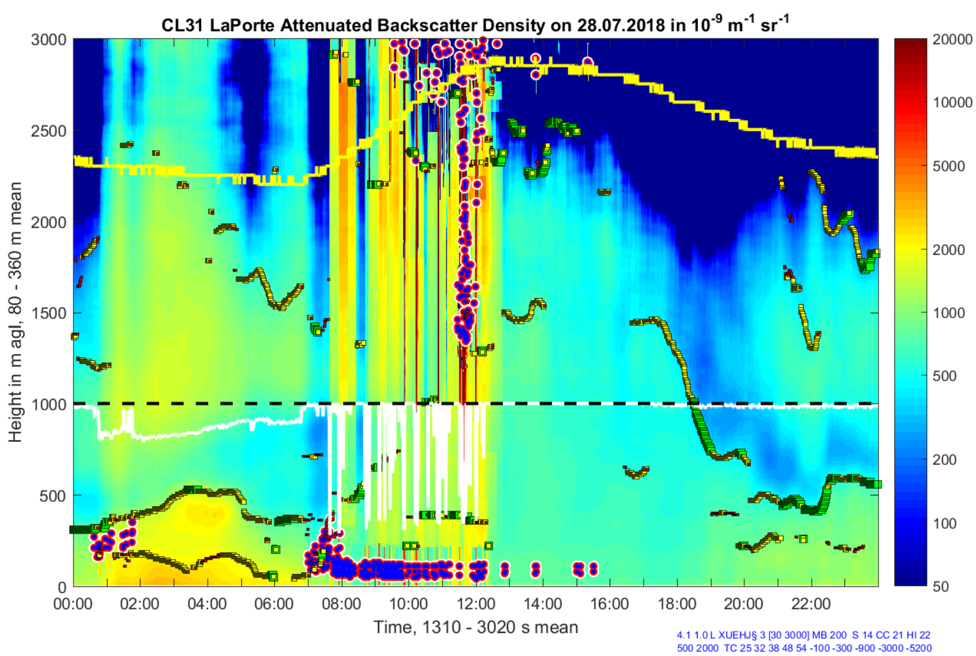

Figure 5-39. LaPorte ceilometer attenuated backscatter density for July 28. Blue filled circles indicate the presence of cloud and yellow squares indicate regions of strong vertical gradients in backscatter.

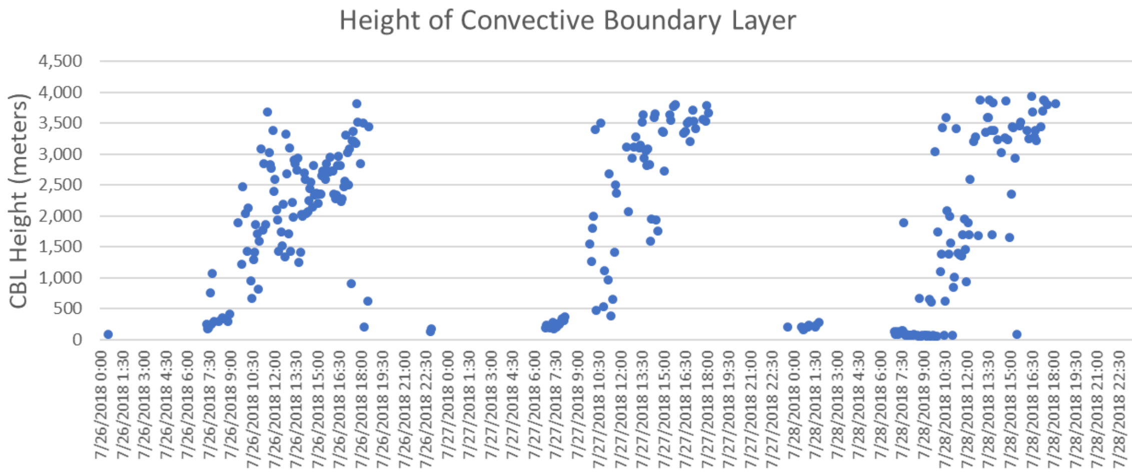

Figure 5-40. July 26-28, 2018 convective boundary layer depth over the LaPorte measurement site as diagnosed by University of Houston based on LaPorte ceilometer data.

5.2.4 Speciated $PM_{2.5}$ Measurements

Speciated $PM_{2.5}$ data can be used to determine whether emissions from fires influenced a monitor. The presence of the sugar anhydride levoglucosan (1,6-anhydro-β-D-glucopyranose) is a marker that is specific to biomass burning (e.g. Simoneit et al., 1999; Cheng et al., 2013; Zhang et al., 2013). Levoglucosan and its isomers mannosan and glactosan are released when cellulose or starches burn but is not released during the combustion of fossil fuels. The ratio of levoglucosan to other species (e.g. mannosan, Cheng et al., 2013) can be used to distinguish among different types of biomass burning. Fire plumes often contain elevated levels of organic carbon (OC) and may also enriched in water soluble potassium (Watson et al., 2001).

Speciated PM measurements for two Houston monitors (Clinton CAMS 403 and UH West Liberty CAMS 699) were provided to the TCEQ by the University of Houston. Data were provided for both monitors for the periods July 25-30, August 22-25 and September 17-18. Figure 5-41 shows the levoglucosan concentrations for each of these days at UH West Liberty CAMS 699 northeast of downtown Houston. Figure 5-42 shows measurements of organic carbon and soluble potassium. The measurements indicate the presence of the biomass burning marker levoglucosan at ground level in Houston on July 26 and 27 and August 23 as well as the presence of soluble potassium during July 26-28 and August 23-24. Soluble potassium is also associated with biomass burning plumes. Aside from levoglucosan, all other measured sugars (e.g. mannosan and galactosan) had zero concentration except for arabitol for at UH, but the arabitol concentrations are smaller than the uncertainty in the measurement and are not included here.

Concentrations of organic and elemental carbon and measured attenuation from black carbon were also enhanced during July 26-27 and August 23-24 relative to July 29-30 and September 16-18, the two non-event periods for which data were available (Figure 5-43, Figure 5-44). Measured attenuation from brown carbon was lower during July 26-28 and August 23-24 than during the July 29-30 and September 16-18 periods (Figure 5-45).

At Clinton CAMS 403, levoglucosan was present on August 23-24, but not during July 26-28. Soluble potassium was present during August 23-24. Concentrations of organic and elemental carbon and measured attenuation from black carbon were generally slightly larger during August 23-24 relative to July 29-30 and September 16-18, the two non-event periods for which data were available. There was no brown carbon attenuation at Clinton CAMS 403 during the July and August episode periods (Figure 5-50).

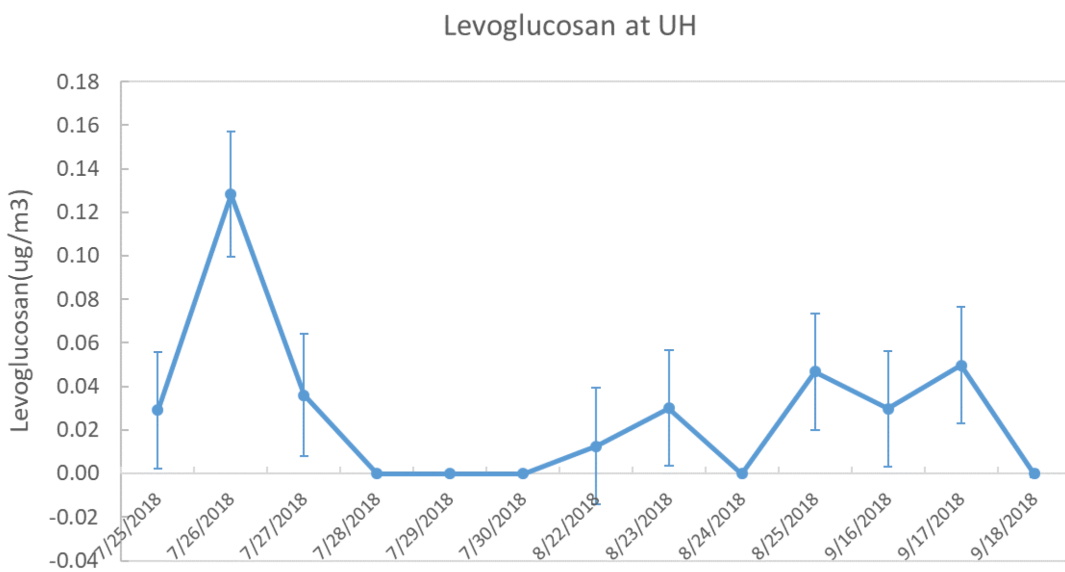

Figure 5-41. Levoglucosan measurements (solid blue) measurements and uncertainty bounds provided by the University of Houston from speciated PM data collected at UH West Liberty CAMS 699.

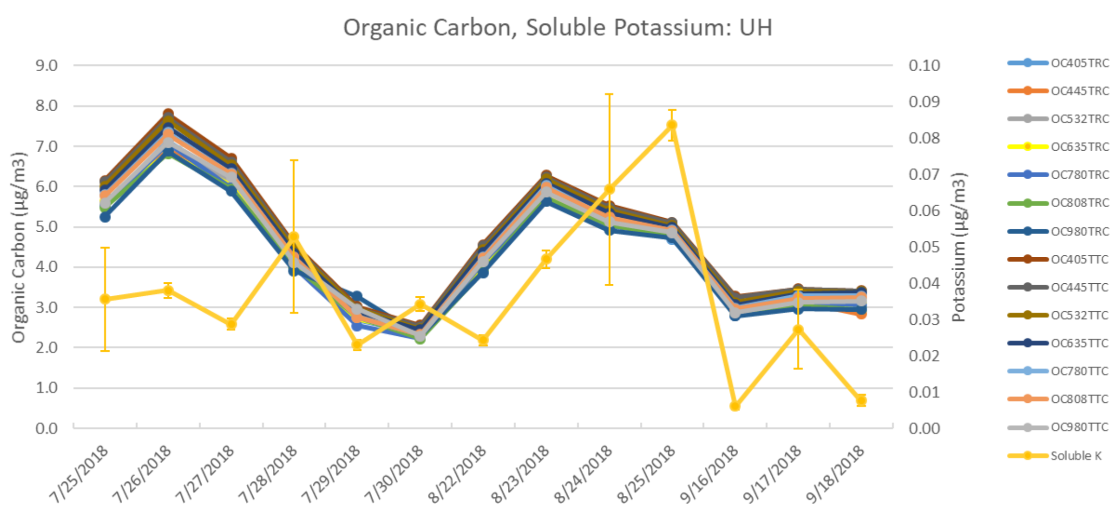

Figure 5-42. Organic carbon and soluble potassium measurements provided by the University of Houston from speciated PM data collected at UH West Liberty CAMS 699.

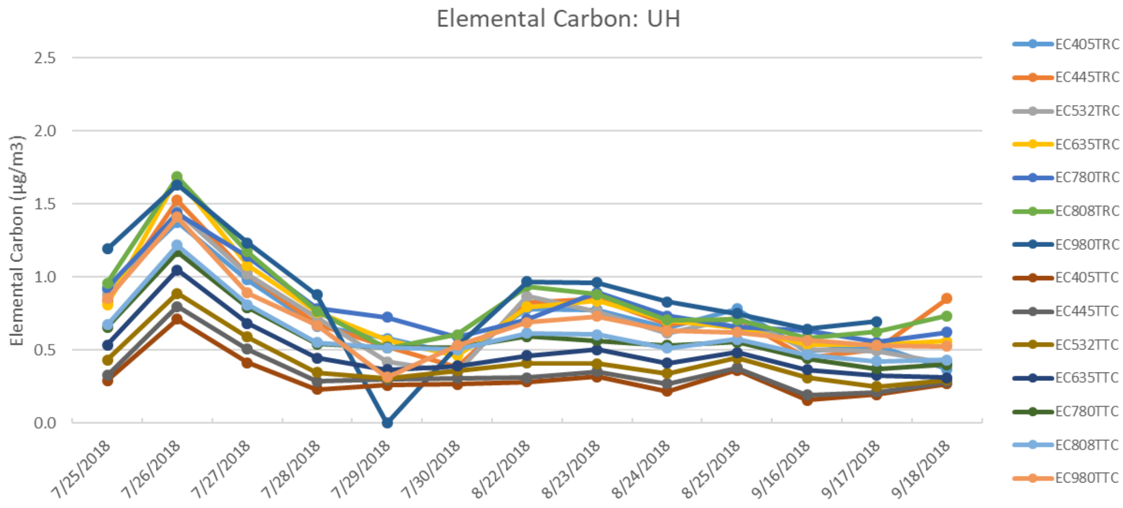

Figure 5-43. Elemental carbon measurements provided by the University of Houston from speciated PM data collected at UH West Liberty CAMS 699.

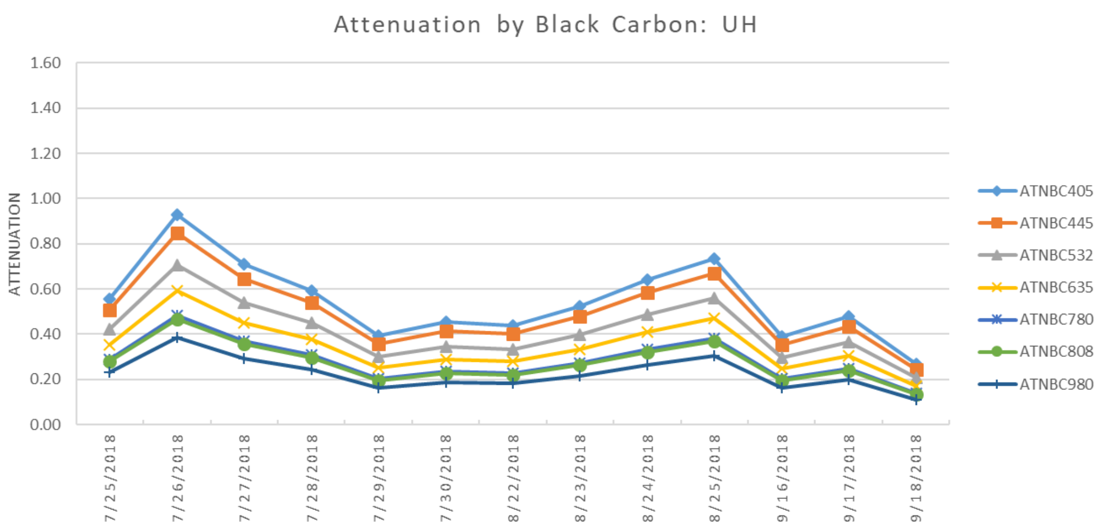

Figure 5-44. Black carbon attenuation measurements made by the University of Houston at UH West Liberty CAMS 699.

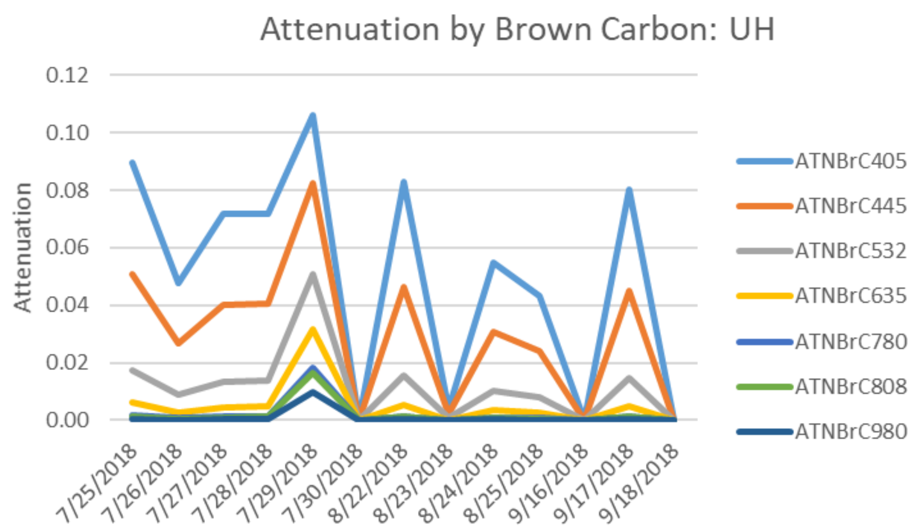

Figure 5-45. Brown carbon attenuation measurements made by the University of Houston at UH West Liberty CAMS 699.

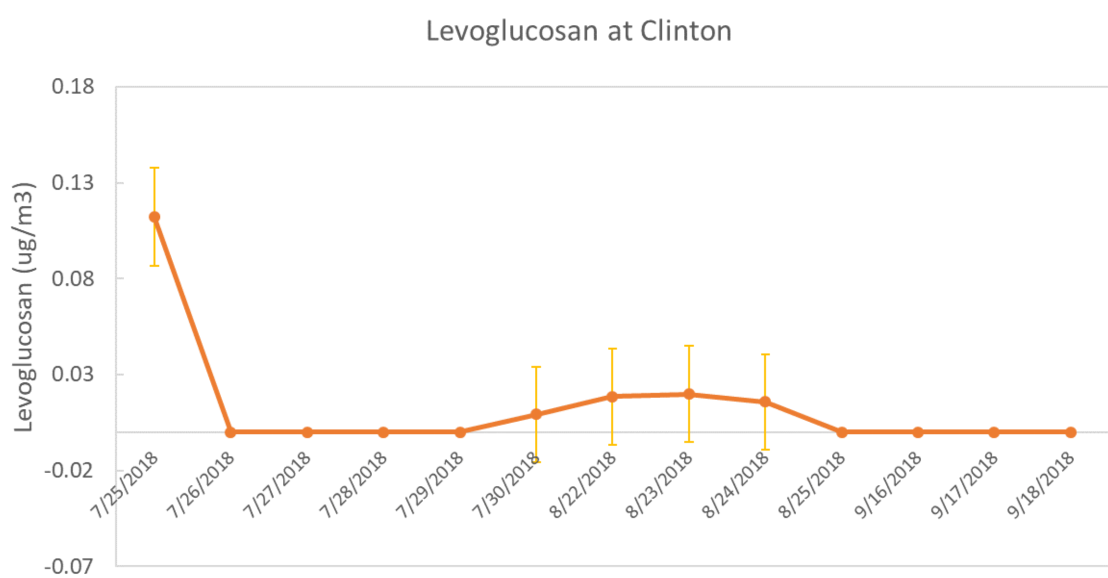

Figure 5-46. Levoglucosan (solid orange) measurements and uncertainty bounds provided by the University of Houston from speciated PM data collected at Clinton CAMS 403.

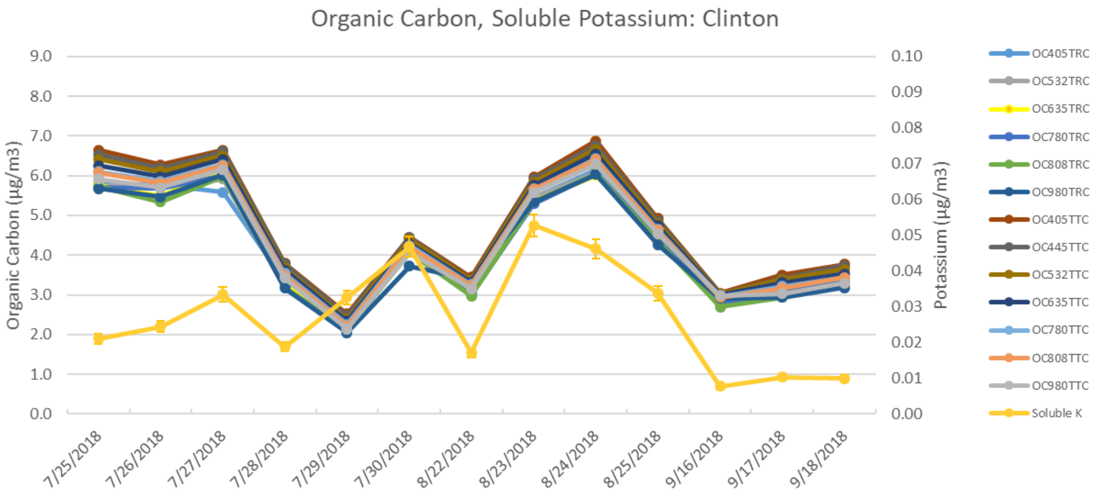

Figure 5-47. Organic carbon and soluble potassium measurements provided by the University of Houston from speciated PM data collected at Clinton CAMS 403.

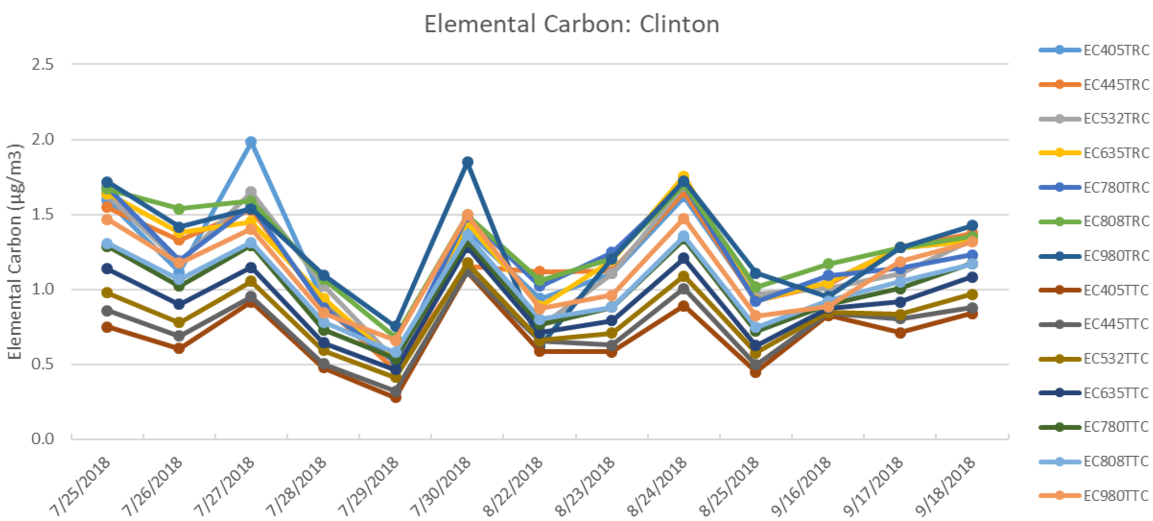

Figure 5-48. Elemental carbon measurements provided by the University of Houston from speciated PM data collected at Clinton CAMS 403.

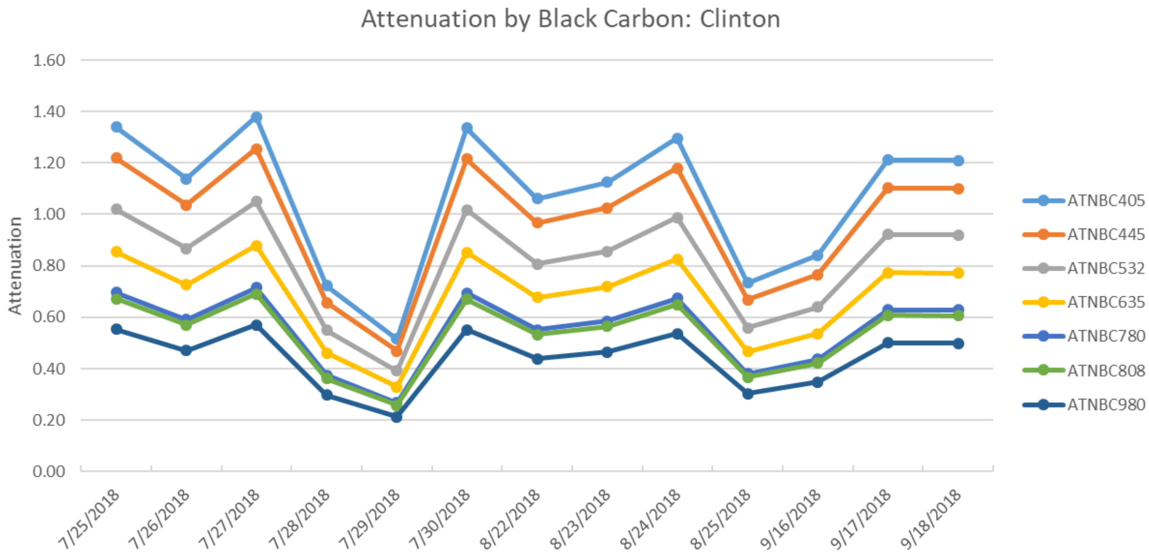

Figure 5-49. Black carbon attenuation measurements made by the University of Houston at Clinton CAMS 403.

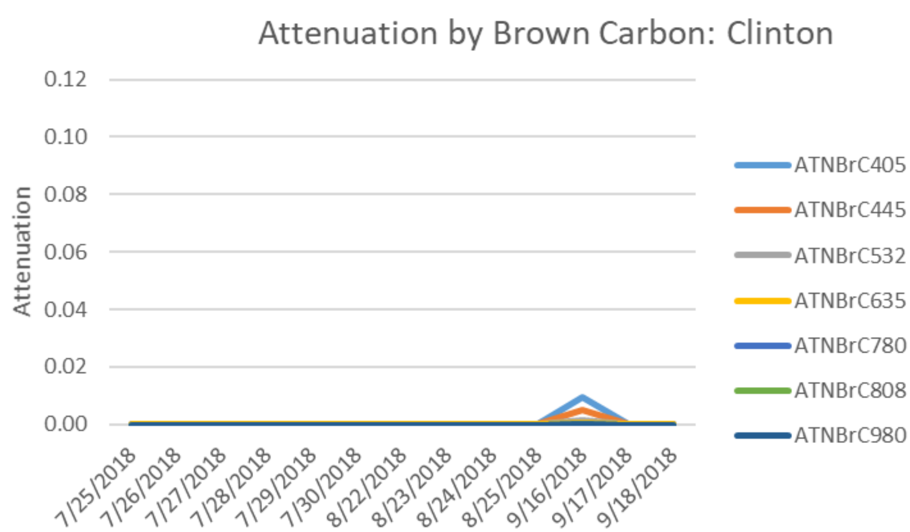

Figure 5-50. Brown carbon attenuation measurements made by the University of Houston at Clinton CAMS 403.

5.2.5 Satellite Aerosol Optical Depth Retrievals over the Houston Area during July – August Episode Days

The TCEQ analyzed satellite imagery from NASA's EOSDIS Worldview website[16] and NOAA's Aerosol Watch website[17] to evaluate whether smoke was present over Houston during the July and August

[16] https://worldview.earthdata.nasa.gov/

[17] https://www.star.nesdis.noaa.gov/smcd/spb/aq/AerosolWatch/

2018 ozone episode days. Retrieval of AOD is not possible in the presence of clouds and so cloudy areas appear as areas of missing data in the AOD images in this section. The AOD and Angstrom aerosol exponent (AAE) images were developed by NOAA using the Deep Blue algorithm, which is optimized for retrievals over land, so the AOD and AAE fields are displayed for land areas only. AOD values of less than 0.1 indicate low levels of aerosol characteristic of clear blue sky, bright sun and maximum visibility. Values greater than 0.5 indicate the presence of aerosol.

The left panel of Figure 5-51 shows satellite images of AOD over the Houston area with values ranging from approximately 0.4-0.7 indicating that there were enhanced levels of aerosol in the atmosphere over Houston on June 26. Values of the Angstrom aerosol exponent (AAE) over Houston area range from 0 (olive green) to 1.77 (purple) (right panel of Figure 5-51). Values of the AAE exceeding 1 are associated with fine particles, suggesting particles of a size consistent with smoke were present over Houston on July 26.

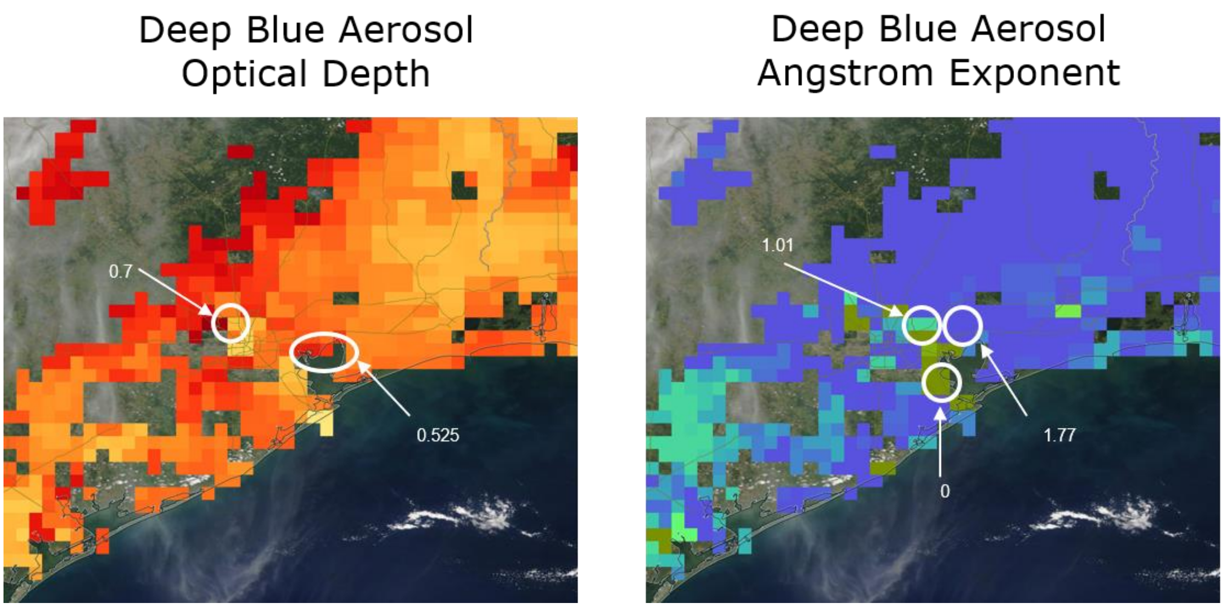

Figure 5-51. NASA EOSDIS Aqua/MODIS imagery for July 26, 2018. Left panel shows Deep Blue AOD and right panel shows Deep Blue Aerosol Angstrom Exponent. Grid cell values are shown in white type

AOD values over the Houston stayed high on July 27 and July 28 (Figure 5-52 and Figure 5-53). On July 27, AOD ranged from approximately 0.075 to 0.485 indicating that there were continuing enhanced levels of aerosol in atmosphere over Houston. Values of the AAE over the Houston area on July 27 ranged from 0 (olive green) to 1.78 (blue) suggesting particles of a size consistent with smoke were present on July 27. AOD and AAE values remained high on July 28, with AAE greater than 1 over most of the region, indicating the continuing presence of smoke.

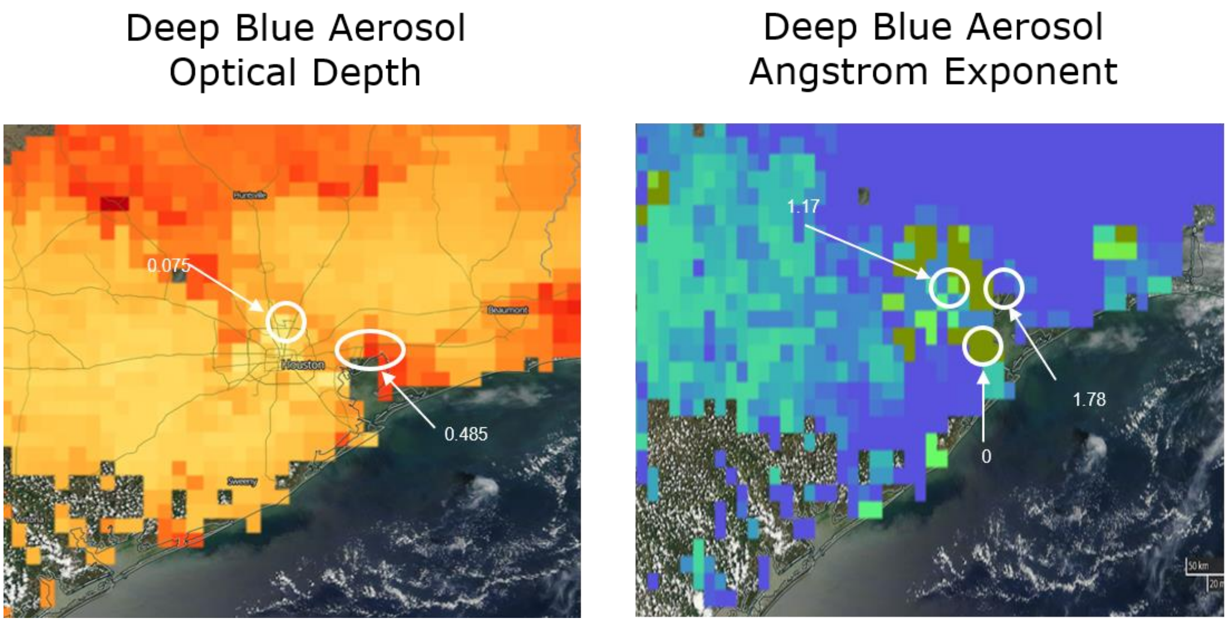

Figure 5-52. Terra/MODIS imagery for July 27, 2018. Left panel shows AOD and right panel shows Deep Blue Aerosol Angstrom Exponent. Grid cell values are shown in white type.

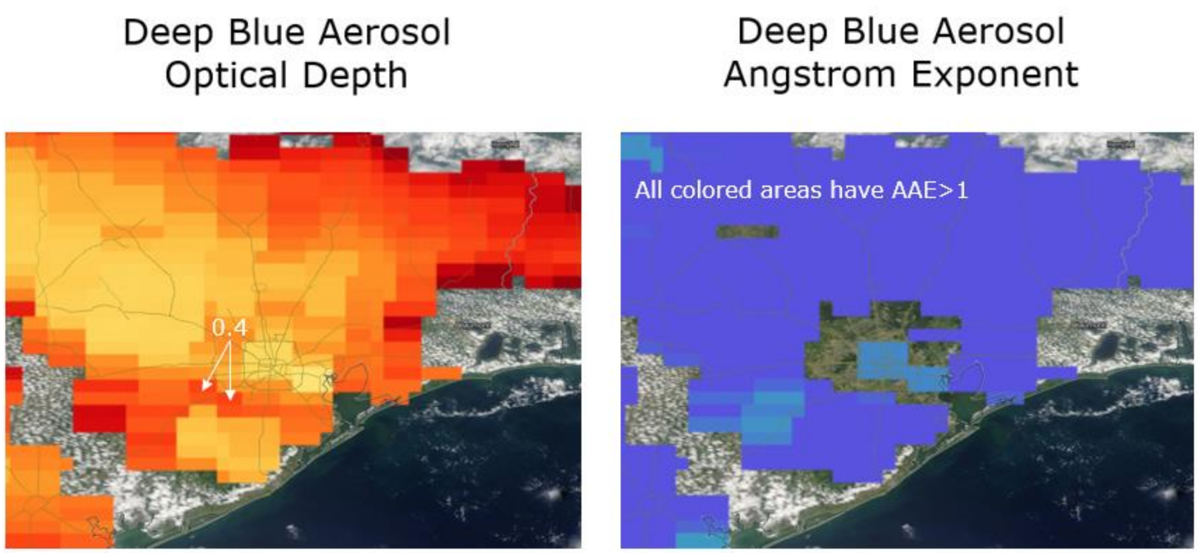

Figure 5-53. Terra/MODIS imagery for July 28, 2018. Left panel shows AOD and right panel shows Deep Blue Aerosol Angstrom Exponent. Grid cell values are shown in white type.

NOAA Aerosol Watch imagery from the GOES 16 satellite also shows the presence of enhanced aerosol levels over the Houston area and surrounding areas of Texas and Louisiana during July 26-28 (Figure 5-54 through Figure 5-56). The spatial coverage of the AOD retrieval is reduced by the presence of fair weather cumulus clouds, but enhanced levels of aerosols over Houston are intermittently visible.

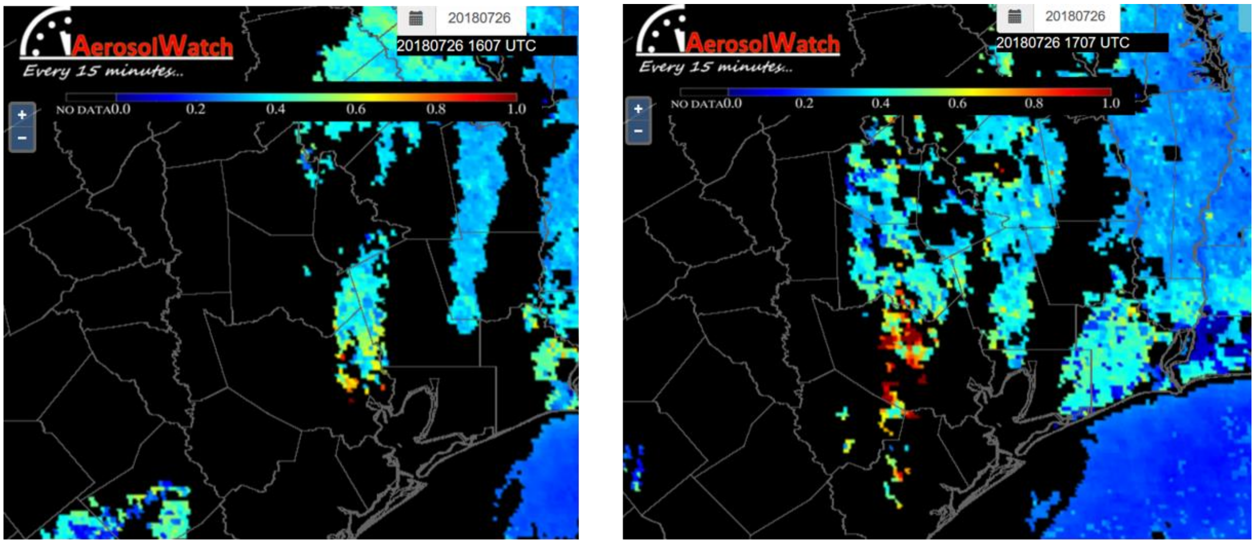

10:07 AM (CST) 11:07 AM (CST)

Figure 5-54. GOES-16 AOD imagery at 10:07 am (CST) and 11:07 am (CST) on July 26, 2018.

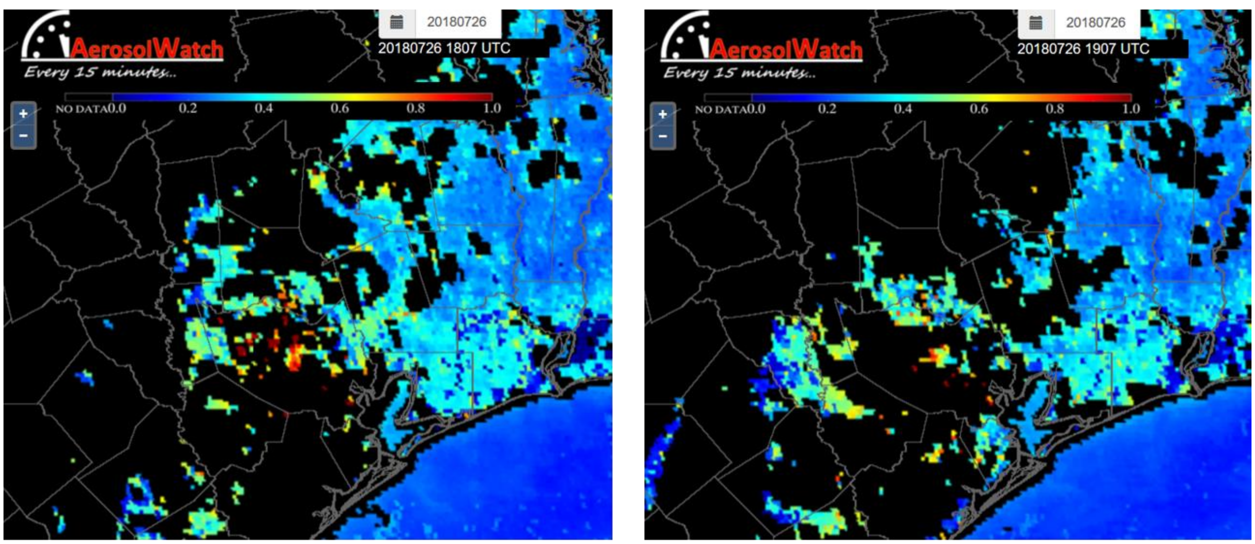

12:07 PM (CST) 1:07 PM (CST)

Figure 5-55. GOES-16 AOD imagery at 12:07 pm (CST) and 1:07 pm (CST) on July 26, 2018.

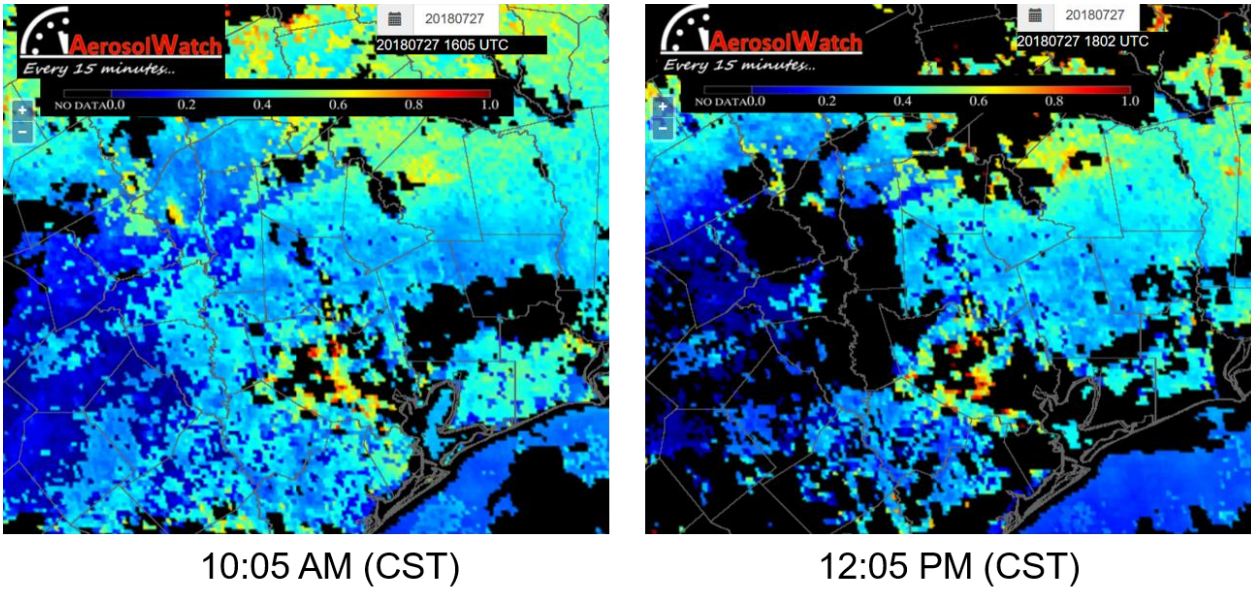

Figure 5-56. GOES-16 AOD imagery at 10:05 AM (CST) and 12:05 pm (CST) on July 27, 2018.

The preceding satellite AOD images show column integrated quantities that provide information on the total amount of aerosol between the satellite instrument and the earth's surface. Total column AOD retrievals cannot distinguish between an aerosol layer close to earth's surface and one high in the atmosphere that does not affect ground level air quality. The Cloud-Aerosol Lidar and Infrared Pathfinder Satellite Observation (CALIPSO) satellite carries an active lidar instrument with passive infrared and visible imagers that allows retrieval of information on the vertical structure and properties of clouds and aerosols. CALIPSO data indicate the altitude of aerosol layers in the atmosphere. Because the satellite is a polar orbiter and the laser instrument has a narrow field of view, there was only one CALIPSO overpass of the Houston area during the July 26-28 and August 23-24 episodes. Figure 5-57 shows TCEQ's analysis of imagery from a CALIPSO overpass of the Houston Area on July 27. The CALIPSO retrieval shows a deep layer of aerosol over Houston at an altitude of approximately 0-3 km. CALIPSO analysis product indicates the aerosol layer is consistent with biomass burning and polluted dust. The UH ceilometer data (Figure 5-38) indicate that aerosols between 0-3 km are within the mixed layer during July 27, consistent with an aerosol layer that mixed down to the ground.

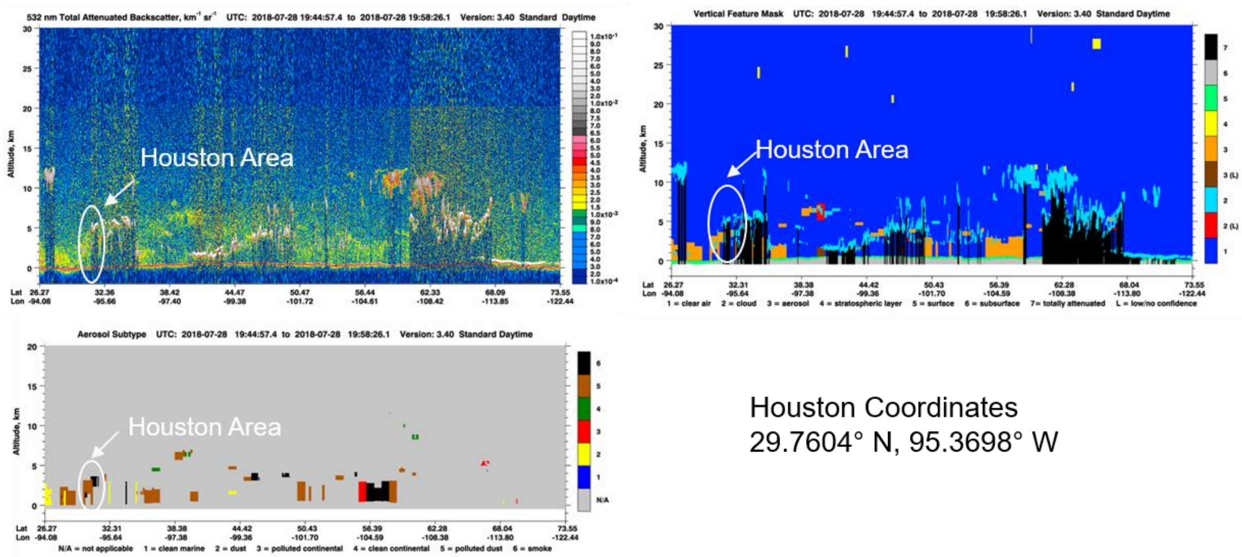

Figure 5-57. CALIPSO total attenuated backscatter (upper left panel), vertical feature mask (upper right panel) and aerosol subtype (lower left panel) from an overpass of the Houston area on approximately 3:50 pm CST July 27, 2018[18].

On August 23, AOD values over the Houston area ranged from approximately 0.185 to 0.7 indicating that there were heightened levels of aerosol in atmosphere over Houston (Figure 5-58). Values of the Houston area range from 0 (olive green) to 1.78 (purple) suggesting particles of a size consistent with smoke were present on August 23. NOAA Aerosol Watch imagery from the GOES 16 satellite also shows the presence of enhanced aerosol levels over the Houston area and surrounding areas of Texas and Louisiana and the Gulf of Mexico during August 23 (Figure 5-59). The spatial coverage of the AOD retrieval is reduced by the presence of clouds, but the signal of enhanced levels of aerosols over Houston is visible.

[18] https://www-calipso.larc.nasa.gov/products/lidar/browse_images/show_detail.php?s=production&v=V3-40&browse_date=2018-07-28&orbit_time=19-18-00&page=3&granule_name=CAL_LID_L1-ValStage1-V3-40.2018-07-28T19-18-00ZD.hdf

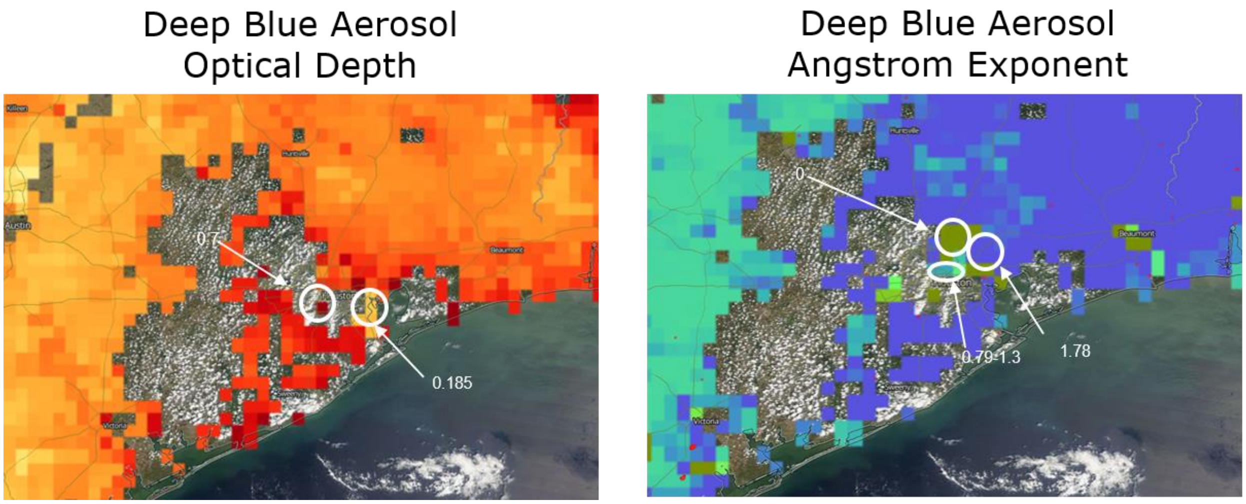

Figure 5-58. Terra/MODIS imagery for August 23, 2018. Left panel shows AOD and right panel shows Deep Blue Aerosol Angstrom Exponent. Grid cell values are shown in white type.

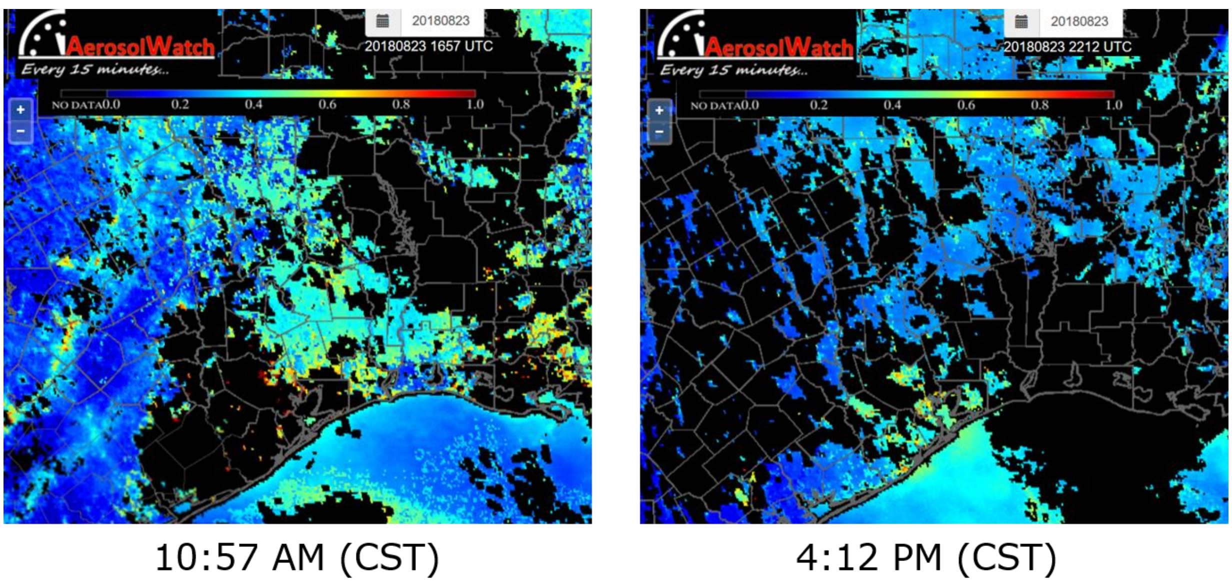

Figure 5-59. GOES-16 AOD imagery at 10:57 AM (CST) and 4:12 pm (CST) on August 23, 2018.

On August 24, AOD values over the Houston area ranged from approximately 0.240 to 0.7 indicating that there were heightened levels of aerosol in atmosphere over Houston (Figure 5-60). Values of the Houston area range from 0.57 (aqua) to 1.78 (purple) suggesting particles of a size consistent with smoke were present on August 24.

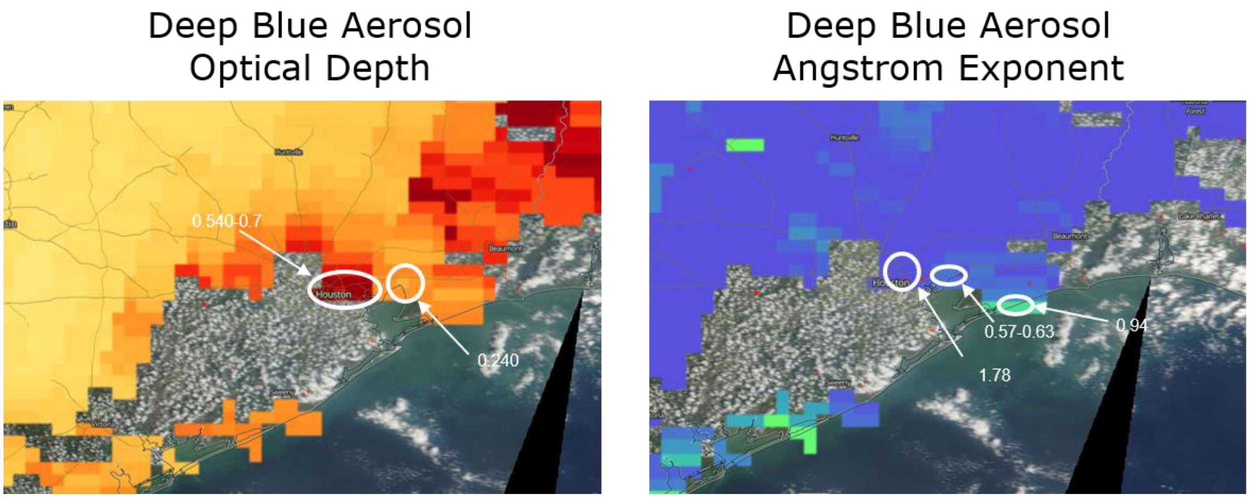

Figure 5-60. Terra/MODIS imagery for August 24, 2018. Left panel shows AOD and right panel shows Deep Blue Aerosol Angstrom Exponent. Grid cell values are shown in white type.

5.3 Evidence that the Fire Emissions were Transported to the Monitors

In this section, we present evidence that fire emissions and their chemical products were transported to the Houston Bayland Park CAMS 53 and Aldine CAMS 8. We analyze HYSPLIT back trajectories to evaluate source-receptor relationships in Section 5.3.1 and review evidence of transport from satellite and meteorological data products in Section 5.3.2.

5.3.1 HYSPLIT Back Trajectory Analysis

We used NOAA's Hybrid Single-Particle Lagrangian Integrated Trajectory (HYSPLIT) model with three-dimensional, gridded, archived weather forecast model data to evaluate the source-receptor relationships for wildfires preceding high ozone at Houston Bayland Park CAMS 53 and Aldine CAMS 8. Because the LaPorte ceilometer measurements (Figure 5-40) indicated a mixed layer depth reaching upwards of 3,000 m at times during the July episode, we prepared trajectories ending at three different altitudes: 500 m, 1,000 m and 2,500 m. This is to allow for the presence of vertical wind shear within the mixed layer which can cause air to be transported to Houston from different directions at different altitudes. Because back trajectories can vary depending on the meteorological analysis used to drive HYSPLIT, we used three meteorological analyses for each back trajectory: the National Centers for Environmental Prediction (NCEP) North American Model (NAM) 12 km analysis, the NCEP Eta Data Assimilation System (EDAS) 40 km analysis and the NCEP North American Regional Reanalysis (NARR) 36 km analysis.

5.3.1.1 July Episode HYSPLIT Trajectory Analysis

We began by preparing HYSPLIT back trajectories that began at Bayland Park CAMS 53 at the time of peak 1-hour average ozone on July 26 (Figure 5-61) and at Aldine CAMS 8 at the time of peak 1-hour average ozone on July 27 (Figure 5-62) and July 28 (Figure 5-63). 5-day HYSPLIT[19] back trajectories using the NAM 12 km, EDAS 40 km and NARR 36 km meteorological analyses are consistent in showing that air arriving at 500 m and 1,000 m above ground level at Bayland Park and Aldine on July

[19] The National Oceanographic and Atmospheric Administration's (NOAA's) Hybrid Single-Particle Lagrangian Integrated Trajectory (HYSPLIT) model.

26 and 27 travelled southward from the Midwest and southern Ontario through the Mississippi Valley and Louisiana before arriving in Houston. For air parcels arriving at 2,500 m above Houston on July 26-27, the back trajectories for the three analyses indicate different origins. The NAM and EDAS analysis 5-day back trajectories extend northwest from Houston toward California, Oregon and British Columbia, while the back trajectories for the NARR analysis are consistent with the lower level back trajectories and extend northward from Houston toward the central US and southern Canada.

We also prepared a HYSPLIT frequency analysis using on-line tools provided by NOAA through their READY website. In the frequency analysis, a back trajectory was begun every three hours during July 26-28 and allowed to run backward for 120 hours (5 days). A 1°x1° grid was laid out on the domain and the number of trajectory points in each grid cell was tabulated. Plots of the resulting trajectory frequency field are shown in Figure 5-64.

The back trajectory frequency field gives a more comprehensive view of the origins of air during the July 26-28 episode. The results are consistent with the back trajectories for the times of peak 1-hour average ozone in suggesting that air arriving in the lowest 1,000 m of the atmosphere travelled from Canada and the Midwest through the Mississippi Valley and Louisiana before arriving in Houston. For air parcels arriving at 2,500 m above Houston on July 26-27, all three analyses show back trajectories extending back through California, Oregon and British Columbia, however these trajectories are less frequent in the NARR analysis than in the NAM and EDAS analyses.

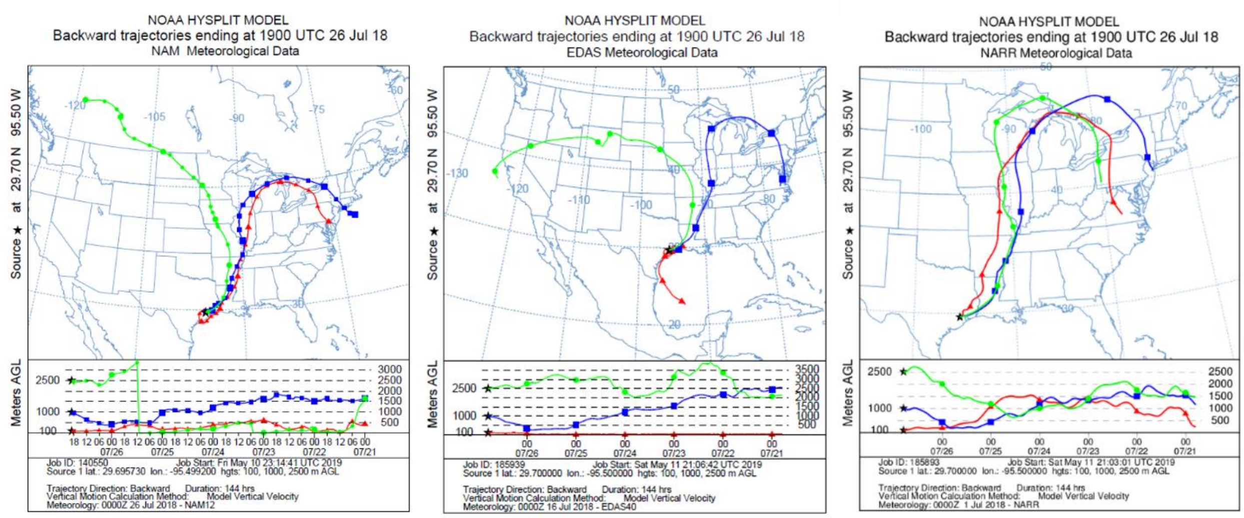

Figure 5-61. HYSPLIT 5-day back trajectories ending at Bayland Park CAMS 53 on July 26, 2018 at 1 pm CST, the time of the maximum daily 1-hour average ozone.

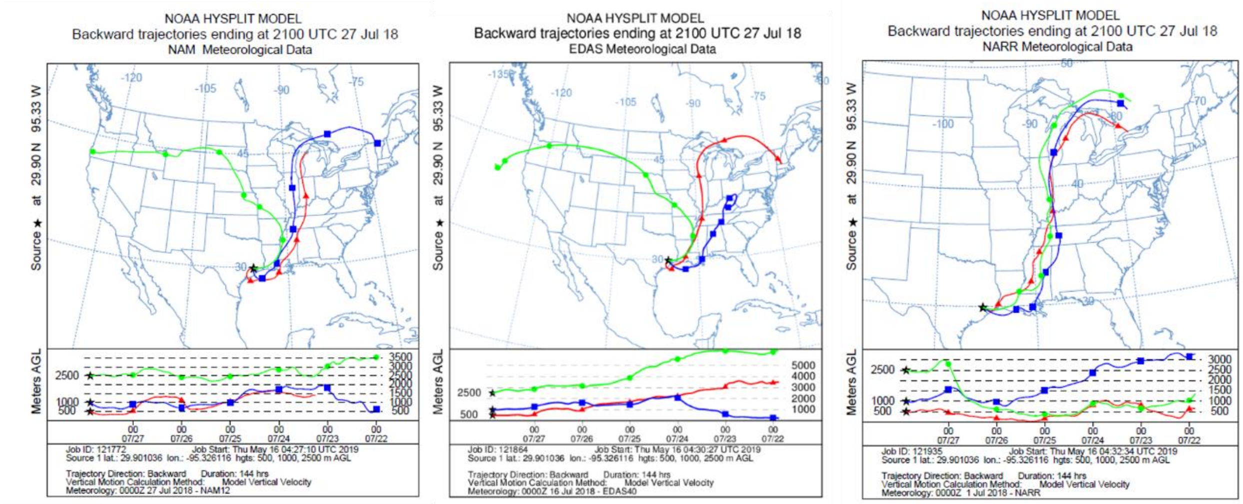

Figure 5-62. HYSPLIT 5-day back trajectories ending at Aldine CAMS 8 on July 27, 2018: MDA1 at 3 pm CST, the time of the maximum daily 1-hour average ozone.

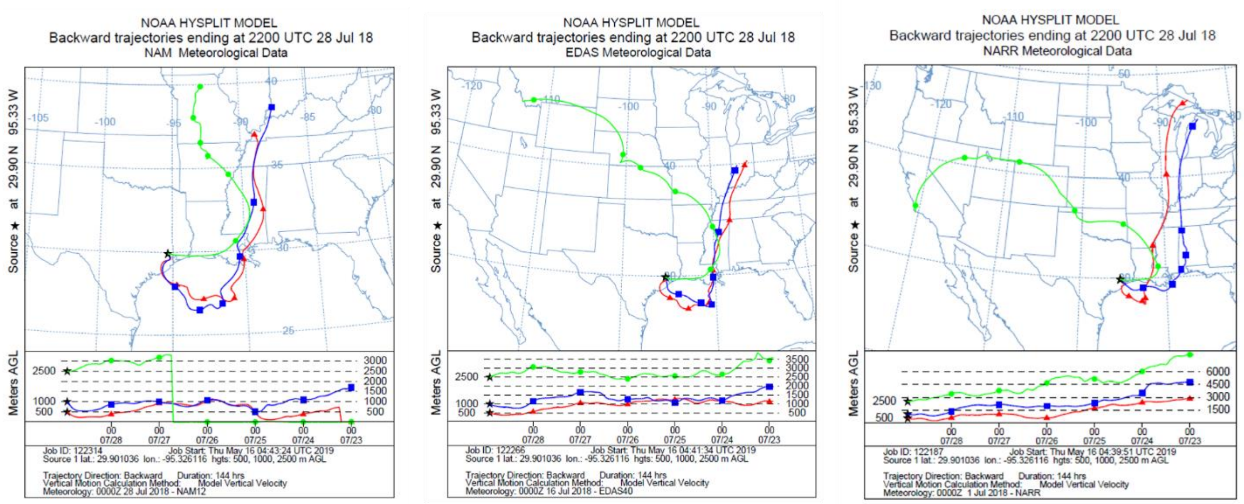

Figure 5-63. HYSPLIT 5-day back trajectories ending at Aldine CAMS 8 on July 28, 2018: MDA1 at 4 pm CST, the time of the maximum daily 1-hour average ozone

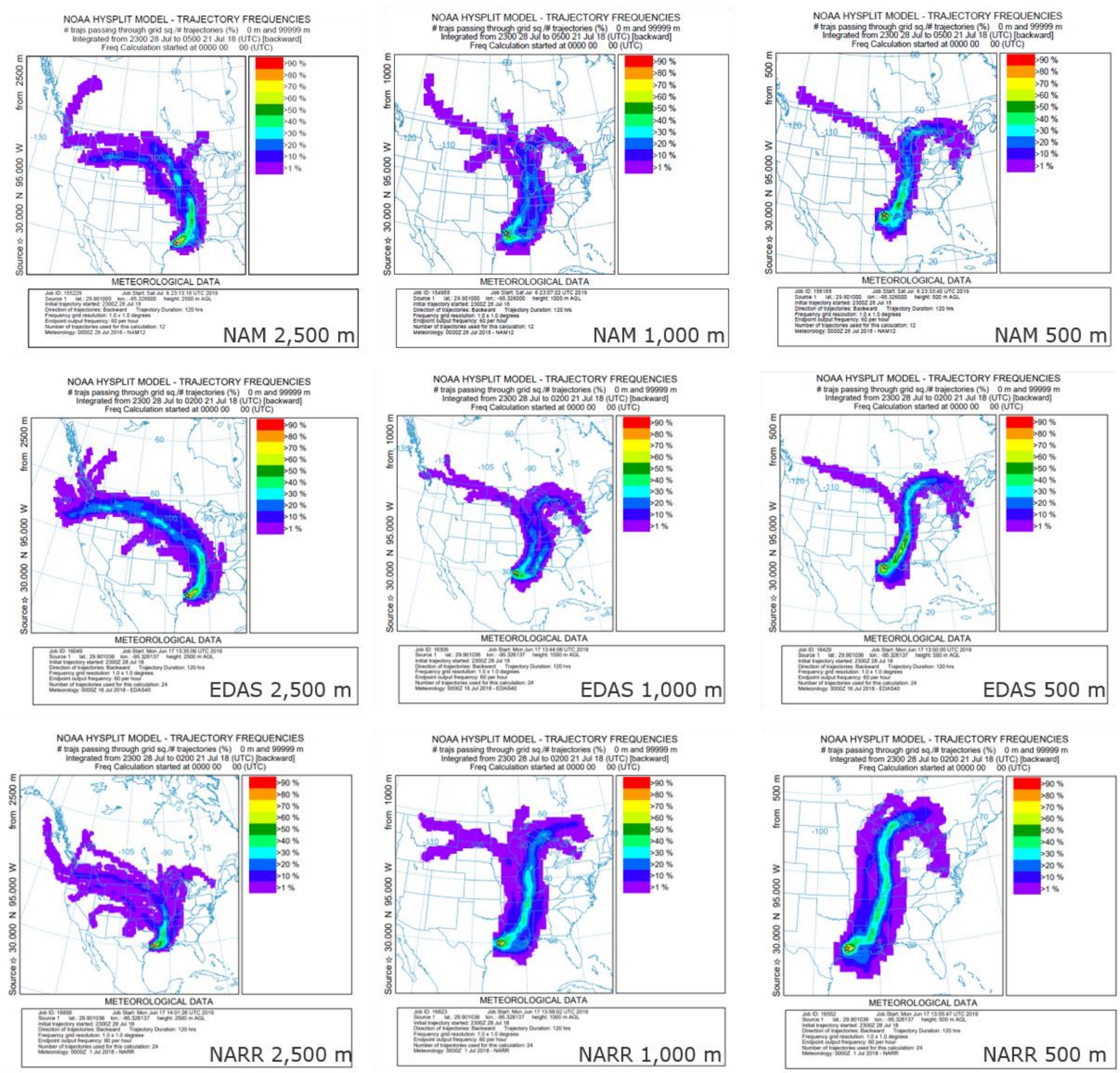

Figure 5-64. HYSPLIT 5-day back trajectory frequency analysis for the July 26-28 episode. Upper panels: HYSPLIT back trajectories using the NAM 12 km meteorological analysis ending in Houston at 2,500 m (left panel), 1,000 m (center panel) and 500 m (right panel). Middle panels: as in upper panels for HYSPLIT back trajectories run with the EDAS 40 km meteorological analysis. Lower panels: as in upper panels for HYSPLIT back trajectories run with the NARR 36 km meteorological analysis.

We reviewed the FINN fire emission inventory to identify large wildfires that were upwind of Bayland Park CAMS 53 and Aldine CAMS 8 during July 26-28 (Figure 5-65). The largest fires burning during the week before the Houston high ozone episode were the Ferguson Complex in central California, the Garner and South Umpqua Complexes in southwest Oregon, the North Bay Complex near the Ontario/Quebec border and fires on the Ontario/Manitoba border. Next, we ran a matrix of 5-day forward trajectories from areas encompassing the fire complexes to establish whether a source-receptor relationship existed for the fire complex regions and Aldine CAMS 8 and Bayland Park CAMS 53.

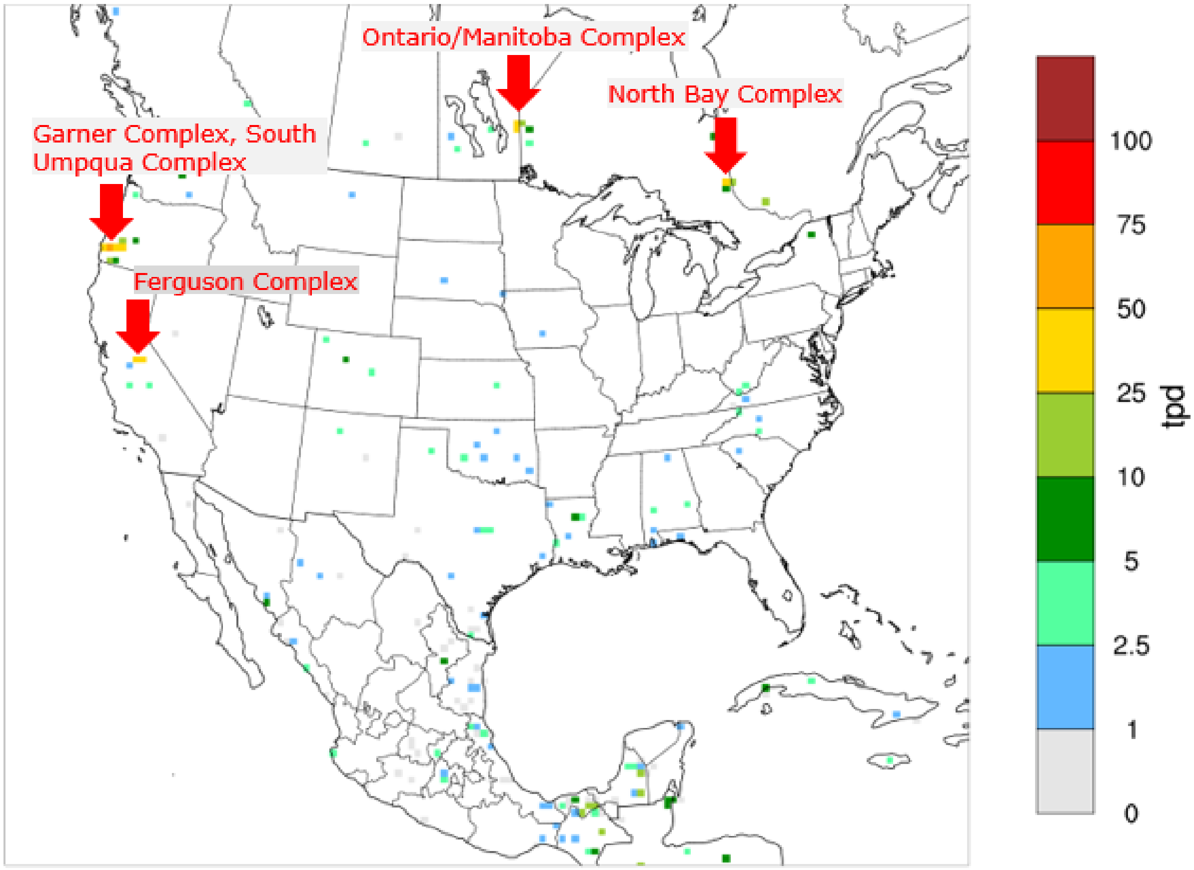

Figure 5-65. FINN fire NOx emissions (tpd) for July 21, 2018. Red arrows indicate large fire complexes determined to be upwind of Houston based on HYSPLIT back trajectory analysis (Figure 5-64).

Figure 5-66 shows HYSPLIT forward trajectories prepared with the EDAS, NARR and NAM analyses and originating at multiple heights indicate that air moved from the North Bay Complex region southward through the Mississippi Valley and Louisiana and into East Texas and the Houston area. Figure 5-67 indicates that air originating from the fire complex on the Ontario/Manitoba border did not travel toward Houston but circulated in a counter clockwise direction before being advected toward the eastern Canada and the northeast US. Forward trajectory matrices for July 21 had a similar pattern and did not suggest a transport path between the Ontario/Manitoba border fires and Houston (not shown). Figure 5-68 showed that most trajectories originating in a matrix encompassing the California/Oregon area did not travel toward Houston, but that air generally moved offshore or eastward across the US without curving southward toward Texas. However, several trajectories starting at 3,000 m showed a transport path between the fire region and Texas did exist.

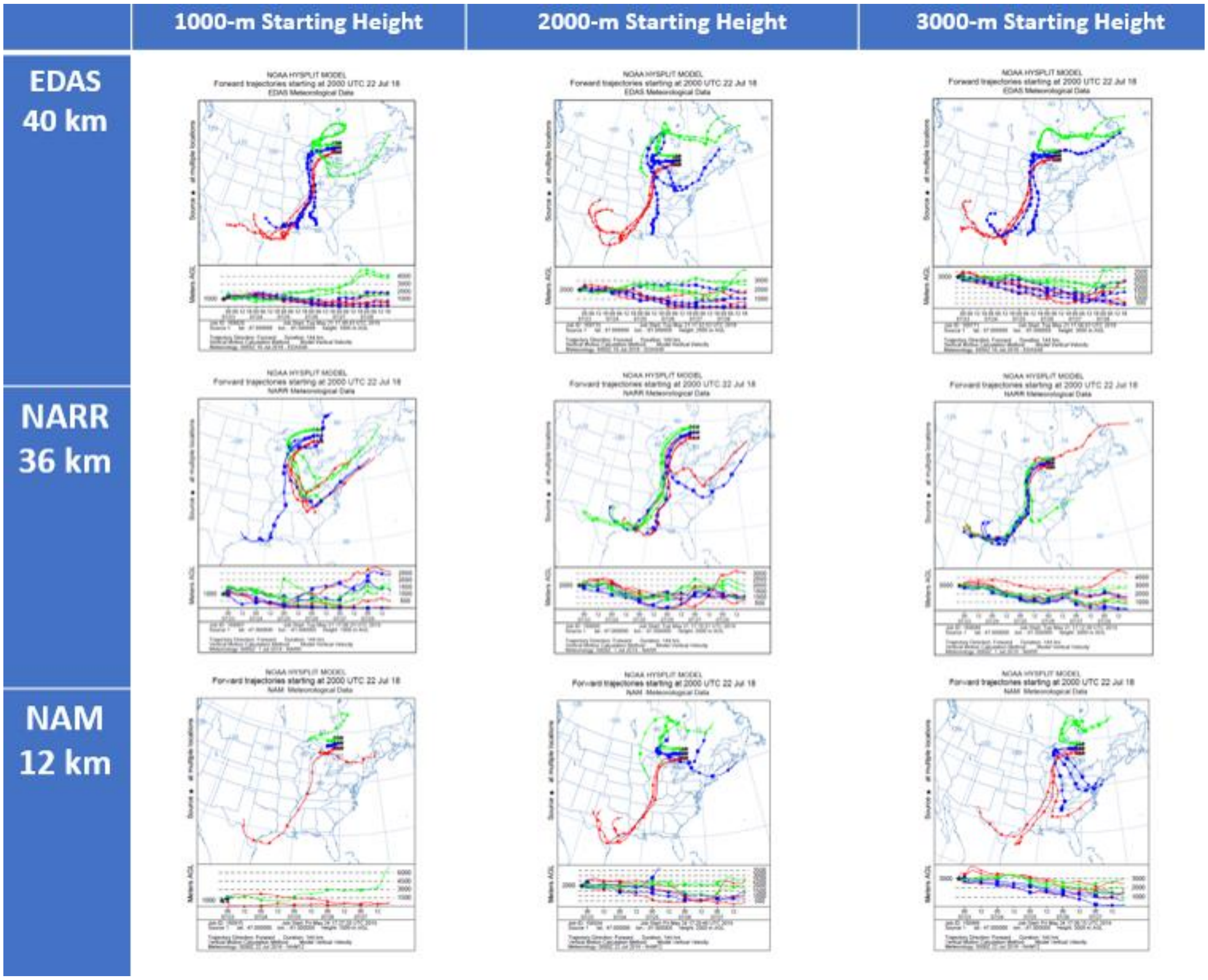

Figure 5-66. HYSPLIT 5-day forward trajectory matrices starting from North Bay Fire Complex region Ontario on 20 UTC July 22, 2018.

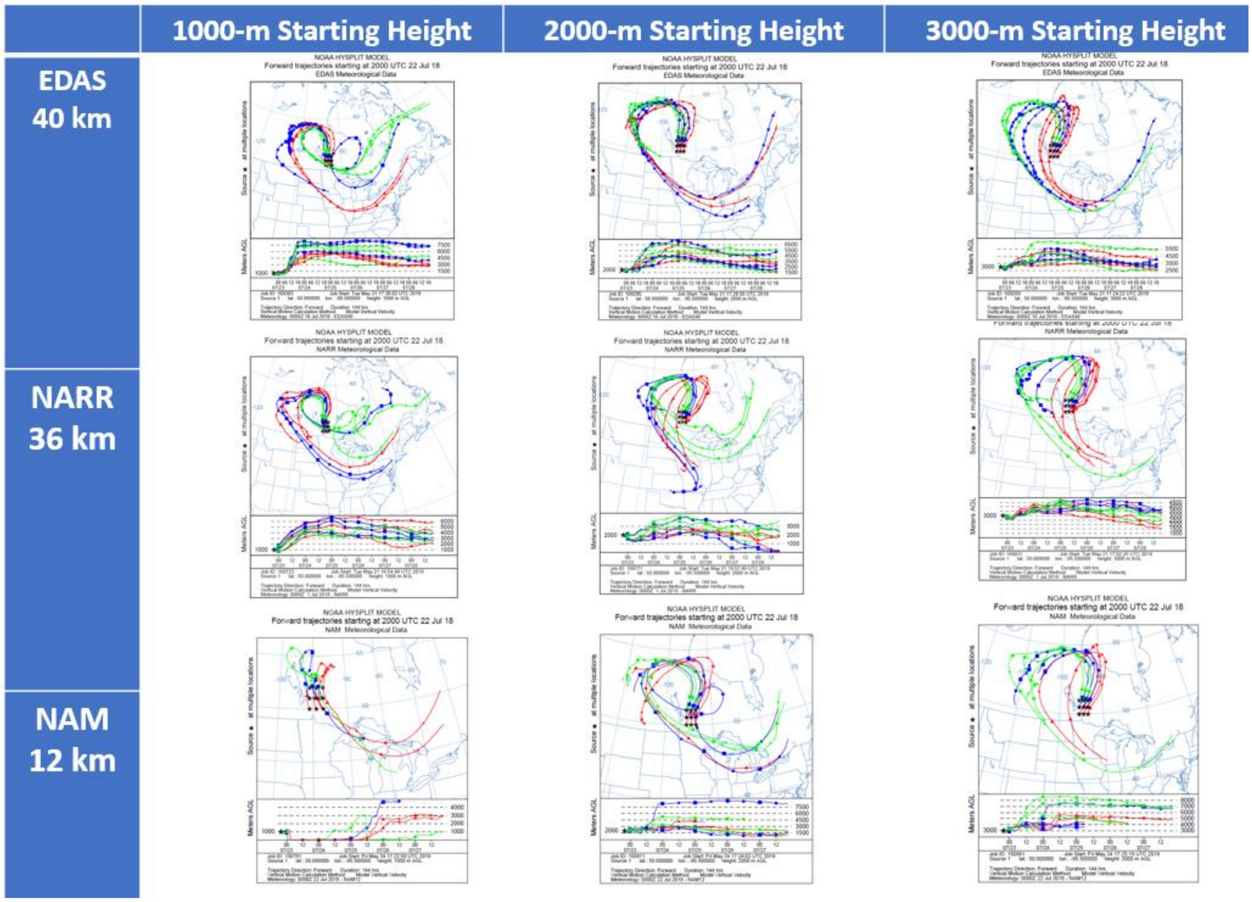

Figure 5-67. HYSPLIT 5-day forward trajectory matrices starting from the Ontario/Manitoba border fire area 20 UTC July 22, 2018.

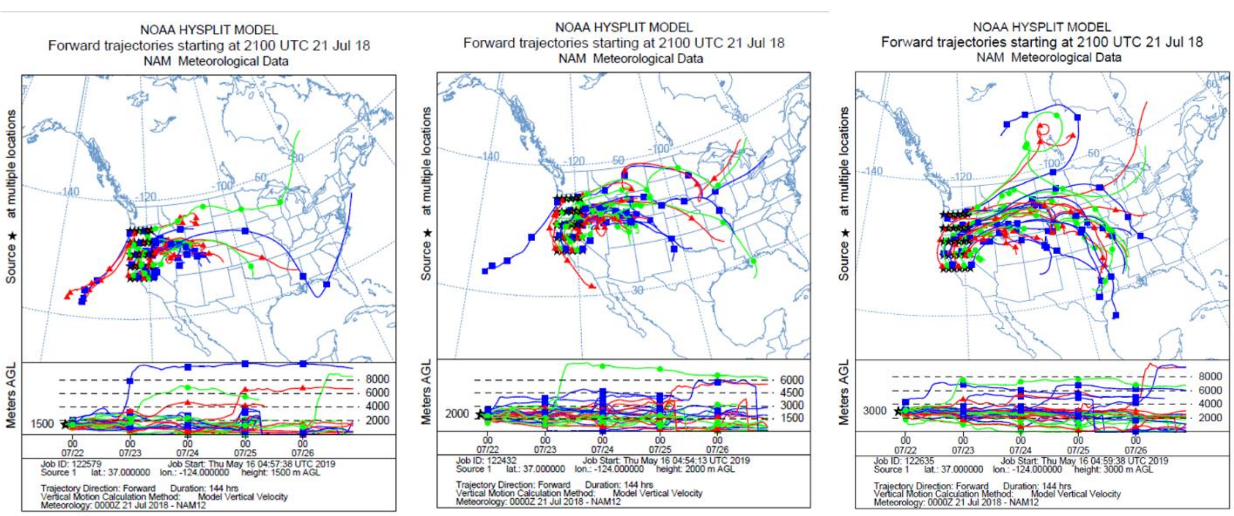

Figure 5-68. HYSPLIT 5-day forward trajectory matrices starting from a region encompassing the California and Oregon fire complexes 21 UTC July 21, 2018.

Based on the results of the forward trajectory matrix screening, we focused on the North Bay Complex in Ontario and the Garner and South Umpqua Complexes in Oregon to isolate whether the actual fire locations showed evidence of transport from the fires to Houston. We ran forward trajectories for the location of the FINN fire emissions shown in Figure 5-65 for each hour for a three-day period starting June 21 and running through June 23. For each hour, we ran HYSPLIT forward trajectories from the fire location starting at 1,000, 2,000 and 3,000 m. We used a variety of starting heights because we did not have information on plume rise altitude for the fires. The HYSPLIT forward trajectories indicate that there was the potential for air to be transported from the North Bay Complex southward through Louisiana toward Houston arriving there during the July 26-28 period.

For the South Umpqua and Garner Complex fires, there were three trajectories that showed transport between these fires and Houston (Figure 5-72). This suggests that transport from these fires to Houston was possible but did not occur over a sustained period sufficient to make a significant contribution to a multi-day ozone episode.

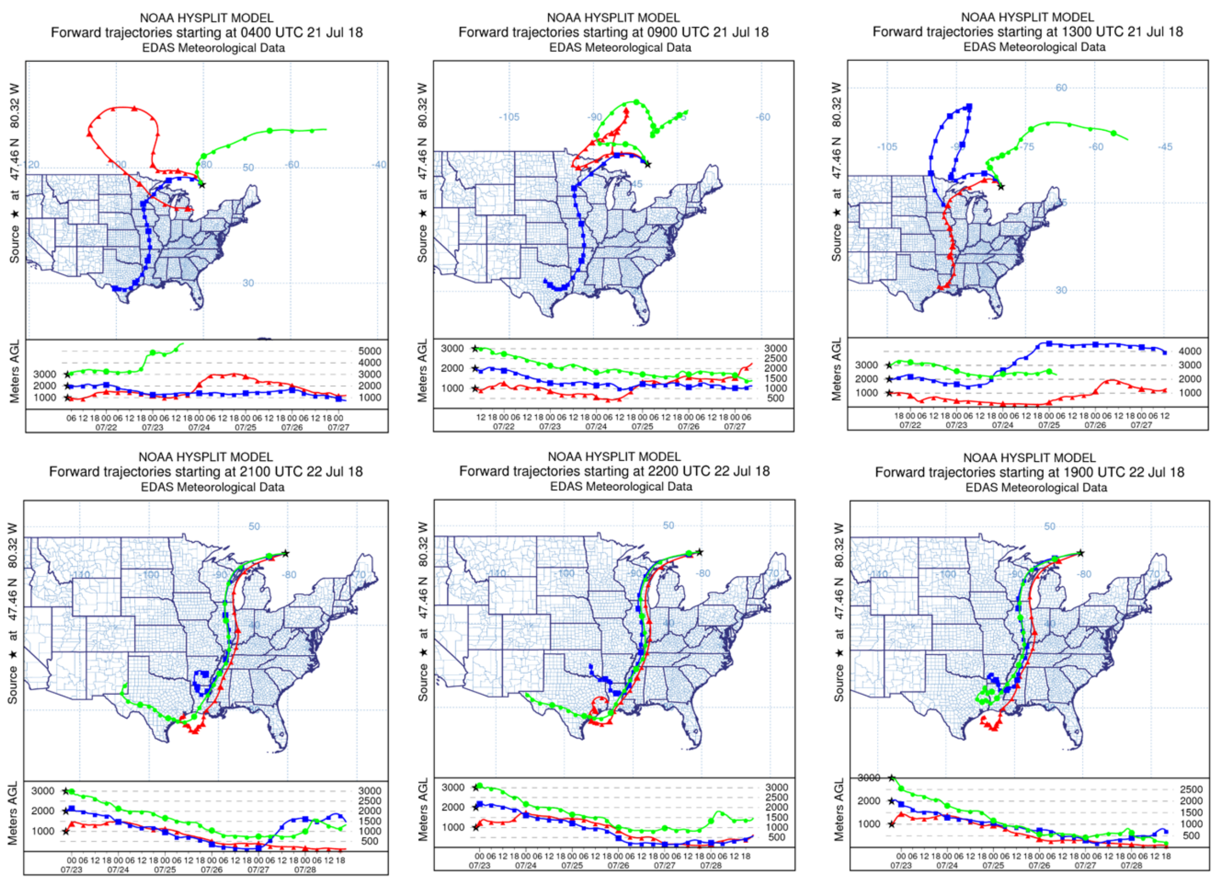

Figure 5-69.   HYSPLIT 5-day forward trajectories starting from the North Bay Complex that used the EDAS meteorological analysis and showed a transport path between the fires and Houston.

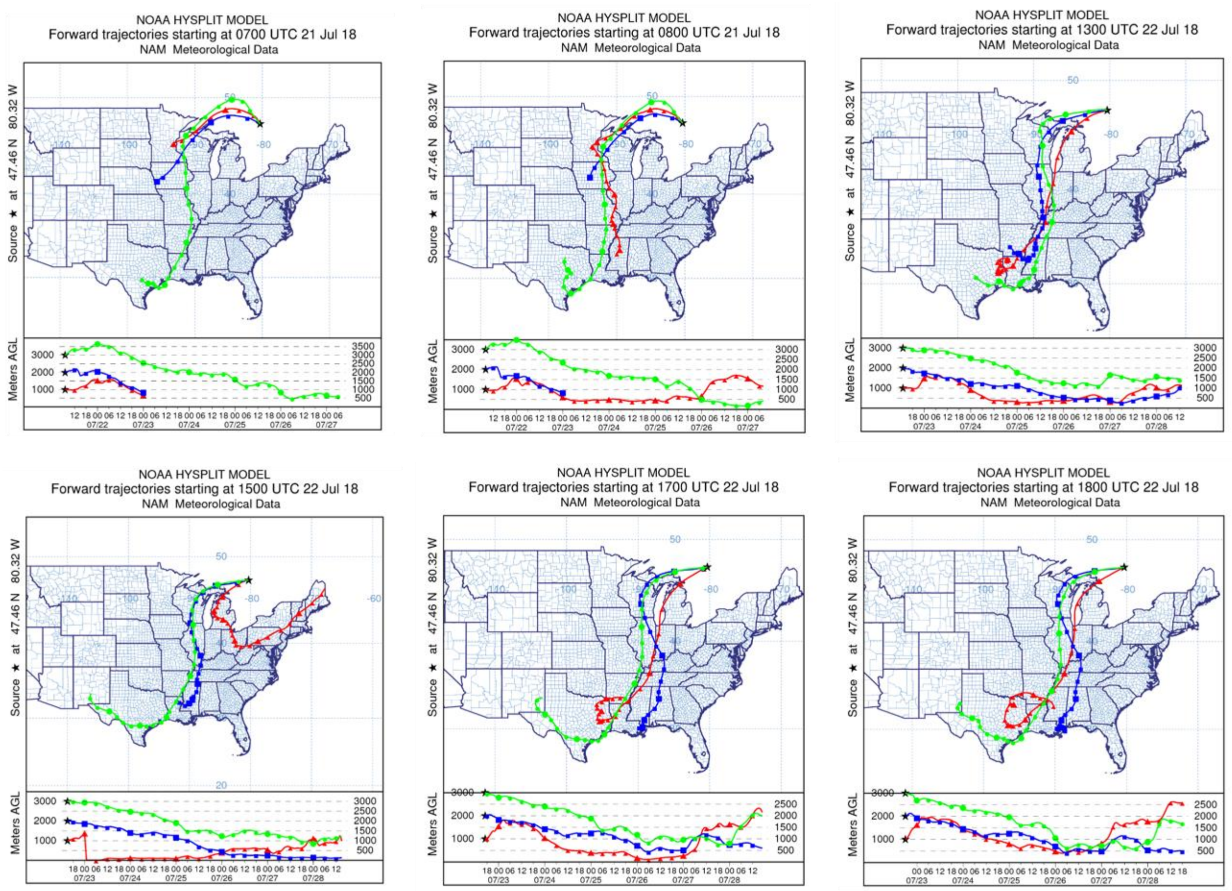

Figure 5-70. HYSPLIT 5-day forward trajectories starting from the North Bay Complex that used the NAM meteorological analysis and showed a transport path between the fires and Houston.

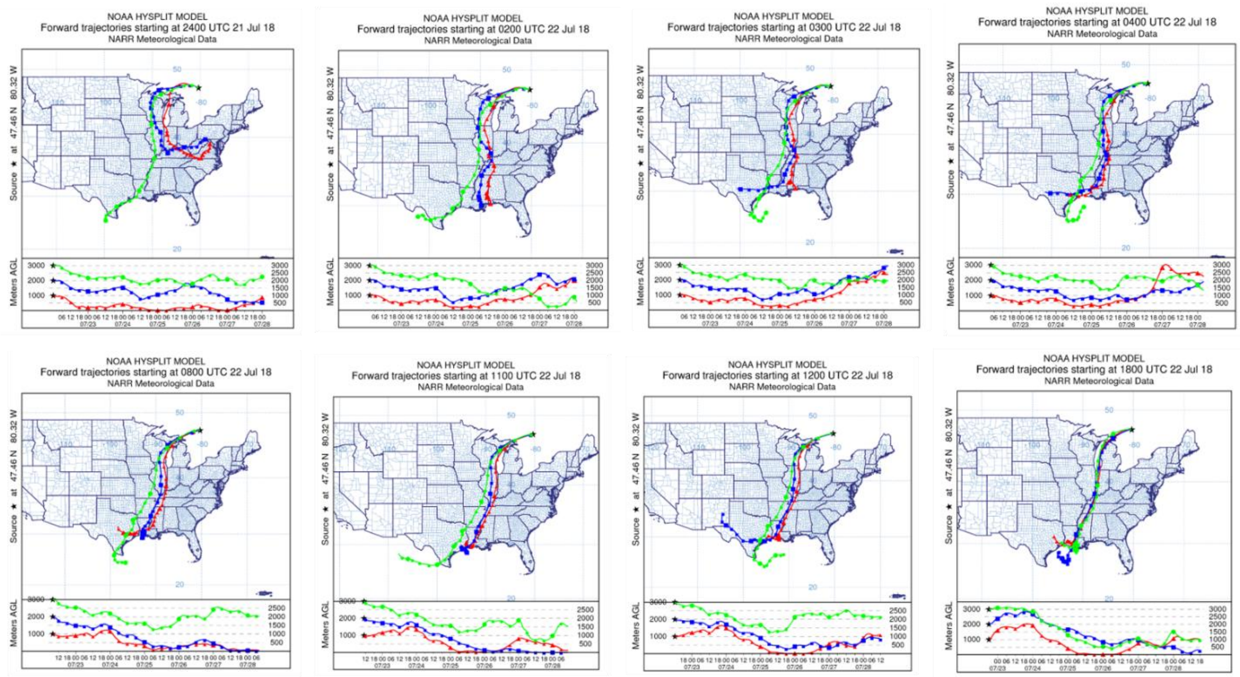

Figure 5-71. HYSPLIT 5-day forward trajectories starting from the North Bay Complex that used the NAM meteorological analysis and showed a transport path between the fires and Houston.

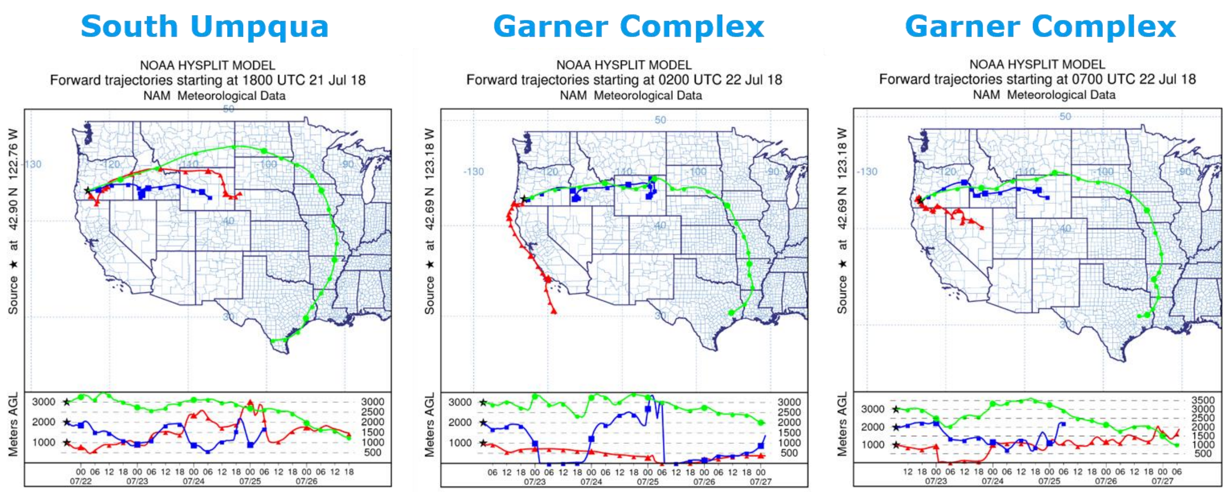

Figure 5-72. HYSPLIT 5-day forward trajectories starting from the South Umpqua Complex and the Garner Complex that used the NAM meteorological analysis and showed a transport path between the fires and Houston. No trajectories that used the EDAS or NARR analyses had a transport path between these fire complexes and Houston.

Consistent with the back trajectories in Figure 5-61 through Figure 5-63, HYSPLIT forward trajectories from the South Umpqua, Garner and North Bay Complexes all travelled through Louisiana on their way to Houston. The FINN emission inventory showed the presence of fires burning in Louisiana in the days leading up to and including the July 26-28 Houston ozone episode. We evaluated the potential for these fires to affect air quality in Houston from July 26-28. We were not able to determine names for these fires or find news reports describing them.

Back trajectories in Figure 5-61 and Figure 5-62 show that air travelling southward toward Houston on July 26 and 27 passed through Louisiana. Figure 5-73 and Figure 5-75 show forward trajectory matrices starting in Louisiana on July 25 and July 26, respectively and indicate that winds were favorable for transport from Louisiana fires circled in red in the FINN emissions plot to Houston during this period. We ran HYSPLIT forward trajectories from the largest of the Louisiana fires on July 25 and July 26 for all hours of the day and found multiple hours had trajectories favorable for transport from the fire to Houston. Figure 5-74 shows an example of a forward trajectory extending from one of the fires circled in the FINN emission figure in the right panel toward Houston and arriving during the day on July 26.

Figure 5-76 shows FINN fire emissions for July 26 (upper left panel) and the HMS smoke product and fire location for July 26 (upper right panel). A large smoke plume extends southwest toward Houston from a fire burning in a rural area west of Alexandria, LA and a plume from a second fire in Texas northeast of Houston is also visible. HYSPLIT back trajectories from the Alexandria fire indicate that winds were favorable for transport from the fire to Houston (lower panels for EDAS analysis and Figure 5-77 for the NARR analysis). Analysis of hourly forward trajectories from the fire northeast of Houston in Figure 5-76 indicate that the plume passed well north of Houston during the entire day of July 26 (not shown).

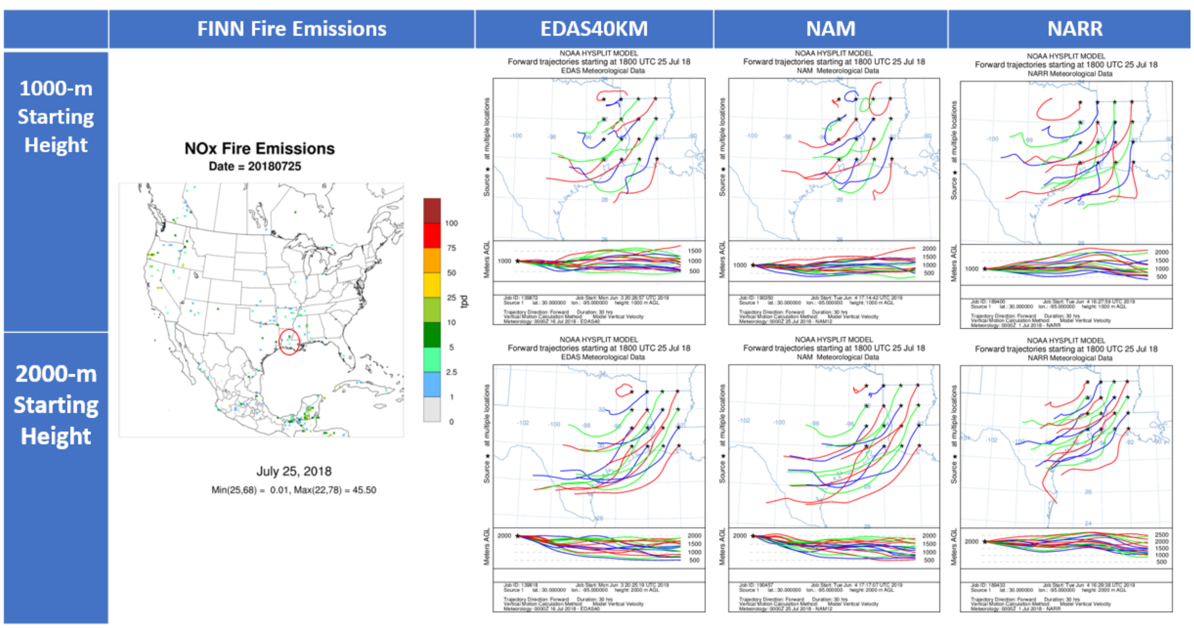

Figure 5-73. HYSPLIT 30-hour forward trajectory matrices for July 25 from Louisiana wildfire regions.

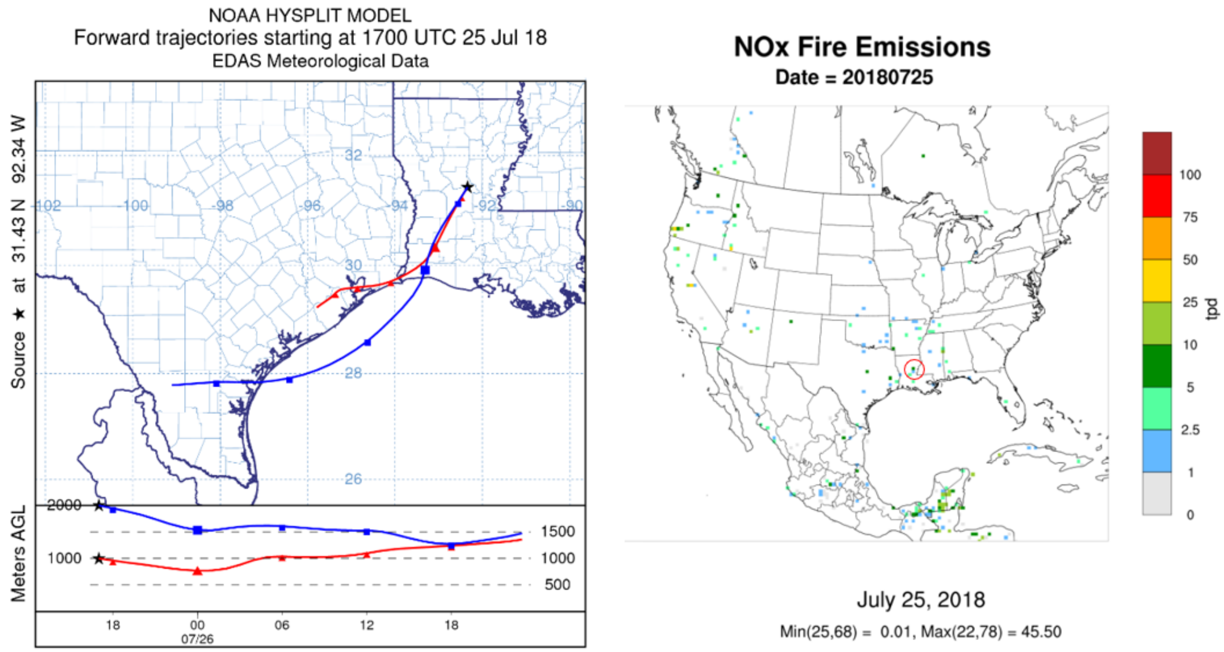

Figure 5-74. Left panel shows HYSPLIT 30-hour forward trajectories for July 25 fire in Louisiana circled in red in FINN fire emissions plot in right panel.

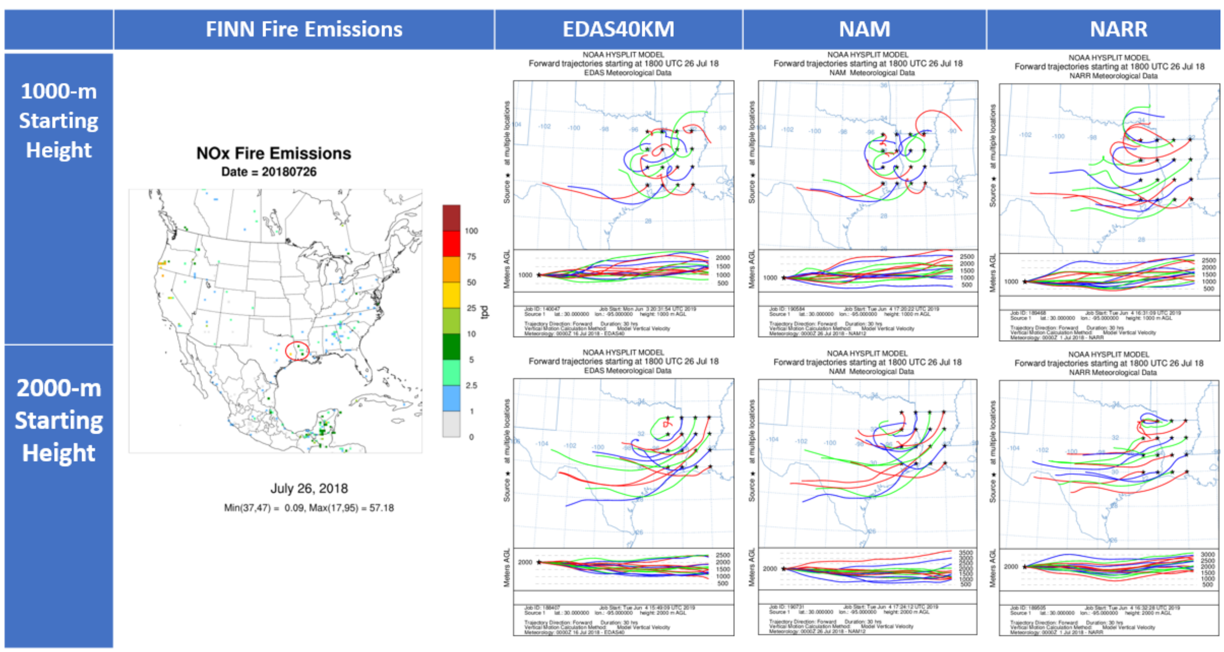

Figure 5-75. HYSPLIT 30-hour forward trajectory matrices for July 26 for Louisiana and Texas areas with wildfire activity.

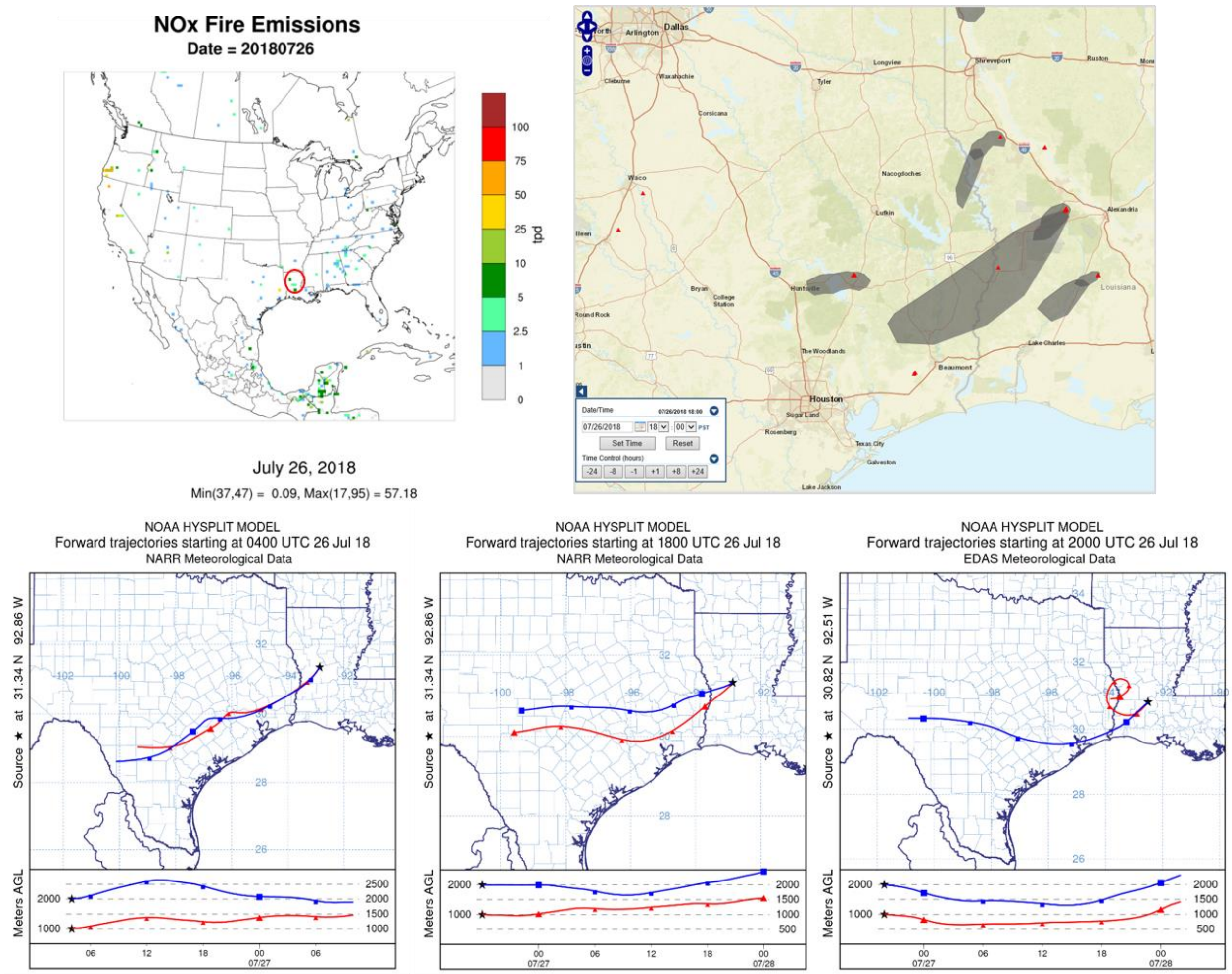

Figure 5-76. Upper left panel: FINN fire emissions for July 26, with the fire location circled. Upper right panel: Airnowtech.org screenshot showing fire location as red triangle (MODIS thermal anomaly) and HMS smoke product showing a plume extending from the fire location toward Houston. Lower left and center panels: HYSPLIT 30-hour forward trajectories for the fire west of Alexandria Louisiana on July 26 starting at 0400 and 1800 UTC. Lower right panel: forward trajectory for fire southeast of the Alexandria fire.

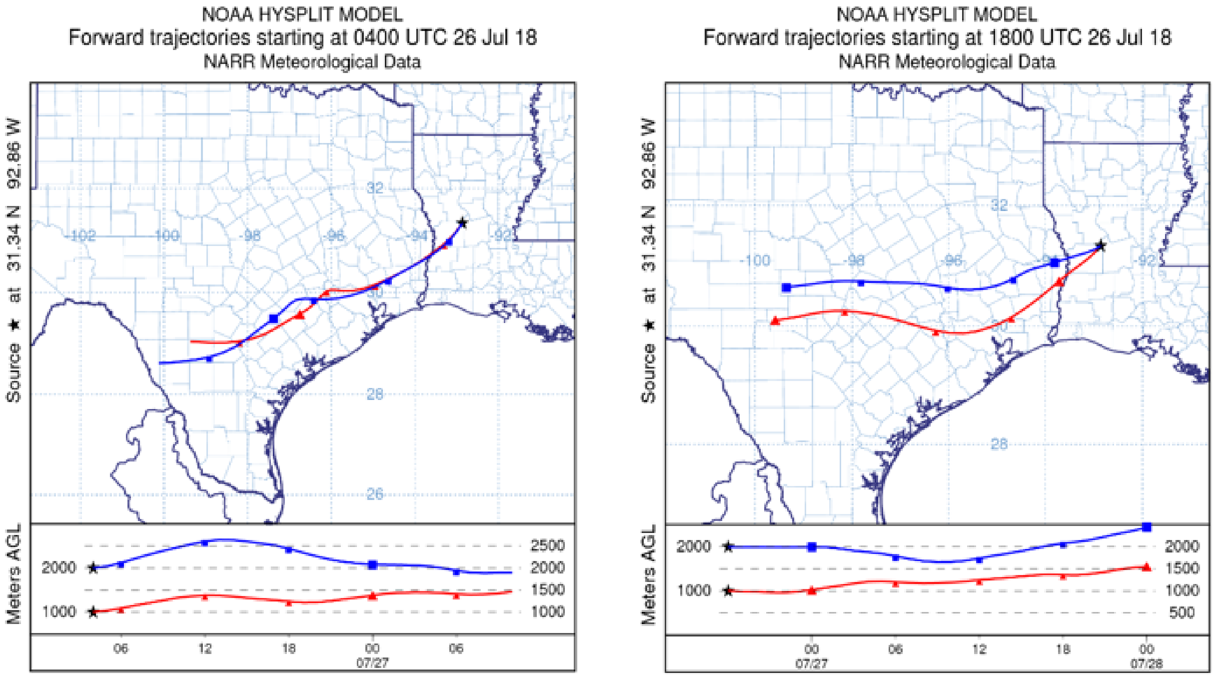

Figure 5-77. HYSPLIT 30-hour forward trajectories for the Louisiana fire west of Alexandria as previous figure but with NARR meteorological analysis.

Given the proximity of the Alexandria fire to Houston, the intensity and orientation of the HMS smoke plume and the source-receptor relationship diagnosed with HYSPLIT, we evaluated the potential for a Tier 2 analysis for this fire. We evaluated the Q/D ratio for the fire on July 26 and found that it was less than 1, which is well below the 100 tons/km EPA threshold for a Tier 2 analysis (Figure 5-78).

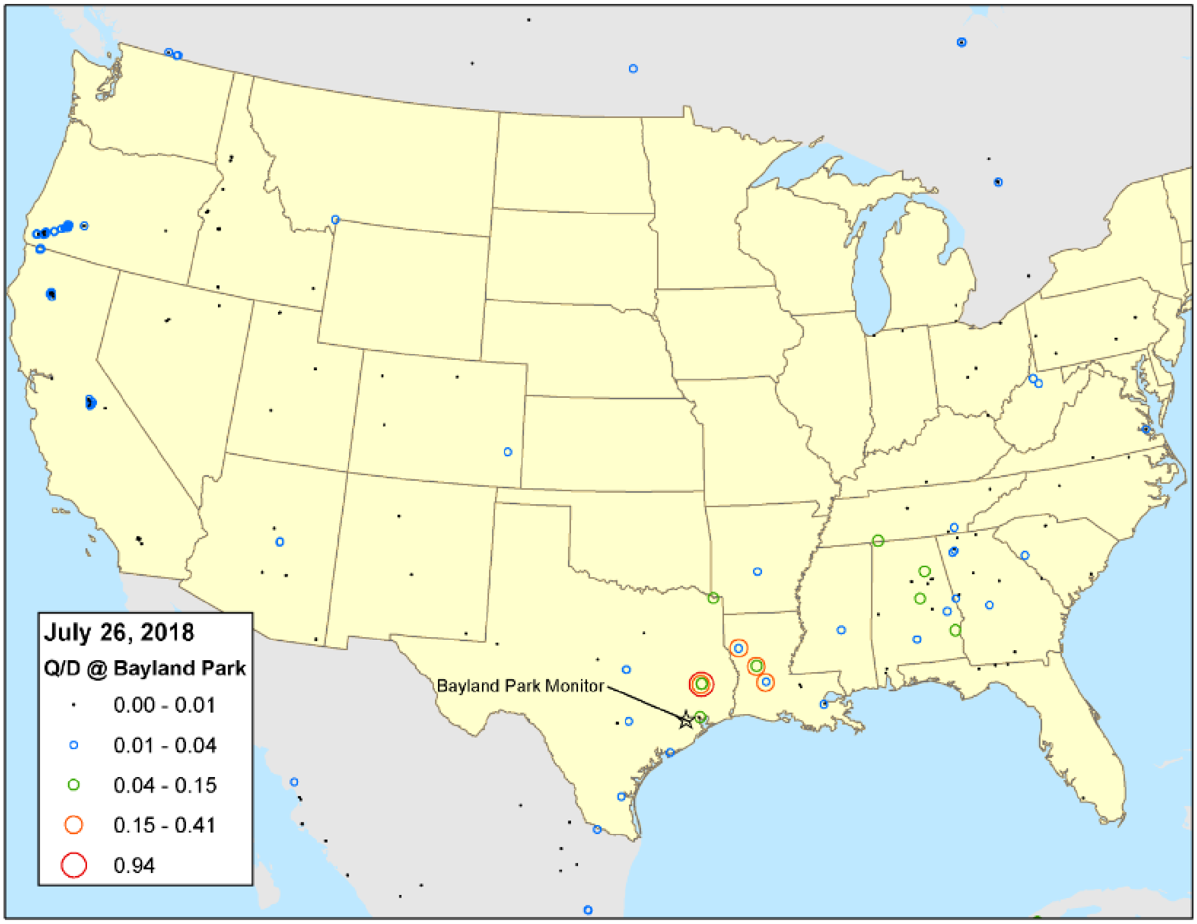

Figure 5-78. July 26 Q/D ratios (tpd/km) for all FINN fires for Bayland Park CAMS 53. EPA threshold for a Tier II analysis is 100 tpd/km.

By July 27, the FINN emission inventory shows only one fire in Louisiana, and the HYSPLIT forward trajectory matrix suggests that winds were not favorable for transport of the fire plume to Houston (Figure 5-79). Forward trajectories from the fire for start times throughout the day on July 27 curve northward away from Houston (not shown). On July 28, the FINN inventory shows no fires in Louisiana, possibly due to the presence of extensive cloud cover that would potentially prevent satellite detection of hot spots.

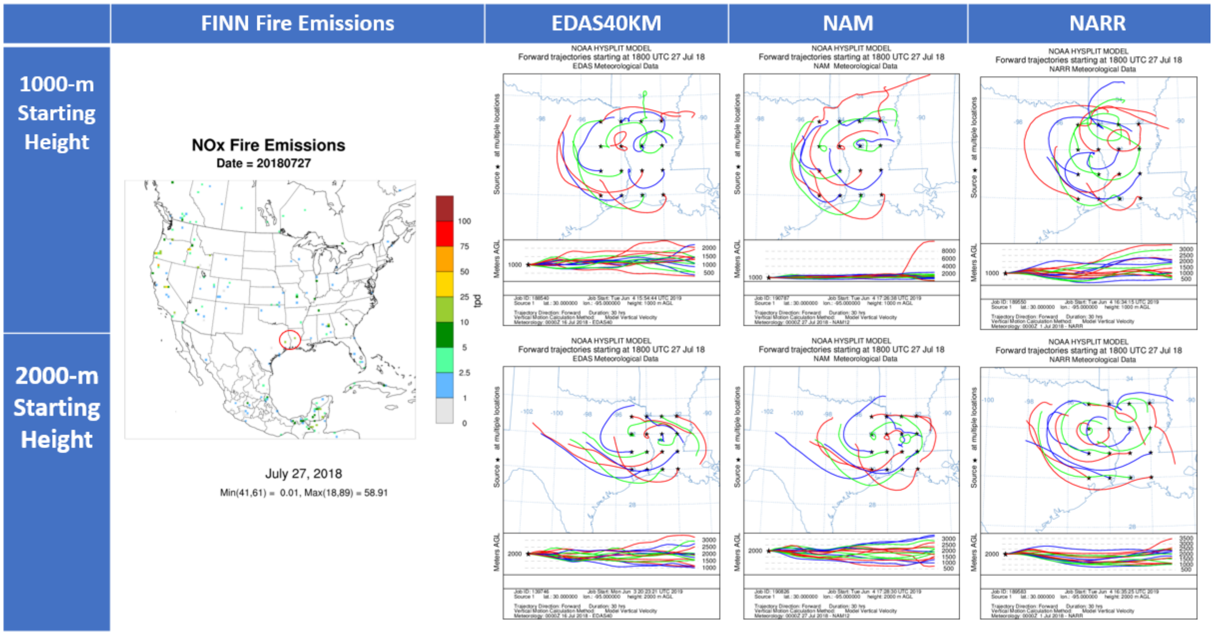

Figure 5-79. HYSPLIT 30-hour forward trajectory matrices for July 27.

5.3.1.2 August Episode HYSPLIT Trajectory Analysis

We prepared HYSPLIT back trajectories ending at Bayland Park CAMS 53 at the time of peak 1-hour average ozone on August 23 (Figure 5-80) and at Aldine CAMS 8 time of peak 1-hour average ozone on August 24 (Figure 5-81). 5-day HYSPLIT back trajectories using the NAM 12 km, EDAS 40 km and NARR 36 km meteorological analyses are consistent in showing that air arriving at 100 m above ground level at Bayland Park on August 23 and Aldine on August 24 travelled northwest across the Gulf of Mexico before arriving in Houston (Figure 5-80 and Figure 5-81). Although low-level parcels arriving at the monitors have a maritime influence, there is significant vertical wind shear on both days, and air further aloft originates over the continental US. For air parcels arriving at 2,500 m above Bayland Park on August 23, the back trajectories for the EDAS, NAM and NARR analyses extend back over California, Nevada and Oregon. The NAM and EDAS analysis 5-day 1,000 m back trajectories are similar to the 100 m back trajectory, extending southeast over the Gulf of Mexico, while the back trajectories for the NARR analysis extend northward toward the central US and southern Canada.

We prepared a HYSPLIT frequency analysis using on-line tools provided by NOAA through their READY website. In the frequency analysis, a back trajectory was begun every three hours during August 23-24 and allowed to run backward for 120 hours (5 days). A 1°x1° grid was laid out on the domain and the number of trajectory points in each grid cell was tabulated. Plots of the resulting trajectory frequency field are shown in Figure 5-82.

The back trajectory frequency field gives a more comprehensive view of the origins of air during the August 23-24 episode. The results are consistent with the back trajectories for the times of peak 1-hour average ozone in suggesting that air arriving in the lowest 1,000 m of the atmosphere travelled northward over the Gulf of Mexico before arriving in Houston. For air parcels arriving at 2,500 m above Houston on August 23-24, all three analyses show back trajectories extending westward toward California, Oregon and Washington.

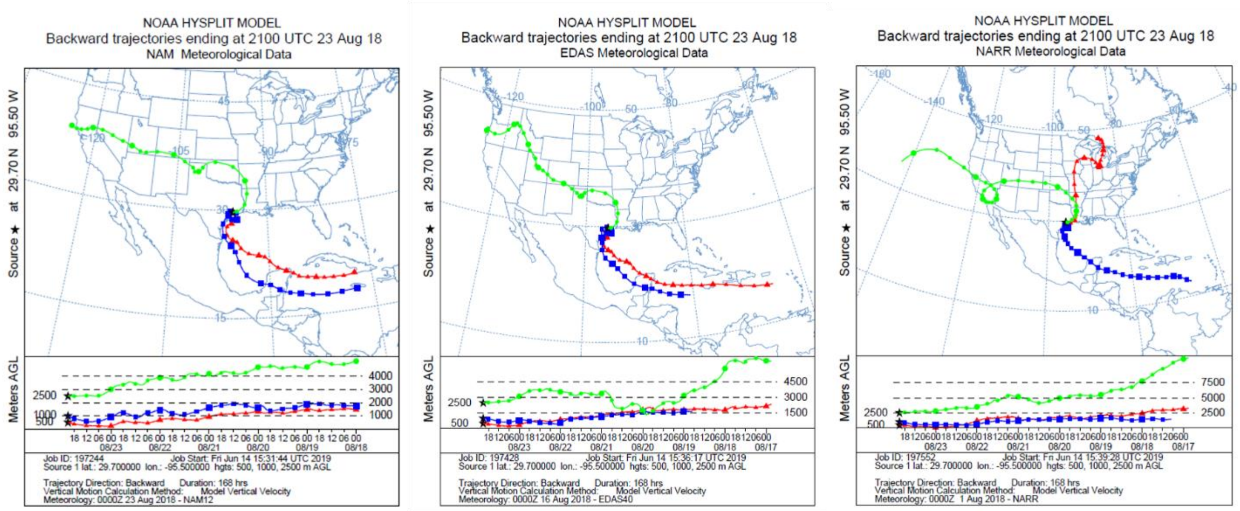

Figure 5-80. HYSPLIT 5-day back trajectories ending at Bayland Park CAMS 53 on August 23, 2018 at 3 pm CST, the time of the maximum daily 1-hour average ozone.

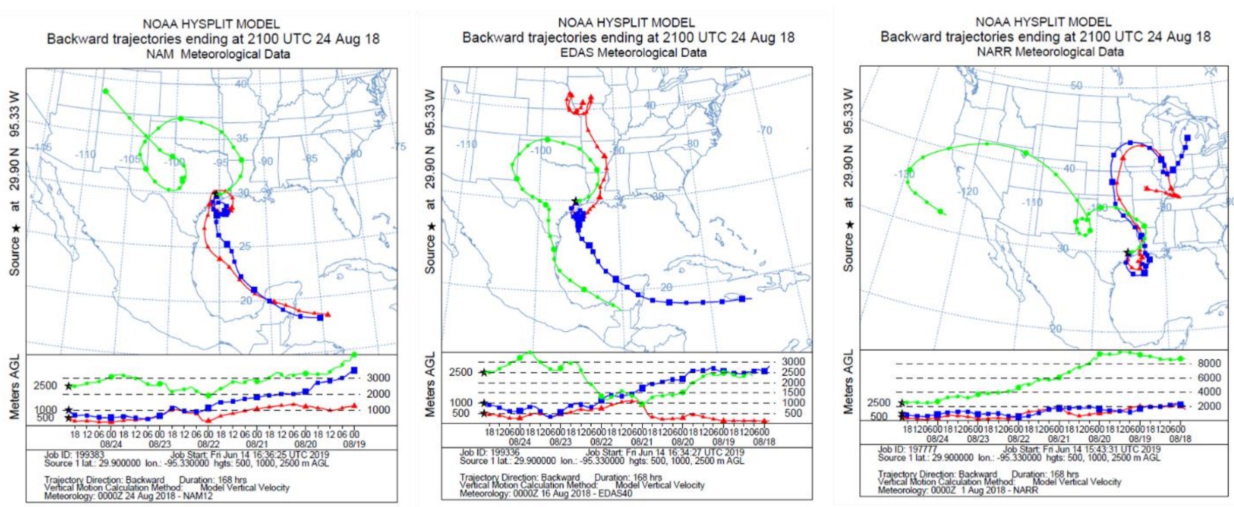

Figure 5-81. HYSPLIT 5-day back trajectories ending at Aldine CAMS 8 on August 24, 2018 at 3 pm CST, the time of the maximum daily 1-hour average ozone

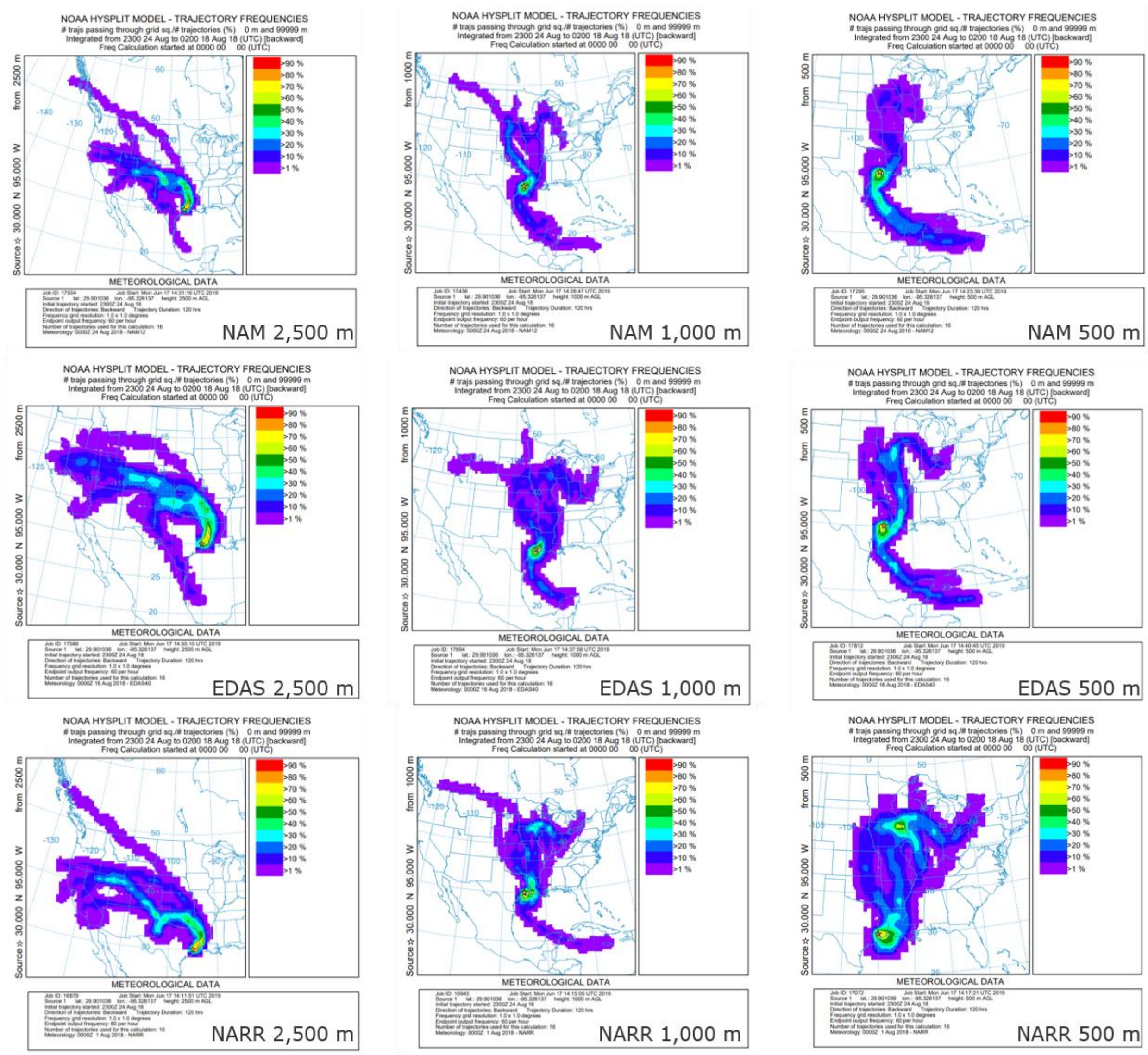

Figure 5-82. HYSPLIT 5-day back trajectory frequencies for the August episode. Upper panels: HYSPLIT back trajectories using the NAM 12 km meteorological analysis ending in Houston at 2,500 m (left panel), 1,000 m (center panel) and 500 m (right panel). Middle panels: as in upper panels for HYSPLIT back trajectories run with the EDAS 40 km meteorological analysis. Lower panels: as in upper panels for HYSPLIT back trajectories run with the NARR 36 km meteorological analysis.

Based on the origins of air arriving at Houston monitors during the August 23-24 high ozone episode, we reviewed the FINN fire emission inventory to identify large fires that were upwind of Houston during the days preceding the August 23-24 high ozone episode. Figure 5-83 shows FINN fire emissions for August 18. Large wildfire complexes were burning in California, Oregon and British Columbia, Canada. Next, we ran a matrix of 5-day forward trajectories from areas encompassing the fire complexes to establish whether a source-receptor relationship existed for that fire complex and Aldine CAMS 8 and Bayland Park CAMS 53.

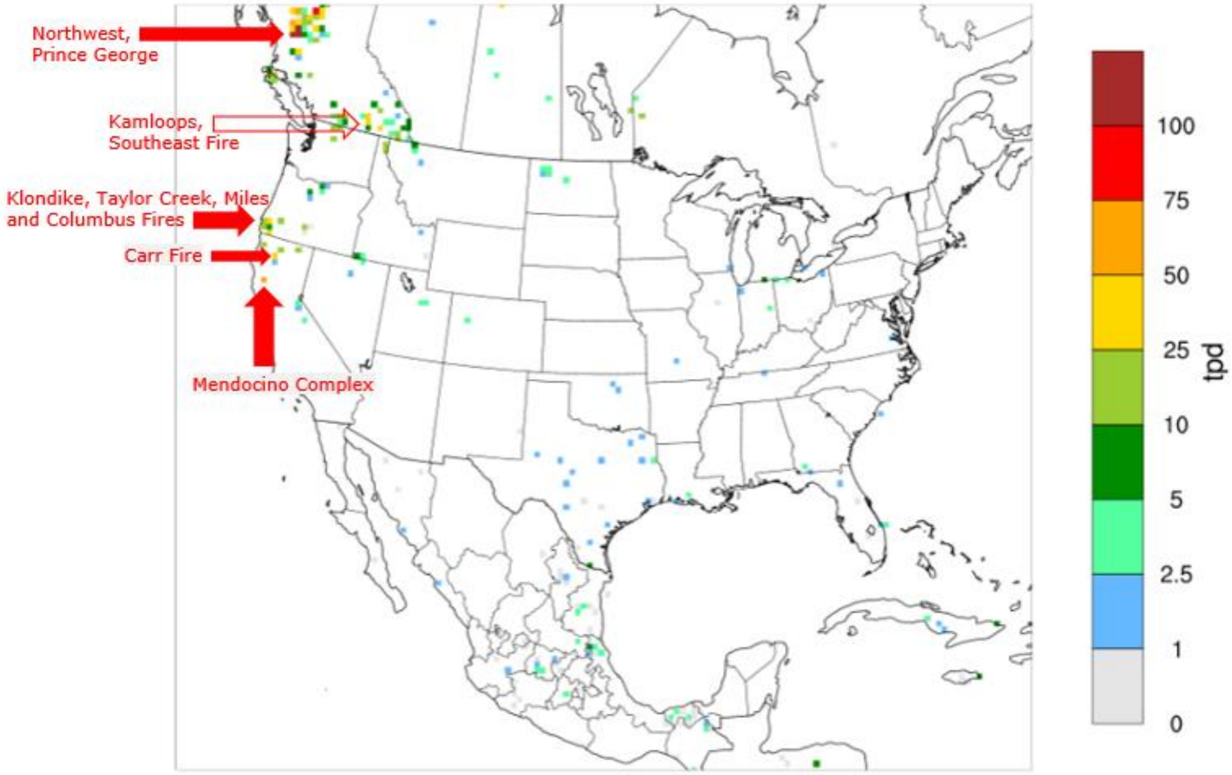

Figure 5-83. FINN fire NOx emissions (tpd) for August 18, 2018. Red arrows indicate large fire complexes determined to be upwind of Houston based on HYSPLIT back trajectory analysis.

Figure 5-84 shows HYSPLIT forward trajectories prepared with the EDAS, NAM and NARR meteorological analyses and originating at multiple heights indicate that air moved from the region containing the southwest Oregon fires, the Carr Fire and the Mendocino Complex fires east across US. The 3,000 m forward trajectories using the NARR analysis show transport to southeast Texas and all trajectories for all three analyses show transport to the southeast US. Figure 5-85, Figure 5-86, Figure 5-87 show forward trajectories from each of these fire complexes that suggest transport of air from the fire to the Houston area. HYSPLIT forward trajectory matrices for fires in Washington and British Columbia had trajectories that extended east across the US and into Canada but did not travel south toward Texas (not shown).

Figure 5-88 shows HYSPLIT forward trajectory frequency plots for the Sugarloaf, NV fires. The HYSPLIT forward trajectories indicate that these large fires were also upwind of the Houston area during the week before the Houston high ozone episode and could have contributed to the plumes traveling toward Houston that were generated by upwind fires in California and Oregon.

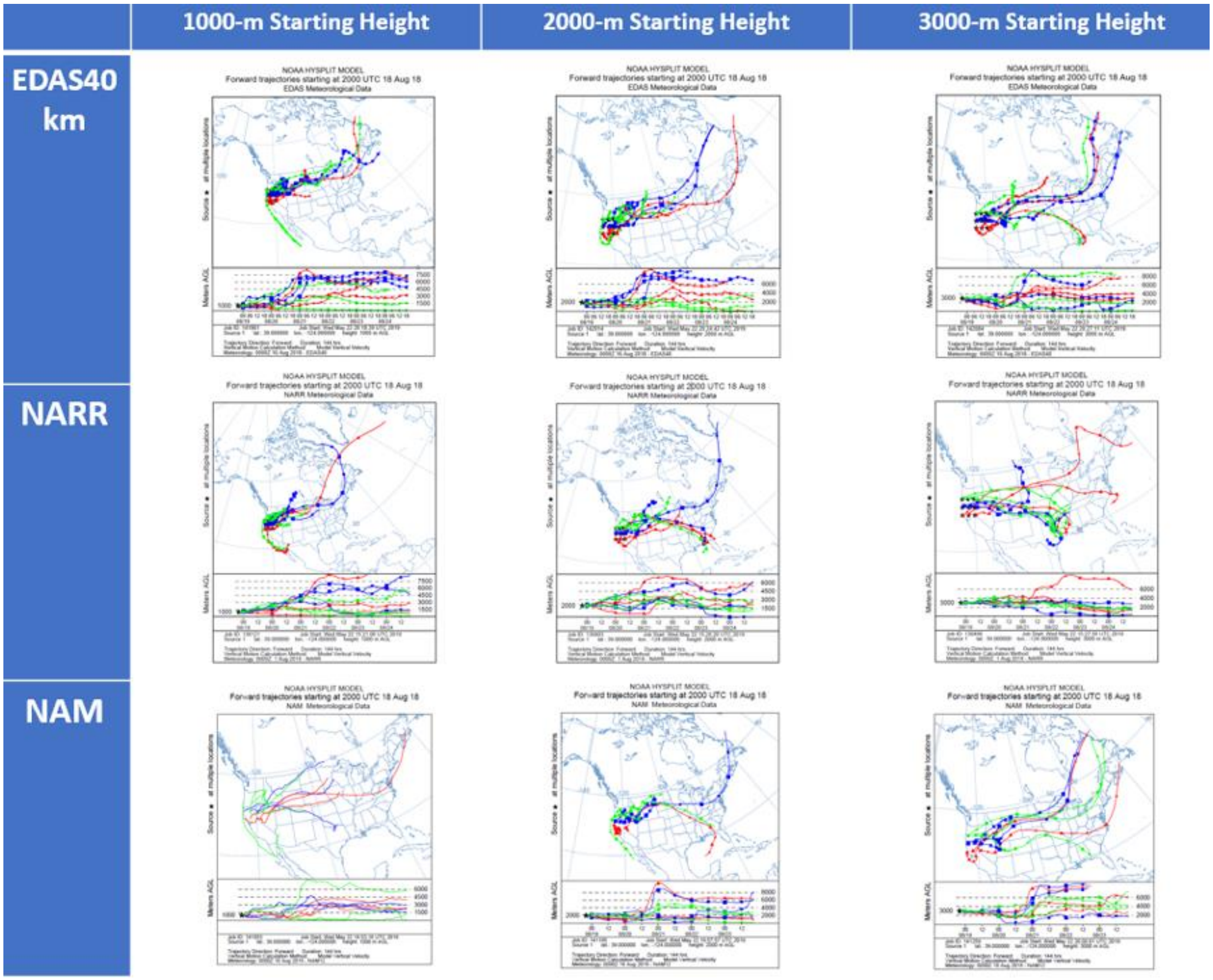

Figure 5-84. HYSPLIT 5-day forward trajectory matrices for August 18 for California areas with wildfire activity.

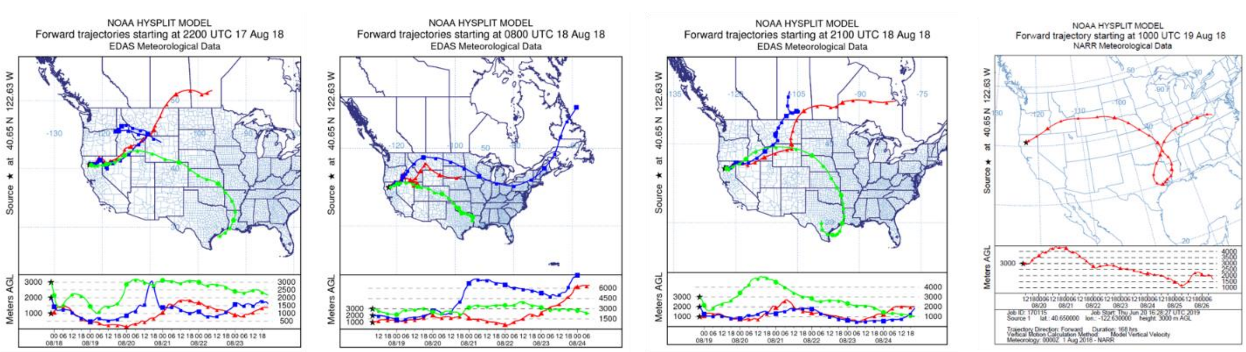

Figure 5-85. HYSPLIT 5-day forward trajectories from the Carr fire in California for times during August 17-19 using the EDAS and NARR analyses.

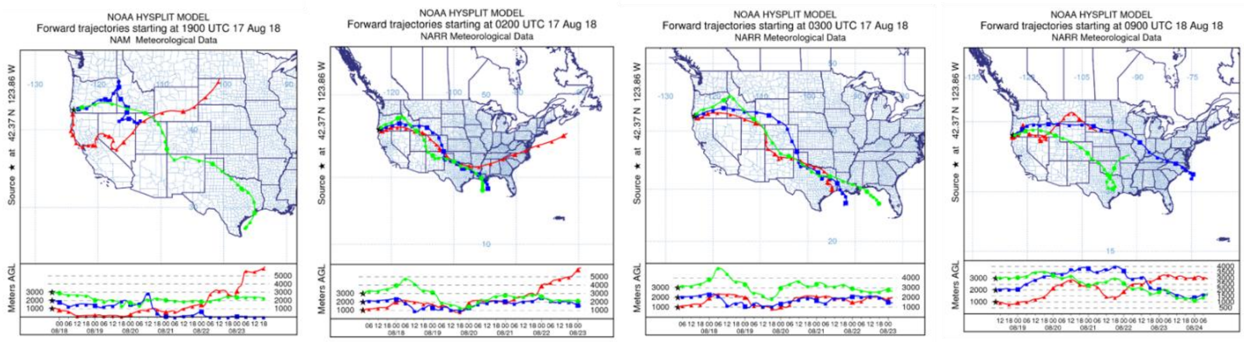

Figure 5-86. HYSPLIT 5-day forward trajectories from the Klondike/Taylor Creek/Miles Complex fires using the NAM and NARR analyses.

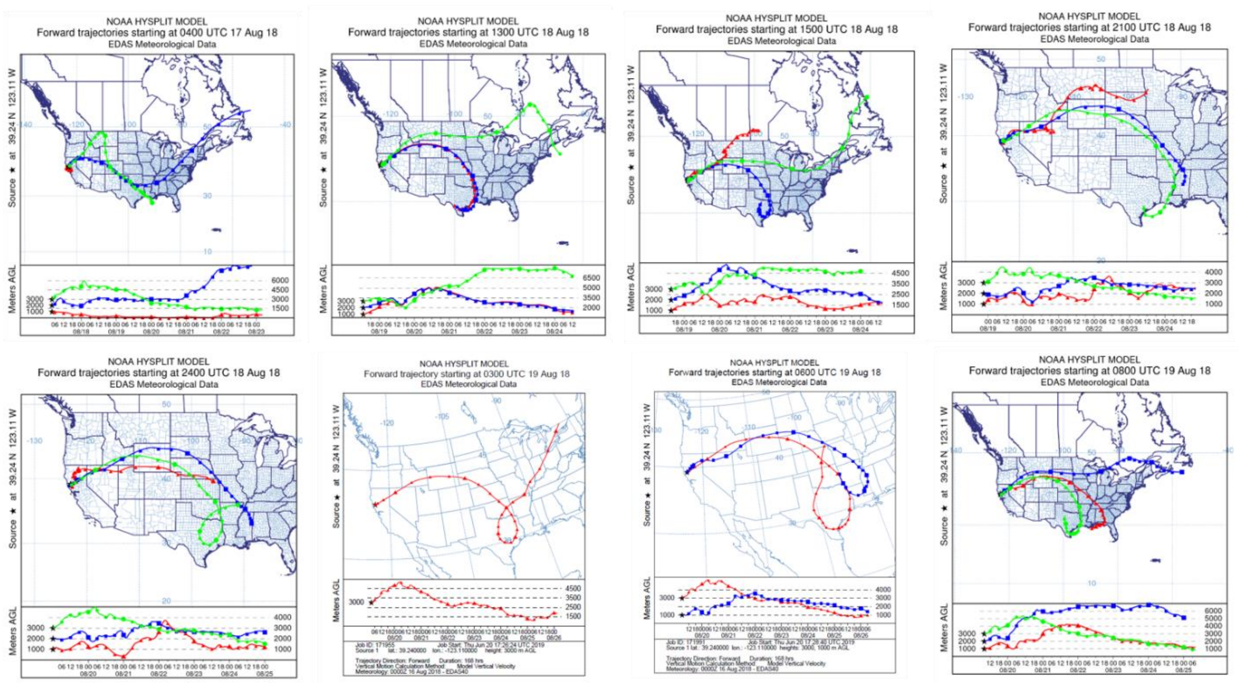

Figure 5-87. HYSPLIT 5-day forward trajectories from the Mendocino Complex using the EDAS analysis.

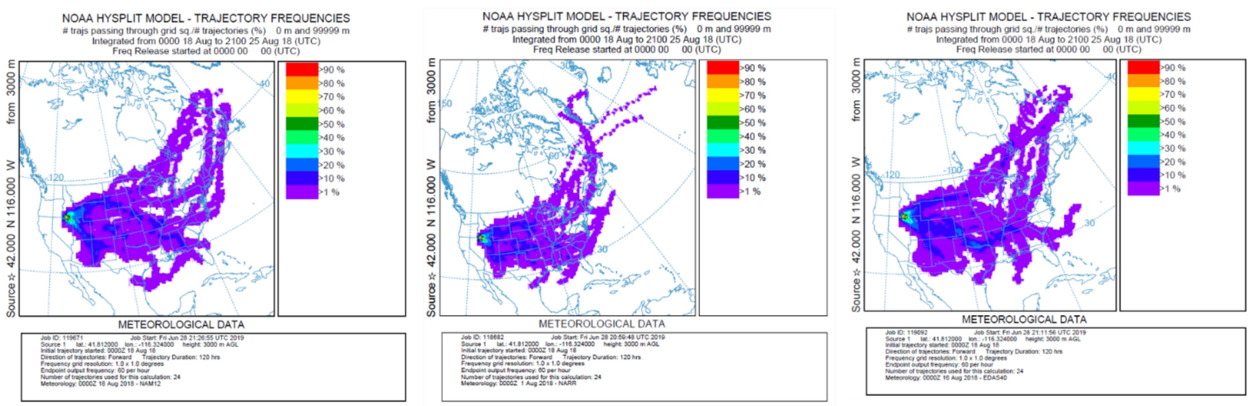

Figure 5-88. Forward trajectories from the Sugarloaf fire complex in Nevada.

Back trajectories in Figure 5-80 and Figure 5-81 show that air travelling southward toward Houston on August 23 and August 24 passed through Louisiana. Figure 5-89 and Figure 5-91 show forward trajectory matrices starting in Louisiana on August 22 and August 23, respectively and indicate that winds were favorable for transport from Louisiana fires circled in red in the FINN emissions plot to Houston during this period. We ran HYSPLIT forward trajectories from the largest of the Louisiana fires on August 22 and August 23 for all hours of the day and found multiple hours had trajectories favorable for transport from the fire to Houston. Figure 5-90 shows an example of a forward trajectory extending from one of the fires circled in the FINN emission figure in the right panel toward Houston and arriving during the day on August 23.

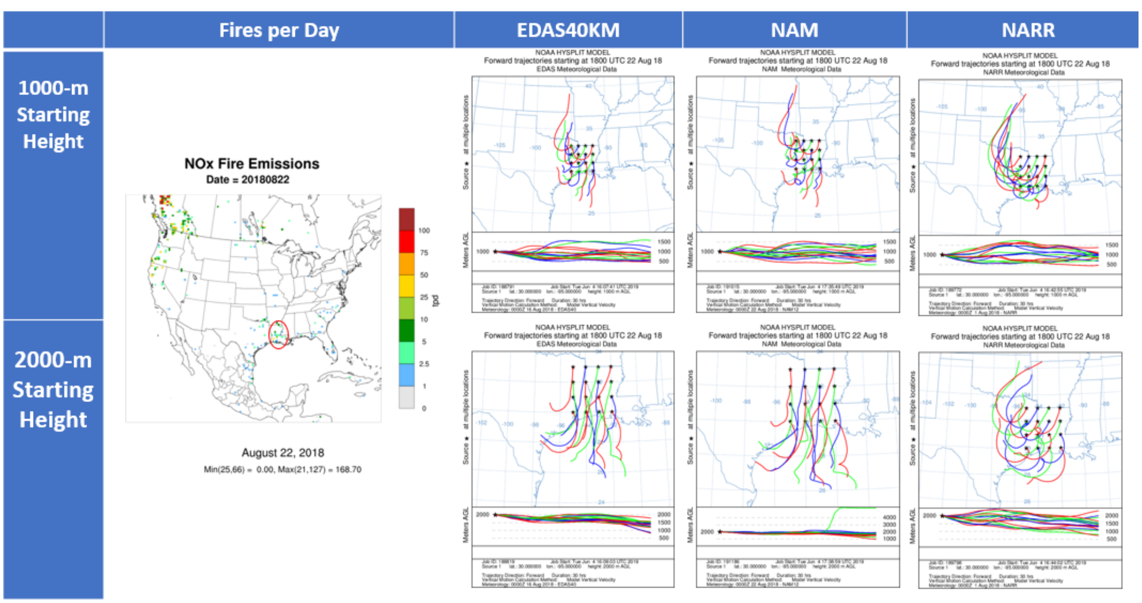

Figure 5-89. HYSPLIT 30-hour forward trajectory matrices for Louisiana fires beginning at 18 UTC on August 22.

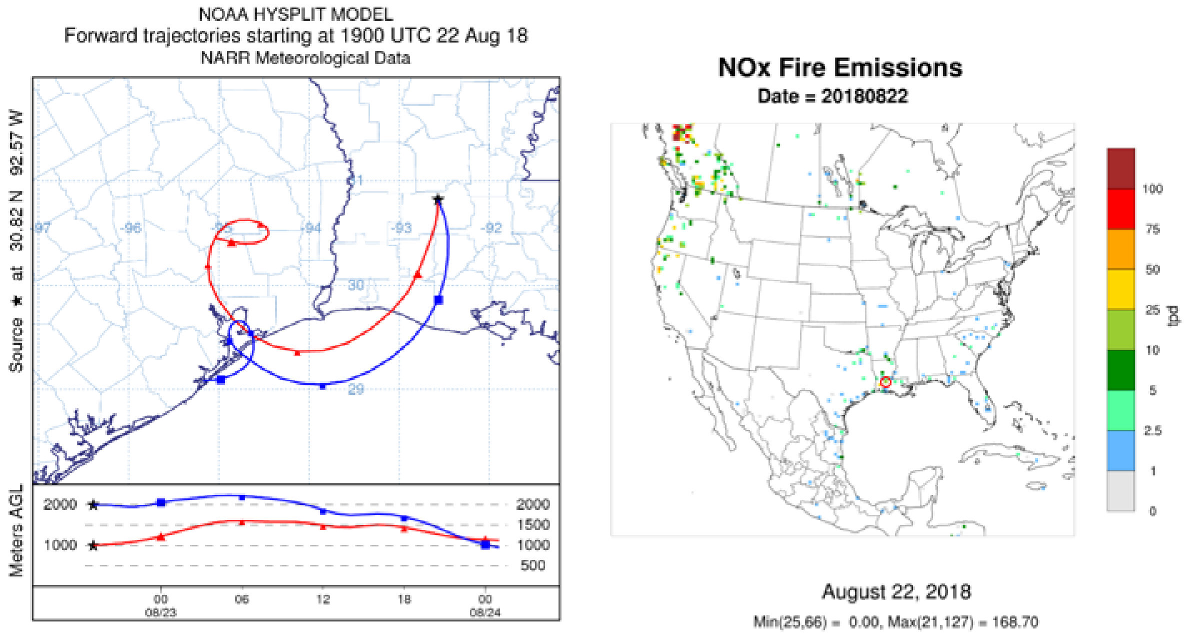

Figure 5-90. Example August 22 HYSPLIT 30-hour forward trajectory.

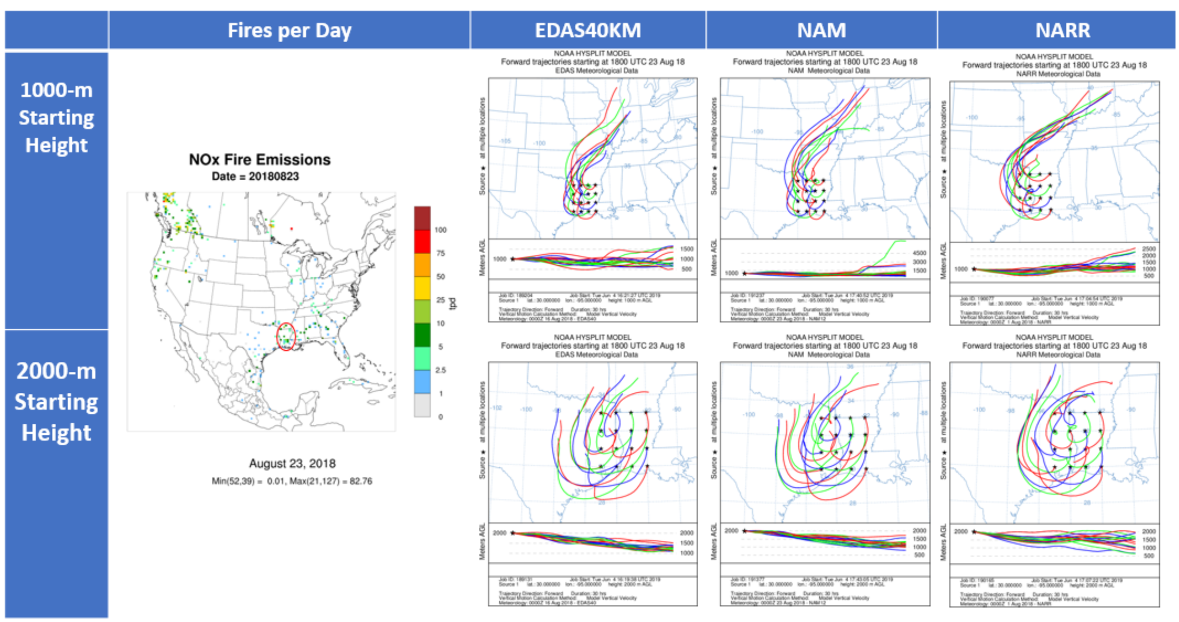

Figure 5-91. HYSPLIT 30-hour forward trajectory matrices for Louisiana fires beginning at 18 UTC on August 23.

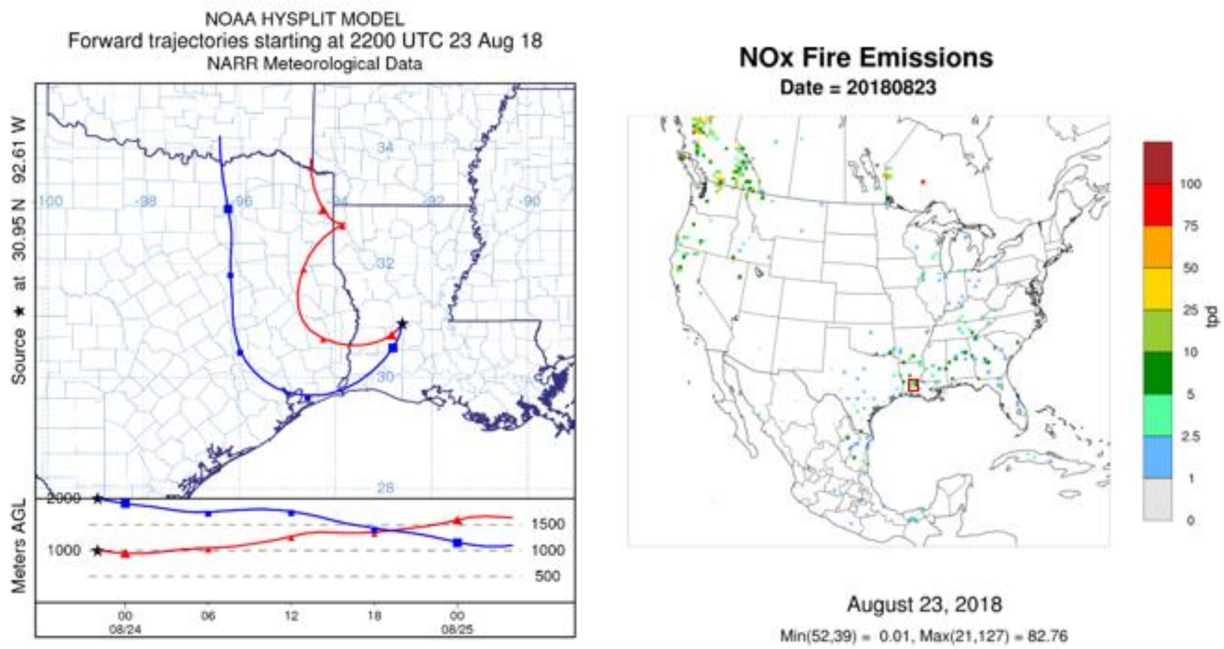

Figure 5-92. Example HYSPLIT 30-hour forward trajectories. August 23.

5.3.2 Satellite Imagery of Plume with Evidence of Plume Impacting the Ground

In this section, we review evidence from satellite imagery for transport of fire emissions from wildfires to the Bayland Park CAMS 53 and Aldine CAMS 8 during the July and August Houston high ozone episodes.

5.3.2.1 July Episode

In Figure 5-93, the true color image and the NOAA HMS smoke product for July 22 show the location of fires (red icons) and associated smoke plumes in southern Oregon and central California (Ferguson Complex) and in Ontario (Ontario/Manitoba and North Bay Complexes). The Canadian fire complexes are partly obscured by cloud cover. In the NOAA HMS map, smoke plumes are also associated with fires in British Columbia and in northern Ontario in the Canadian Shield. The AIRS CO signature from the North Bay and Ontario/Manitoba Canadian complexes is evident, but the California and Oregon fires fall in a data gap in the satellite overpasses. The signatures of the Ferguson Complex and the Oregon fires are apparent in the July 22 AOD plot, while the Canadian fires are in a cloudy region, and only a few pixels are assigned AOD values. However, the available pixels do show high levels of AOD. Clouds are associated with storm systems with surface low pressure centered in Ohio and northern Manitoba. The cyclonic circulation around the low pressure system centered over Ohio moved the plume from the North Bay Complex westward and then southward into the US. The July 22 500 mb height field is dominated by high pressure centered over New Mexico and a broad ridge and westerly winds over the western US.

By July 23 (Figure 5-94), the plume from the North Bay Complex is visible as an area of smoke and enhanced AOD curving southward into Wisconsin, northern Illinois and driven by the cyclonic wind field from the low pressure system over the eastern US. A broad trough in the 500 mb wind field with north-south axis oriented along a line between Georgia and Michigan creates northerly flow that moves the plume from the North Bay Complex south toward the Mississippi Valley. The plume of smoke extending from Ontario south into the US is also visible in the HMS smoke product and in the

AIRS CO retrieval. The AOD, CO and visible images show that the plume from the fires in British Columbia remains north of the US-Canada border and the plumes from the Ferguson fire and the Oregon fires remain largely confined to California and Oregon. In the CO and AOD retrievals, there is no evidence of plume extending east from these fires toward the central US and Texas, however, the NOAA HMS product does show a smoke plume extending east to North Dakota and Nebraska. The AOD retrieval shows that the plume from the fires at the Ontario/Manitoba border extends eastward toward the Hudson Bay and does not extend south toward Texas.

On July 24 (Figure 5-95), the 500 mb plot shows that the ridge of high pressure over the western US and the trough over the east US continue to dominate the flow pattern over the US. Winds aloft over the Mississippi Valley are northerly. At the surface, high pressure builds over Nebraska behind a southward-moving cold front. Clouds associated with the low pressure system and the gap in the CO data to the overpass pattern limit the data available in the region of the southward moving plume from the North Bay Complex, however the HMS smoke product shows the plume's continued southward movement. Figure 5-96 shows the GOES-16 true color image and AOD retrieval for four times during July 24-25. An area of enhanced AOD appeared along the Illinois/ Indiana border at 10:17 CDT on July 24, and moved southward during the day, consistent with the 500 mb wind pattern. The southward movement of this region of enhanced AOD continued on July 25, and Louisiana appears as a region of AOD on the order of 0.5 by July 25.

Smoke plumes emanating from the California and Oregon fires extend east across Oregon, but the signature of this plumes is not apparent east of the Oregon and California borders in the true color image and there is no area of enhanced AOD over the Rocky Mountain states between California/Oregon and Texas in the GOES-16 retrieval. In the AOD image in Figure 5-95, smoke from the Oregon fires is visible as an area of enhanced AOD extending from the fires northeast across Idaho and Montana. There is little evidence of a plume turning southeast toward Texas. The plume from the Ferguson fire is directed toward southern California. This is consistent with the HMS smoke product.

By July 25 (Figure 5-97), the cold front has sagged south into Texas, Louisiana and Mississippi and the 500 mb trough axis continues to move east and the ridge covers most of the western US. At 500 mb, winds continue to be northerly over Texas, Arkansas and Louisiana. Accordingly, the HMS product shows southward movement of the North Bay Complex plume further into Texas and Louisiana. Over the Mississippi Valley, the AOD retrieval has many areas of missing data due to the presence of clouds, however an area of enhanced AOD is visible in southern Louisiana and Mississippi. The AOD impact of two fires north of Houston can be seen, although they are surrounded by areas of cloud where no AOD value is retrieved. The CO retrieval, however, shows only mild enhancement over Texas and Louisiana. The NOAA NESDIS Descriptive Text Narrative for Smoke/Dust Observed in Satellite Imagery for July 25 notes, "*The smoke over the Western and Central US was likely attributed to wildfire activity over the Western US. The mass of thin to moderately dense smoke stretching from the Great Lakes region to the Gulf Coast was more likely being transported southward from Canada with the source potentially from wildfires in Canada and even now possibly from the longer range transport from Europe/Asia.*"

By July 26 (Figure 5-98), the HMS smoke field no longer covers a broad swath of Texas and Louisiana, as it did on July 25. The area of dense, regional smoke has retreated well north of Oklahoma and Arkansas and the only smoke signal over East Texas and Louisiana now comes from smaller fires, whose individual plumes appear in the HMS smoke product plot. Smoke plumes associated with fires in Texas and Louisiana appear in the true color images (Figure 5-99) as well as in the AOD (Figure

5-100). The AOD signal from the fire west of Alexandria, LA can be seen extending southwest from the fire location as well as in the HMS smoke product. There is a broad area of enhanced (>0.5) AOD and CO over East Texas, including Houston, that extends into Louisiana and Arkansas. The 500 mb and surface weather maps indicate that a region of high pressure is located over Texas. The 500 mb wind field is weak and disorganized over East Texas, indicating there is no strong synoptic forcing over Houston on July 26.

Synoptic forcing remains weak on July 27 (Figure 5-101). There is a stationary front located over North Texas and the 500 mb wind field is disorganized. The HMS smoke product indicates the intense smoke plumes covering much of the US remained well north of Texas. The only smoke plumes in the region are from smaller local fires north of Houston and in Louisiana. AOD levels remain enhanced over Louisiana and north Texas but are lower in southeast Texas than on July 26.

On July 28, AOD levels remain enhanced northeast of Houston, but are relatively low (,0.3) southwest of Houston. This is consistent with the onset of low level southerly winds which bring clean Gulf air into Houston. Fire activity in southeast Texas and Louisiana has diminished and there are no HMS smoke plumes emanating from the fires that are there.

5.3.2.2 August Episode

On August 18, large wildfires were burning in British Columbia, Washington, Oregon, California and other western states. Smoke plumes from these wildfires stretched across Canada and much of the northern US (Figure 5-103). The NOAA NESDIS Smoke Narrative for August 18 reads, *"Much of Canada and the Northern United States....The ongoing wildfire activity affecting portions of the western United States and western Canada continues to produce enormous amounts of smoke that covers most of Canada and the northern portion of the United States. The areas of densest smoke extend from western and southern British Columbia across Alberta, Saskatchewan, Manitoba, Ontario, and southern Quebec in Canada and northern California, southern Oregon, all of the northern border states from Washington to Michigan, Wisconsin, Iowa, Illinois, and Missouri in the United States. Lighter-density smoke extends over the U.S. southern Plains, northern Alberta and British Columbia, northern Quebec, and over the northern Atlantic Ocean."*

The true color image for August 18 (Figure 5-103) shows smoke plumes originating from the Mendocino Complex, the Carr Fire and the southwest Oregon Fires (Klondike, Taylor Creek, Miles and Columbus Fires) as well as numerous fires in British Columbia. The 500 mb height field shows that winds are zonal over Canada, so that smoke from the fires in British Columbia is transported directly to the east rather than southeast toward Texas. There is high pressure over the southwestern US and a shortwave in the 500 mb height field over Idaho. The wind field over northern California and southern Oregon is northwesterly and favorable for transport toward the southeast. The AOC, CO and HMS smoke product all show the signature of fire plumes extending far downwind from these fires.

By August 19, the shortwave at 500 mb has deepened into a low centered over Nebraska and a surface low is located over Kansas (Figure 5-104). A cold front associated with the surface low stretches across northwest Texas and a band of clouds along the cold front is visible in the true color image. The flow at 500 mb is northwesterly and favorable for transport from the fires toward the southeast. Clouds within the low pressure system cause data gaps in the AOD retrieval, but an area of enhanced AOD is visible over Kansas as well as enhanced CO. The HMS smoke product shows south-westward movement of the area of very dense smoke from the fires in British Columbia.

The surface low and upper level low moved east by August 20. An area of smoke moving southeast behind the front is visible in the true color image (Figure 5-105; Figure 5-106). The cyclonic flow associated with the low brings the smoke from the western fires southeast toward Texas. By August 20 three is an area of enhanced AOD (AOD>1) over north Texas, as well as an area of enhanced CO. The HMS smoke product also shows dense smoke entering Texas from the north. The NOAA NESDIS Smoke Narrative for August 20 noted," The *ongoing wildfire activity in the western U.S. and western Canada continues to produce enormous amounts of smoke of varying density that covers most of southern Canada and the northern United States. The densest smoke within this area extended from the Texas Panhandle north to eastern Montana and also extending offshore the Pacific Northwest to western British Columbia*."

On August 21, the cold front is just north of Houston and the surface low is now over the Great Lakes (Figure 5-107). The 500 mb height field over Texas is flat, with high pressure dominating the area. An area of high AOD coincides with the visible smoke plume that extends from Kansas across Oklahoma and Northeast Texas into Louisiana and Mississippi. This feature also appears in the HMS smoke product, which shows most of the US to be covered with smoke.

By August 22, the smoke has reached Houston (Figure 5-108) and is clearly visible in the true color image as well as the AOD and CO retrievals and the HMS smoke product. Figure 5-109 shows an expanded view of the true color MODIS image showing smoke over the region including Houston. Smoke is still present over Houston on August 23 (Figure 5-110) as evidenced enhanced values of AOD. The GOES-16 smoke mask product also indicates that smoke was present over Houston on August 23 (Figure 5-111). The NOAA HRRR surface smoke forecast for August 23 (Figure 5-112) shows smoke plumes from several fires in Louisiana extending toward Houston and suggests that these fires as well as transport from distant wildfires contributed to smoke over Houston on August 23. There is a stationary front over Houston and the 500 mb height field shows high pressure over Texas; these features are consistent with weak synoptic forcing over Houston.

On August 24, the 500 mb height field over Texas remains flat and the surface wind field in the southeast is influenced by anticyclonic flow around the areas of high pressure over the mid-Atlantic states (Figure 5-113). By August 24, the HMS smoke product no longer shows evidence of region-wide smoke over Texas. There are a few small smoke plumes emanating from fires in northern Louisiana a but winds on August 24 transported these plumes northward away from Houston. The AOD retrieval shows enhanced levels (AOD > 0.5) over Houston and over southern Louisiana.

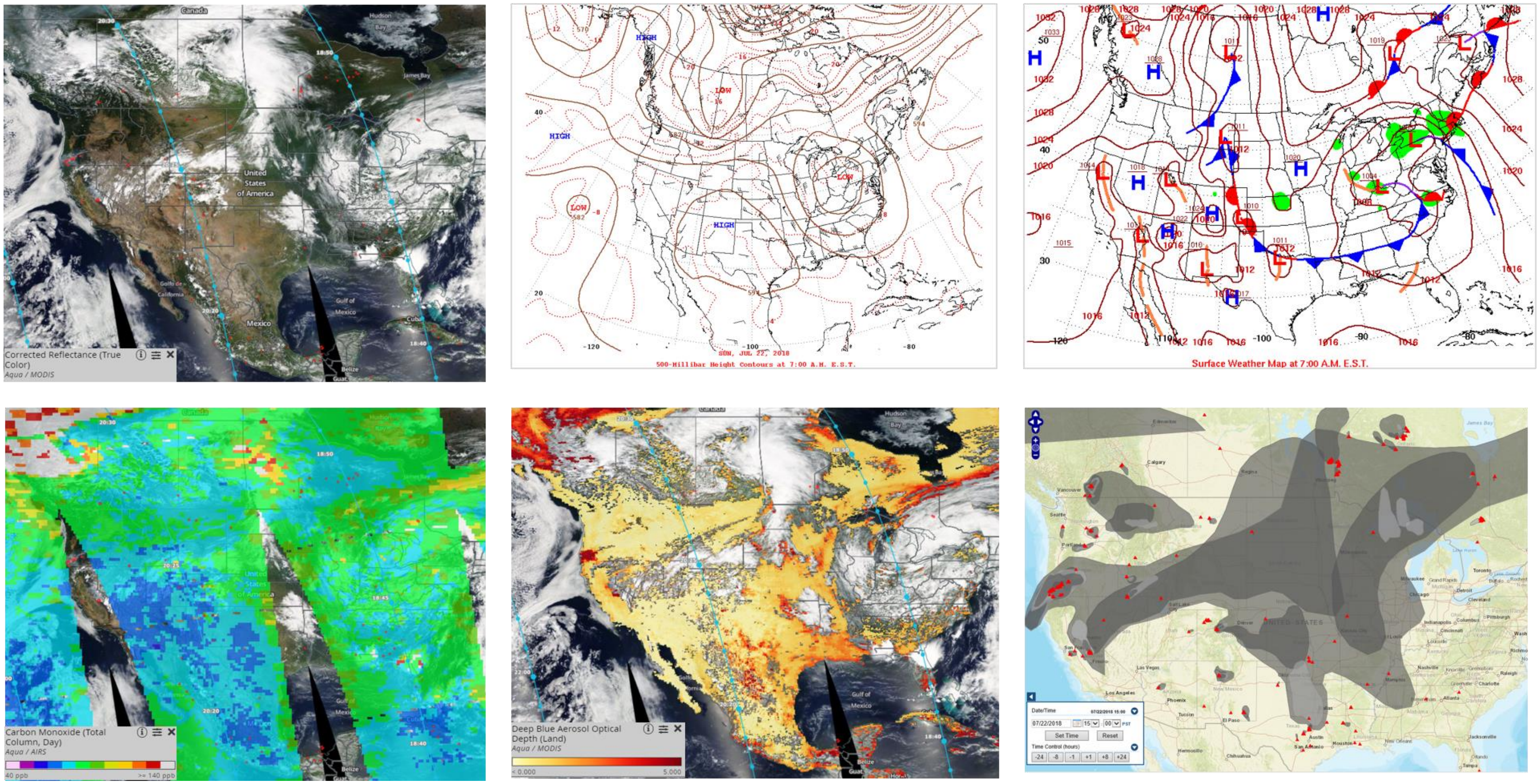

Figure 5-93. NASA EOSDIS images for July 22, 2018. Upper left panel: Aqua/MODIS corrected reflectance (true color) image and Aqua/MODIS fires/thermal anomalies (red icons). Time stamp for the Aqua satellite overpass is noted on the blue traces. Upper middle panel: National Weather Service (NWS) Daily Weather Map 500 mb height field for 7 am EST July 22. Upper right panel: NWS surface analysis at 7 am EST. Lower left panel Aqua/AIRS CO column retrieval. Lower center panel: Aqua/MODIS Deep Blue AOD. Lower right panel: airnowtech.org map showing NOAA HMS fire detections (red triangles) and NOAA HMS smoke product (gray shading) for July 22. Darker shading indicates heavier smoke.

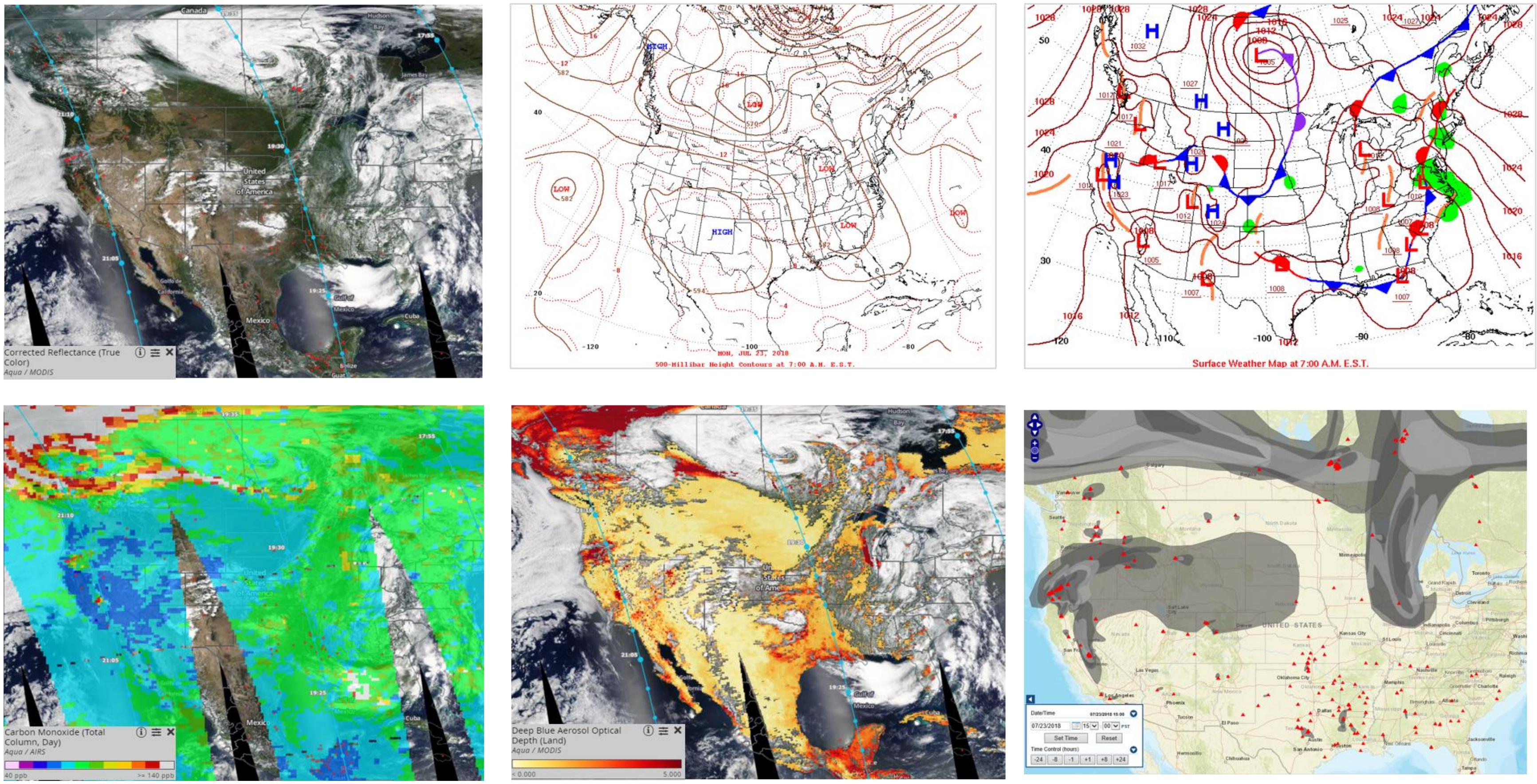

Figure 5-94. As in Figure 5-93, for July 23, 2018.

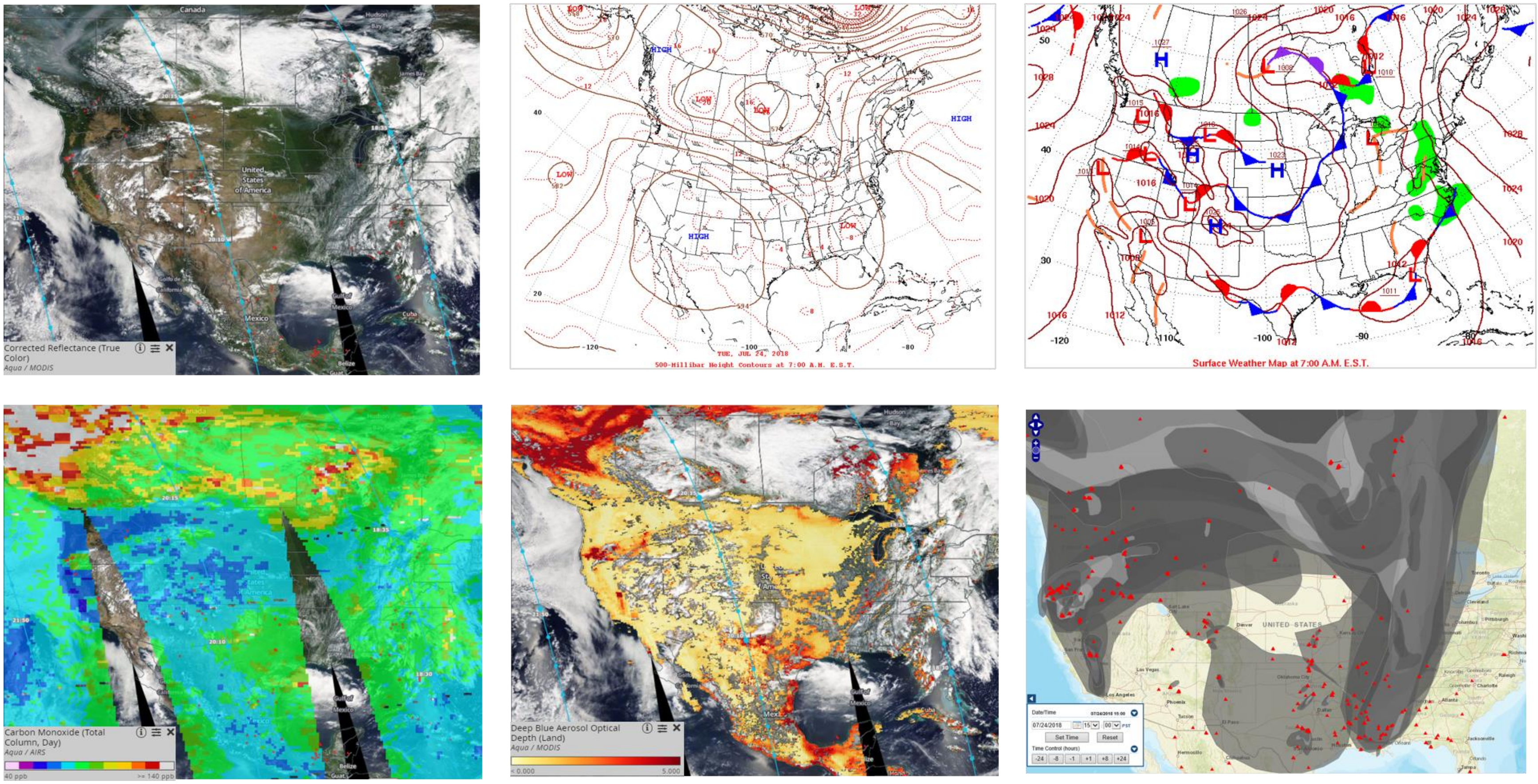

Figure 5-95. As in Figure 5-93, for July 24, 2018.

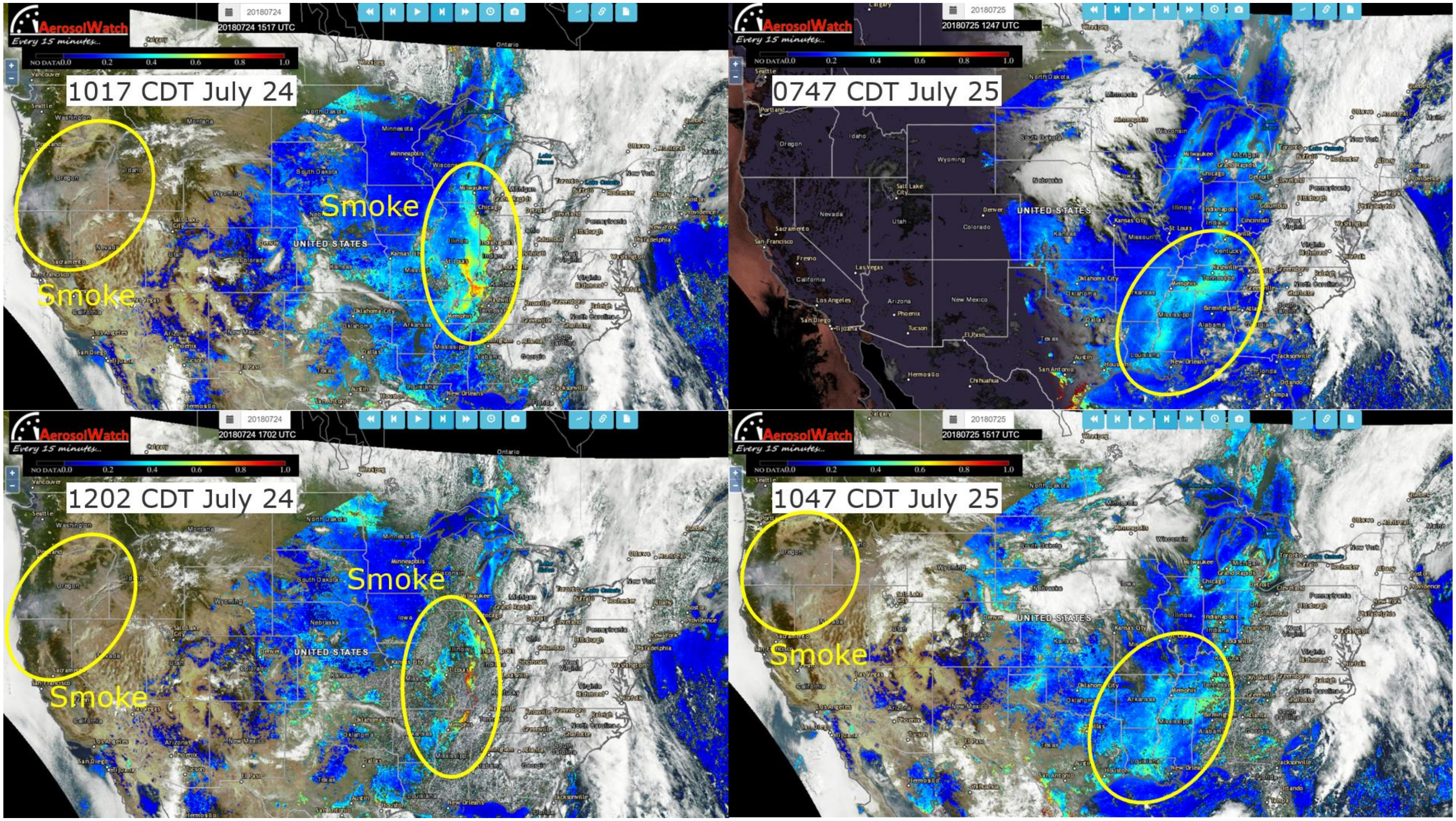

Figure 5-96. Aerosol Watch GOES 16 AOD and true color background. Images show southward movement of smoke on July 24-25.

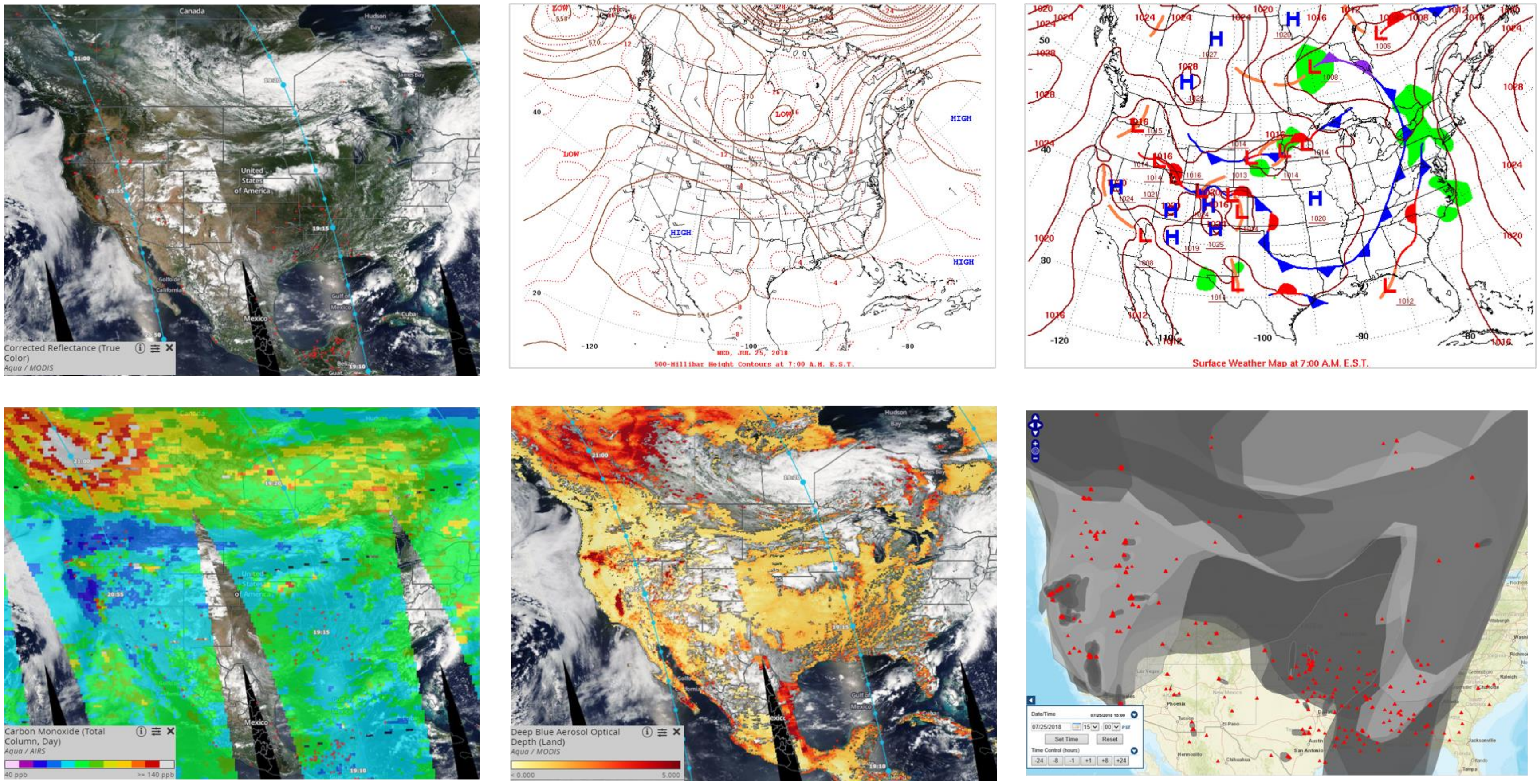

Figure 5-97. As in Figure 5-93, for July 25, 2018.

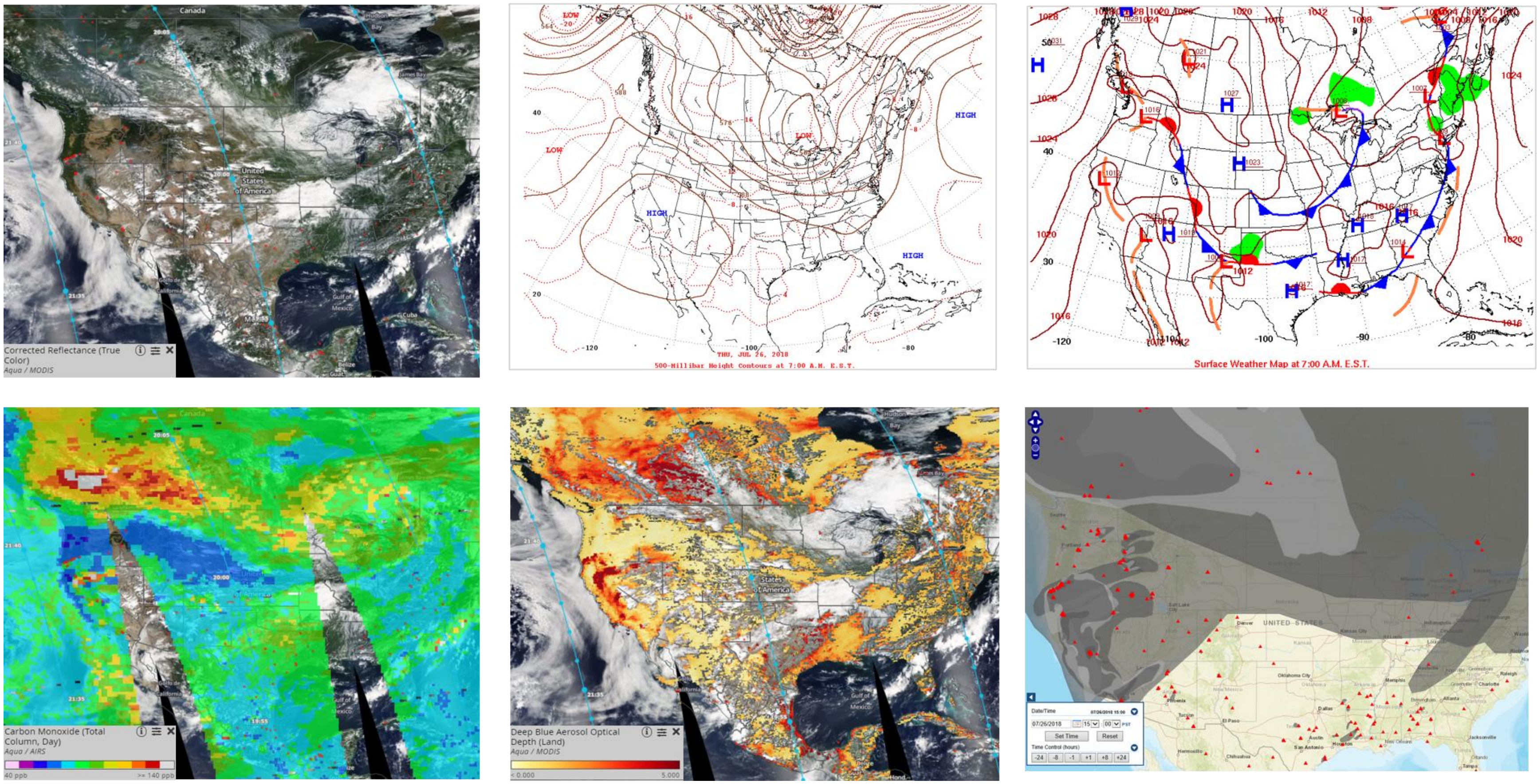

Figure 5-98. As in Figure 5-93, for July 26, 2018.

Figure 5-99. July 26, 2018.

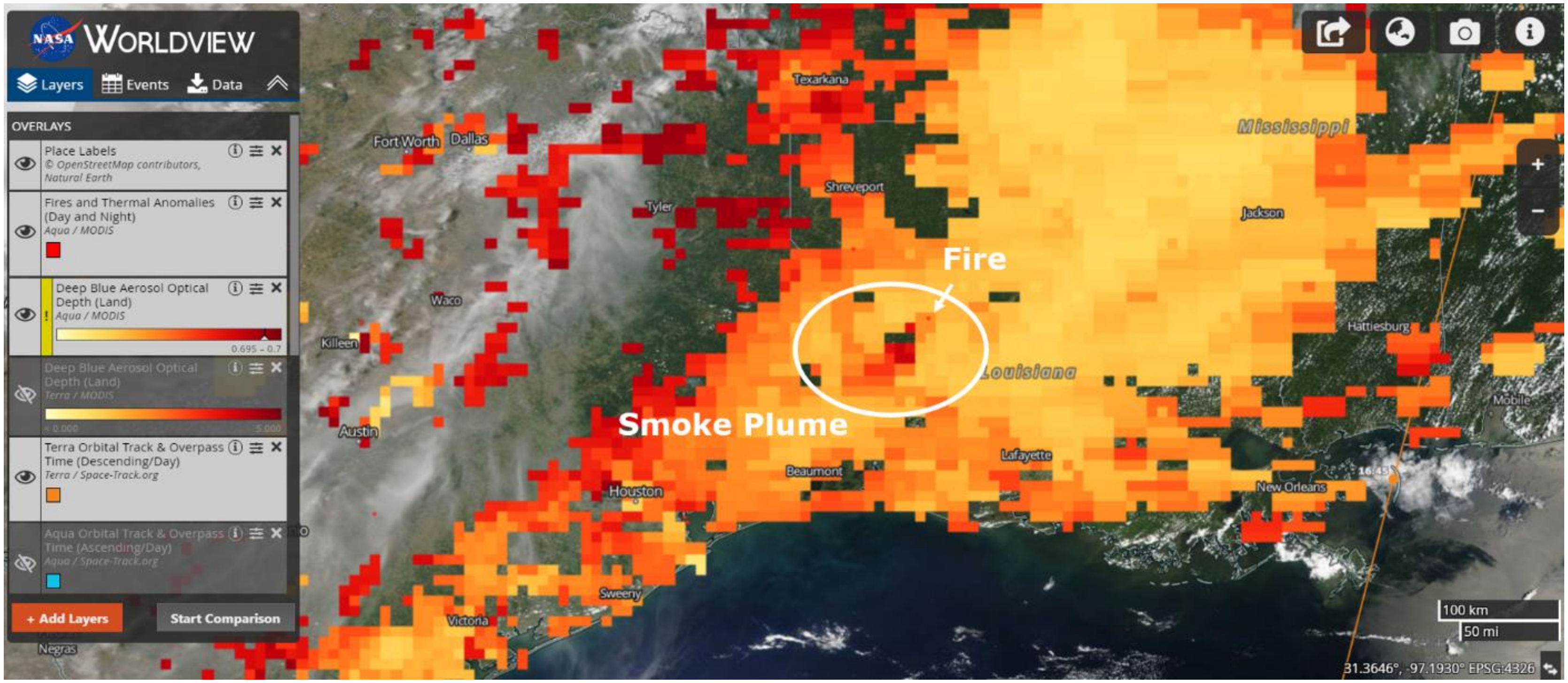

Figure 5-100. July 26, AOD.

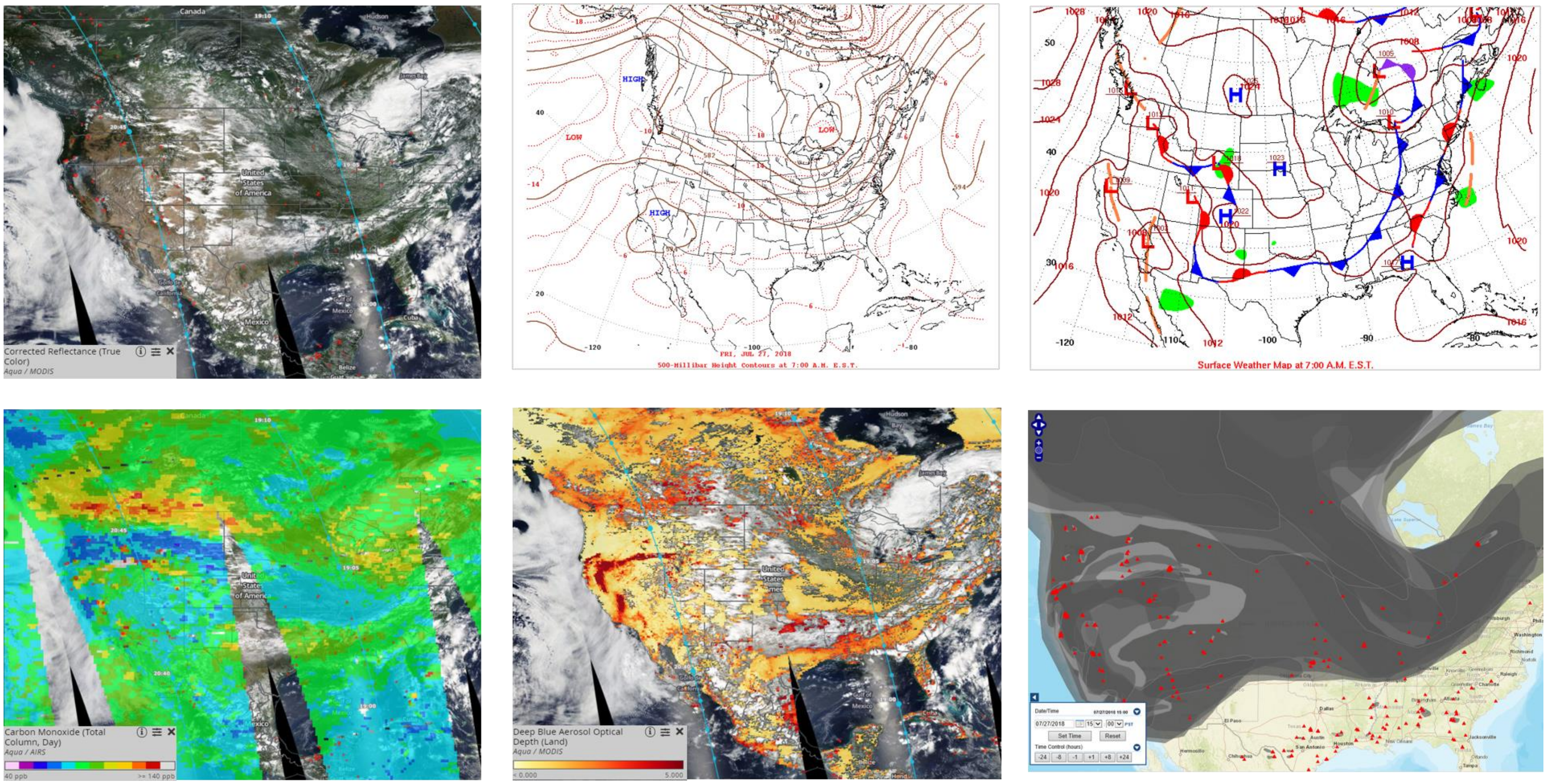

Figure 5-101. As in Figure 5-93, for July 27, 2018.

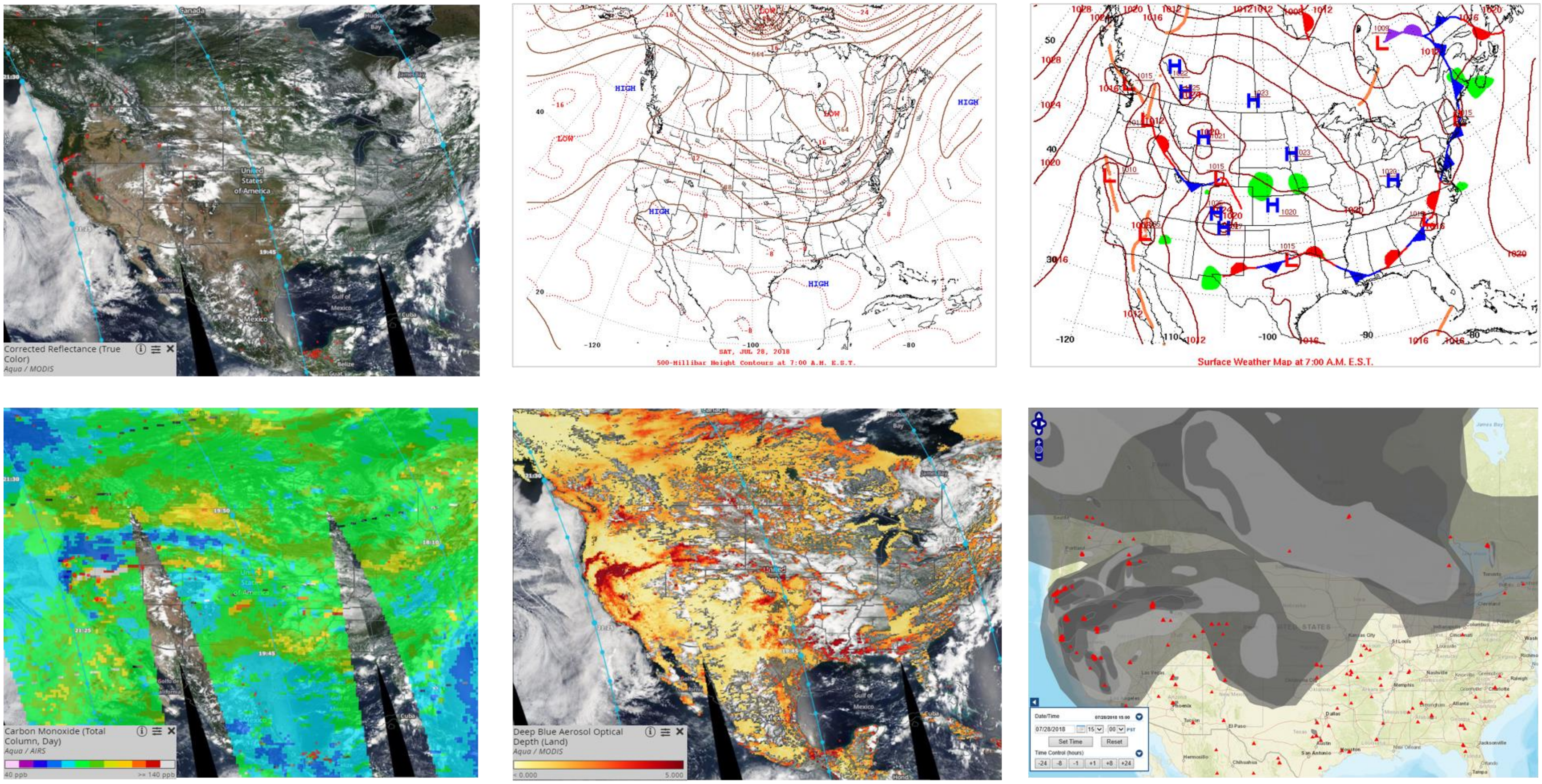

Figure 5-102. As in Figure 5-93, for July 28, 2018.

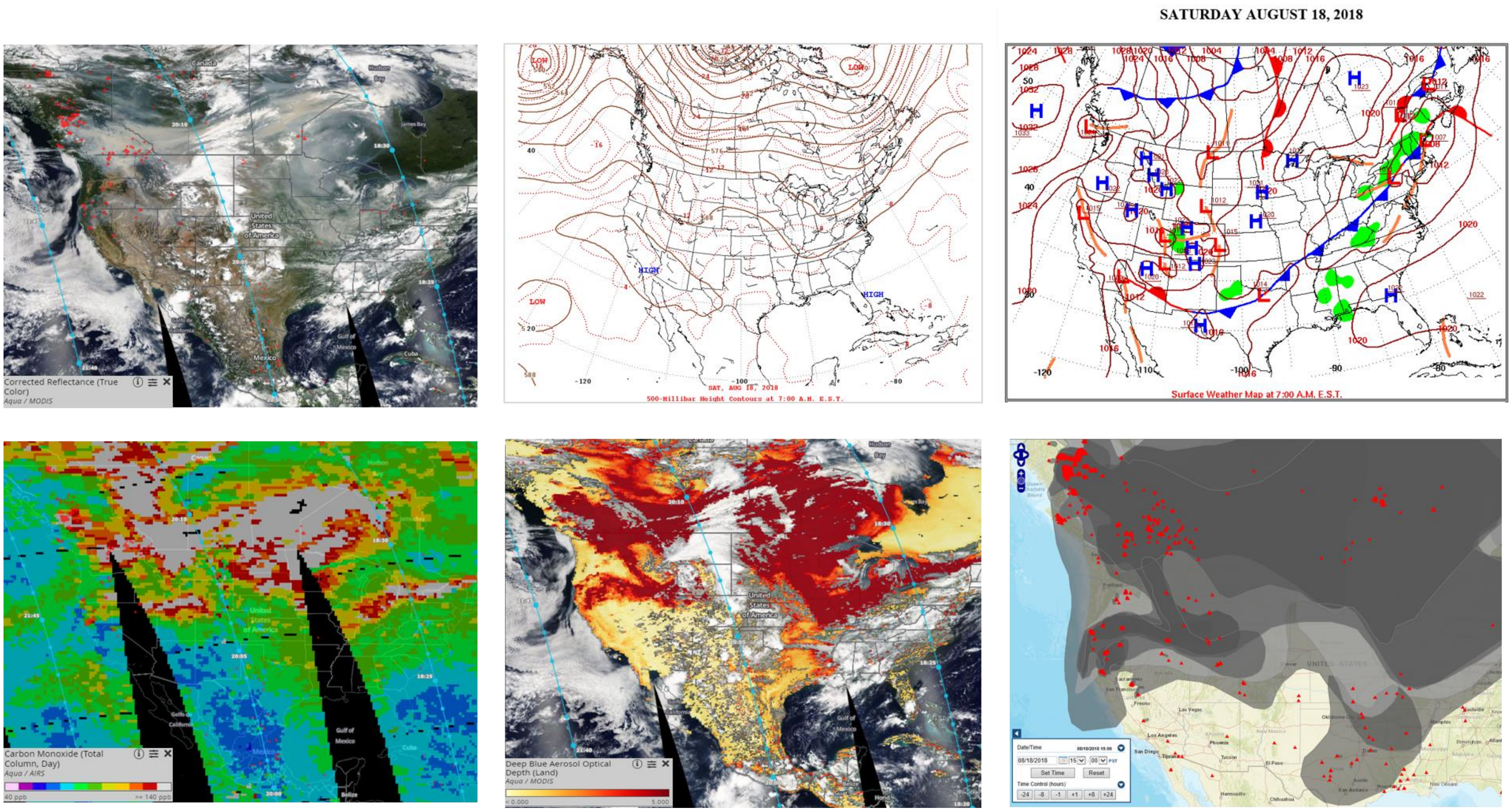

Figure 5-103. As in Figure 5-93, for August 18, 2018.

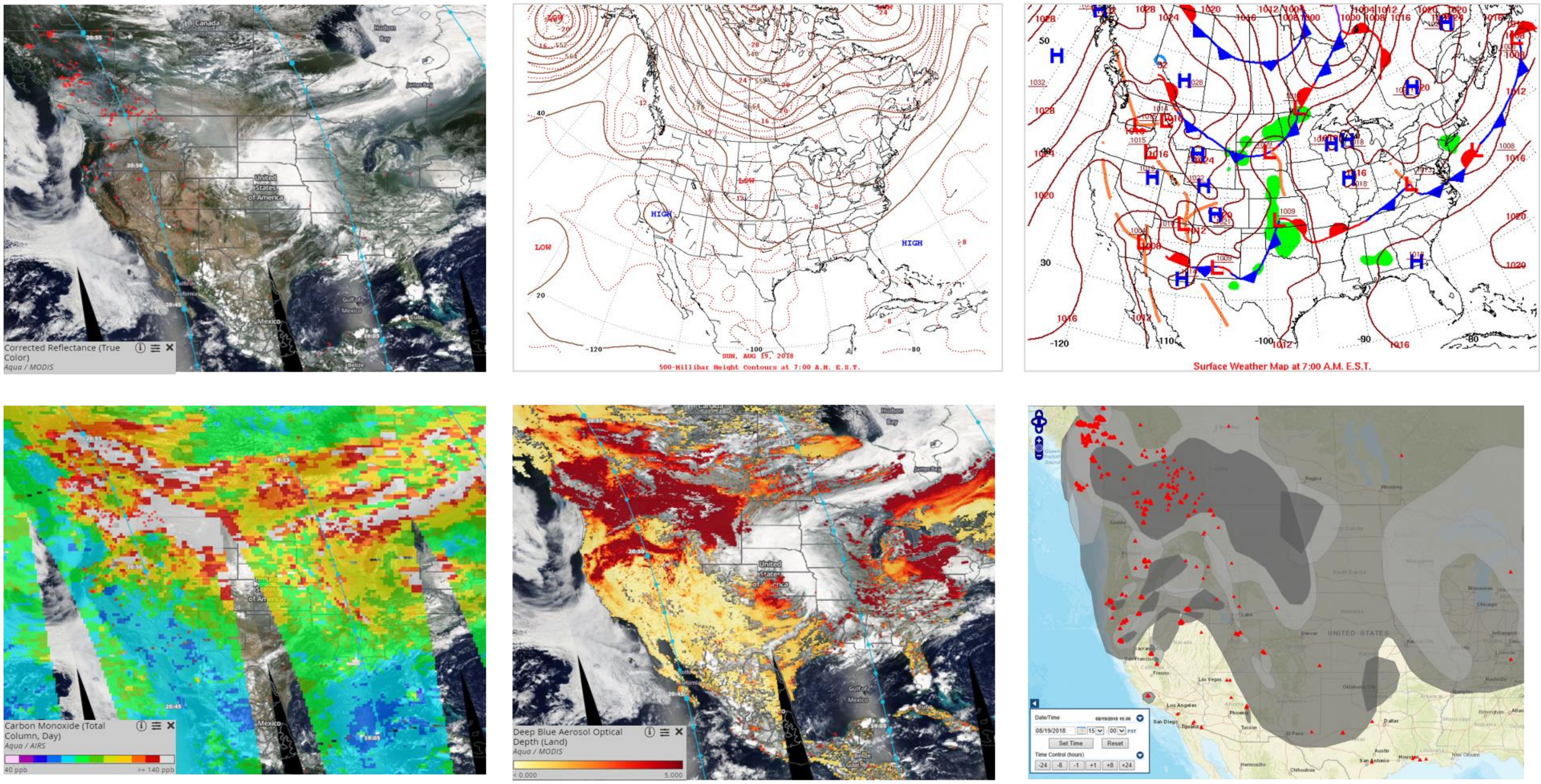

Figure 5-104. As in Figure 5-93, for August 19, 2018.

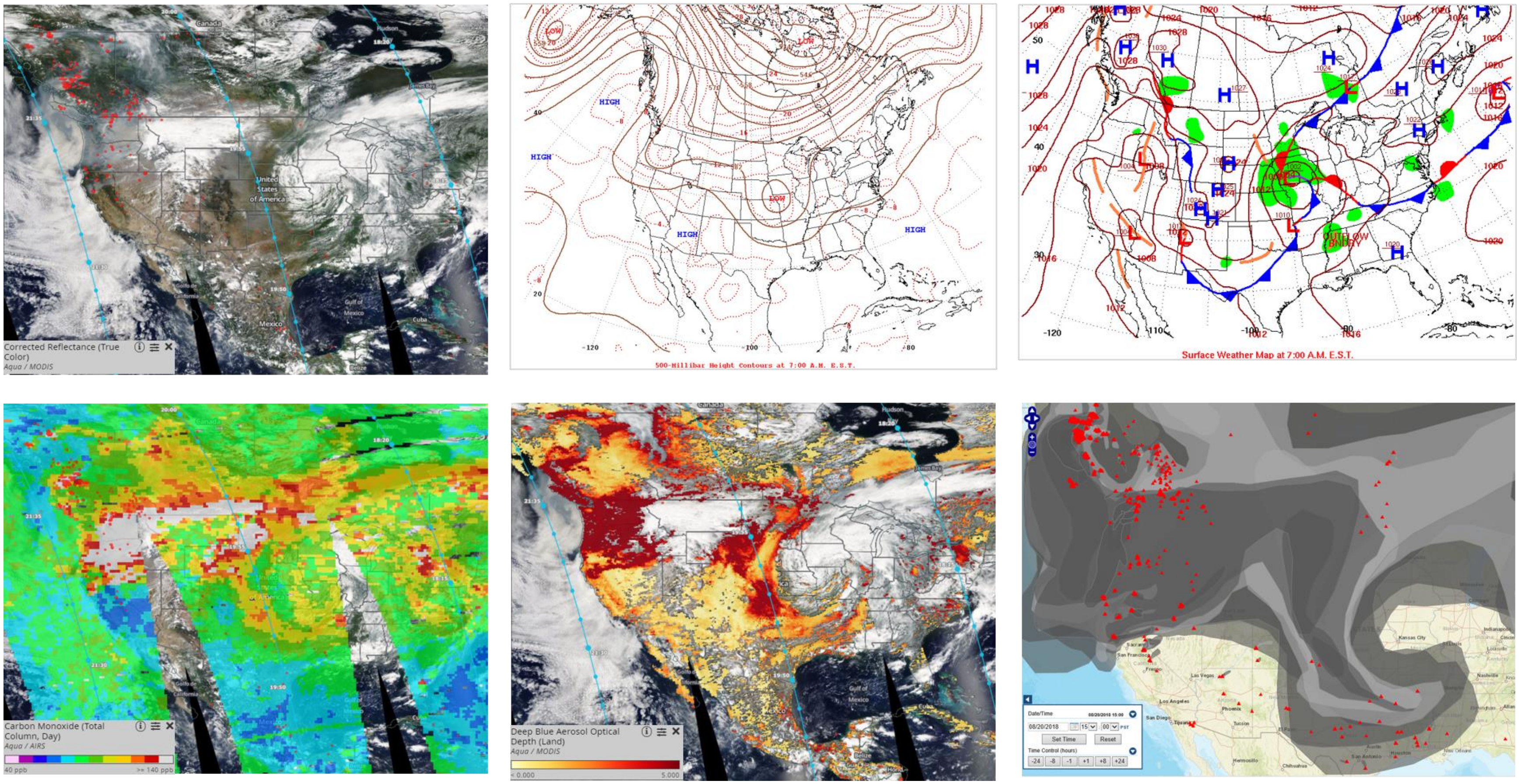

Figure 5-105. As in Figure 5-93, for August 20, 2018.

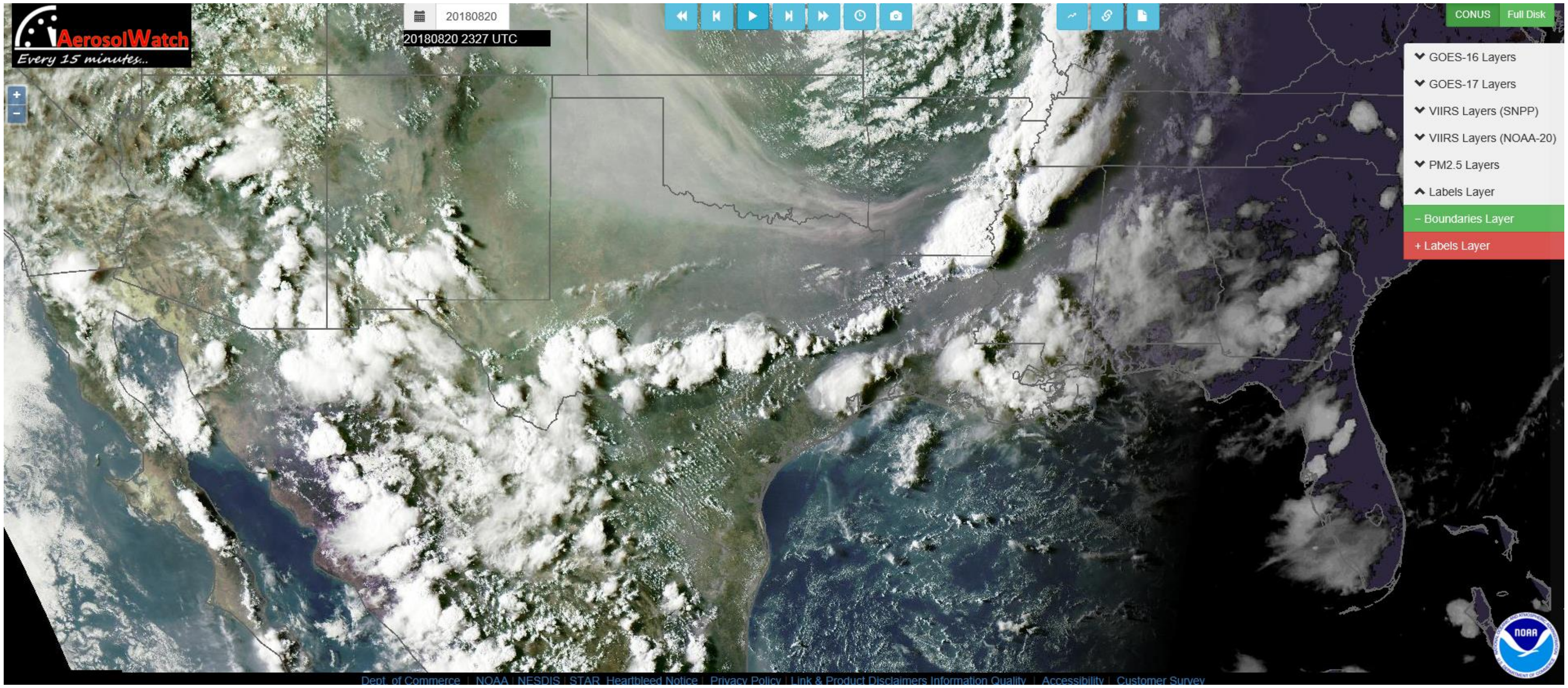

Figure 5-106. On August 20, smoke from fires in the western US and Canada advances southward into Texas behind a cold front. True color GOES-16 image from Aerosol Watch.

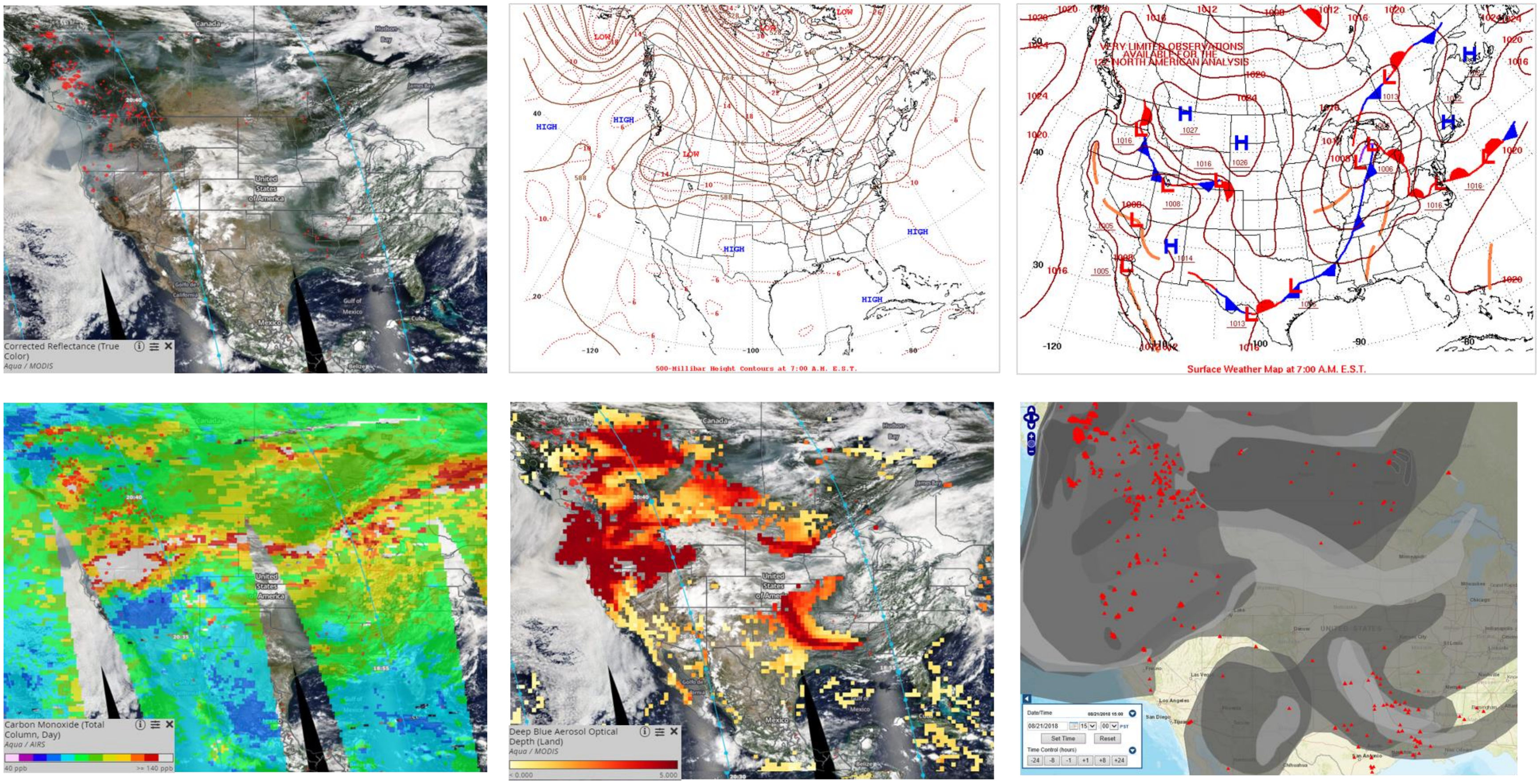

Figure 5-107. As in Figure 5-93, for August 21, 2018.

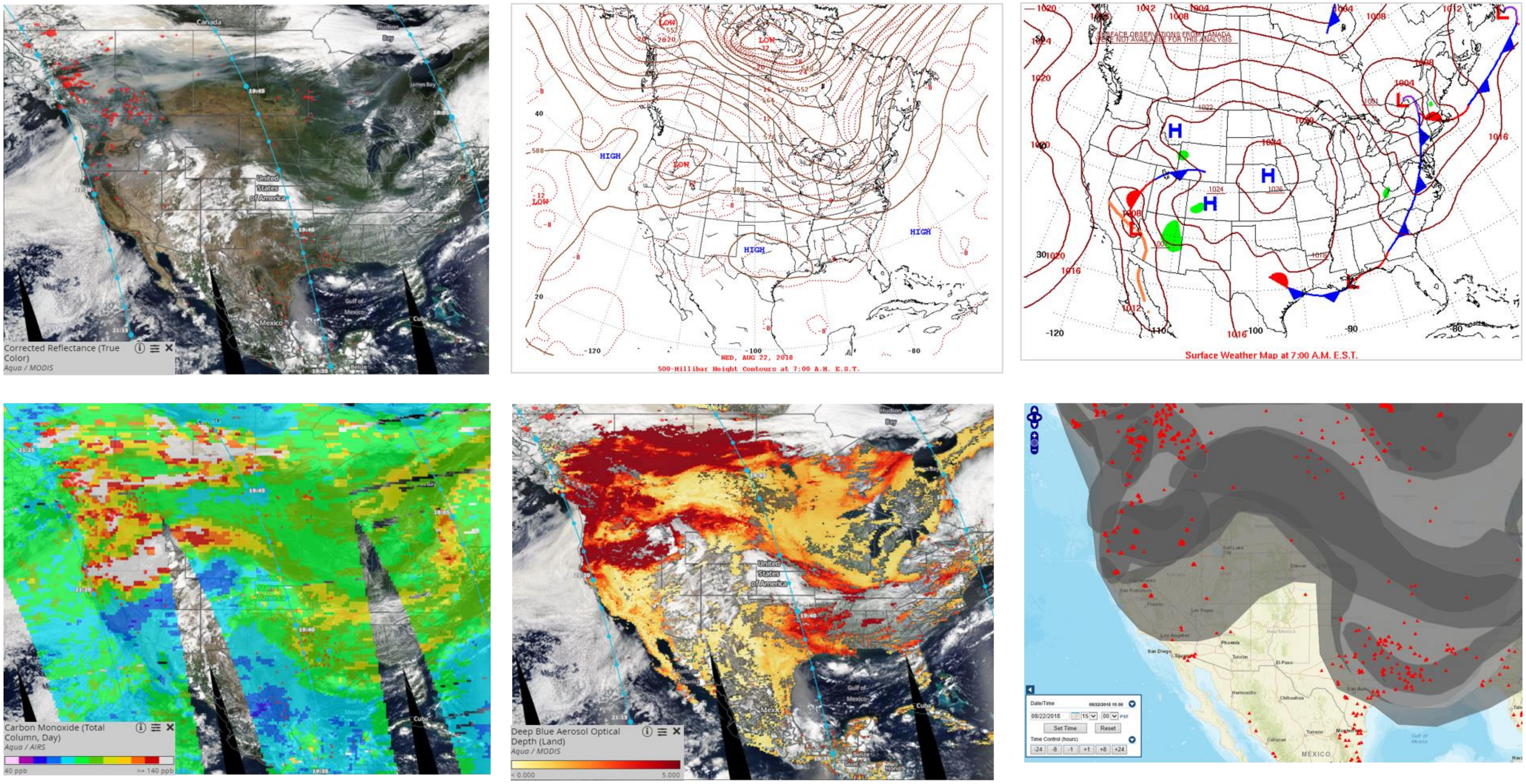

Figure 5-108. As in Figure 5-93, for August 22, 2018.

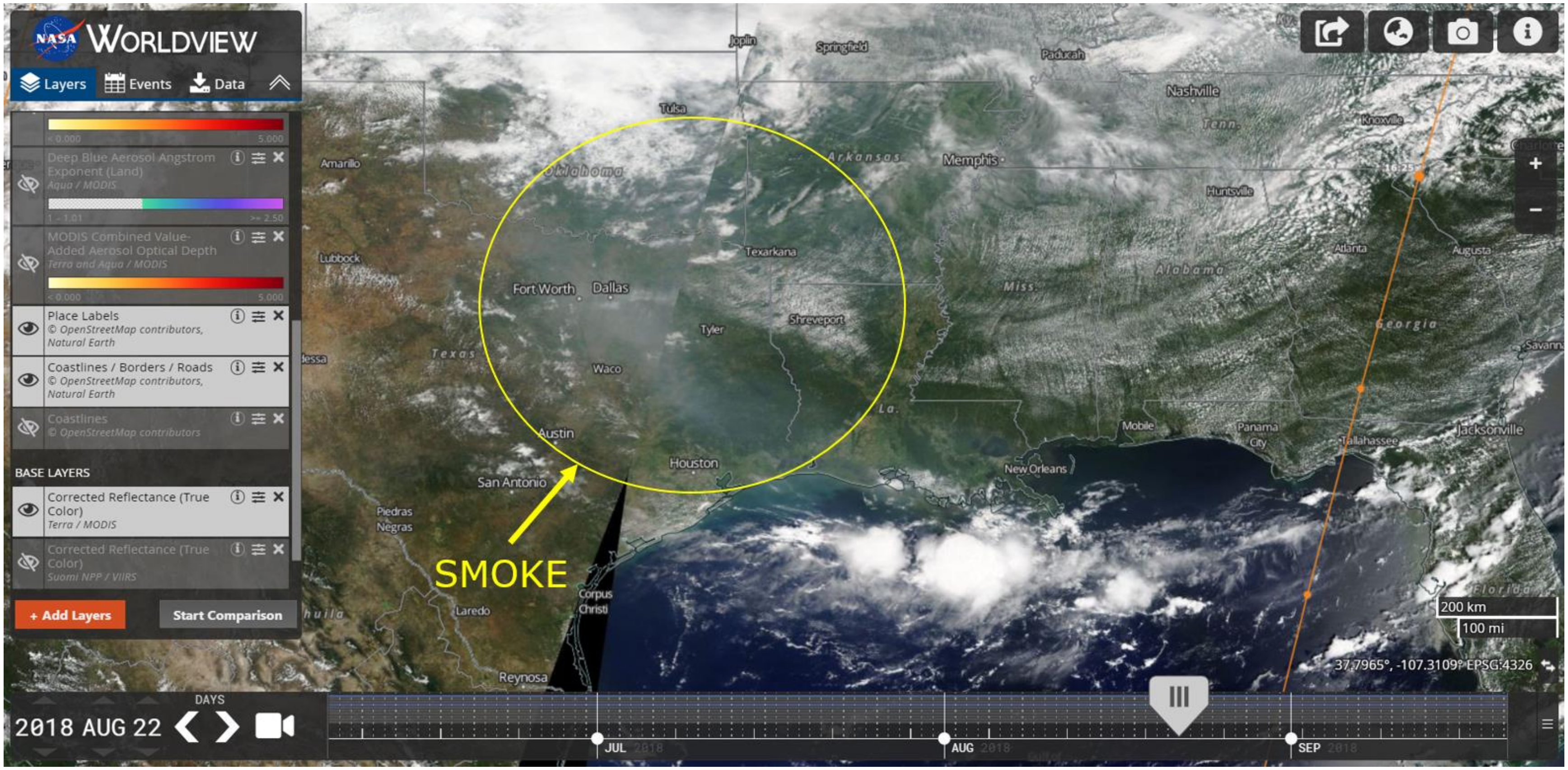

Figure 5-109. EOSDIS August 22 corrected reflectance (true color) image showing smoke over East Texas and over Houston.

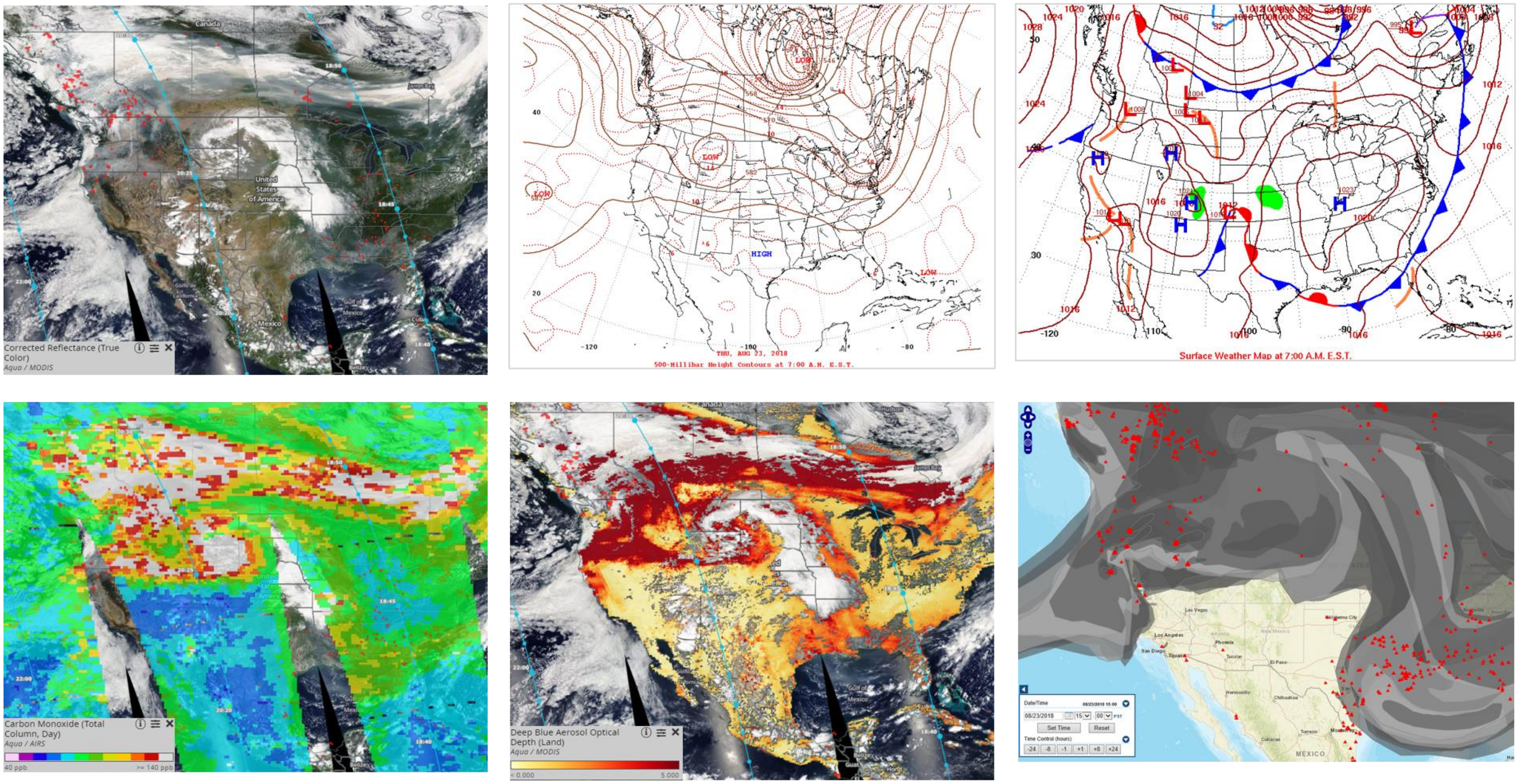

Figure 5-110. As in Figure 5-93, for August 23, 2018.

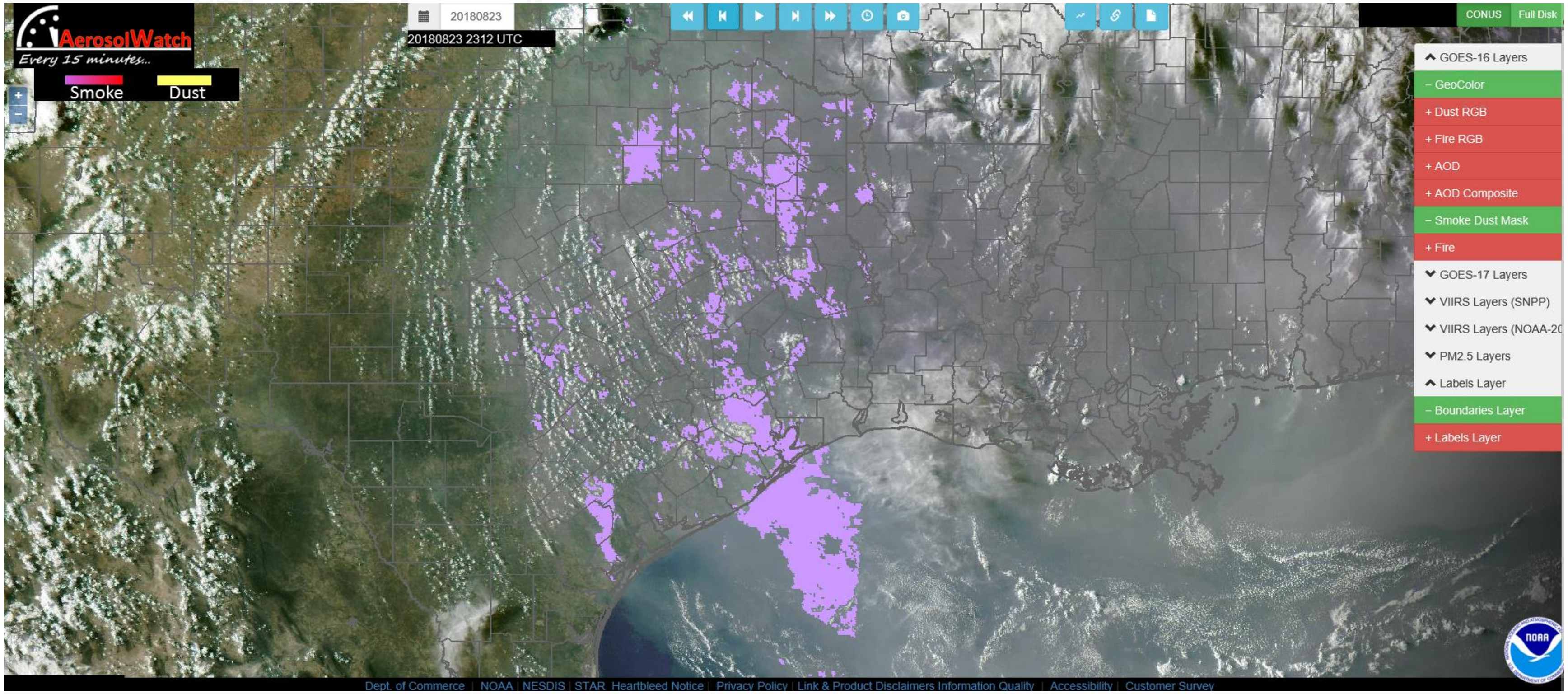

Figure 5-111. August 23. Aerosol Watch GOES 16 true color image with smoke mask product (purple) showing the presence of smoke over Houston.

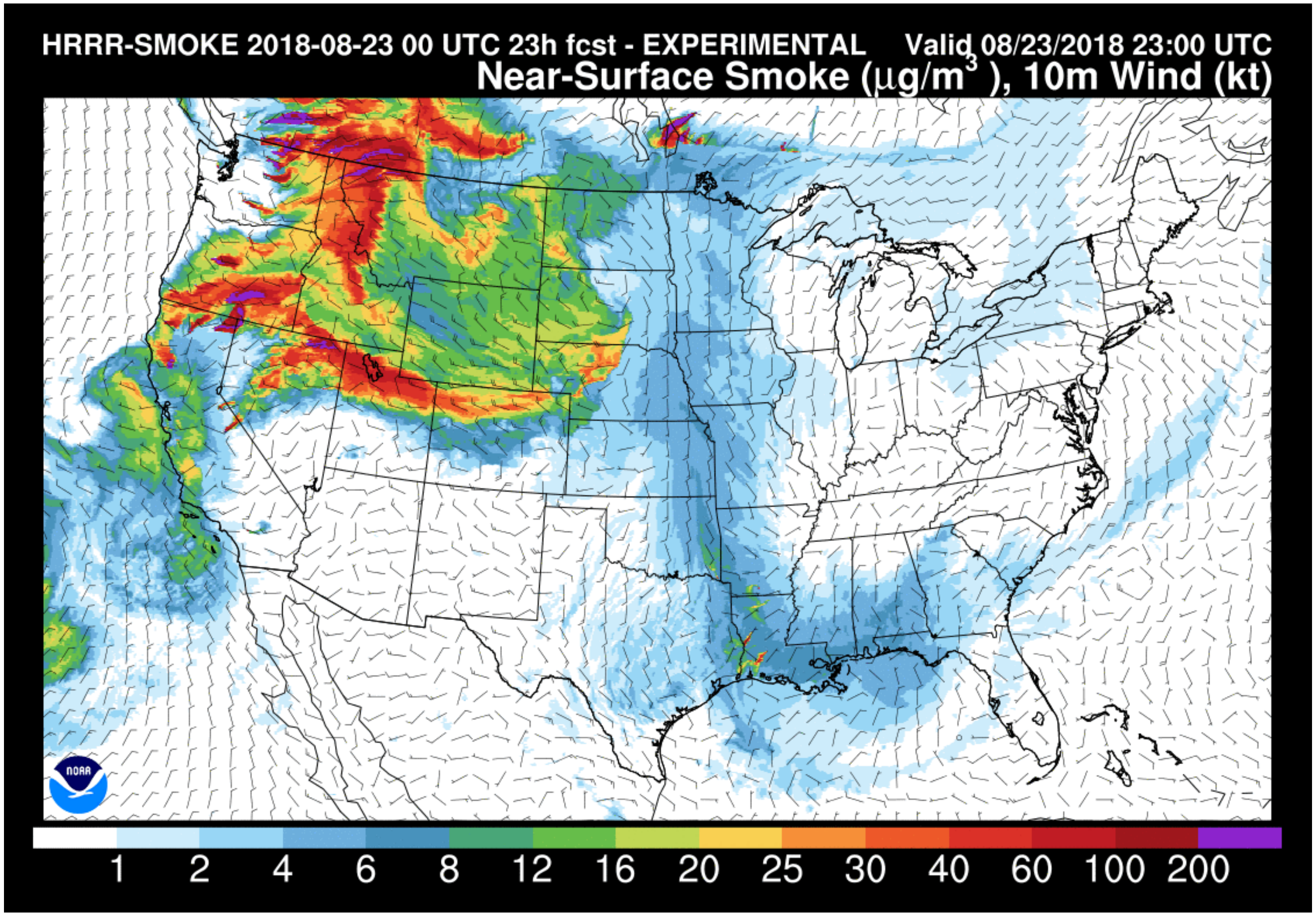

Figure 5-112. NOAA HRRR Near-Surface Smoke Product for August 23 showing smoke from distant fires superposed with plumes from fires in Louisiana.

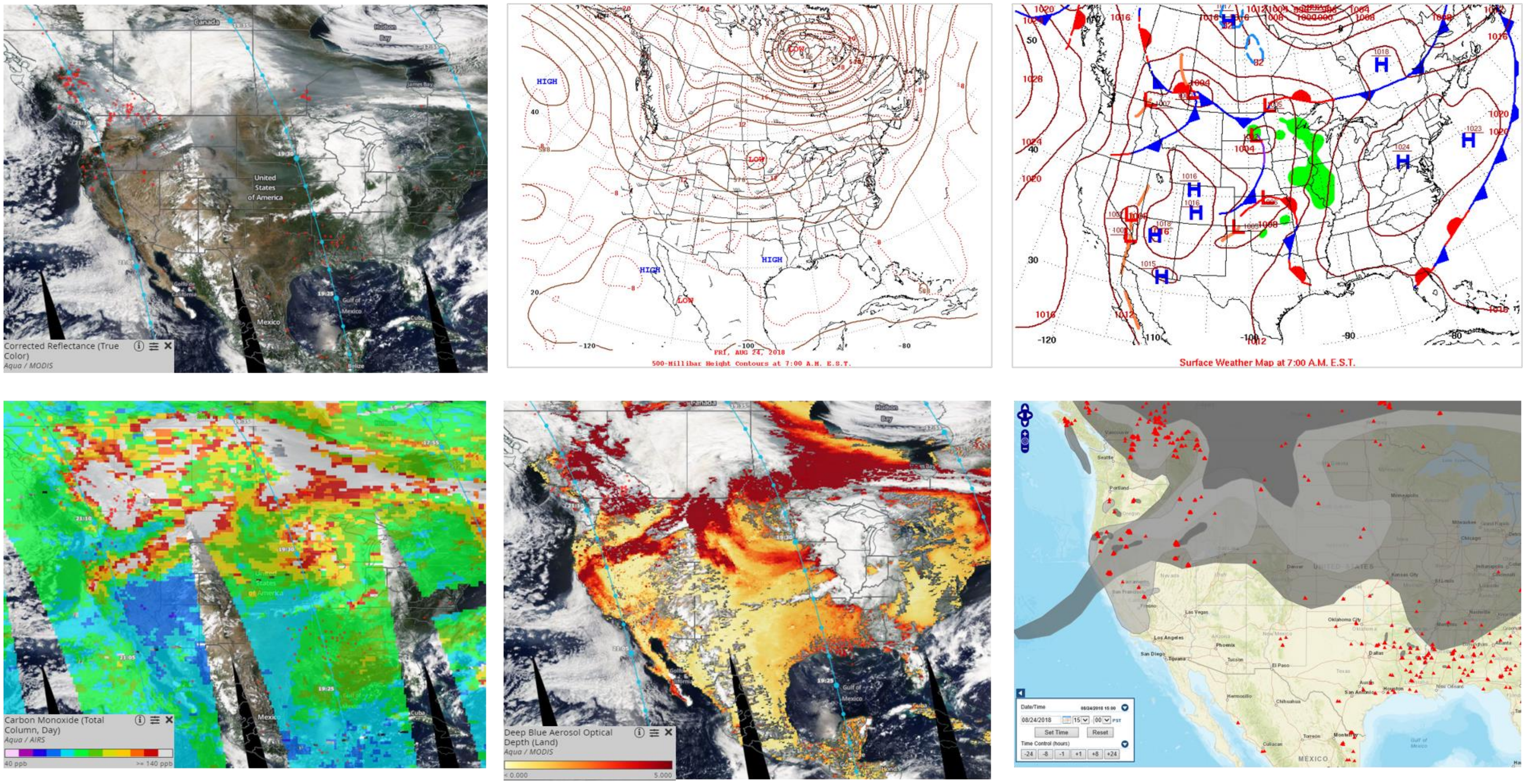

Figure 5-113. As in Figure 5-93, for August 24, 2018.

5.4 Additional Evidence that Wildfire Emissions Caused the Ozone Exceedances at Bayland Park CAMS 53 and Aldine CAMS 8

EPA Guidance on Exceptional Event Demonstrations (EPA, 2016) notes that air agencies may develop supporting evidence for a clear, causal relationship between wildfire(s) and ozone exceedance(s) using photochemical modeling, matching day analyses and statistical regressions. All three of these analyses were performed for this Tier 3-level analysis and we describe the methods and results for each In Section 5.4.

5.4.1 NRTEEM Photochemical Modeling of Wildfire Contributions to Houston Ozone

In 2018, Ramboll operated a Near-Real Time Exceptional Event Modeling (NRTEEM) system for the TCEQ (Johnson et al., 2018). The NRTEEM system uses the Weather, Research and Forecasting (WRF) meteorological model and the Comprehensive Air Quality Model with Extensions (CAMx) air quality model. The modeling system encompasses Houston, which is simulated at 4 km spatial resolution, and all of the continental US. NRTEEM is an operational system run in near-real time (NRT) mode with input data that were readily available at the time of the simulations. The NRTEEM model configuration is similar to that used for the TCEQ's State Implementation Plan (SIP) modeling and is described below.

5.4.1.1 Modeling Cycle and Meteorology

The NRTEEM system runs daily and simulates 24 hours (1 full day from midnight to midnight in CST) that continue from the preceding simulation day. Ramboll uses 0.25 degree Global Forecasting System (GFS) data assimilation system (GDAS) analysis data (Ek et al., 2014) as initial conditions for the WRF meteorological model. This GDAS data is also used for boundary conditions and data assimilation. The NRTEEM system runs a modeling cycle with at least a 1-day lag to acquire satellite-derived wildfire emissions, observations and analyses for the WRF model for the entire modeling cycle; therefore, no GFS forecast data needs to be used. We are not able to utilize the NAM (North American Mesoscale) data assimilation system (NDAS) analysis data because it does not cover the expanded 36 km domain (includes all of Mexico and parts of Central America) used in the NRTEEM system.

We are utilizing WRF v3.9.1.1 (released August 2017; Skamarock et al., 2008) for the NRTEEM system, the latest version of the model available in at the start of the 2018 TCEQ NRTEEM project. Complete WRF physics configuration is available in Johnson et al., (2018).

5.4.1.2 CAMx Model Configuration

Ramboll selected CAMx version 6.40 (released December 2016; Ramboll 2016) for the NRTEEM system, the latest version of the model at the start of the 2018 NRTEEM project. We use the following CAMx inputs for the NRTEEM system:

- Initial conditions and boundary conditions extracted from NRT Whole Atmosphere Community Climate Model (WACCM) chemical forecasts from NCAR (https://www.acom.ucar.edu/waccm/forecast/). Chemical forecasts are run each day using WACCM, driven by GEOS-5 meteorology and including the standard (100 species) chemical mechanism.
- WRFCAMx v4.6 using YSU Kv methodology
- Kv landuse patch up to 100 m and Kv cloud patch applied
- O3MAP: 2016 monthly averages from 1 degree TOMS satellite ozone column data
- Photolysis rates files generated using O3MAP 2016 monthly averages

5.4.1.3 Anthropogenic Emissions

The anthropogenic emission inventory used for the NRTEEM 2018 modeling is TCEQ's 2017 future year inventory that is projected from 2012 and does not contain day-specific emissions. 2010 Emissions Database for Global Atmospheric Research (EDGAR) global 0.1 degree emissions based on EPA's Hemispheric Transport of Air Pollution (HTAP) emissions modeling platform are used outside the TCEQ 36 km domain.

5.4.1.4 Biogenic Emissions

Biogenic emissions use Model of Emissions of Gases and Aerosols from Nature (MEGAN; Guenther et al., 2006) v2.10 using contemporaneous WRF modeling cycle meteorology with isoprene emissions factors that incorporate aircraft flux measurements as in (Yu, et. al., 2015). Leaf Area Index (LAI) inputs include urban enhancements in Texas (Kota, et. al., 2015).

5.4.1.5 Wildfire Emissions

In summer 2018, Ramboll used Fire INventory of NCAR (FINN) v1.0 fire emissions in the original NRTEEM modeling for the period preceding the July 26-28 and August 23-24 high ozone periods.

Instead of relying on reports from fire agencies, FINN fire emissions are obtained from Moderate Resolution Imaging Spectroradiometer (MODIS) instruments flying aboard two polar-orbiting satellites, Terra and Aqua. As these two satellites orbit the Earth, traveling from pole to pole while the earth rotates beneath them, a given area of the Earth will experience an overpass from Terra and Aqua approximately twice a day. MODIS instruments detect fires as thermal anomalies (i.e., hot spots seen against a cooler background) at a spatial resolution of approximately 1 km. Fire emissions derived from the MODIS data include NOx, CO, VOC and PM species. The FINN fire emissions inventory development approach is described by Wiedinmyer et al. (2006; 2011), and Wiedinmyer and Friedli (2007).

Since the initial NRTEEM modeling in summer 2018, NCAR has released an updated version of the FINN fire emissions (v1.5). Ramboll processed the FINN v1.5 emissions for use in the NRTEEM modeling platform for this project.

The FINN fire emission inventory shows large wildfire complexes burning in California, Oregon, British Columbia and along the Ontario/Manitoba and Ontario/Quebec borders during the days leading up to the July 26-28 high ozone days in Houston (Figure 5-114). Figure 5-115 shows a similar plot for the large wildfire complexes burning in California, Oregon, Washington, Nevada and British Columbia during the week before the August 23-24 high ozone days in Houston.

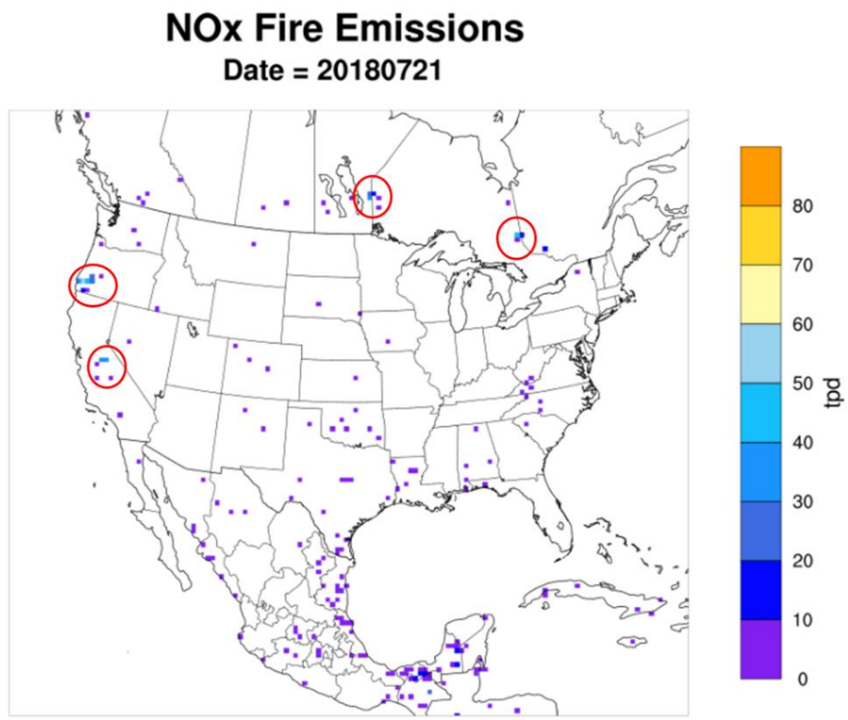

Figure 5-114. FINN NOx emissions for July 21, 2018. Fire complexes circled in red are being investigated as potential contributors to Houston ozone on July 26-28 via long-range transport.

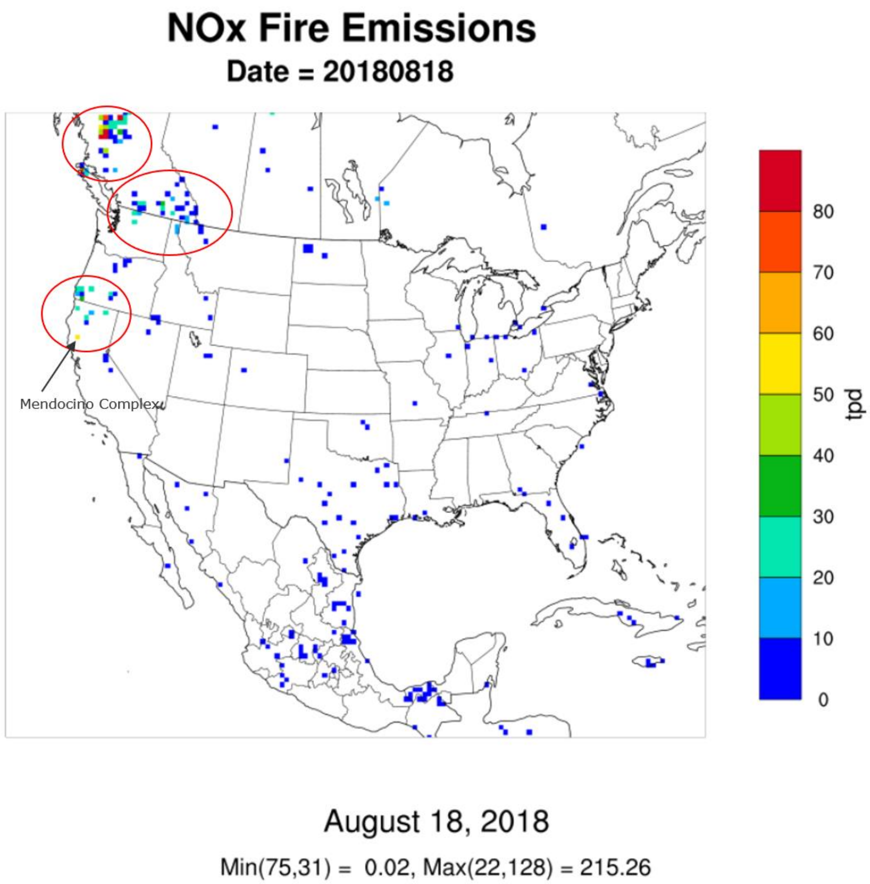

Figure 5-115. FINN NOx emissions for August 18. Circles indicate locations of large fire complexes in the western US and Canada.

5.4.2 Fire Emission NOx Speciation

The NRTEEM model re-speciates the FINN fire NOx emissions species to simulate more realistic (rapid) NOx to NOy conversion observed in fire plumes (Lonsdale et al., 2014). This approach applies vegetation type-dependent speciation factors for NOx emissions (see Table 5-4) and was developed in the 2015 Texas Air Quality Research Program (AQRP) Fires project (McDonald-Buller et al., 2015) and applied for the 2018 TCEQ NRTEEM project. The speciation factors partition FINN NOx into several Carbon Bond 6 revision 2 (CB6r2) NOy species: NO2, PAN, PANX, NTR2 and HNO3.

Table 5-4. NOx-to-NOy FINN fire emissions species mapping factors by vegetation type.

FINN NOx ->	NOy Species					
Vegetation Type Scale Factor	**NO**	**NO2**	**PAN**	**PANX**	**NTR2**	**HNO3**
A	0	0.736	0.056	0.008	0.02	0.18
B	0	0.421	0.144	0.104	0.05	0.28
C	0	0.451	0.128	0.072	0.05	0.3

A: Grasslands/Savanna/Woody Savanna/Shrublands/Croplands
B: Tropical Forest
C: Temperate Forest

For the 2018 TCEQ NRTEEM project, Ramboll evaluated the impact of the NOx-to-NOy conversion by developing a sensitivity simulation with the re-speciated FINN emissions (NOx2NOy) for the April 28, 2017 Mexico/Central America biomass burning episode (Johnson et al., 2017). Figure 5-116 shows the extent of the smoke plume ($PM_{2.5}$ tracer in left panel), base model NOx concentrations (middle) and NOx impacts (NOx2NOy-base) from the new FINN fire emissions. NOx concentrations decrease from the re-speciation. The magnitude of this impact is over 50 ppb where fires are burning. This finding is consistent with the AQRP Fires study (McDonald-Buller et al., 2015).

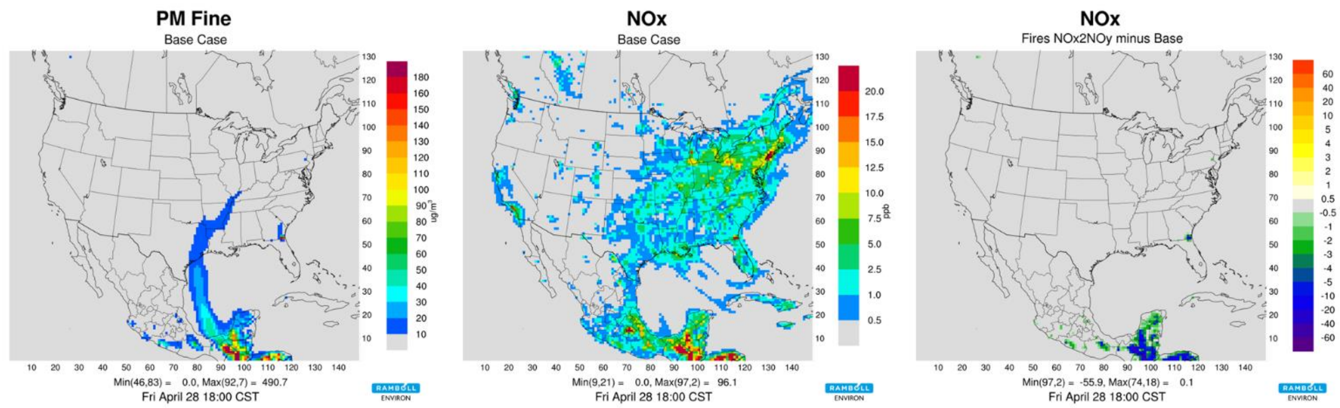

Figure 5-116. Hourly $PM_{2.5}$ smoke tracer (left), NOx (middle) and NOx difference (NOx2NOy-base) concentrations for April 28, 2017 18:00 CST.

Next, we evaluated ozone impacts from the FINN fire emissions re-speciation Figure 5-117. The left panel is the same as in Figure 5-116. The middle and right panels are similar to Figure 5-116 but show ozone concentrations instead of NOx. We found that the lower NOx emissions after re-speciation lead to ozone decreases in the smoke plume. The magnitude of this impact is up to 5 ppb in East Texas. Additionally, we found ozone increases in areas where NOx was titrating ozone in the base run. This finding is also consistent with the AQRP Fires study (McDonald-Buller et al., 2015).

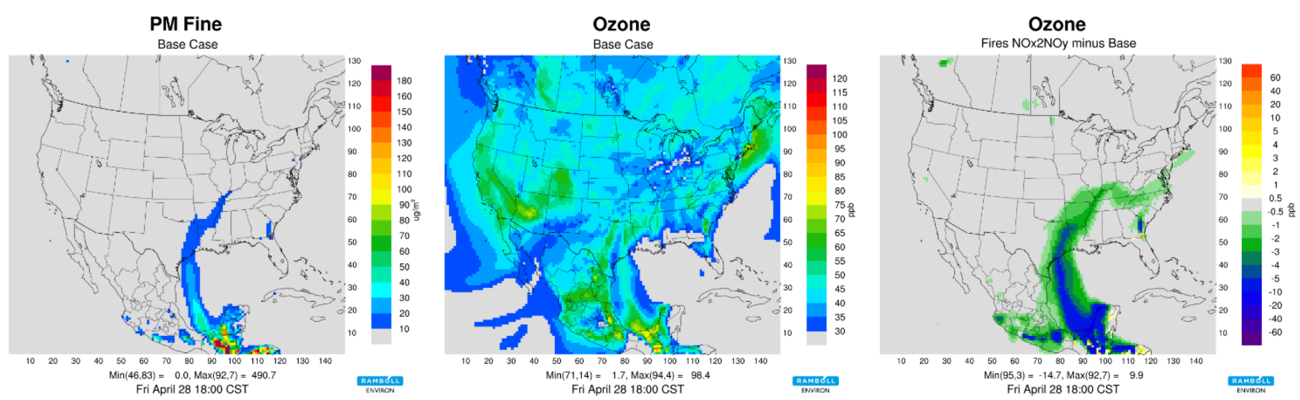

Figure 5-117. Hourly $PM_{2.5}$ smoke tracer (left), Ozone (middle) and Ozone difference (NOx2NOy-base) concentrations for April 28, 2017 18:00 CST.

Temporal and Spatial Allocation

NRTEEM utilizes the EPS3 emissions model, which incorporates the Western Regional Air Partnership (WRAP) methodology to temporally and vertically allocate the FINN fire emissions[20]. The virtual area[21] is used to classify each fire into one of five fire size bins, which determines the values used to calculate the fraction of emissions allocated to the first vertical layer in CAMx and the heights of the plume bottom and top for each hour of the day. Since the FINN fire inventories consist of fires that are always less than or equal to 1 km^2 in size because of the pixel size of the MODIS instrument, fire points that are within 5 km of one another are assumed to be part of the same fire; the virtual areas of each of these points are added together so they have characteristics of a larger fire.

5.4.2.2 CAMS Site Selection

Since the NRTEEM modeling was performed in summer 2018, TCEQ staff have validated all monitoring data collected in Houston during 2018. Ramboll re-downloaded and re-processed all Houston monitoring data.

We have also prepared model performance statistics and time series with the validated monitoring data to evaluate the model's ability to accurately simulate Houston air quality during these periods.

We examine wildfire impacts on ozone and model performance at four CAMS sites:

- Aldine C8
- Bayland Park C53
- Conroe Relocated C78
- UH West Liberty C699

We selected Conroe Relocated C78 and UH West Liberty C699 because they are expected to be upwind on days with transport of continental air into Houston from the north/northeast.

[20] http://www.wrapair.org/forums/fejf/documents/WRAP_2002_PhII_EI_Report_20050722.pdf

[21] Virtual area is a measure of fire size, fire type (prescribed burn or wildfire) and fuel loading

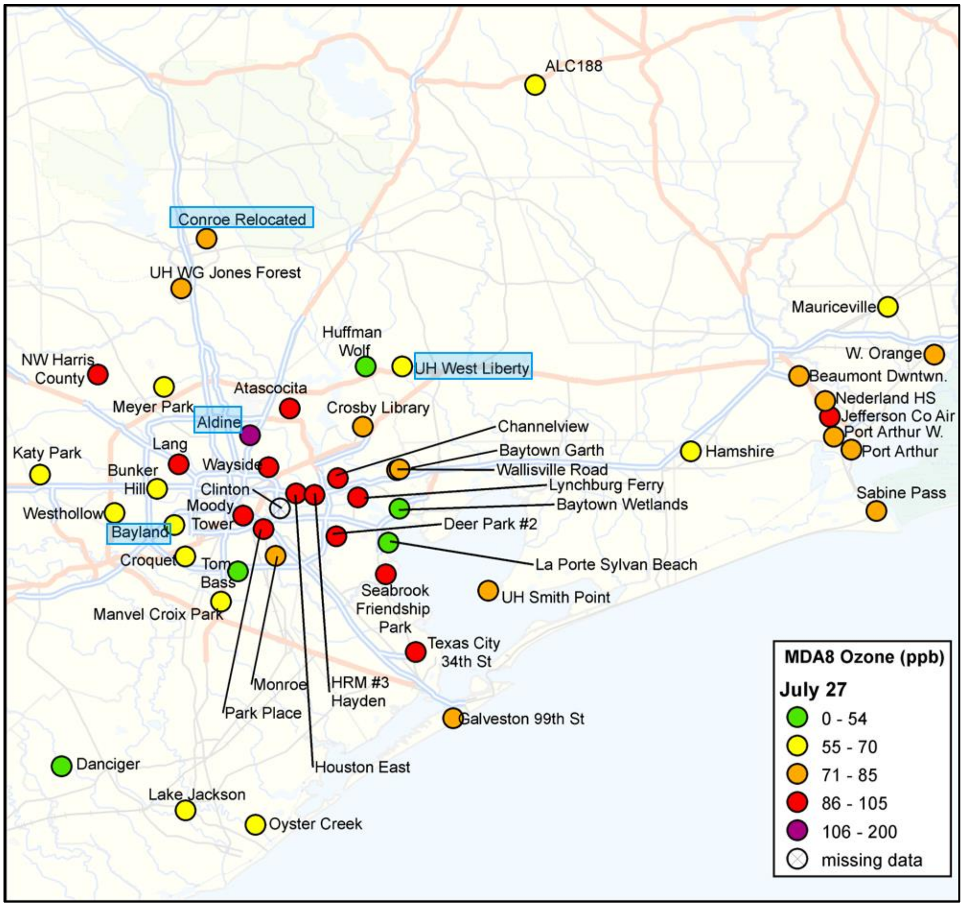

Figure 5-118. Map of Houston and Beaumont area CAMS. Four selected CAMS highlighted in blue.

5.4.2.3 July 26-28, 2018

The TCEQ is evaluating high ozone values at Bayland Park CAMS 53 on July 26, 2018 and Aldine CAMS 8 on July 27, 2018 and July 28, 2018.

Wildfire Impacts on Ozone at the Bayland Park, Aldine and Upwind Monitors

NRTEEM modeling shows wildfire impacts on 1-hour ozone at the Bayland Park (Figure 5-119) and Aldine (Figure 5-120) CAMS were equal to or less than 1 ppb during July 26-28. MDA8 ozone impacts from wildfires is 0.6 ppb at Bayland Park on July 26, 2018 and 0.5 ppb at Aldine on July 27, 2018.

Similar figures for upwind monitors Conroe Relocated and UH West Liberty are shown in Figure 5-121 and Figure 5-122, respectively. Late on July 25, Conroe shows a maximum 1-hour impact of 8.7 ppb, suggesting that modeled wildfire smoke plumes passed to the north of the Bayland Park and Aldine monitors. This wildfire plume had only a small impact at the UH West Liberty monitor, as modeled ozone impacts from fires were under 1 ppb for July 25-28.

Model performance for 1-hour ozone was good[22] at Bayland Park during July 26-28, but the model greatly underestimated peak ozone at Aldine on July 26 (observed: 144 ppb, modeled: 62 ppb) and July 27 (observed: 92 ppb, modeled: 69 ppb). The model reproduced July 26-28 ozone at the UH West Liberty site reasonably well[23], which suggests that the model did not have large biases in simulating the regional background ozone entering Houston. We present model statistics charts for the four CAMS for July 20-28, 2018 in the Appendix.

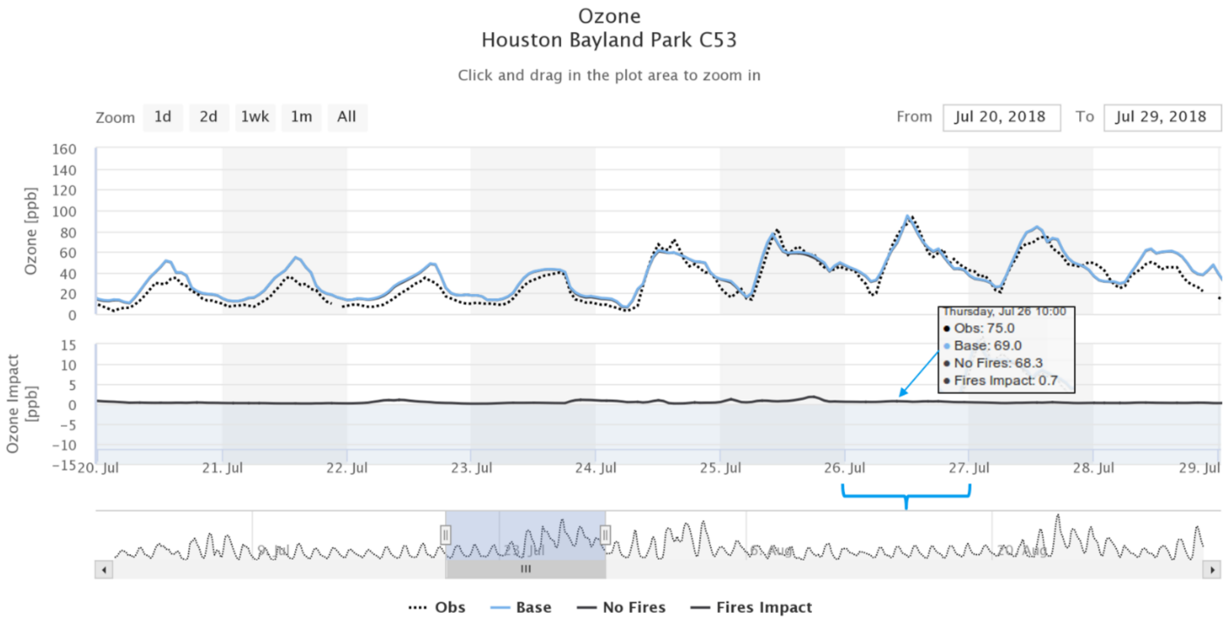

Figure 5-119. Observed (black dotted line), base model (blue) and Fires Impact (dark grey) ozone time series for July 20-28, 2018 at Bayland Park C53 in Houston. Maximum 1-hour ozone impact from wildfires on July 26, 2018 shown in box.

[22] Daily mean normalized bias of 1% on July 26, 6% on July 27 and 20% on July 28

[23] Daily mean normalized bias ≤10% on July 25-27 and 22% on July 28

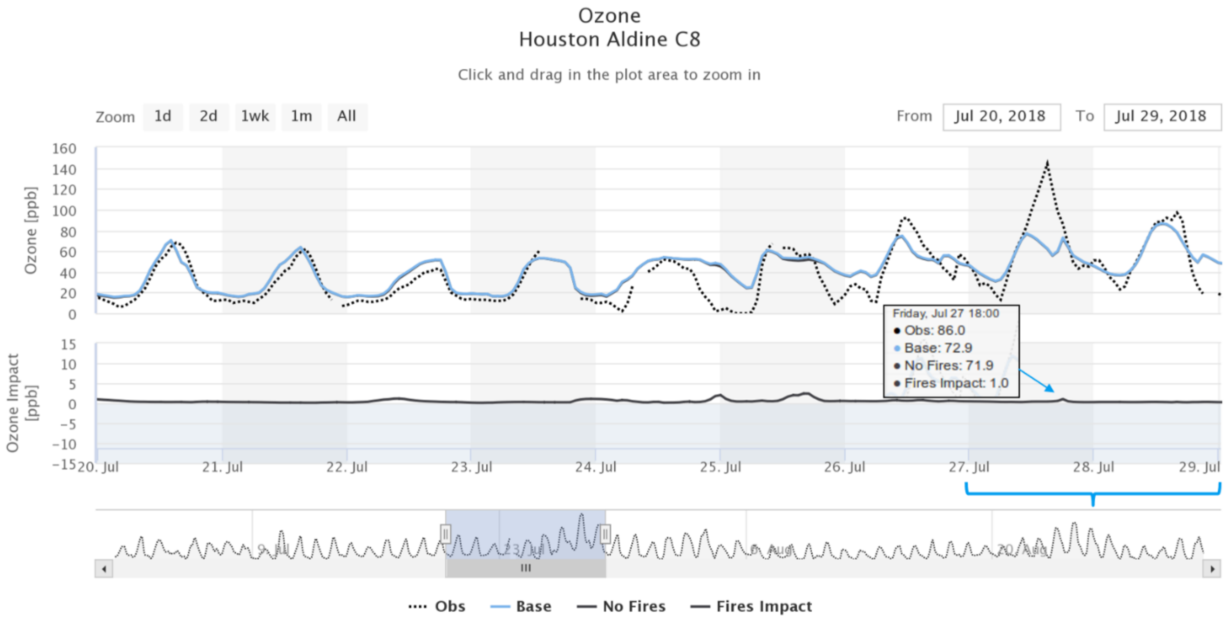

Figure 5-120. Observed (black dotted line), base model (blue) and Fires Impact (dark grey) ozone time series for July 20-28, 2018 at Aldine C8 in Houston. Maximum 1-hour ozone impact from wildfires on July 27, 2018 shown in box.

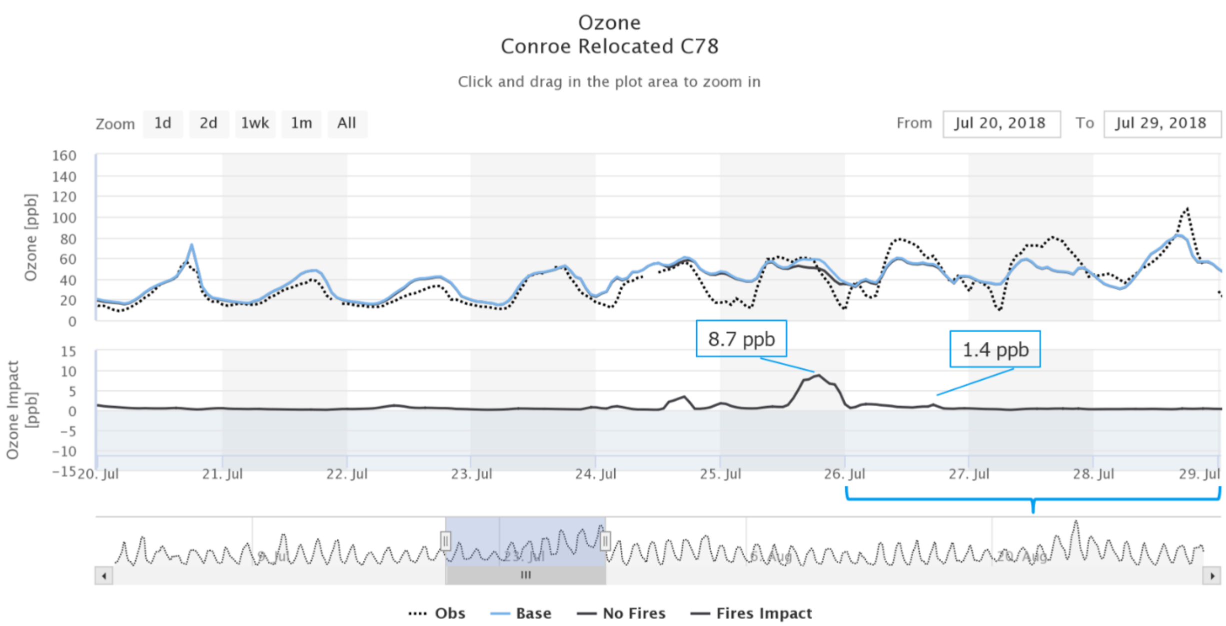

Figure 5-121. Observed (black dotted line), base model (blue) and Fires Impact (dark grey) ozone time series for July 20-28, 2018 at Conroe Relocated C78 in Houston. Maximum 1-hour ozone impact from wildfires on July 25 and 26, 2018 shown.

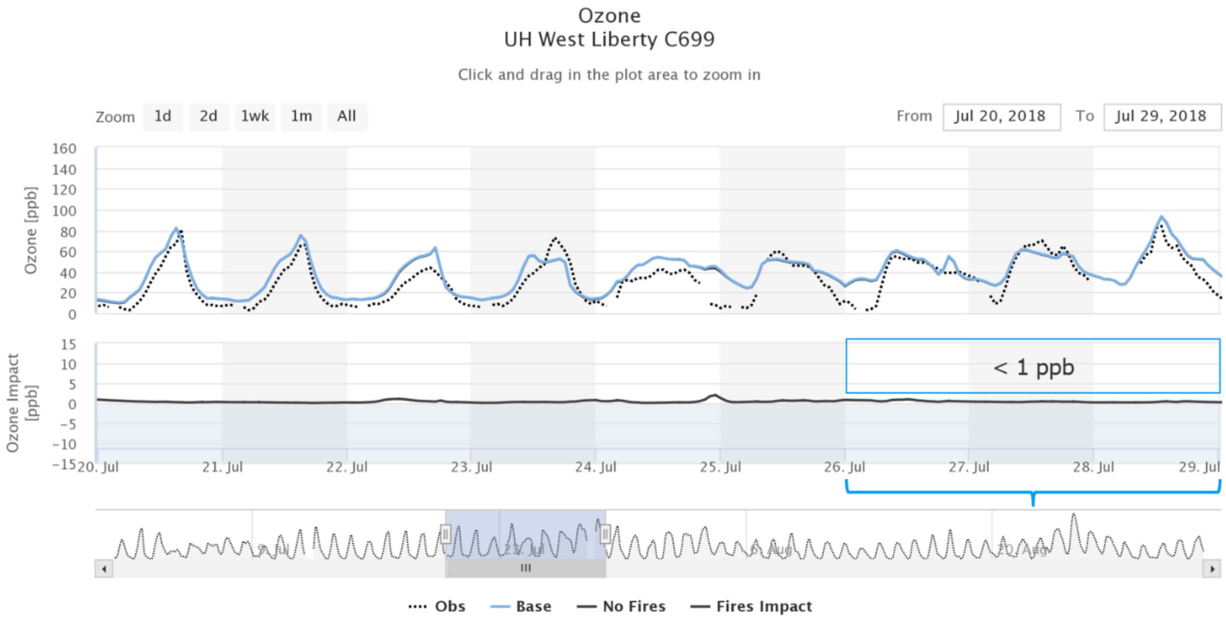

Figure 5-122. Observed (black dotted line), base model (blue) and Fires Impact (dark grey) ozone time series for July 20-28, 2018 at UH West Liberty C699 in Houston.

NRTEEM smoke tracer plots for July 23-28, 2018 (Figure 5-123) indicate that several fires in Louisiana and Texas influenced the Houston area. However, the most intense parts of these fire plumes stayed north of Houston (see Figure 5-124). The NRTEEM model's smoke tracer results were consistent with the NOAA HRRR smoke modeling (see Figure 5-125) in suggesting that fires in Louisiana played a more important role than distant fires in the western US in determining the concentrations of smoke over Houston on July 26-28.

Figure 5-126 shows similar plots as in Figure 5-123, but for MDA8 ozone impacts. These plots suggest that fires in Louisiana were more important than the distant fires in Canada and the western US in transporting ozone to the Houston area in the NRTEEM modeling. On July 26, a fire plume with wildfire MDA8 ozone enhancements exceeding 10 ppb passed north of Houston. We examine model performance for NRTEEM winds in the next section.

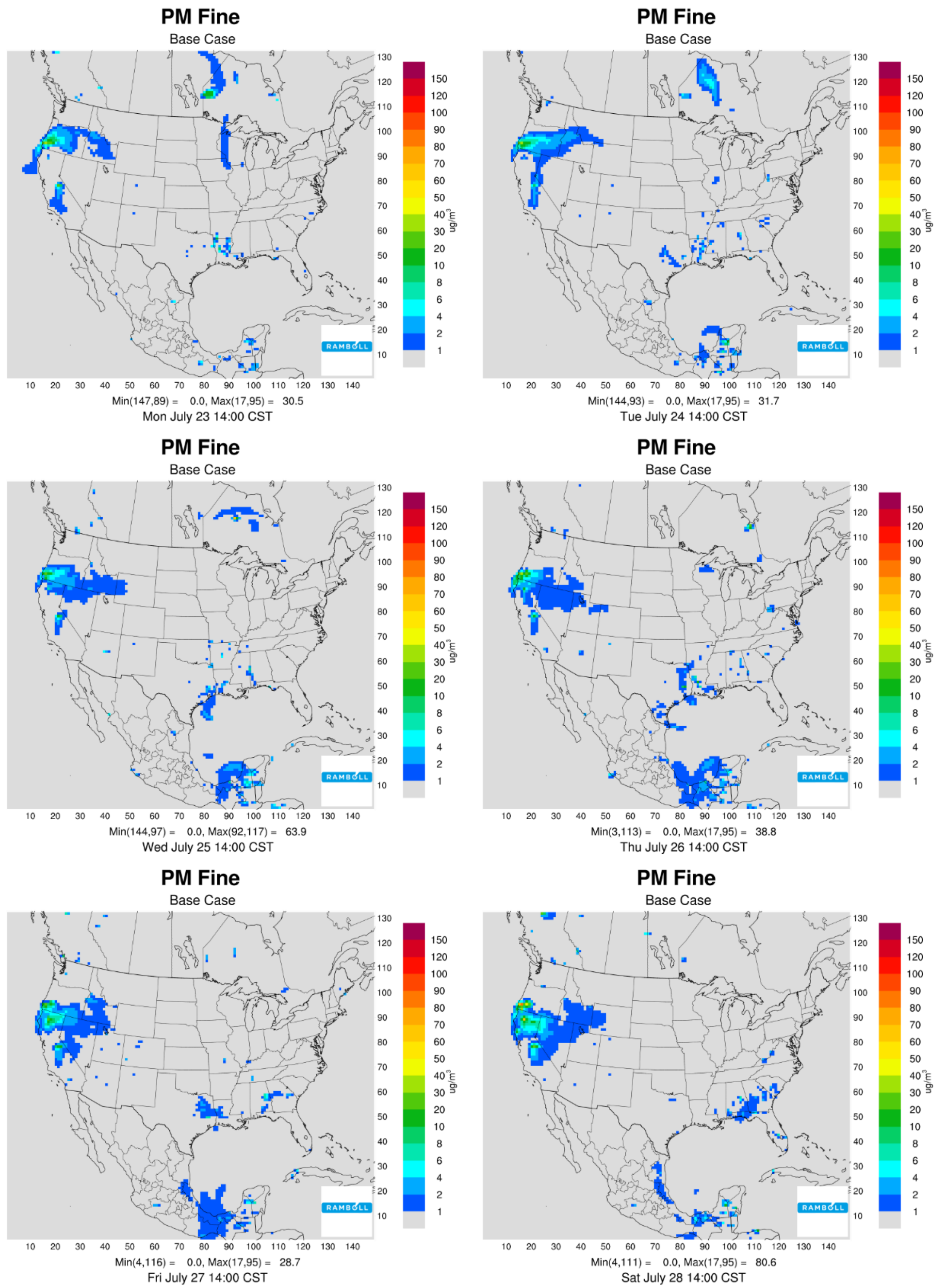

Figure 5-123. NRTEEM $PM_{2.5}$ wildfire smoke tracer impacts for the 36 km domain for July 23-28, 2018 at 2 PM CST.

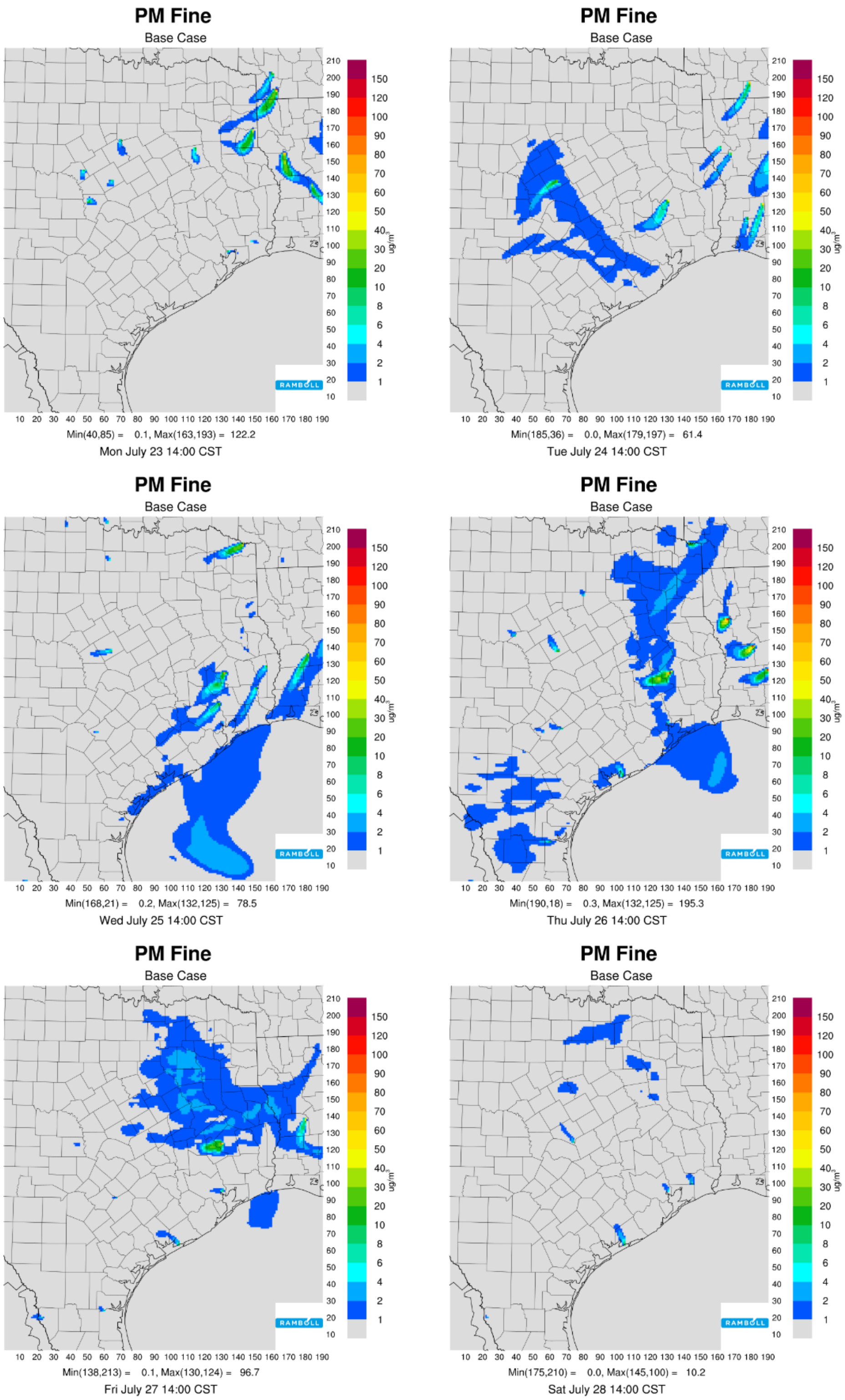

Figure 5-124. NRTEEM $PM_{2.5}$ wildfire smoke tracer impacts for the 4 km domain for July 23-28, 2018 at 2 PM CST.

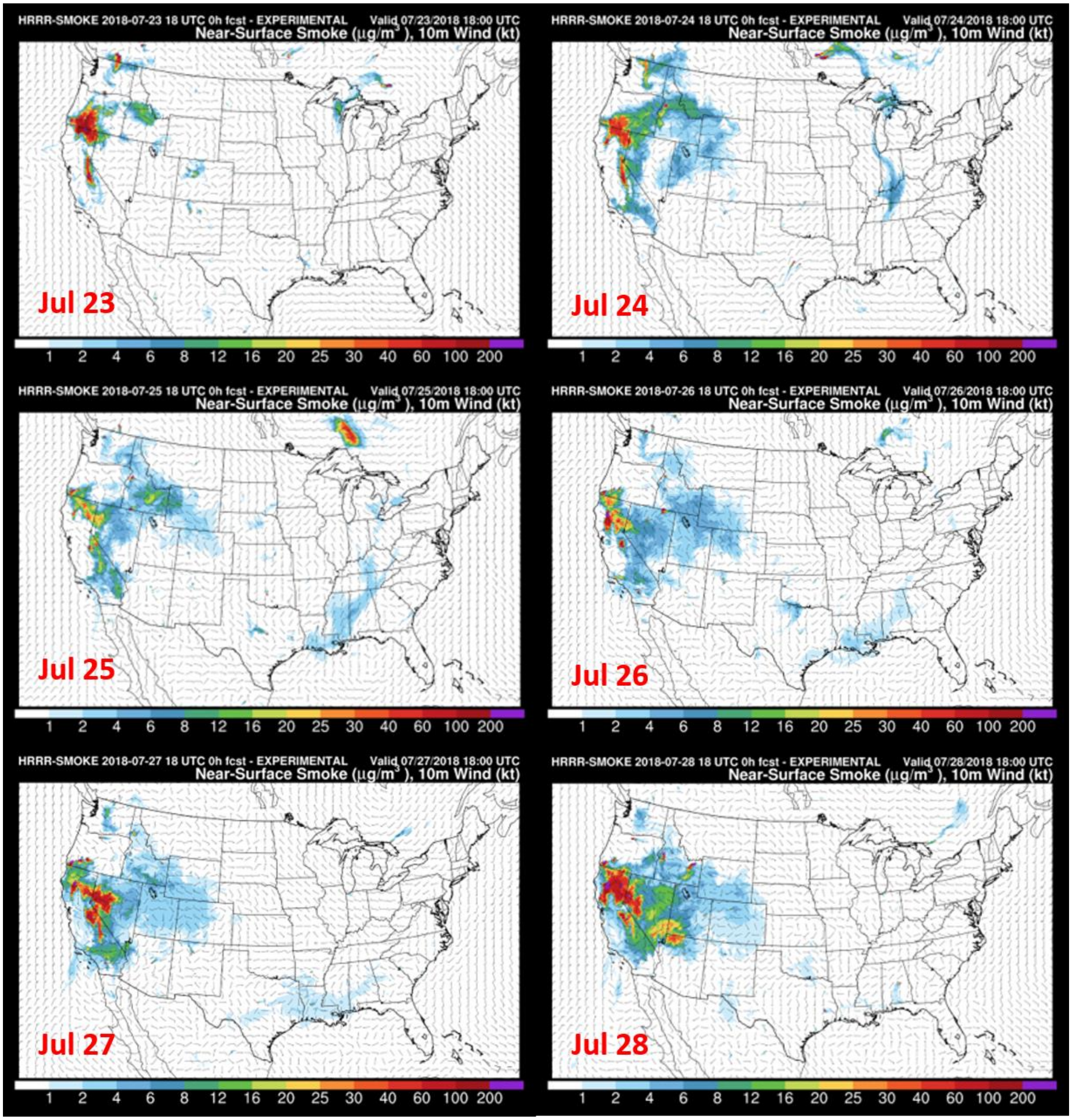

Figure 5-125. NOAA HRRR Near-Surface Smoke Product for July 23-28, 2018 showing smoke from distant fires superposed with plumes from fires in Texas and Louisiana.

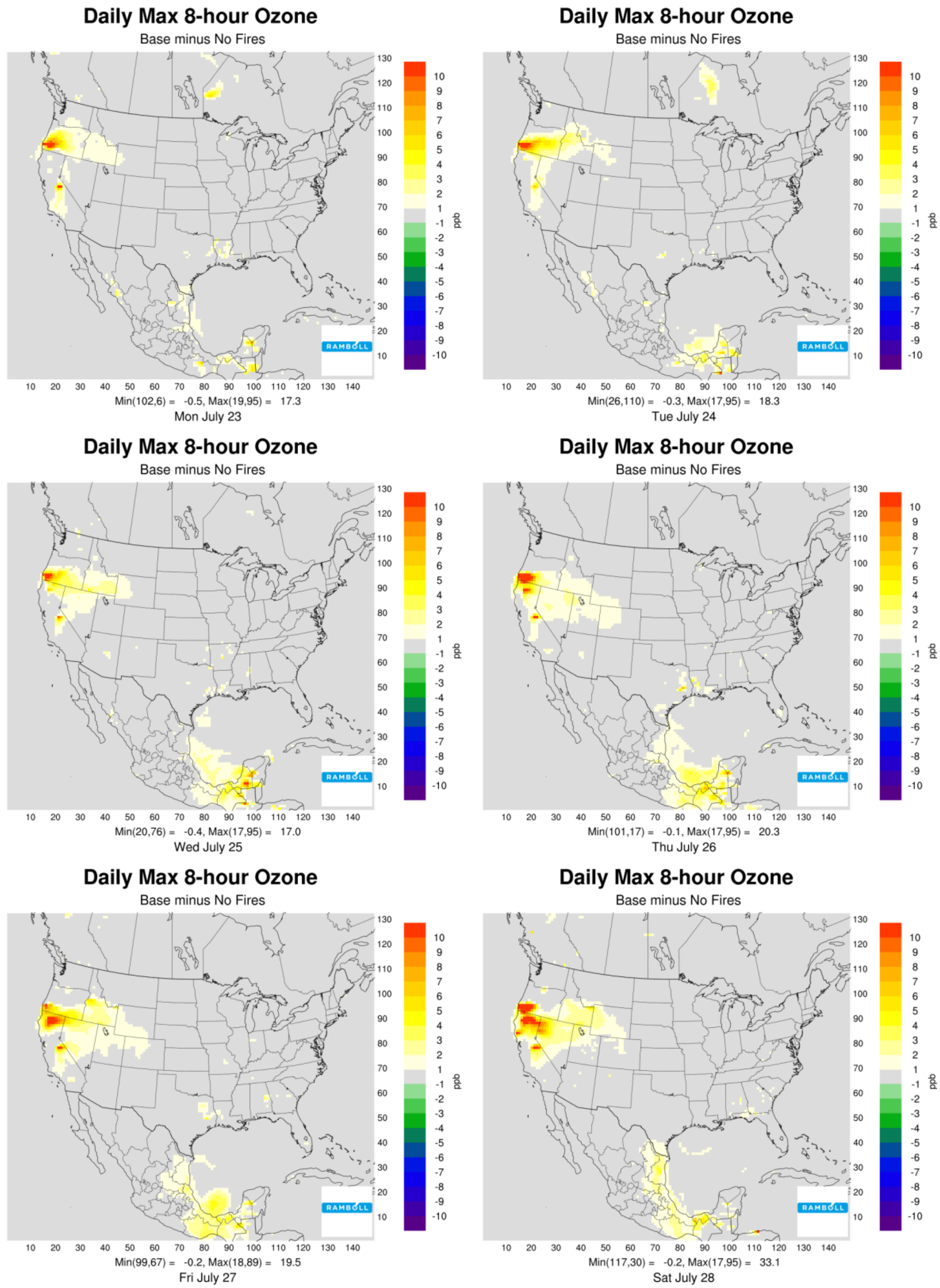

Figure 5-126. NRTEEM wildfire MDA8 ozone impacts for the 36 km domain for July 23-28, 2018.

Wind Performance at the Houston Monitors

Figure 5-127 presents 1-hour wind speed (top) and wind direction (bottom) for the NRTEEM model (blue) and observations (black dotted line) at the Bayland Park monitor for July 20-28, 2018. Similar plots for Aldine, Conroe Relocated and UH West Liberty follow in Figure 5-128, Figure 5-129, and Figure 5-130, respectively.

The NRTEEM model predicts observed wind speed and wind direction reasonably well on the highest observed ozone days (highlighted with blue brace). At each of the monitors, the model performs less well on the days preceding the highest ozone days, July 24-25. On these days, the NRTEEM model shows a more consistent wind direction from the northeast and east while the observations show a clockwise evolution over these two days, returning to east on the afternoon of July 25.

It is possible that wind direction errors on days leading up to high ozone days are leading to underestimated fire impacts at the Bayland Park and Aldine monitors. However, NRTEEM model winds are more consistently from the direction of wildfires (northeast and east) on these days than the observations. In addition, ozone performance at the four monitors on July 25 – just prior to the episode onset – does not appear to be negatively impacted by these wind direction errors.

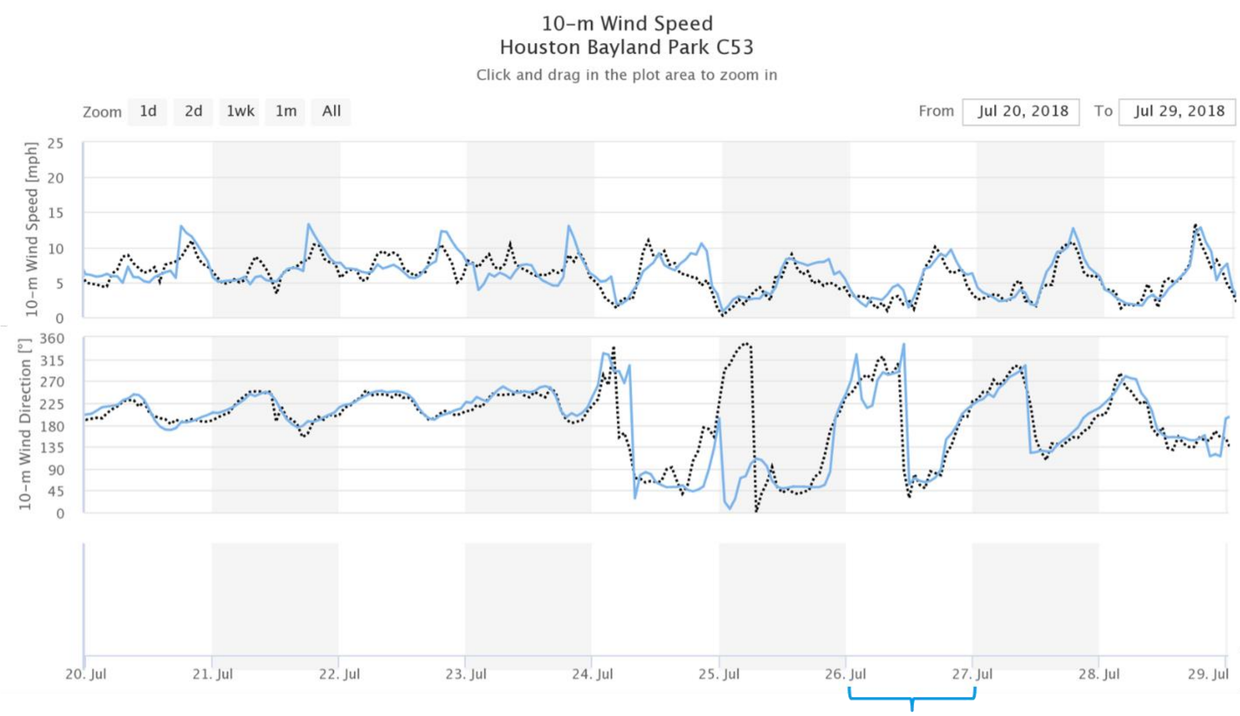

Figure 5-127. Observed (black dotted line) and base model (blue) wind speed (top) and wind direction (bottom) time series for July 20-28, 2018 at Bayland Park C53 in Houston.

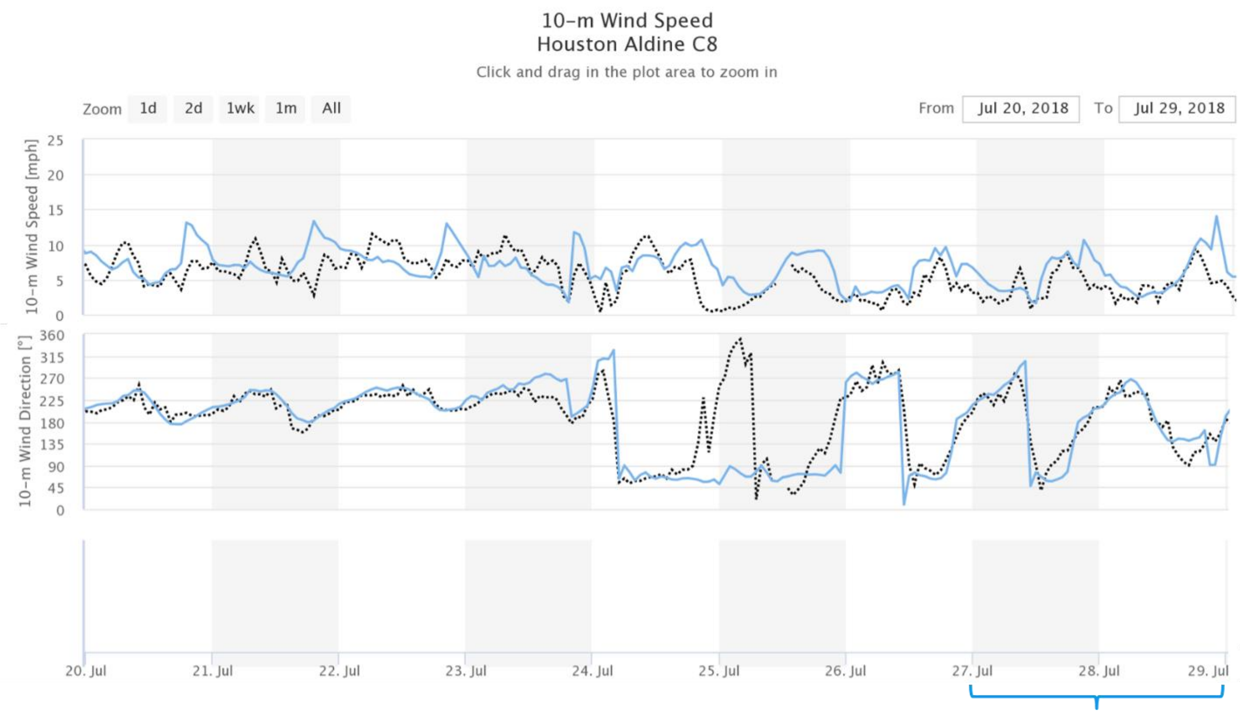

Figure 5-128. Observed (black dotted line) and base model (blue) wind speed (top) and wind direction (bottom) time series for July 20-28, 2018 at Aldine C8 in Houston.

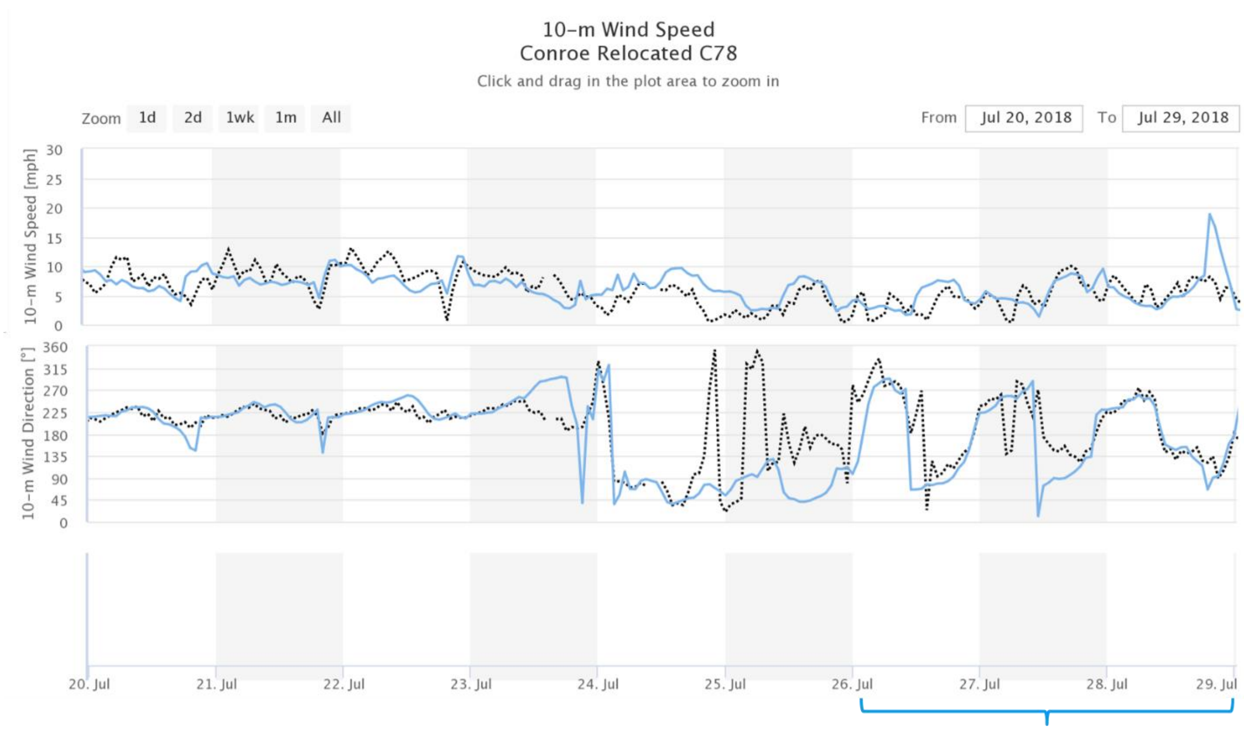

Figure 5-129. Observed (black dotted line) and base model (blue) wind speed (top) and wind direction (bottom) time series for July 20-28, 2018 at Conroe Relocated C78 in Houston.

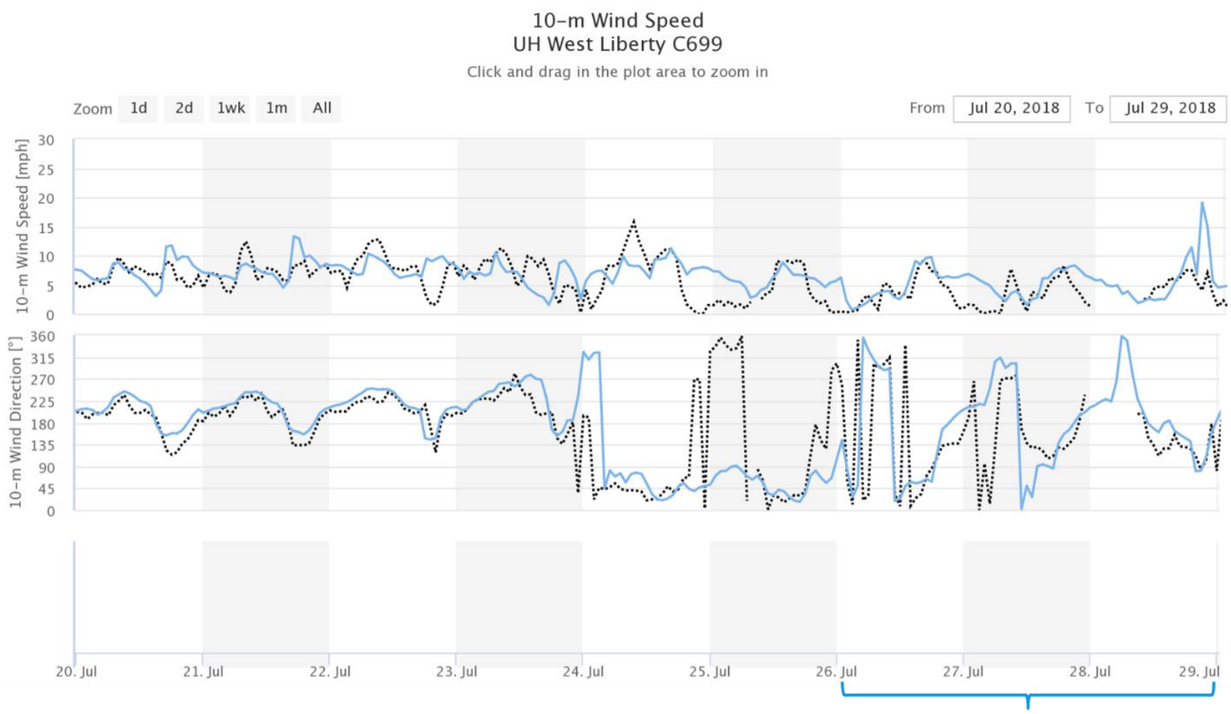

Figure 5-130. Observed (black dotted line) and base model (blue) wind speed (top) and wind direction (bottom) time series for July 20-28, 2018 at UH West Liberty C699 in Houston.

5.4.2.4 August 23-24, 2018

The TCEQ is evaluating high ozone values at Bayland Park CAMS 53 on August 23, 2018 and Aldine CAMS 8 August 24, 2018.

Wildfire Impacts on Ozone at the Bayland Park, Aldine and Upwind Monitors

NRTEEM modeling shows wildfire impacts on 1-hour ozone at the Bayland Park (Figure 5-131) and Aldine (Figure 5-132) CAMS were between 2 and 3 ppb during August 23-24. MDA8 ozone impacts from wildfires is 2.4 ppb at Bayland Park on August 23, 2018 and 2.4 ppb at Aldine on August 24, 2018.

Similar figures for upwind monitors Conroe Relocated and UH West Liberty are shown in Figure 5-133 and Figure 5-134, respectively. On the afternoon of August 23, UH West Liberty shows a maximum 1-hour wildfire ozone impact of 10.1 ppb, suggesting that modeled wildfire smoke plumes passed to the northeast of the Bayland Park and Aldine monitors. This wildfire plume had a smaller impact at the Conroe Relocated monitor, as modeled ozone impacts from fires peaked at 4.1 ppb on August 23. At all four monitors, modeled wildfire ozone impacts stayed around 2 ppb through August 24. This contrasts with the July episode, where modeled wildfire ozone impacts decreased very quickly to near zero after the initial impacts. Small wildfire ozone impacts present for several consecutive days at multiple monitors are consistent with an episode in which a continental air mass influenced by distant wildfires passes through the Houston area. This is in contrast with the impact of a nearby wildfire, which would produce larger impacts over a shorter time period at a few monitors, consistent with a narrow, well-defined fire plume.

The NRTEEM model underestimated peak 1-hour ozone at Aldine by 25-30 ppb on August 23-24. At Bayland Park, peak 1-hour ozone on August 23 was 10 ppb low and occurred 3 hours earlier than the observed peak. On August 24, peak 1-hour ozone was underestimated by about 6 ppb. As in the July episode, the NRTEEM model's performance at the UH West Liberty monitor had smaller biases than at the Aldine and Bayland Park monitors.

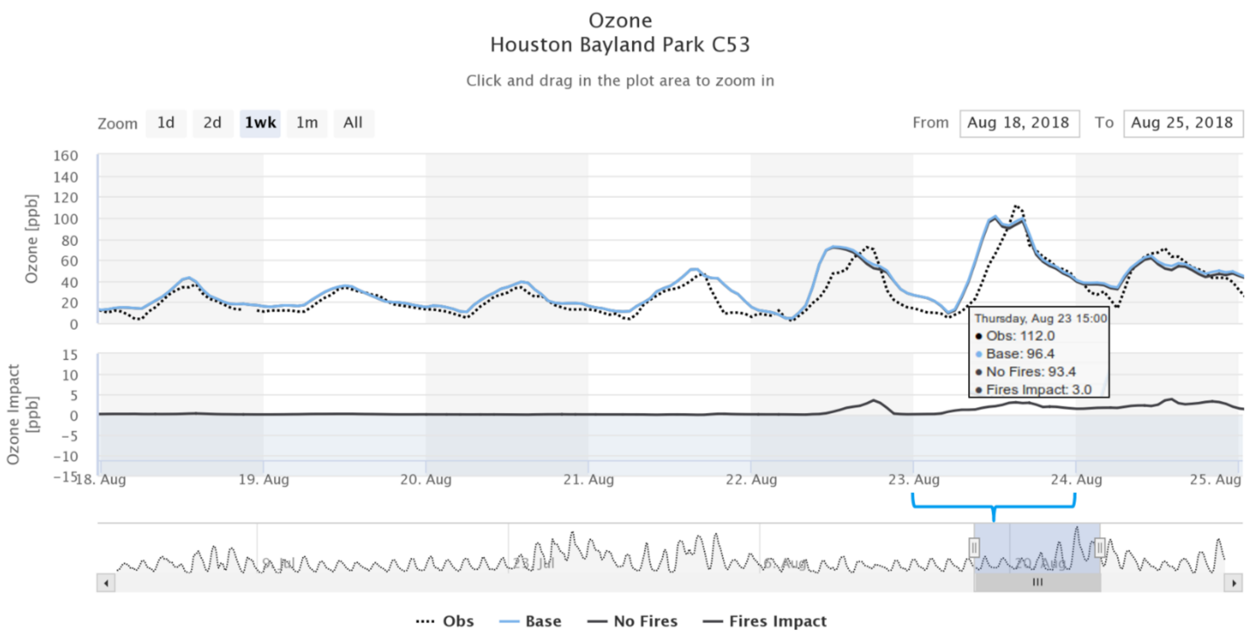

Figure 5-131. Observed (black dotted line), base model (blue) and Fires Impact (dark grey) ozone time series for August 18-24, 2018 at Bayland Park C53 in Houston. Maximum 1-hour ozone impact from wildfires on August 23, 2018 shown in box.

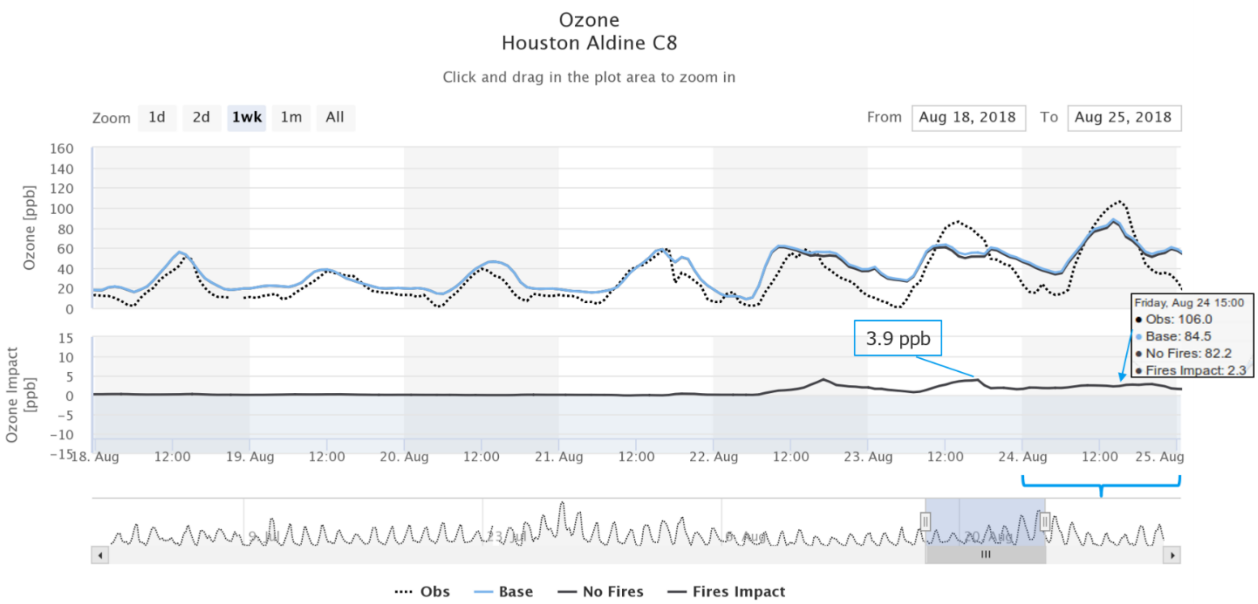

Figure 5-132. Observed (black dotted line), base model (blue) and Fires Impact (dark grey) ozone time series for August 18-24, 2018 at Aldine C8 in Houston. Maximum 1-hour ozone impact from wildfires on August 24, 2018 shown in box.

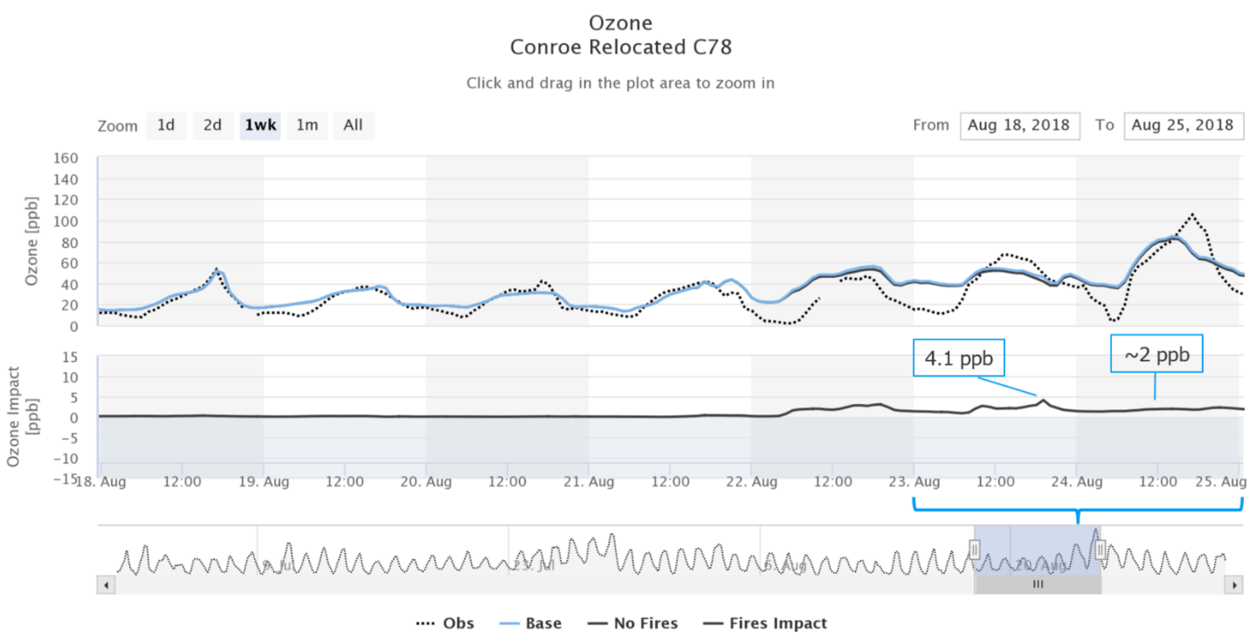

Figure 5-133. Observed (black dotted line), base model (blue) and Fires Impact (dark grey) ozone time series for August 18-24, 2018 at Conroe Relocated C53 in Houston. Maximum 1-hour ozone impact from wildfires on August 23, 2018 shown.

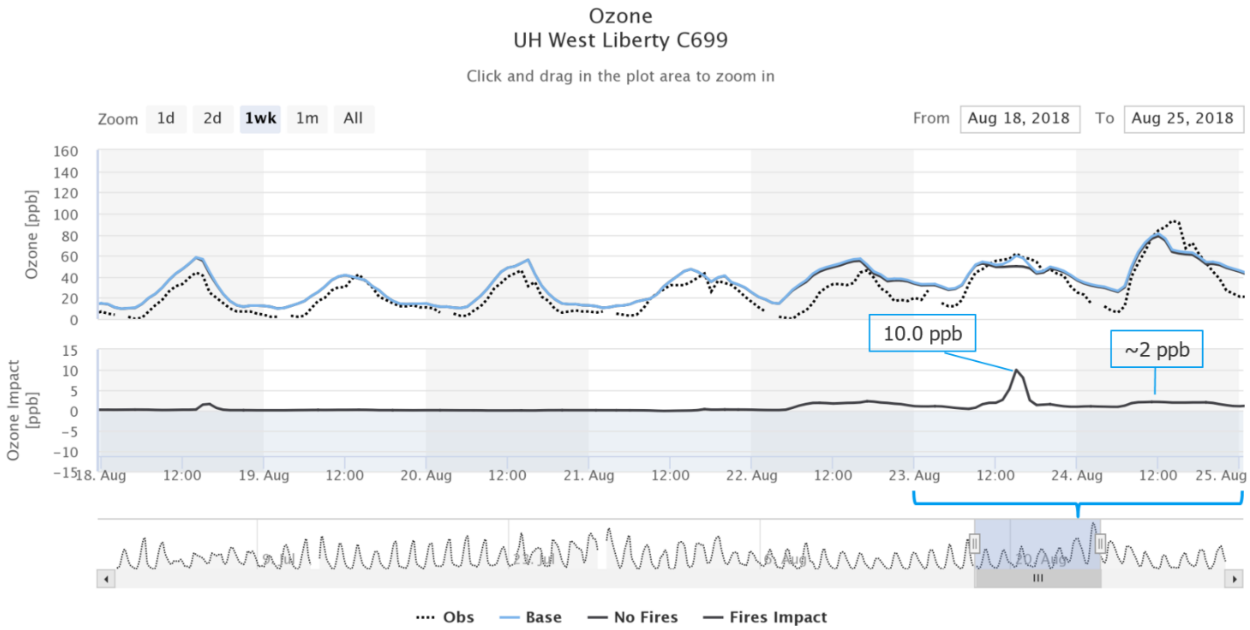

Figure 5-134. Observed (black dotted line), base model (blue) and Fires Impact (dark grey) ozone time series for August 18-24, 2018 at UH West Liberty C699 in Houston. Maximum 1-hour ozone impact from wildfires on August 23, 2018 shown.

The NRTEEM model smoke tracer (Figure 5-135) clearly shows transport of PM from wildfires in British Columbia, California, Oregon, Washington, Colorado, Nevada and to Houston and the evolution of the NRTEEM smoke tracer is consistent with the evolution of wildfire plumes as shown by satellite retrievals of AOD and CO as well as in true color visible images and the NOAA HRRR surface smoke product. We present MODIS true color imagery superposed with fire detections (top left) and MODIS aerosol optical depth (bottom left) compared with NRTEEM $PM_{2.5}$ smoke tracers (top right) and MDA8 ozone (bottom right) for August 19, 2018 in Figure 5-136. Similar figures for August 20-24, 2018 are shown from Figure 5-137 through Figure 5-141. The NRTEEM model smoke tracer also shows that fires in Louisiana contributed smoke to the Houston area.

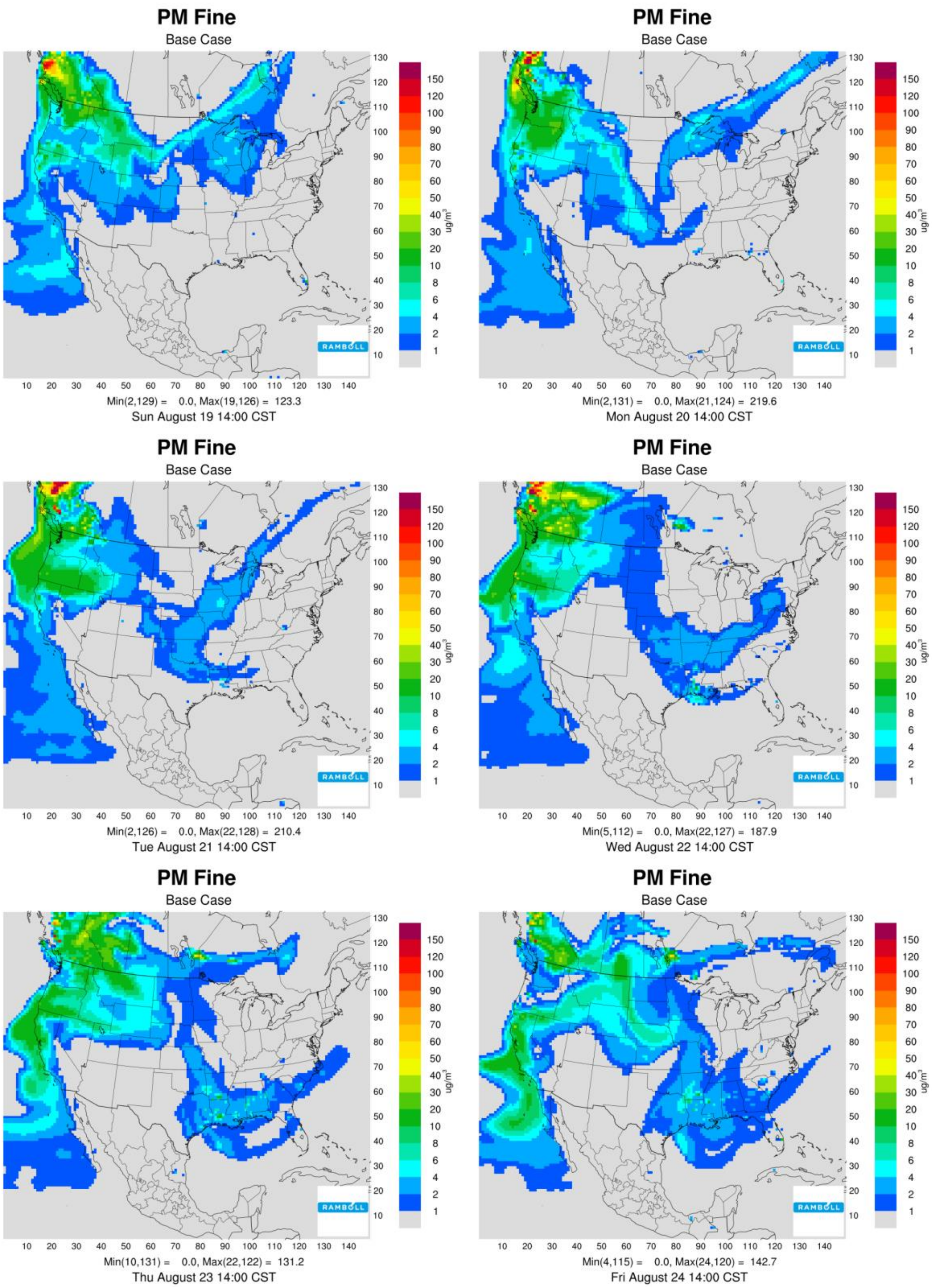

Figure 5-135. NRTEEM $PM_{2.5}$ wildfire smoke tracer plots for the 36 km domain for August 19-24, 2018 at 2 PM CST.

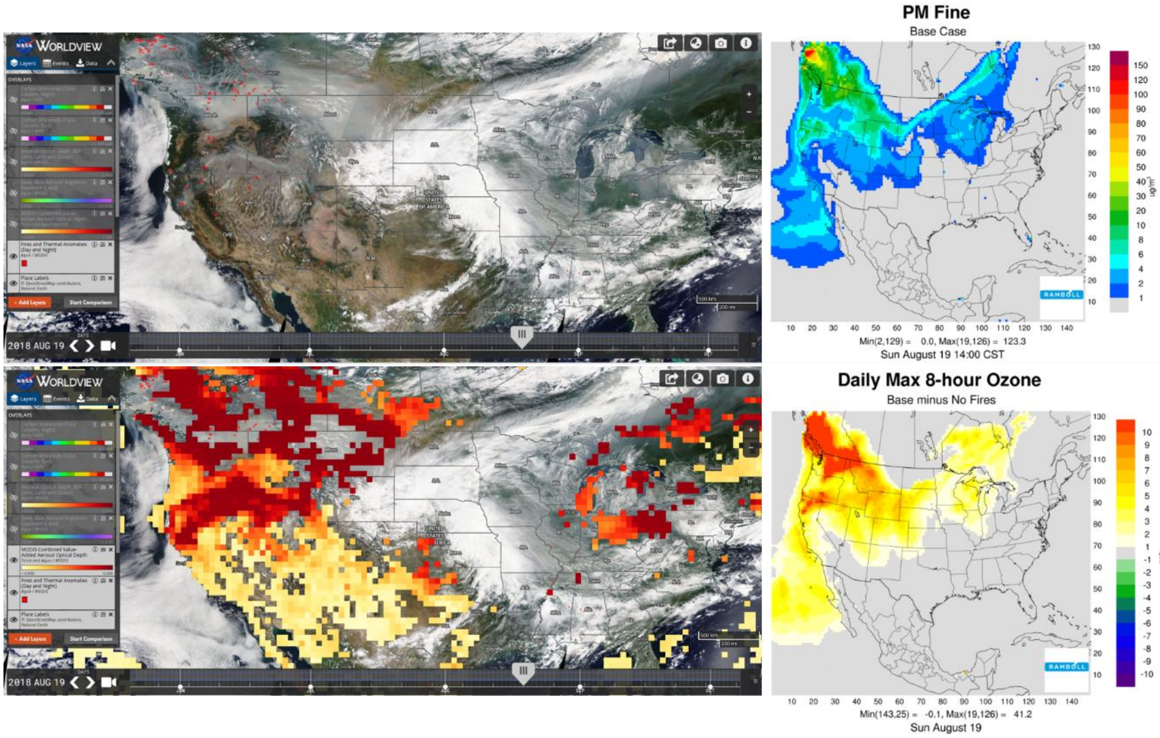

Figure 5-136. Comparison of MODIS True Color imagery superposed with fire detections (top left) and aerosol optical depth (bottom left) and NRTEEM $PM_{2.5}$ smoke tracers (top right) and MDA8 ozone (bottom right) for August 19, 2018.

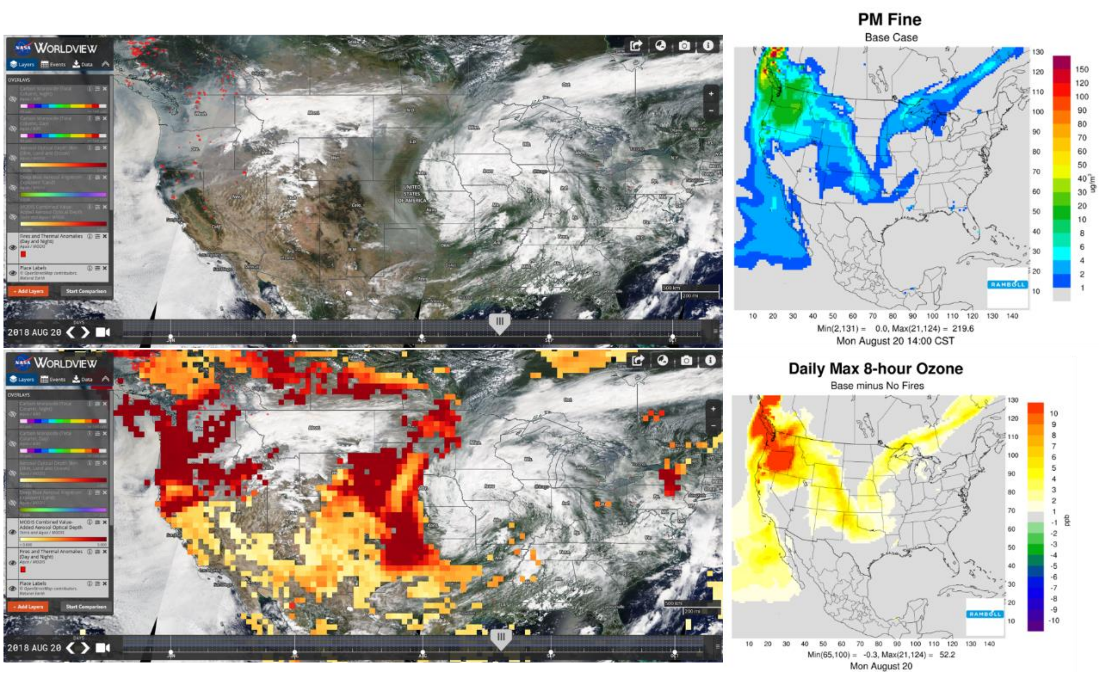

Figure 5-137. Comparison of MODIS True Color imagery superposed with fire detections (top left) and aerosol optical depth (bottom left) and NRTEEM $PM_{2.5}$ smoke tracers (top right) and MDA8 ozone (bottom right) for August 20, 2018.

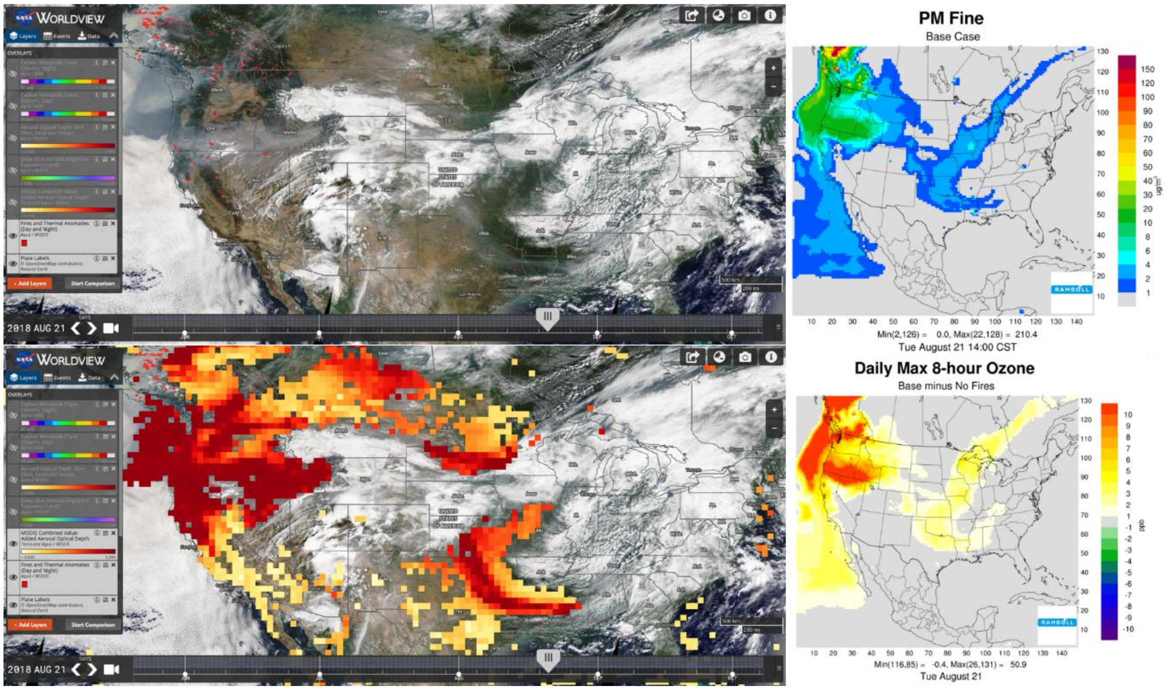

Figure 5-138. Comparison of MODIS True Color imagery superposed with fire detections (top left) and aerosol optical depth (bottom left) and NRTEEM PM$_{2.5}$ smoke tracers (top right) and MDA8 ozone (bottom right) for August 21, 2018.

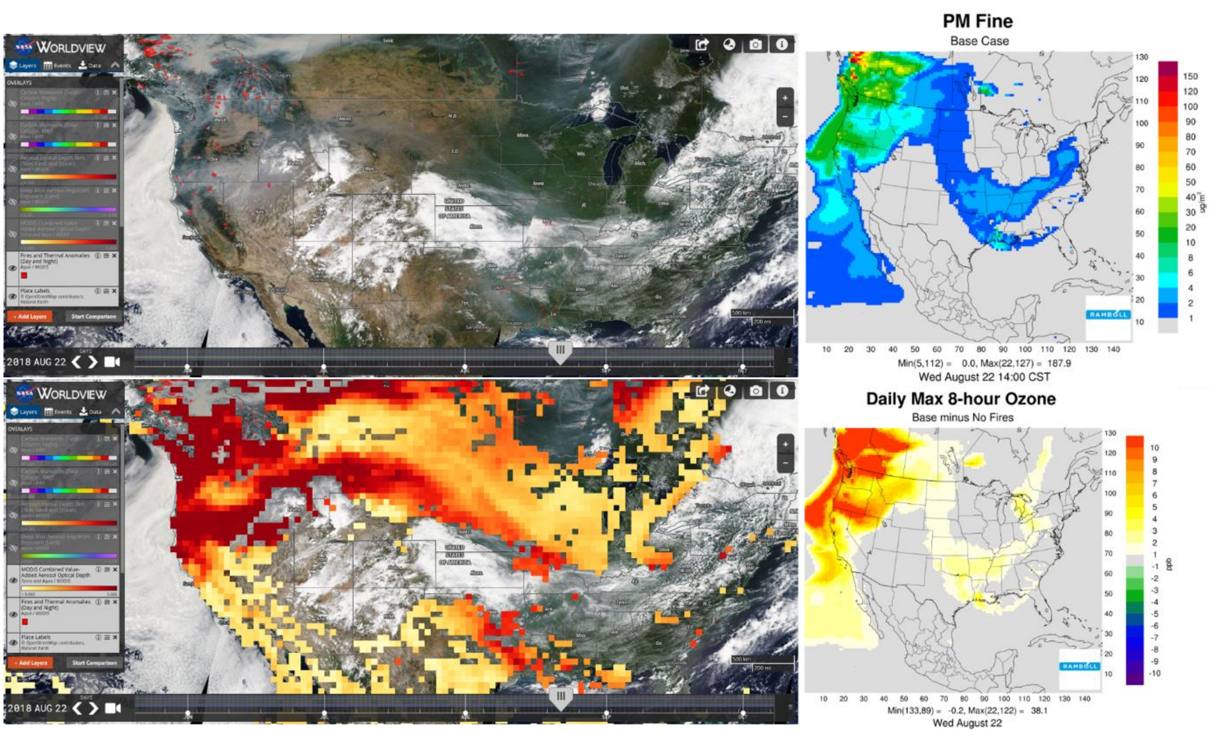

Figure 5-139. Comparison of MODIS True Color imagery superposed with fire detections (top left) and aerosol optical depth (bottom left) and NRTEEM PM$_{2.5}$ smoke tracers (top right) and MDA8 ozone (bottom right) for August 22, 2018.

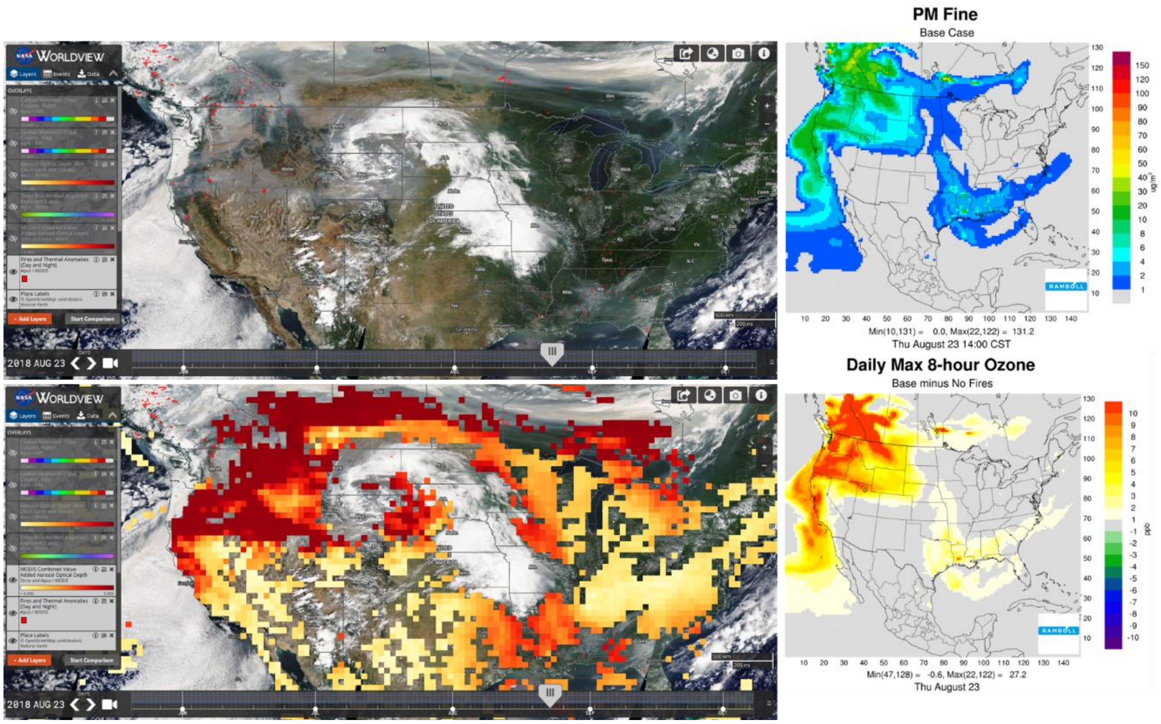

Figure 5-140. Comparison of MODIS True Color imagery superposed with fire detections (top left) and aerosol optical depth (bottom left) and NRTEEM $PM_{2.5}$ smoke tracers (top right) and MDA8 ozone (bottom right) for August 23, 2018.

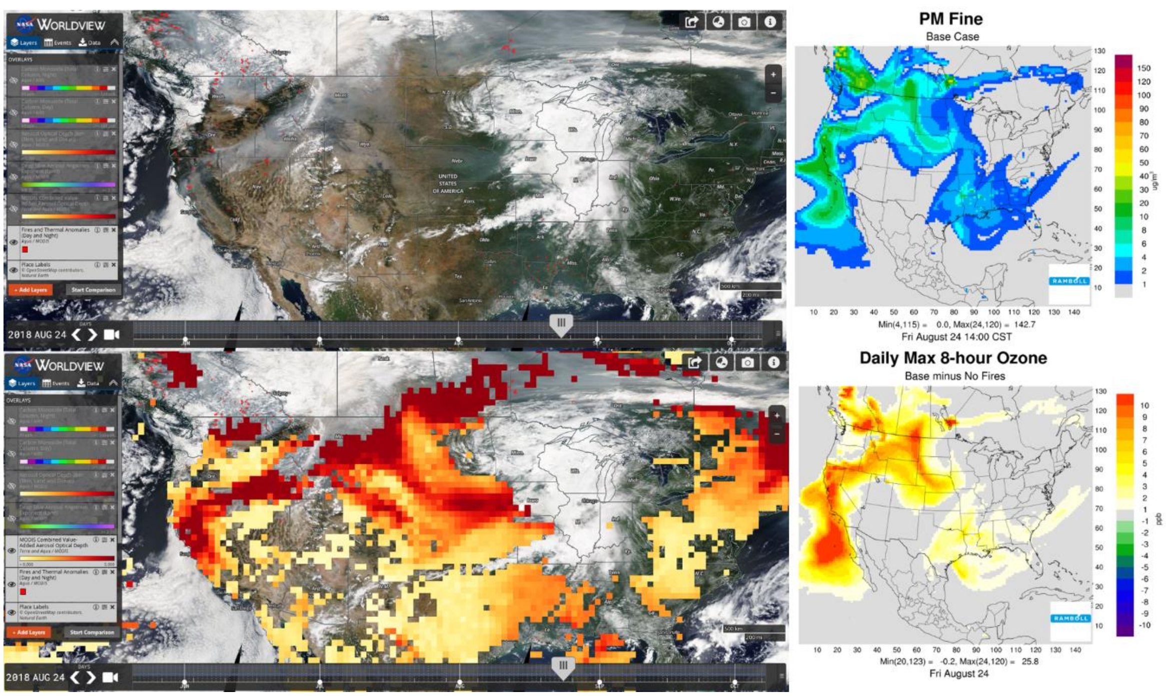

Figure 5-141. Comparison of MODIS True Color imagery superposed with fire detections (top left) and aerosol optical depth (bottom left) and NRTEEM $PM_{2.5}$ smoke tracers (top right) and MDA8 ozone (bottom right) for August 24, 2018.

Wind Performance at the Houston Monitors

Figure 5-142 presents 1-hour wind speed (top) and wind direction (bottom) for the NRTEEM model (blue) and observations (black dotted line) at the Bayland Park monitor for August 18-24, 2018. Similar plots for Aldine, Conroe Relocated and UH West Liberty follow in Figure 5-143, Figure 5-144, and Figure 5-145, respectively.

The NRTEEM model predicts observed wind speed and wind direction reasonably well on the highest observed ozone days (highlighted with blue brace). In contrast with the July episode, the NRTEEM model performs about as well for the highest observed ozone days compared with the days immediately preceding them.

The NRTEEM model does not capture the timing of wind direction shifts on August 22 and 23 at Bayland Park and August 22 at Aldine. The wind direction performance is also negatively impacted by the observed light and variable winds (e.g. UH West Liberty on August 23 and 24) that occur under stagnant conditions, which meteorological models such as WRF have a difficult time replicating. Overall, the NRTEEM model wind model performance is good throughout the August episode and it is unlikely that wind errors substantially impact modeled ozone fire impacts.

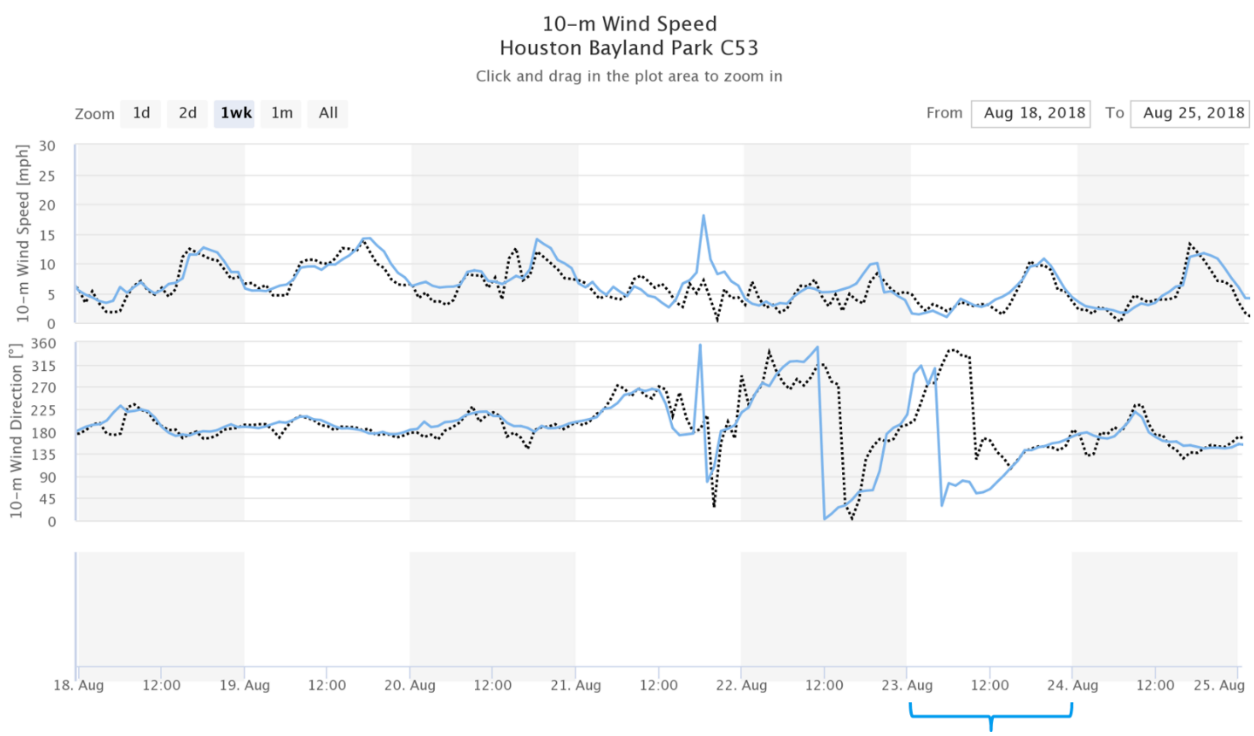

Figure 5-142. Observed (black dotted line) and base model (blue) wind speed (top) and wind direction (bottom) time series for August 18-24, 2018 at Bayland Park C53 in Houston.

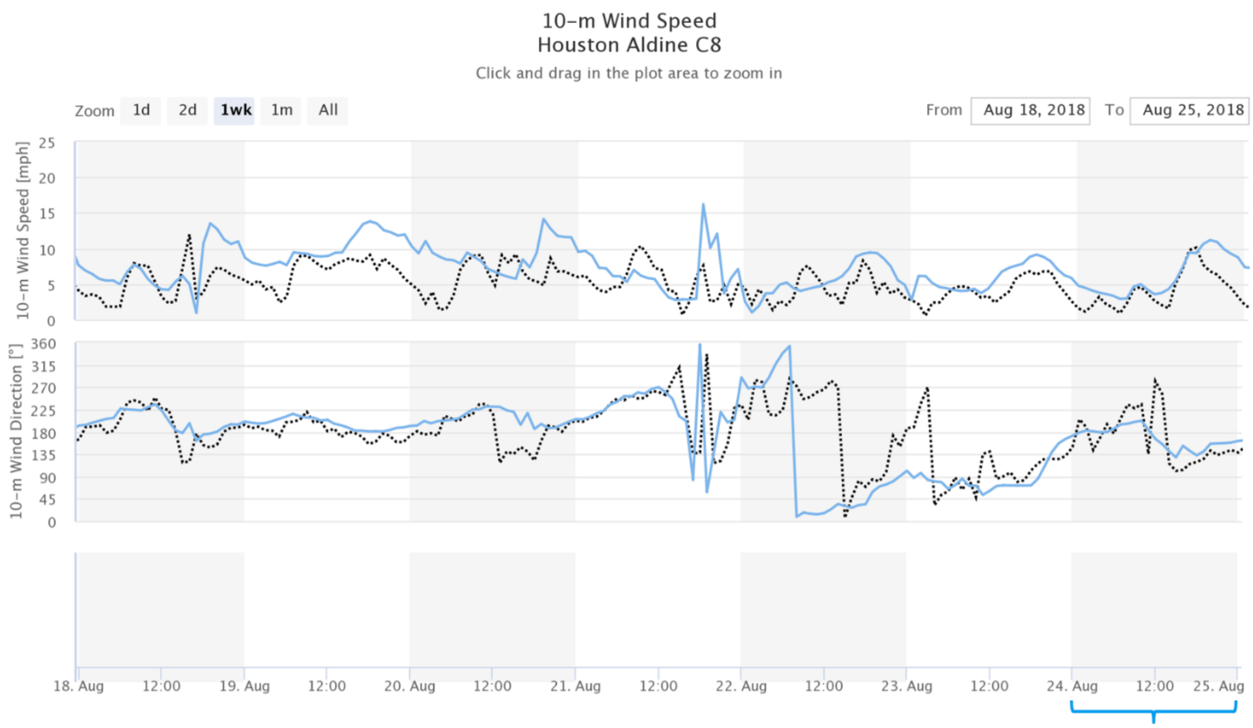

Figure 5-143. Observed (black dotted line) and base model (blue) wind speed (top) and wind direction (bottom) time series for August 18-24, 2018 at Aldine C8 in Houston.

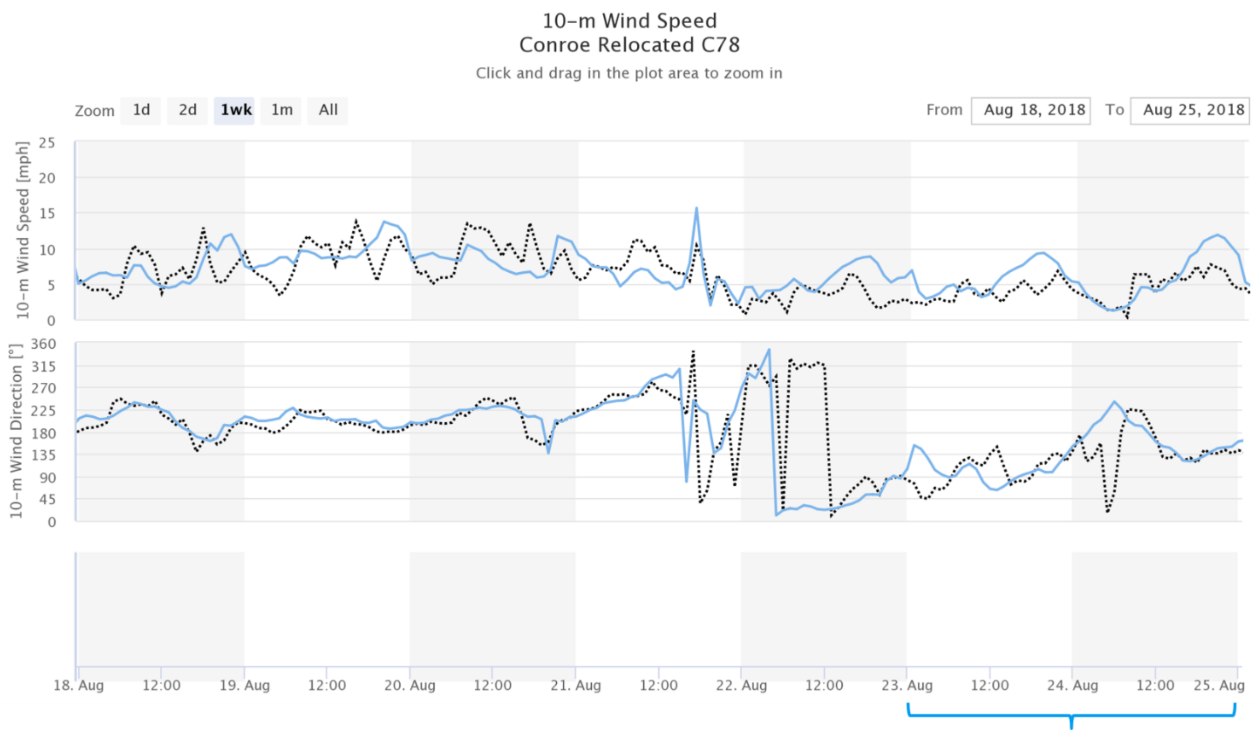

Figure 5-144. Observed (black dotted line) and base model (blue) wind speed (top) and wind direction (bottom) time series for August 18-24, 2018 at Conroe Relocated C78 in Houston.

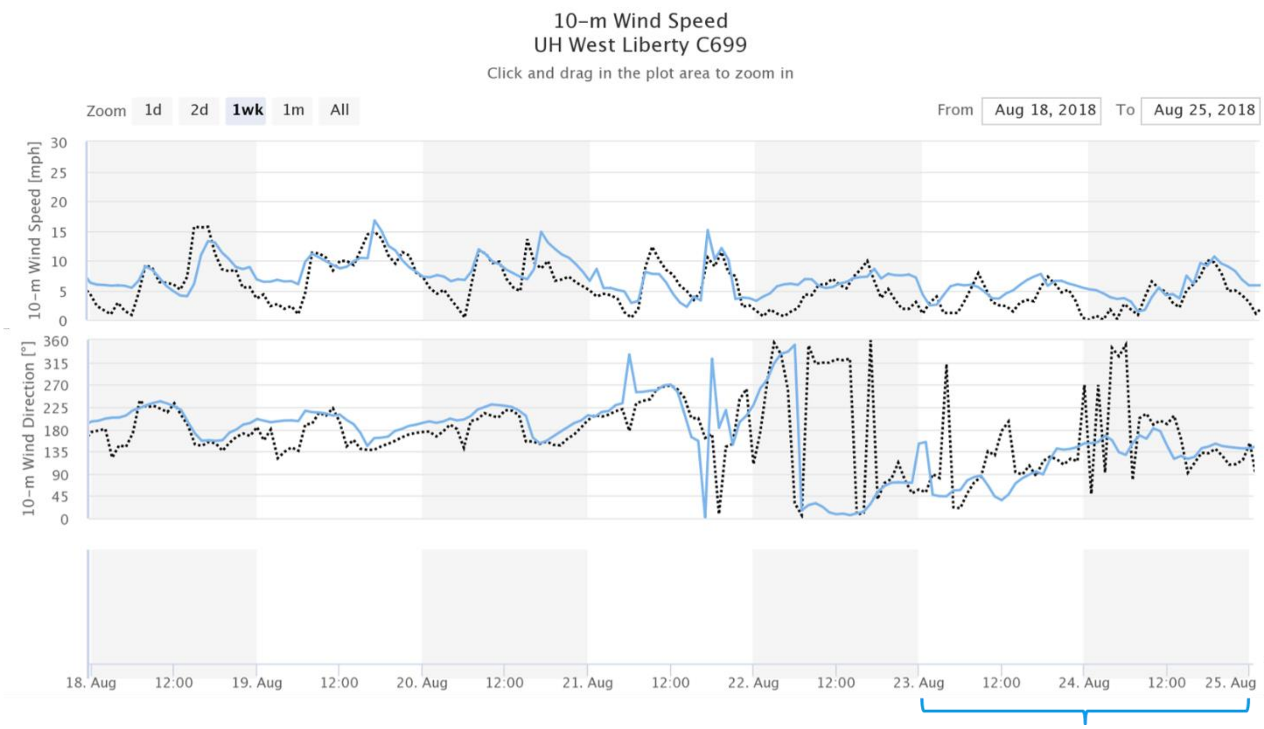

Figure 5-145. Observed (black dotted line) and base model (blue) wind speed (top) and wind direction (bottom) time series for August 18-24, 2018 at UH West Liberty C699 in Houston.

5.4.2.5 Uncertainty in Photochemical Modeling of Fires

Simulation of wildfire impacts on ozone in a photochemical model is challenging (e.g. Baker et al., 2016; Baker et al., 2018). In this section, we give a brief overview of some of the uncertainties that affect the modeling of wildfires and their ozone impacts.

Wildfire plumes are typically not well-resolved at the spatial resolution of a photochemical model. This makes it difficult to simulate the rapid chemical processing of wildfire emissions in the near-field fire plume. The large wildfires in Canada and the western US shown in Figure 4-1 and Figure 4-16 are far from Texas and therefore are modeled at 36 km resolution in NRTEEM. Fires in Louisiana are modeled at either 12 km or 4 km resolution depending on their distance from Texas.

Simulation of fire plume rise must also be parametrized, and this introduces uncertainty into the simulation of plume transport. In the NRTEEM modeling, fire plume rise is a function of the fire size, weather conditions and time of day. Errors in plume rise can affect the transport and dispersion of the fire plume, and this effect is more pronounced where strong vertical wind shear is present. In the real world, intense fires can affect the weather in the surrounding area. For example, pyrocumulus clouds can form above a large wildfire and can affect solar radiation incident on the plume as well as the heat budget in the atmospheric column above the fire. In the NRTEEM modeling system, there are no such feedbacks from fires to meteorology, as the meteorological model must be run before the photochemical model in order to provide weather inputs.

The NRTEEM model is run in near-real time mode and must therefore use a fire emission inventory that is also prepared in near-real time. As described in Section 5.4.1.5, the NRTEEM modeling system uses the FINN fire emission inventory, which is based on satellite fire detections. Satellite fire detection systems have limited ability to detect small (< 100 ha) fires (Wiedinmyer et al., 2011), fires beneath cloud cover and fires that occur between satellite overpasses. Wiedinmyer et al. (2011) list the following additional sources of uncertainty in the FINN emissions estimates: land cover classifications, assumed area burned, biomass loading, the amount of fuel burned, and emission factors. For a modeling system that is not run in near-real time mode, it would be possible to use a more comprehensive fire emission inventory such as EPA fire emissions developed with the BlueSky framework that incorporates ground reports and other data in addition to satellite fire detections into emissions estimates. However, EPA emissions for the July and August 2018 episodes were not available at the time of the NRTEEM modeling.

There are uncertainties in the spatial and temporal allocation of the wildfire emissions. The FINN inventory provides daily emissions which must then be allocated in time for each fire. The allocation is performed within the EPS emissions pre-processor, which assigns to all fires a single temporal profile which has a mid-afternoon peak. This can cause the NRTEEM system to mis-time fire impacts at nearby monitors. For example, if a fire occurred upwind of a monitor in the morning and the fire was no longer burning by afternoon, the timing of the fire impact in the model may be later than is observed because of the strong afternoon peak in temporal profile applied to the daily emissions. Spatial aggregation of pixelated satellite fire detects is also performed within EPS3. Any fire location within 5 km of another fire is assumed to be part of the same fire event. A fire event is therefore defined as a cluster of points meeting this criterion; this aggregation procedure introduces uncertainty into the fire size and, therefore, the plume rise.

Baker et al. (2018) recommend avenues for advancing modeling of wildfires including improvements in speciation of NOx and VOC emissions, vertical mixing within the smoke plume, fuel mapping, and temporal allocation of emissions. Baker et al. note that data from a number of field studies in 2018 and 2019 are expected to provide data for improving the representation of fire and their impacts in photochemical modeling.

5.4.3 Matching Day Analysis

The EPA's *Guidance on Preparation of Exceptional Events Demonstrations for Wildfire Events that May Influence Ozone Concentrations*[24] (EPA, 2016) states that a matching day analysis may be used to support a clear, causal relationship between wildfire and an ozone exceedance. A matching day analysis compares ozone on days with similar weather conditions that differ in their influence from wildfire impacts. Because similar weather conditions for a given area tend to produce similar ozone conditions, the presence of markedly higher ozone on a given day compared to other days with similar weather suggests that day was influenced by an unusual process, such as a wildfire.

EPA's Guidance document recommends basing the matching day analysis on meteorological parameters that are known to have a strong influence on ozone in the area of the exceeding monitor(s). Suggested parameters include daily high temperature, hourly temperature, surface wind speed and direction, upper air temperature and pressure, relative or absolute humidity, atmospheric stability, cloud cover, and solar irradiance. The Guidance recommends matching the meteorological parameters within "an appropriate tolerance" but does not supply specific values.

[24] https://www.epa.gov/sites/production/files/2018-10/documents/exceptional_events_guidance_9-16-16_final.pdf

5.4.3.1 Method and Data

Meteorological Parameters and Matching Criteria

Ramboll selected parameters for the analysis based on EPA Guidance and the TCEQ's conceptual model of ozone in the Houston area[25]. The parameters are shown in Table 5-5. Given the dependence of Houston weather conditions and ozone formation on time of year, matching days were selected from June, July and August days only. Because Houston ozone precursor emissions have been decreasing with time[2], data prior to 2014 were excluded to minimize the influence of emission trends on the matching day analysis. The TCEQ provided 2014 - 2018 hourly meteorological observations from KHOU (William Hobby Airport) and KIAH (George Bush Airport) from the NOAA Integrated Surface Daily (ISD) Archives. We merged these data with hourly meteorological observations from the Aldine (CAMS 8 and Bayland Park CAMS 53 air quality monitoring sites. The resulting hourly data were then processed to produce a set of key meteorological values for each day. Parameters measured at more than one site were averaged to obtain a single daily value to simplify the matching criteria. However, the average morning wind direction and average afternoon wind direction values were computed separately for each monitoring site.

Table 5-5. Criteria for selecting matching days.

Parameter	Description	Matching Criteria
Month	Month	June - August
Tmax	Maximum temperature	Within ±5 °C of target day median
Tmin	Minimum temperature	Within ±5 °C of target day median
Tavg	Average temperature	Within ±5 °C of target day median
SumPrecip	Total precipitation	Average < 0.1 mm/hr
AvgP	Average barometric pressure	Within ±10 hPa of target day median
AvgWS	Average wind speed (scalar average)	Within ±3 m/s of target day median
AvgRH	Average relative humidity	±10%
IntSR	Integrated solar radiation	474 – 618 ly/day
AvgMrngWS	4:00 – 10:00 LST average wind speed at Aldine and Bayland Park	< 2 m/s at both Aldine and Bayland Park
AvgAftWD	14:00 – 20:00 LST average wind direction (resulting unit vector) at Aldine and Bayland Park	67.5° – 157.5° (i.e., ENE – SSE clockwise) at both Aldine and Bayland Park

As shown in Figure 5-146 and Figure 5-147, weather conditions on the five "target" high ozone episode days (July 26-28, 2018 and August 23-24, 2018) were very similar except with respect to relative humidity (RH). RH on the target days falls roughly in two groups: a) 56.9% and 59.3% on July 26 and 27, respectively and b) 70.1% and 69.2% on August 23 and August 24 respectively. The

[25]https://www.tceq.texas.gov/assets/public/implementation/air/sip/hgb/HGB_2016_AD_RFP/AD_Adoption/HGB_AD_SIP_Appendix_D_Adoption.pdf

average RH on July 28 was 66.8%. Thus, the first two July days are a bit drier than the days in August, with the last July day falling just above the midpoint between and the two sets of days.

We identified potential matching days in 2014 – 2017 based on the matching criteria listed in the right hand column of Table 5-5. The wind direction criteria in Table 5-5 were designed to capture the range of daily wind direction shifts observed at Aldine and Bayland Park during the target days as shown in Figure 5-147. In reviewing results of filtering according to the parameters shown in Table 5-5, we found that applying both the morning and afternoon wind direction criteria at all sites was too restrictive and was hampered by frequent missing values at KHOU and KIAH.

The matching day criteria used in our first round of analysis (see Table 1 of our 30 May memo) included a requirement that morning wind directions at either Aldine CAMS 8 or Bayland Park CAMS 53 fall within the range SSW – NNW (clockwise). In the present analysis, we have relaxed the criteria so that morning average wind speeds at both Aldine and Bayland Park must simply be less than 2 m/s regardless of wind direction. Relaxing the morning wind direction requirement was motivated by measurements showing that Houston morning winds on the episode days are light and variable, thus making the directional constraint excessively restrictive. By relaxing the morning wind direction criterion, we identified 50 matching days during the months of June – August in the years 2014 – 2018.

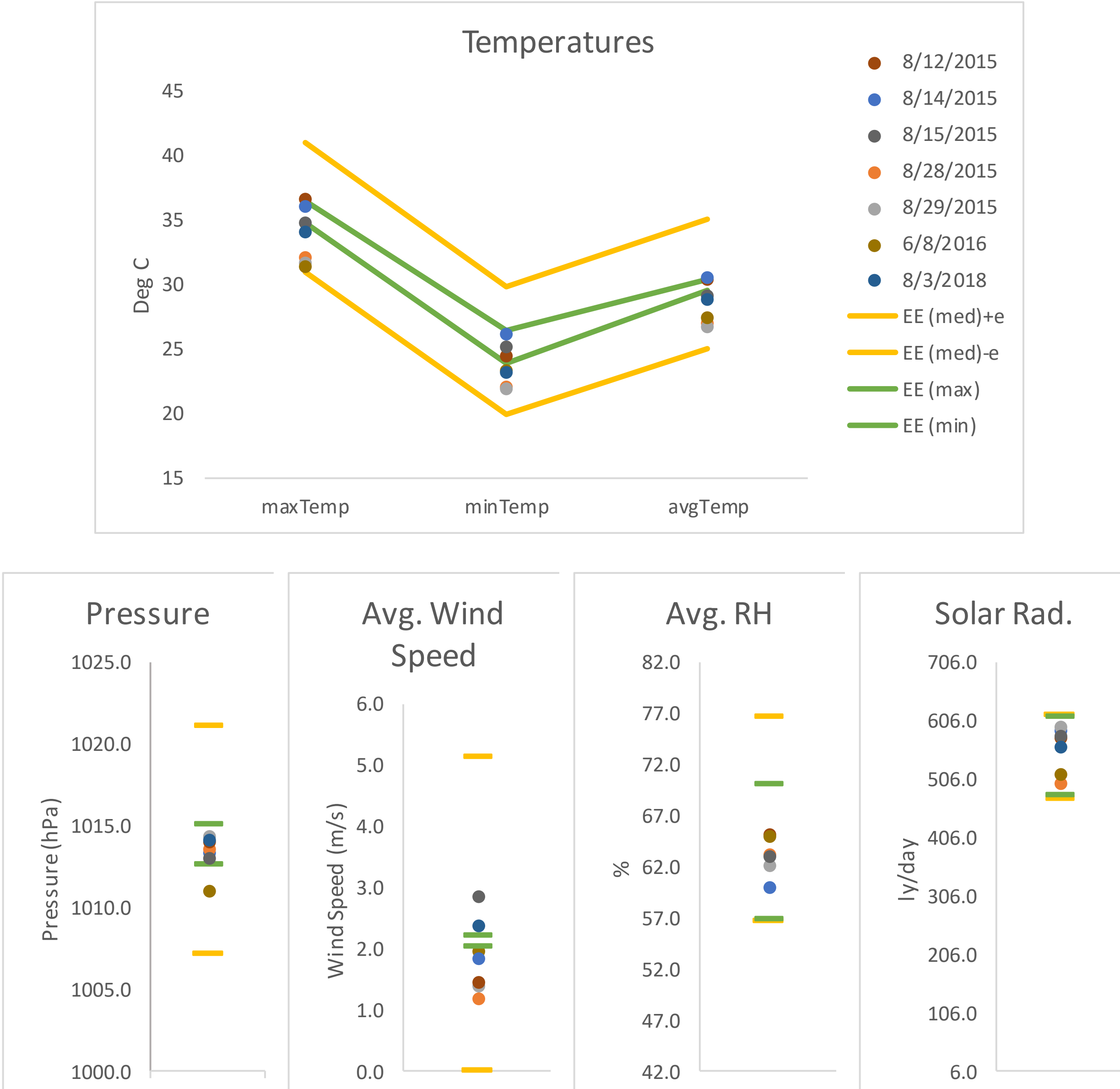

Figure 5-146. Values of surface meteorological parameters in Table 5-5 on candidate matching day (dots). Green lines indicate maximum and minimum values over the episode days; orange lines indicate upper and lower bounds for the matching tolerances (e) listed in Table 5-5.

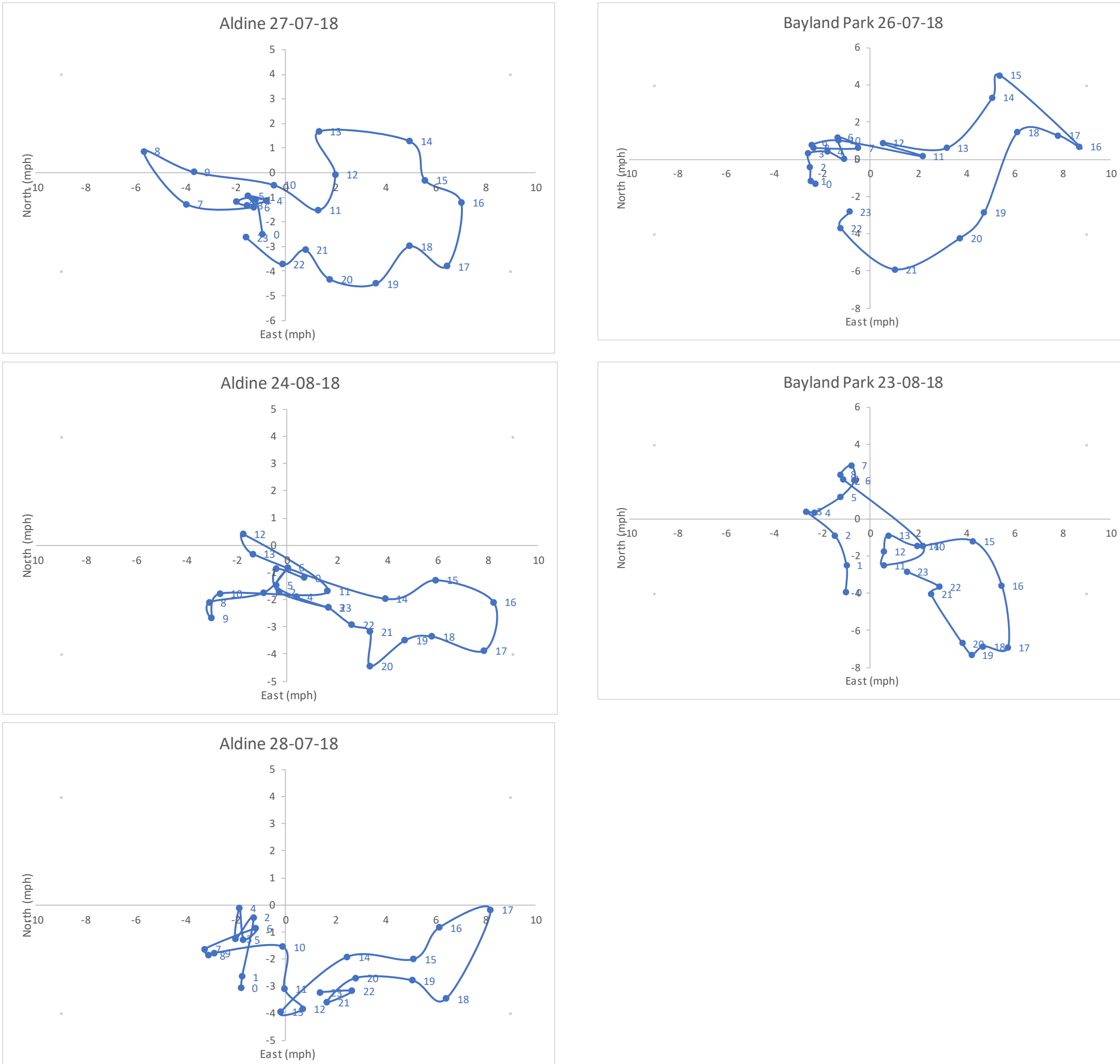

Figure 5-147. Hodograms showing hourly resultant wind direction and speeds: each hourly wind vector points to the axis origin from the blue dot plotted for each hour with time (LST) indicated by the blue numbers; speed (mph) is indicated by the distance from the origin to the hour marker.

We prepared 5-day HYSPLIT back trajectories for all 50 matching days. A review of these results showed that 8 of these days had back trajectories which match the episode days reasonably well: 8/12/15, 8/14/15, 8/15/15, 8/27/15, 8/28/15, 8/29/15, 6/8/16, and 8/3/18. Weather conditions on these 8 days are compared in Figure 5-146 with the range of conditions on the episode days and the matching criteria listed in Table 5-5. In most cases, conditions on the matching days are within the range of or very close to conditions on the episode days, all of which are very similar to each other. Temperatures were cooler than the episode days on 8/28/15, 8/29/15, and 6/8/16. The barometric pressure was lower on 6/8/16; average wind speeds were more than 0.5 m/s lower on 8/12/15, 8/28/15, and 8/29/15 and higher on 8/15/15 and 8/3/18. Relative humidity values on the episode days cover a fairly wide range; RH values on the matching days fall well within these bounds.

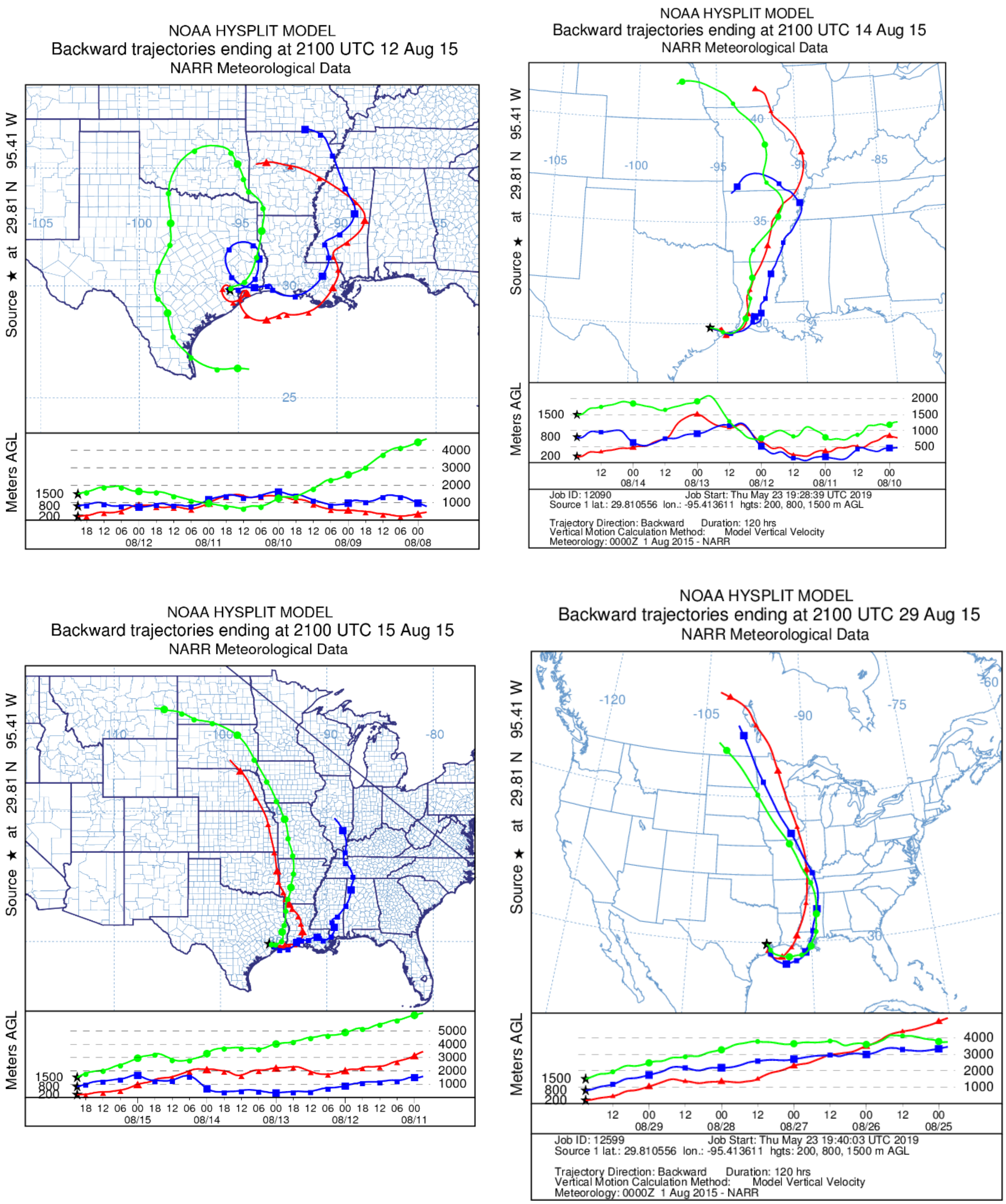

Figure 5-148. HYSPLIT 5-day back trajectories on potential matching days.

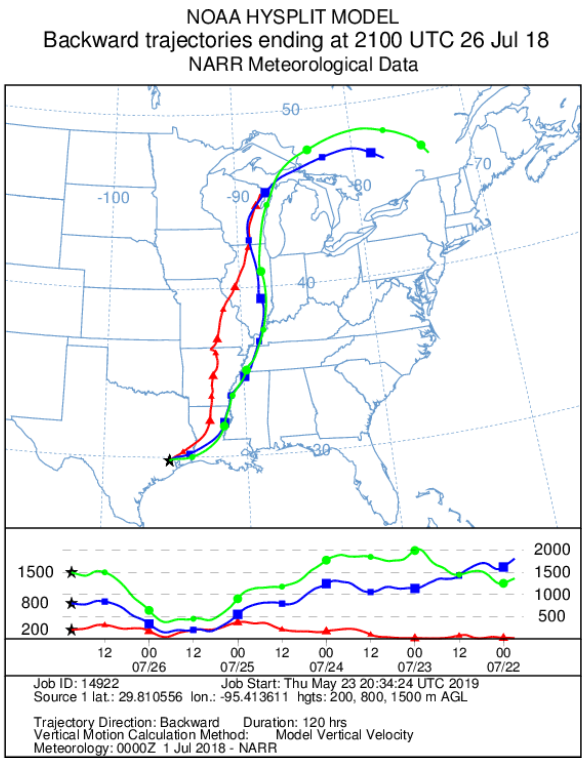
NOAA HYSPLIT MODEL
Backward trajectories ending at 2100 UTC 26 Jul 18
NARR Meteorological Data
Source ★ at 29.81 N 95.41 W
Meters AGL
Job ID: 14922
Job Start: Thu May 23 20:34:24 UTC 2019
Source 1 lat.: 29.810556 lon.: -95.413611 hgts: 200, 800, 1500 m AGL
Trajectory Direction: Backward Duration: 120 hrs
Vertical Motion Calculation Method: Model Vertical Velocity
Meteorology: 0000Z 1 Jul 2018 - NARR

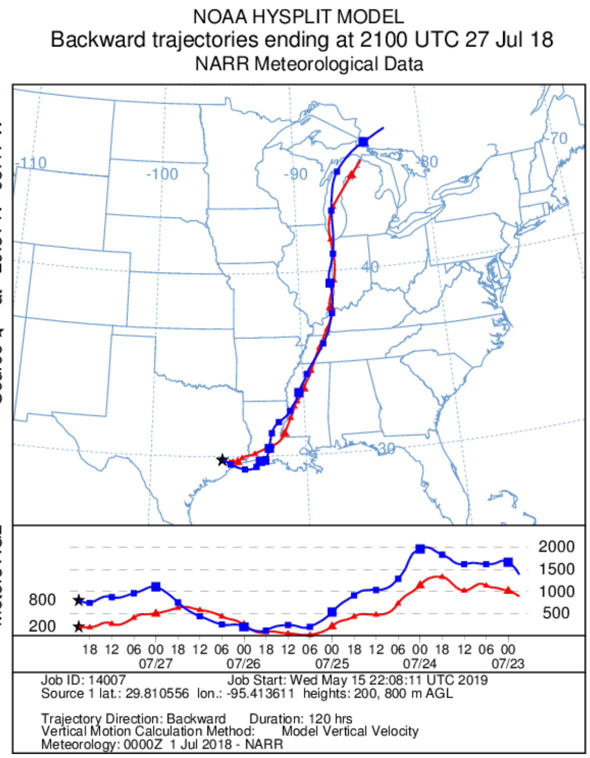
NOAA HYSPLIT MODEL
Backward trajectories ending at 2100 UTC 27 Jul 18
NARR Meteorological Data
Source ★ at 29.81 N 95.41 W
Meters AGL
Job ID: 14007
Job Start: Wed May 15 22:08:11 UTC 2019
Source 1 lat.: 29.810556 lon.: -95.413611 heights: 200, 800 m AGL
Trajectory Direction: Backward Duration: 120 hrs
Vertical Motion Calculation Method: Model Vertical Velocity
Meteorology: 0000Z 1 Jul 2018 - NARR

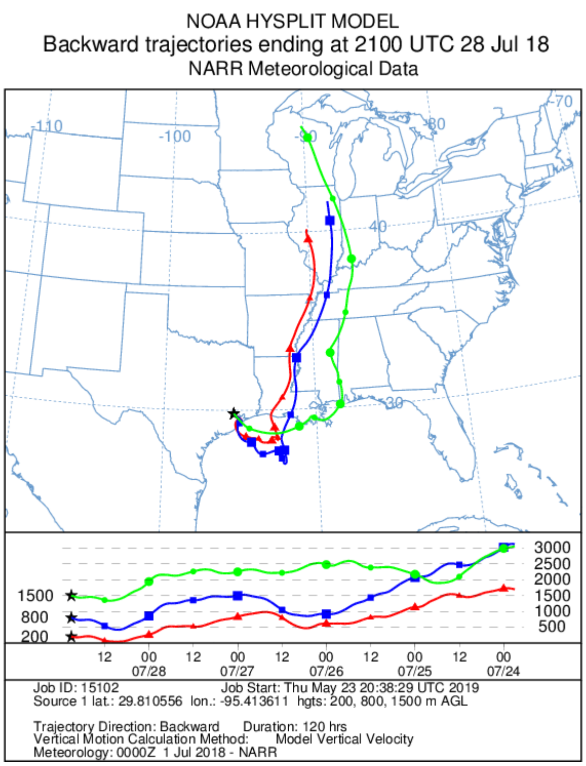
NOAA HYSPLIT MODEL
Backward trajectories ending at 2100 UTC 28 Jul 18
NARR Meteorological Data
Source ★ at 29.81 N 95.41 W
Meters AGL
Job ID: 15102
Job Start: Thu May 23 20:38:29 UTC 2019
Source 1 lat.: 29.810556 lon.: -95.413611 hgts: 200, 800, 1500 m AGL
Trajectory Direction: Backward Duration: 120 hrs
Vertical Motion Calculation Method: Model Vertical Velocity
Meteorology: 0000Z 1 Jul 2018 - NARR

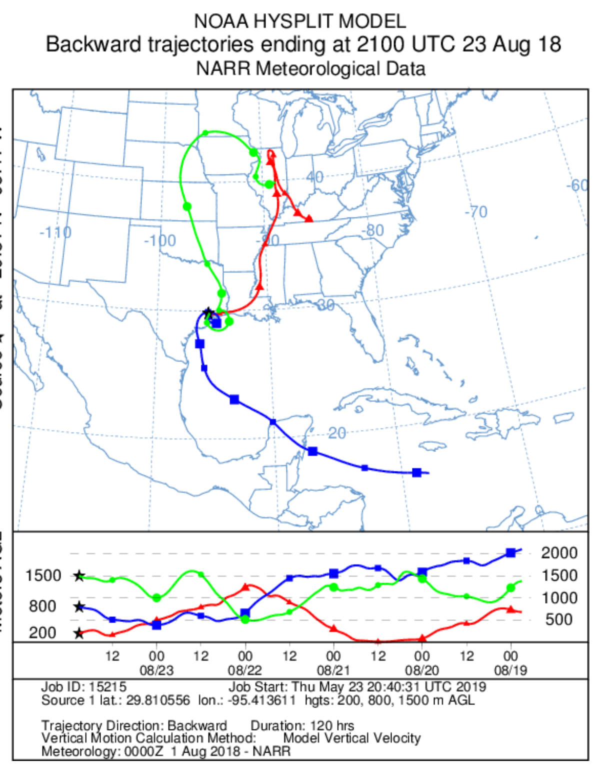
NOAA HYSPLIT MODEL
Backward trajectories ending at 2100 UTC 23 Aug 18
NARR Meteorological Data
Source ★ at 29.81 N 95.41 W
Meters AGL
Job ID: 15215
Job Start: Thu May 23 20:40:31 UTC 2019
Source 1 lat.: 29.810556 lon.: -95.413611 hgts: 200, 800, 1500 m AGL
Trajectory Direction: Backward Duration: 120 hrs
Vertical Motion Calculation Method: Model Vertical Velocity
Meteorology: 0000Z 1 Aug 2018 - NARR

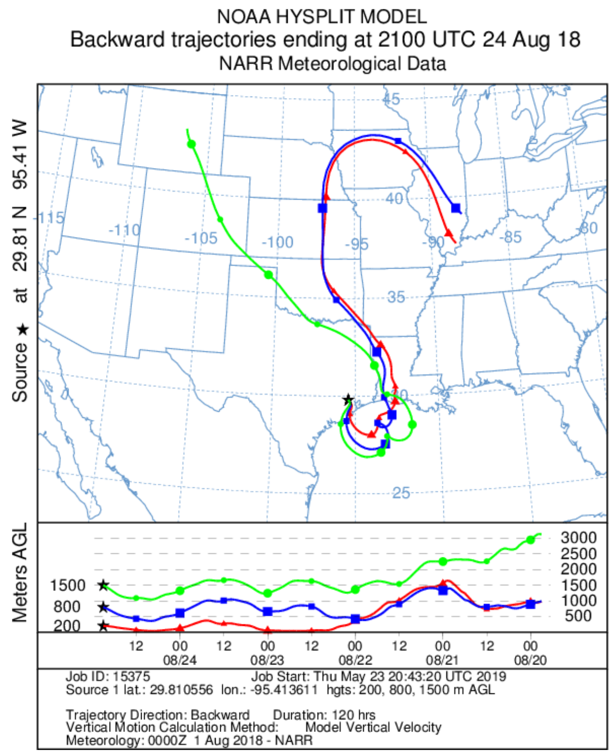

Figure 5-149. HYSPLIT 5-day back trajectories for episode days.

We then examined the NOAA Hazard Mapping System (HMS) smoke analysis product map for each of these 8 days and found that smoke was diagnosed directly over Houston on 4 of them, leaving 4 potential matching days: 8/12/15, 8/14/15, 8/15/15, and 8/29/15. HYSPLIT back trajectories for these four days are shown in for comparison with target episode day back trajectories, which are reproduced in Figure 5-149.

Ozone concentrations on the four potential matching days are summarized in Table 5-6 below. Ozone levels exceeded 90 ppb at multiple sites on 8/12/15 and 8/29/15 but were below 75 ppb at all Houston-Galveston-Brazoria (HGB) monitoring sites on 8/14/15 and 8/15/15.

Table 5-6. Daily maximum 8-hour average ozone concentrations on potential matching days (ppb).

Date	Aldine	Bayland Park	HGB Highest	HGB 2nd Highest
8/12/15	102	98	106 (Moody Tower)	102 (Aldine)
8/14/15	64	61	74 (Sugarland)	73 (La Porte and Westhollow)
8/15/15	62	56	71 (Danciger)	65 (Westhollow)
8/29/15	105	65	105 (Aldine)	93 (Haden Rd.)

HMS charts for the four days in Table 5-6 are shown in Figure 5-150. Areas of smoke are diagnosed by HMS close to although not directly over Houston on 8/14/15 and 8/29/15.[26] Coincident with the nearby smoke were high ozone readings at several monitoring sites on the 29th. However, ozone was also high at several sites on the 12th when the HMS analysis indicates the closest area of smoke to Houston was well north of the Red River. In contrast, ozone readings were low at both Aldine CAMS 8 and Bayland Park CAMS 53 on the 14th and 15th with an HGB-wide maximum of 74 ppb on the 14th and 71 ppb on the 15th. A key difference between the 12th and the 15th is the recirculation pattern within southeast Texas evident in the HYSPLIT back trajectories for the 12th which did not occur on the 15th and also did not occur on any of the episode days (except for the 1,500 m AGL trajectory on 8/23/18). This suggests that the 12th is not necessarily a good match with the episode days, thus leaving 8/15/15 as the best matching day. (Low ozone readings at Aldine and Bayland Park and generally low readings throughout HGB on 8/14/15 suggest that the nearby smoke may not have impacted the area on that day either).

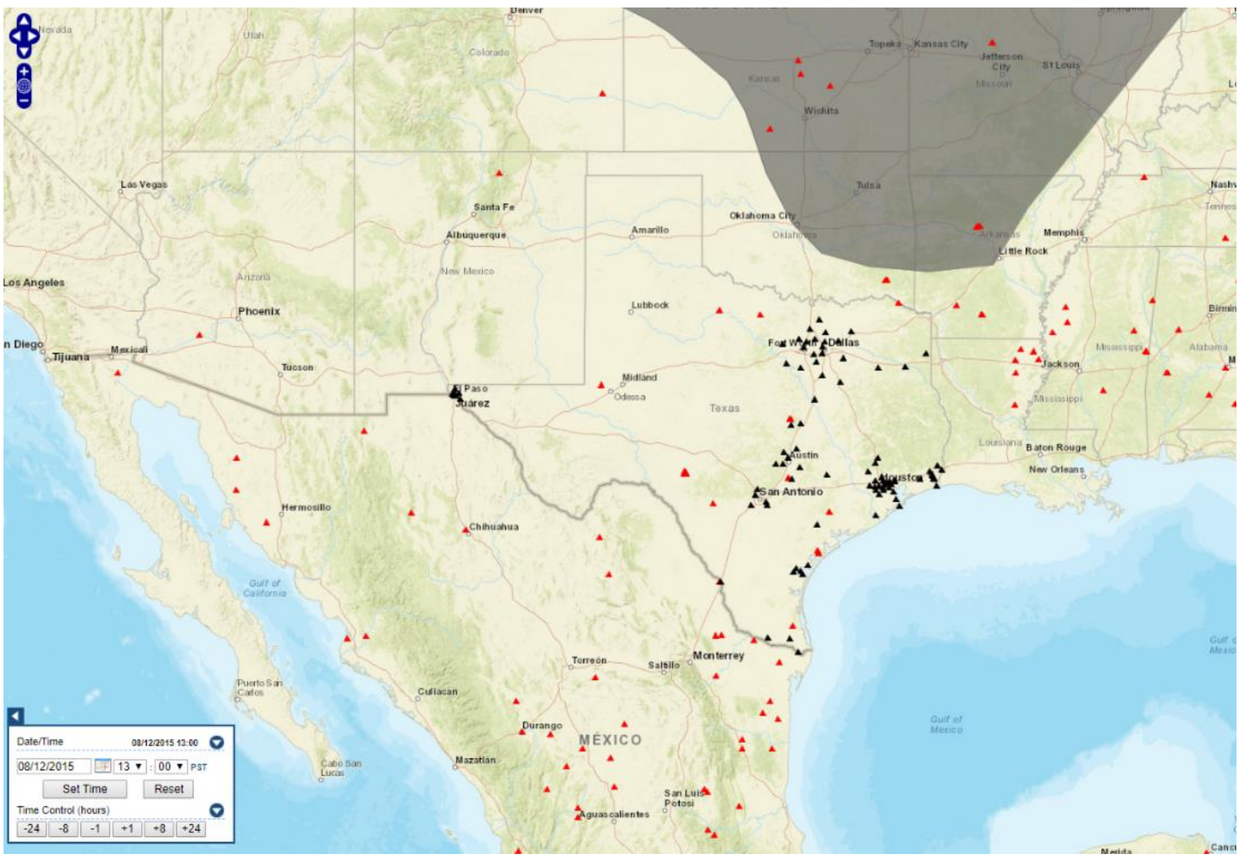

a) HMS diagnosed areas of smoke for 8/12/15 15:00 CST.

[26] It is important to keep in mind when evaluating HMS charts that the analyst will generally avoid indicating areas of smoke where clouds are prevalent and thus preventing satellite AOD retrievals.

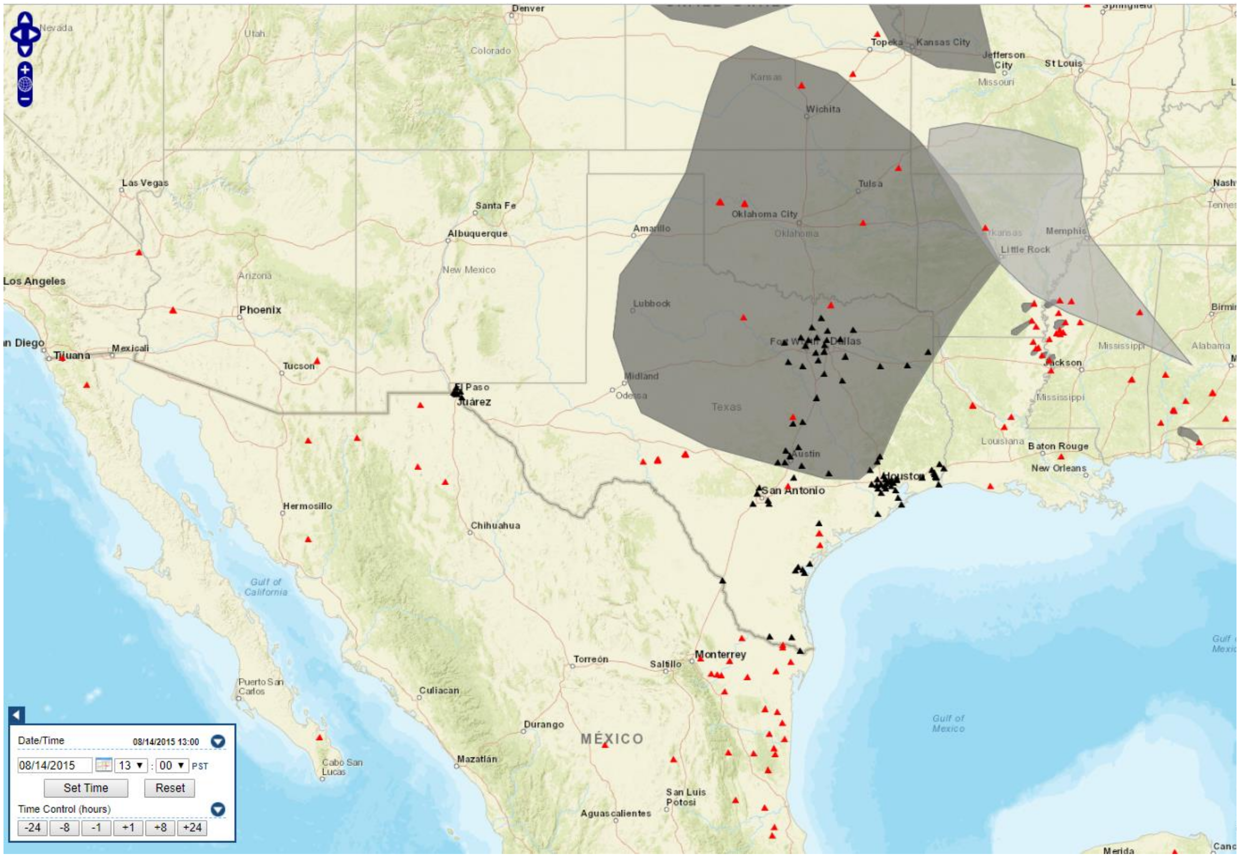

b) HMS diagnosed areas of smoke for 8/14/15 15:00 CST.

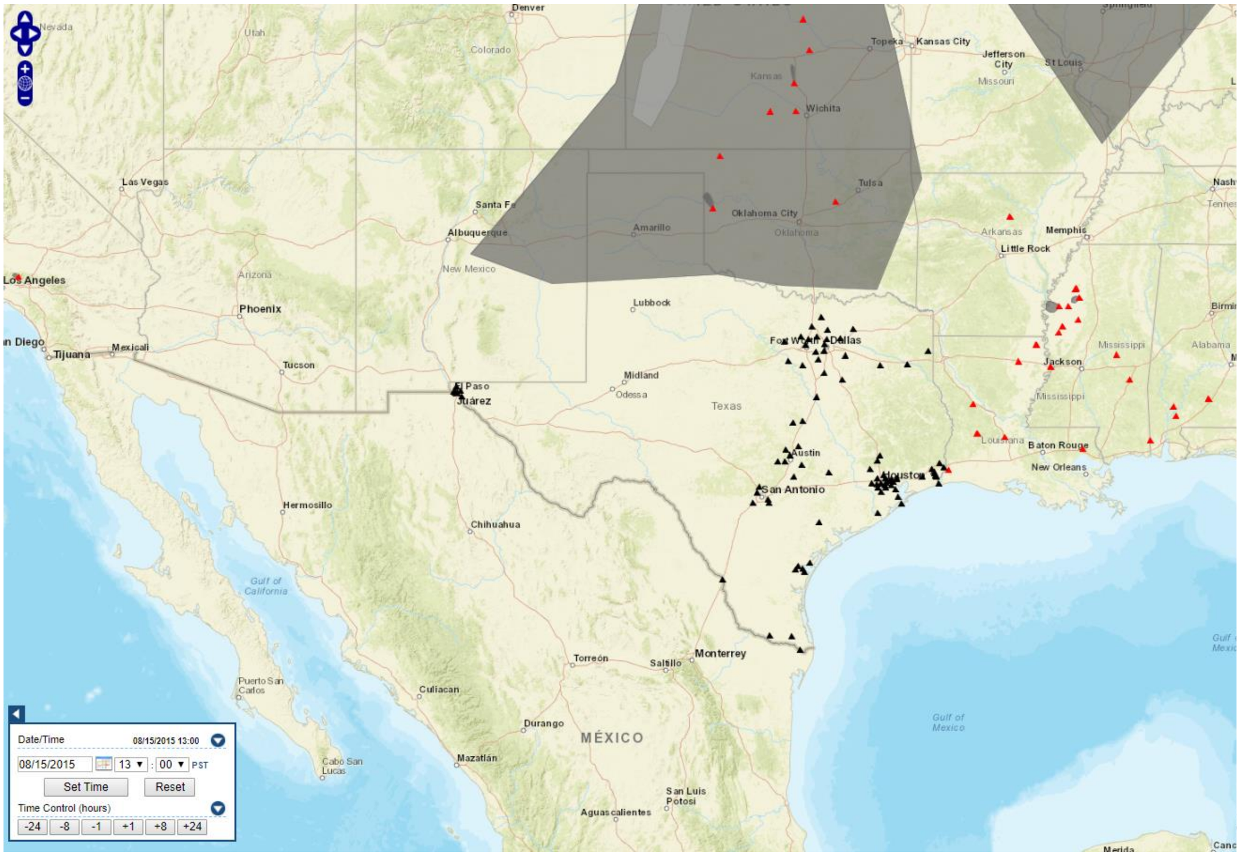

c) HMS diagnosed areas of smoke for 8/15/15 15:00 CST.

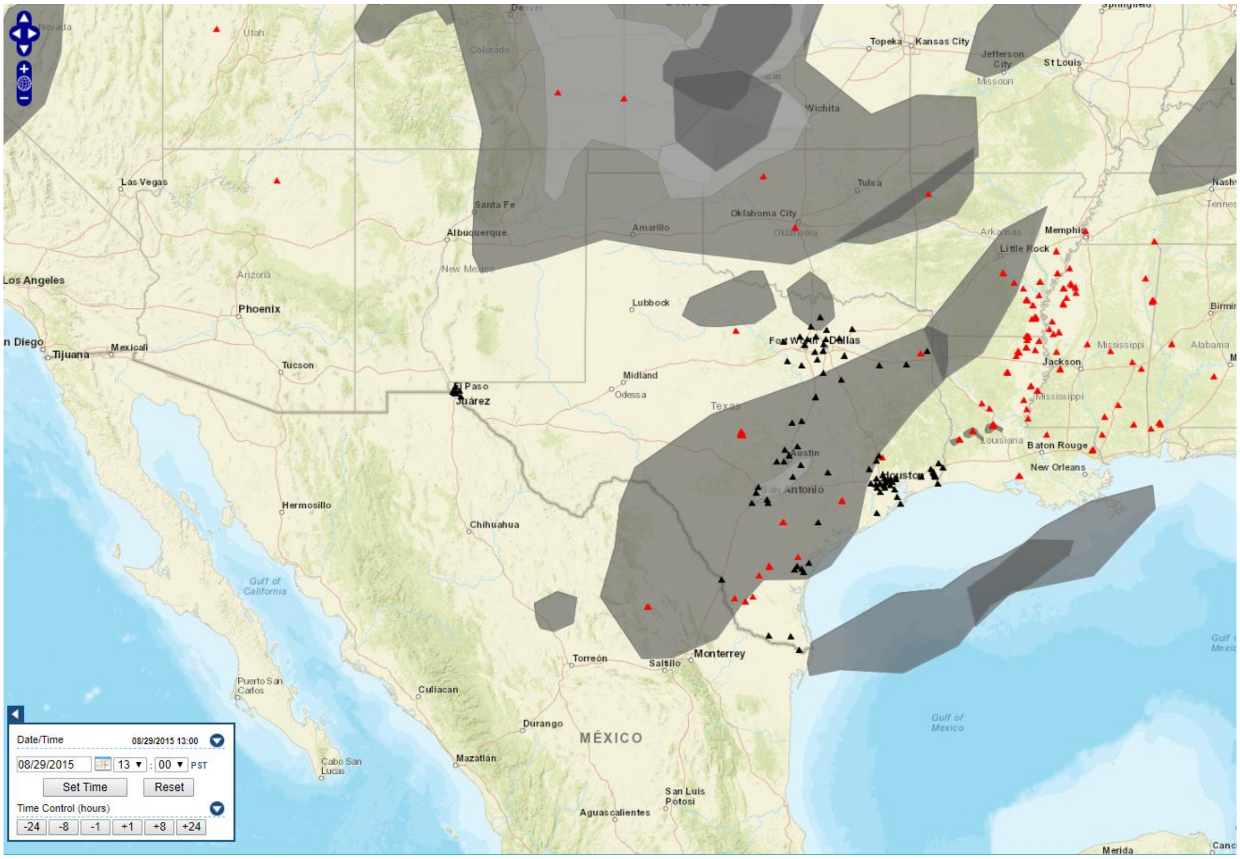

d) HMS diagnosed areas of smoke for 8/29/15 15:00 CST.

Figure 5-150. HMS diagnosed areas of smoke.

Additional evidence supporting the hypothesis that a smoke plume impacted Aldine CAMS 8 on the 8/24/18 target episode day but not on the 8/14/15 or 8/15/15 matching days can be found in the comparisons of hourly $PM_{2.5}$ concentrations on these days as compared to all June – August days 2014 – 2018 (Figure 5-151). $PM_{2.5}$ concentrations on 8/24/18 where unusually high at the time of the peak ozone concentrations (14:00 – 16:00 CST) whereas $PM_{2.5}$ concentrations and ozone were low on both matching days.

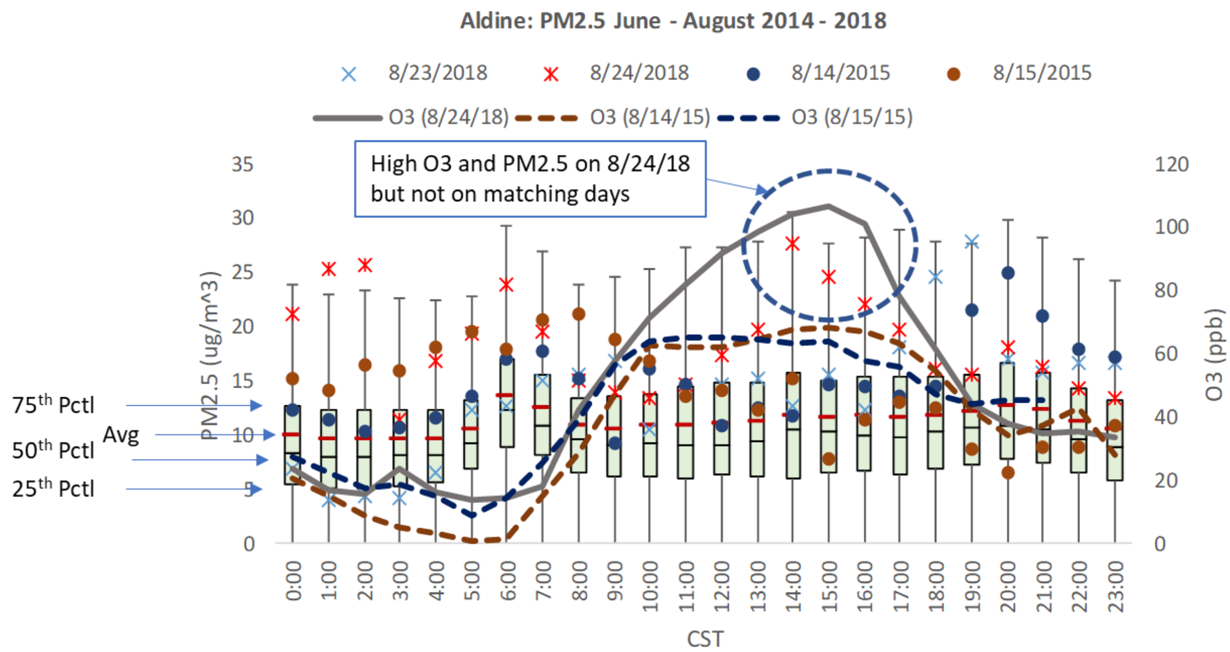

Figure 5-151. Boxplots of hourly PM2.5 concentrations at Aldine on all June-August days 2015-2015 compared to the 8/23/18 and 8/24/18 episode days and the 8/14/15 and 8/15/15 matching days; solid gray line is hourly ozone on 8/24/18.

Hourly ozone, NOx, and $PM_{2.5}$ data from HGB monitoring sites were reviewed to screen for the presence of wildfire smoke at ground level on the 8/14/15 and 8/15/15 matching days as compared to the 2018 episode days. Hourly ozone, NOx, and these two days concentrations for 8/14 – 8/15 2015 at Aldine are shown in Figure 5-151; PM2.5 at other HGB sites on these two days are shown in Figure 5-152 ($PM_{2.5}$ is not monitored at Bayland Park). Hourly ozone, NOx, and $PM_{2.5}$ concentrations at Aldine for the August 23-24, 2018 episode days are shown in Figure 5-153 ($PM_{2.5}$ 5 data are missing for nearly the entire July 26-28, 2018 target episode day period at Aldine). As shown in Figure 5-151, Aldine experienced a $PM_{2.5}$ and NOx peak at 20:00 CST on August 14 in addition to the usual morning commute period peak around 6:00 CST. Examination of the monitoring data (not shown) indicates that the NOx peak is almost entirely associated with an increase in NO_2 and thus not from an immediately local source of fresh emissions. $PM_{2.5}$ concentrations remain mostly above 15 µg/m3 until the morning of the 15th. Neither of the broad afternoon ozone peaks on these two days is coincident with any sharp $PM_{2.5}$ peaks but $PM_{2.5}$ concentrations are somewhat elevated (generally at or above 15 µg/m3) from the evening of the 14th until mid-day on the 15th. Thus, while there is no direct evidence of a $PM_{2.5}$ plume associated with elevated ozone, a source of elevated $PM_{2.5}$ and NOx does appear to have impacted the monitor during at least part of this period. Nevertheless, ozone remained low. As shown in Figure 5-152, $PM_{2.5}$ at other HGB monitoring sites during August 14 -15, 2015 were well correlated with those at Aldine (correlation coefficients ranging from 0.6 to 0.8), supporting the hypothesis that the elevated $PM_{2.5}$ was a regional phenomenon, consistent with the influence of a continental air mass (as indicated by the HYSPLIT back trajectories in Figure 2). Numerous anthropogenic and bio- or geogenic sources – possibly including agricultural burning and wildfires – could have contributed to the $PM_{2.5}$ present in this air mass. However, PM2.5 peak concentrations during August 14 -15, 2015 matching days were ~ 5 µg/m3 lower than during the

August 23-24, 2018 episode days (Figure 5-153) which featured multiple peaks approaching 30 µg/m3. The lower $PM_{2.5}$ concentrations on the matching days makes it less obvious that there was a significant influence from fires on air quality on these days as compared to the episode days. Comparisons of PM composition on these two sets of days may shed further light on this issue. It would also be helpful to compare PM composition data on these days with measurements of similar air masses of continental origin in southeast Texas that can be determined to a high degree of confidence to be smoke free.

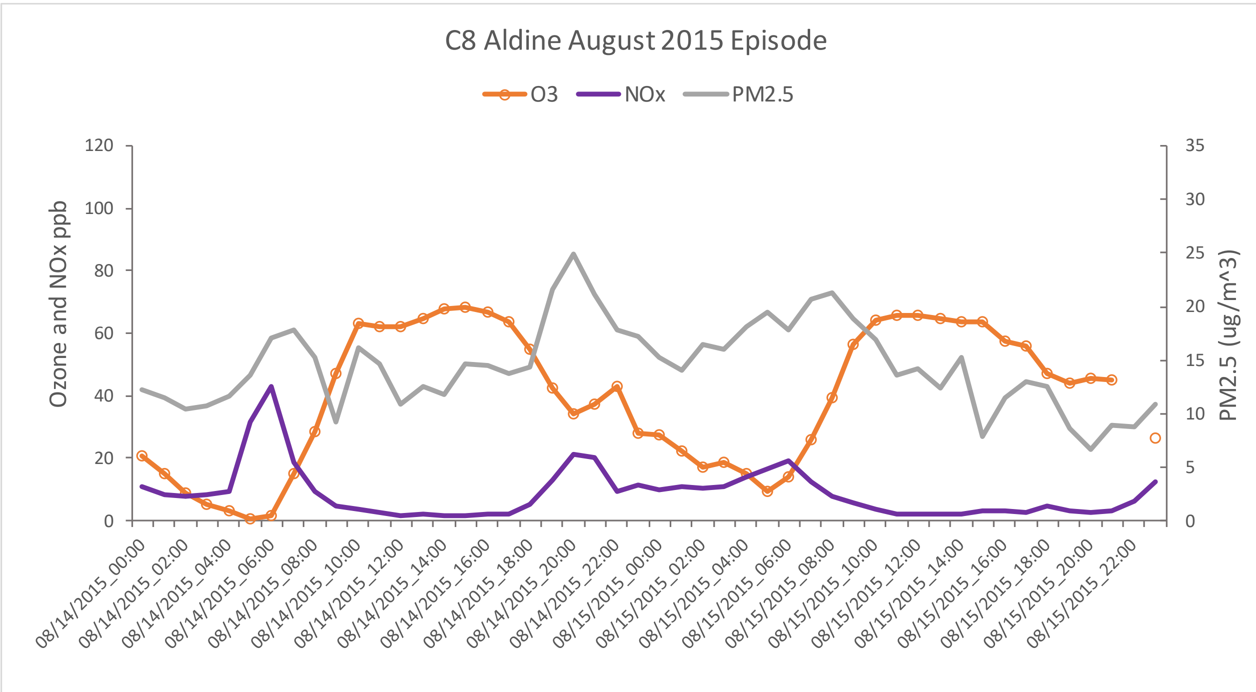

Figure 5-152. Hourly ozone, NOx, and PM2.5 concentrations at Aldine for August 14-15, 2015.

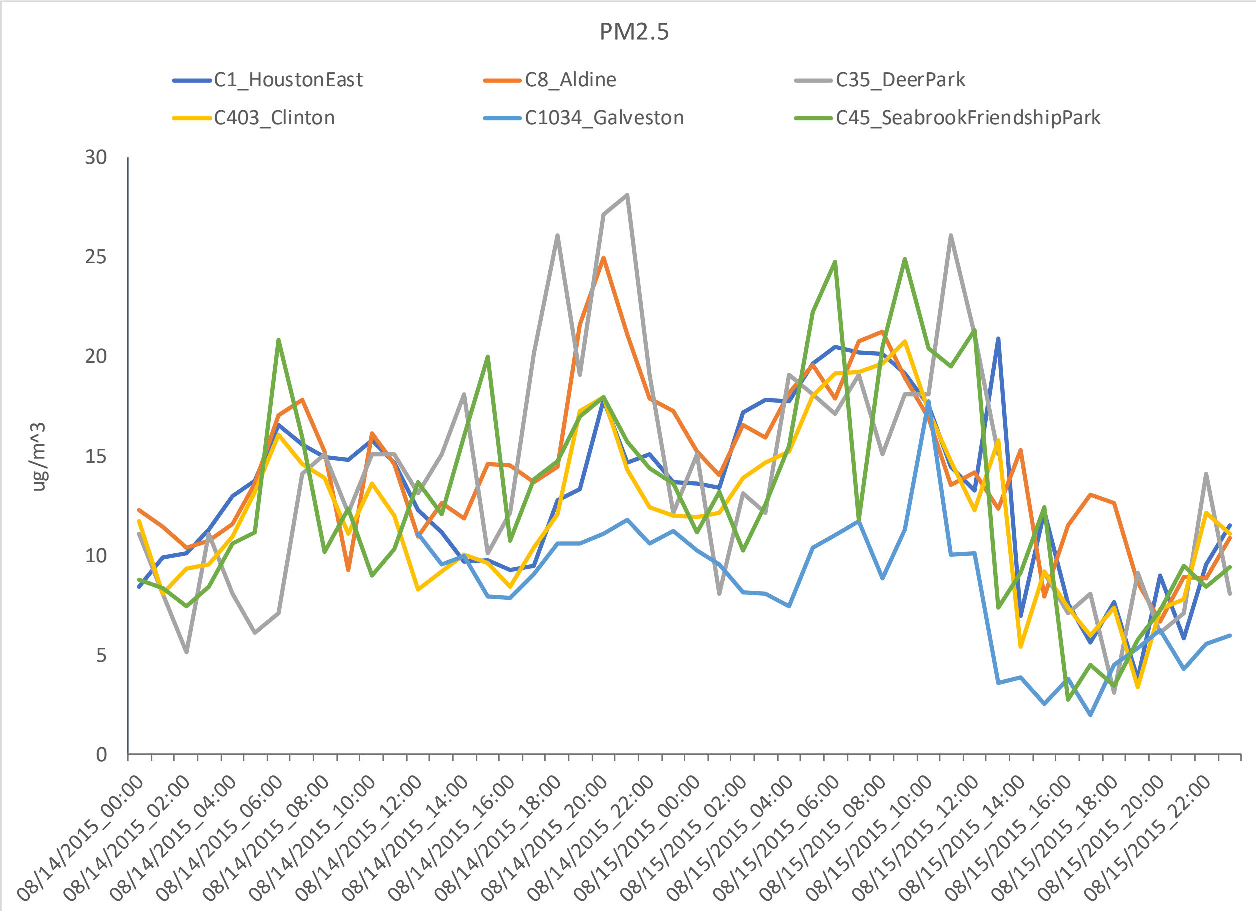

Figure 5-153. Hourly PM2.5 concentrations at HGB area monitors: August 14-15, 2015.

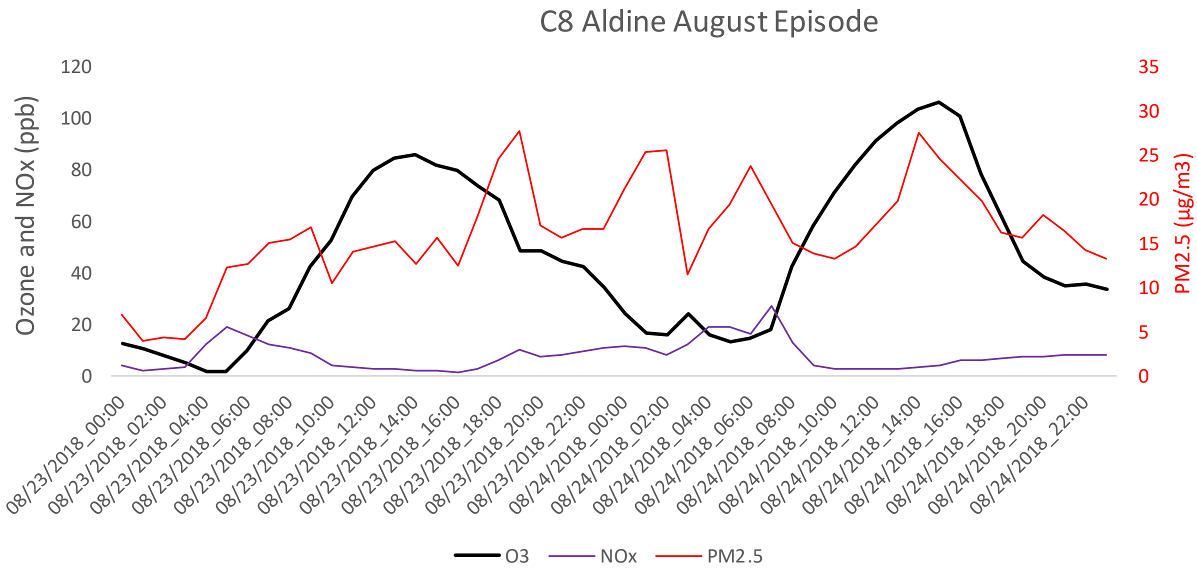

Figure 5-154. Hourly ozone, NOx, and $PM_{2.5}$ concentrations at Aldine for August 23-24, 2018.

Maximum daily 8-hour average (MDA8) ozone concentrations on 8/14/15 and 8/15/15 are compared with MDA8 values on the episode days in Table 3. Ozone values are low (<65 ppb at Aldine and Bayland Park and less than 75 ppb throughout HGB) on these days, particularly on 8/15/15 when the HMS product shows no smoke over Houston. The strong similarity in meteorological conditions between the 8/15/15 matching day and episode days is consistent with the hypothesis that smoke plume impacts are responsible for enhanced ozone on at least some of the episode days.

5.5 Comparison of Synoptic Conditions

North American 500 hPa geopotential height maps, surface weather (synoptic) maps, and precipitation maps for the episode days are presented in Figure 5-155, Figure 5-156 and Figure 5-157, respectively. Similar maps for the selected matching days are presented in Figure 5-158, Figure 5-159 and Figure 5-158. Note that the selected precipitation maps show total precipitation for the 24-hours ending 7:00 EST on the day after the target episode day or matching day; some or all of the indicated precipitation may have fallen after the time of the peak ozone on the target or matching day.

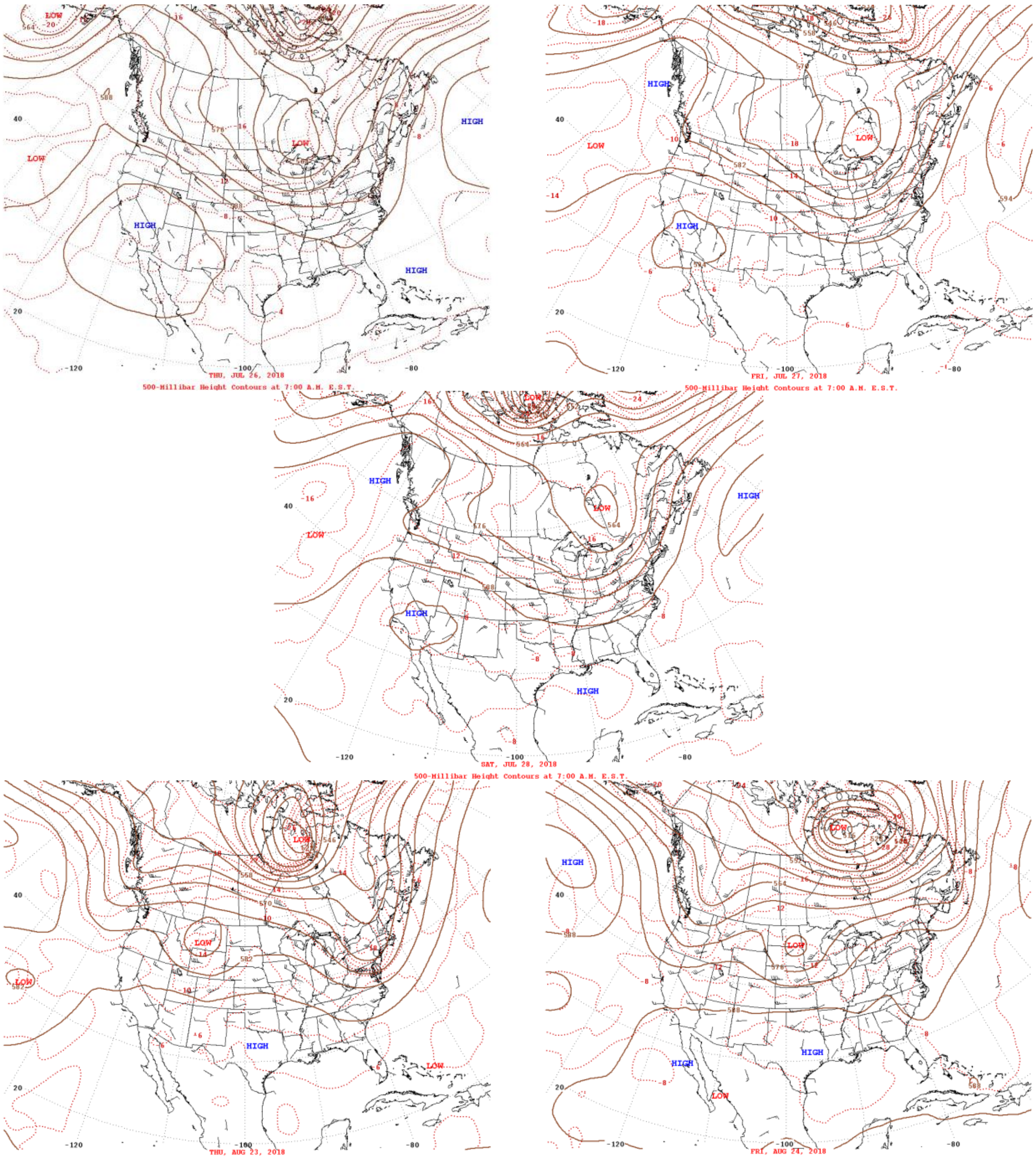

Figure 5-155. 500 hPa geopotential heights (solid contours), winds, and temperatures (dotted contours) for 5 am LST 2018 July 26 and 27 (top), July 28 (middle), and August 23 and 24 (bottom).

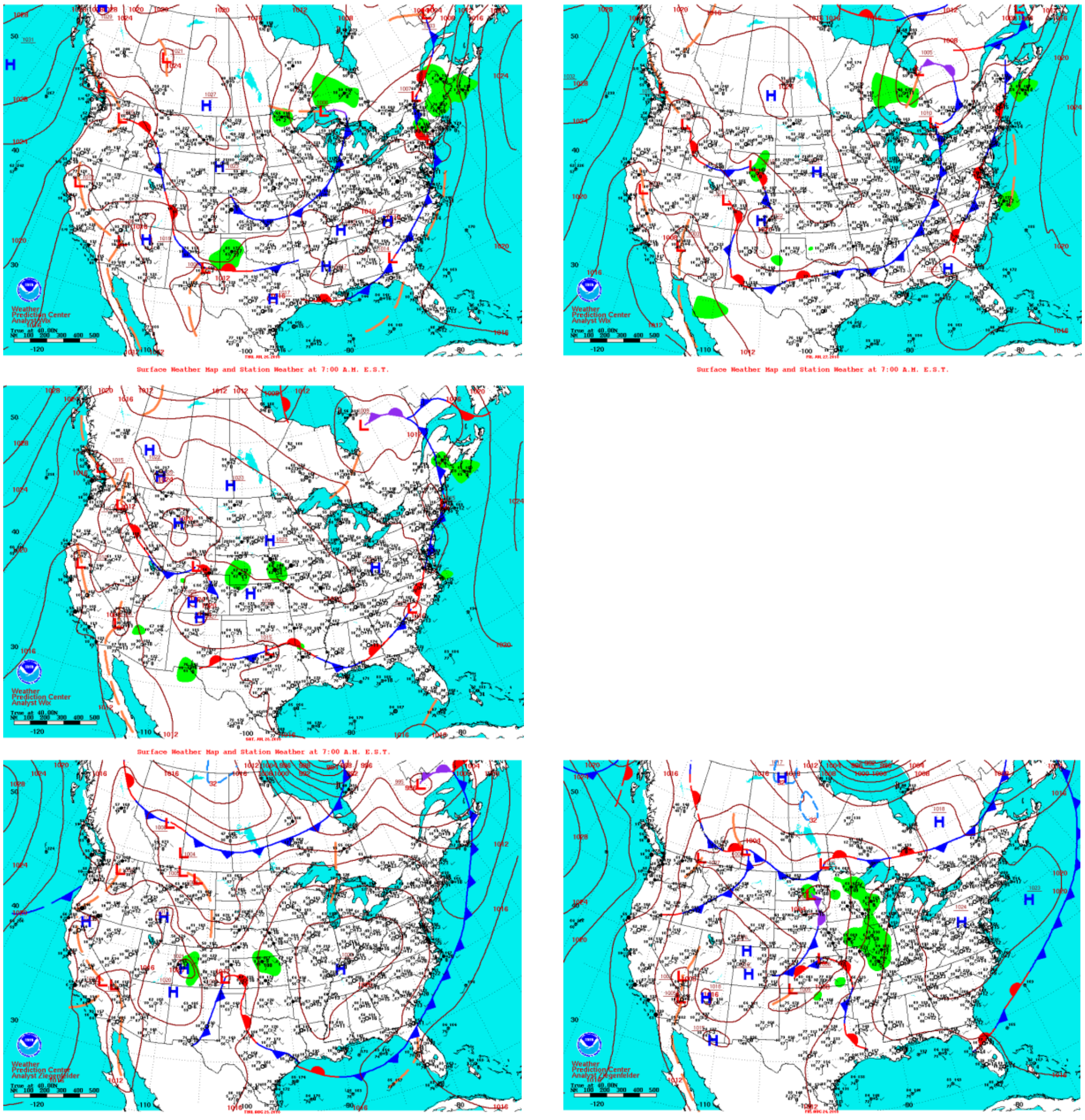

Figure 5-156. Surface weather analysis maps for 6 am LST 2018 July 26 and 27 (top), July 28 (middle), and August 23 and 24 (bottom).

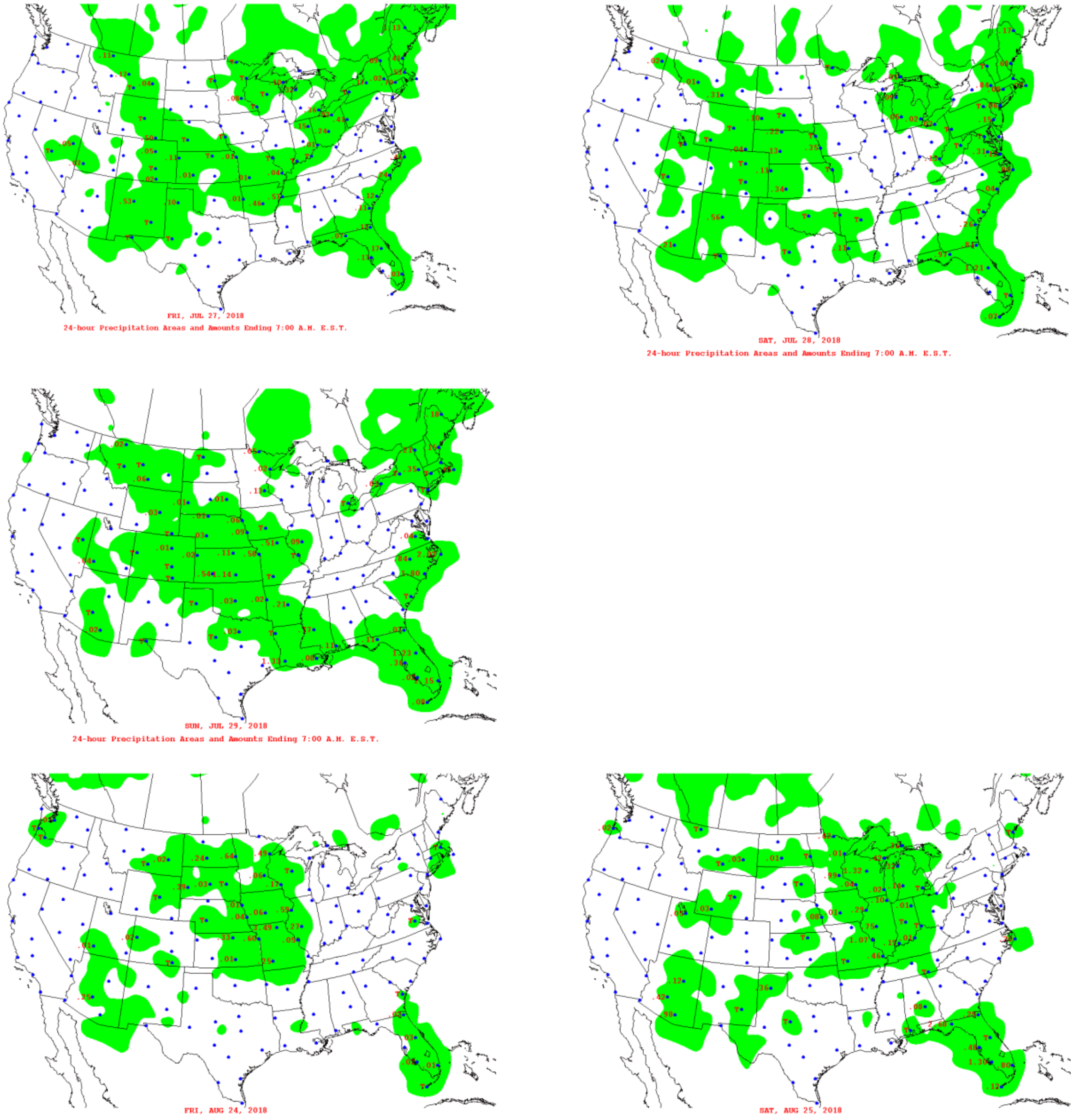

Figure 5-157. Total precipitation for 24-hour period ending at 6 am LST 2018 July 27 and 28 (top), July 29 (middle), and August 24 and 25 (bottom).

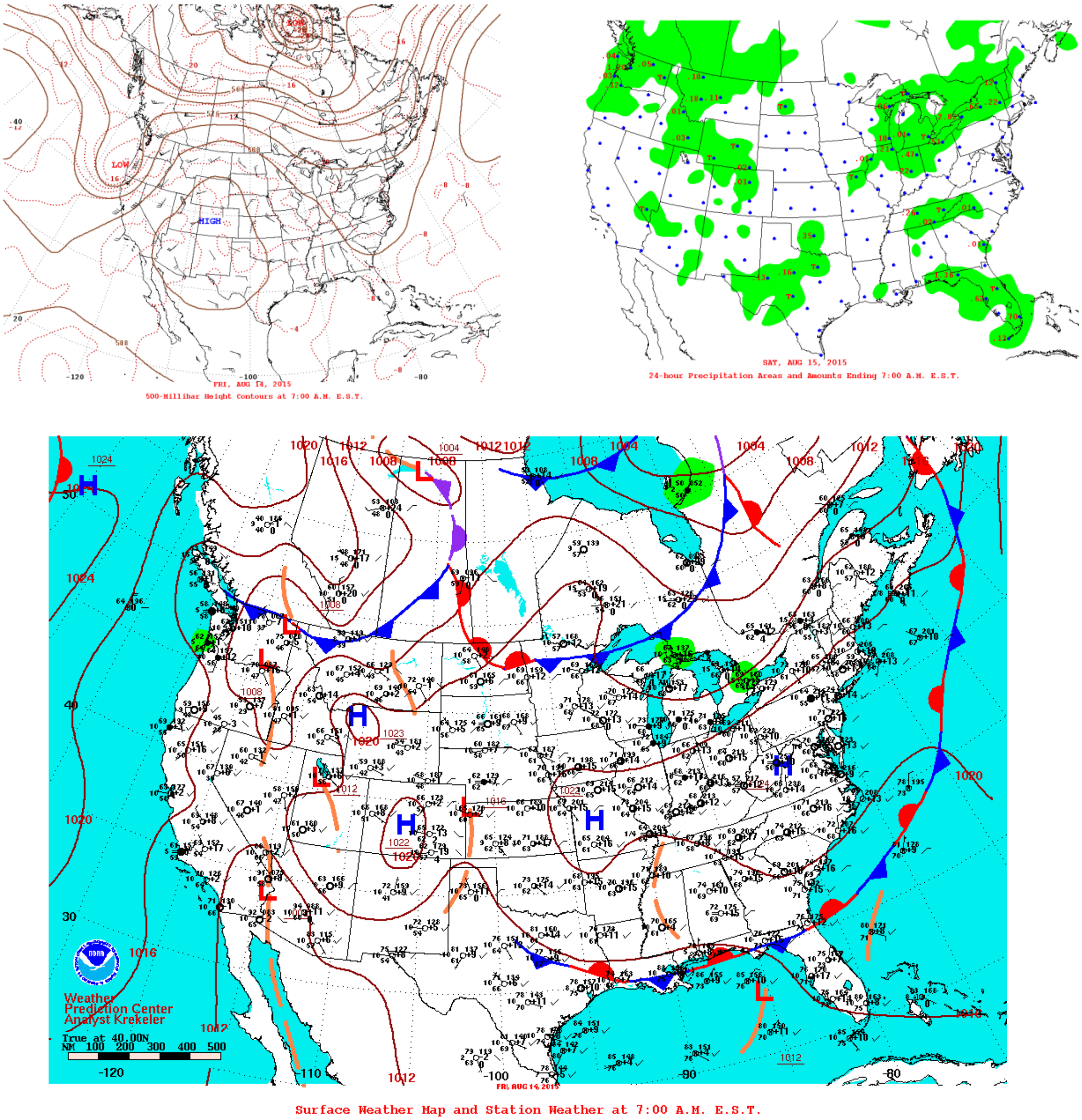

Figure 5-158. 500 hPa (top left), surface analysis (top right), and precipitation (bottom) for 14 August 2015.

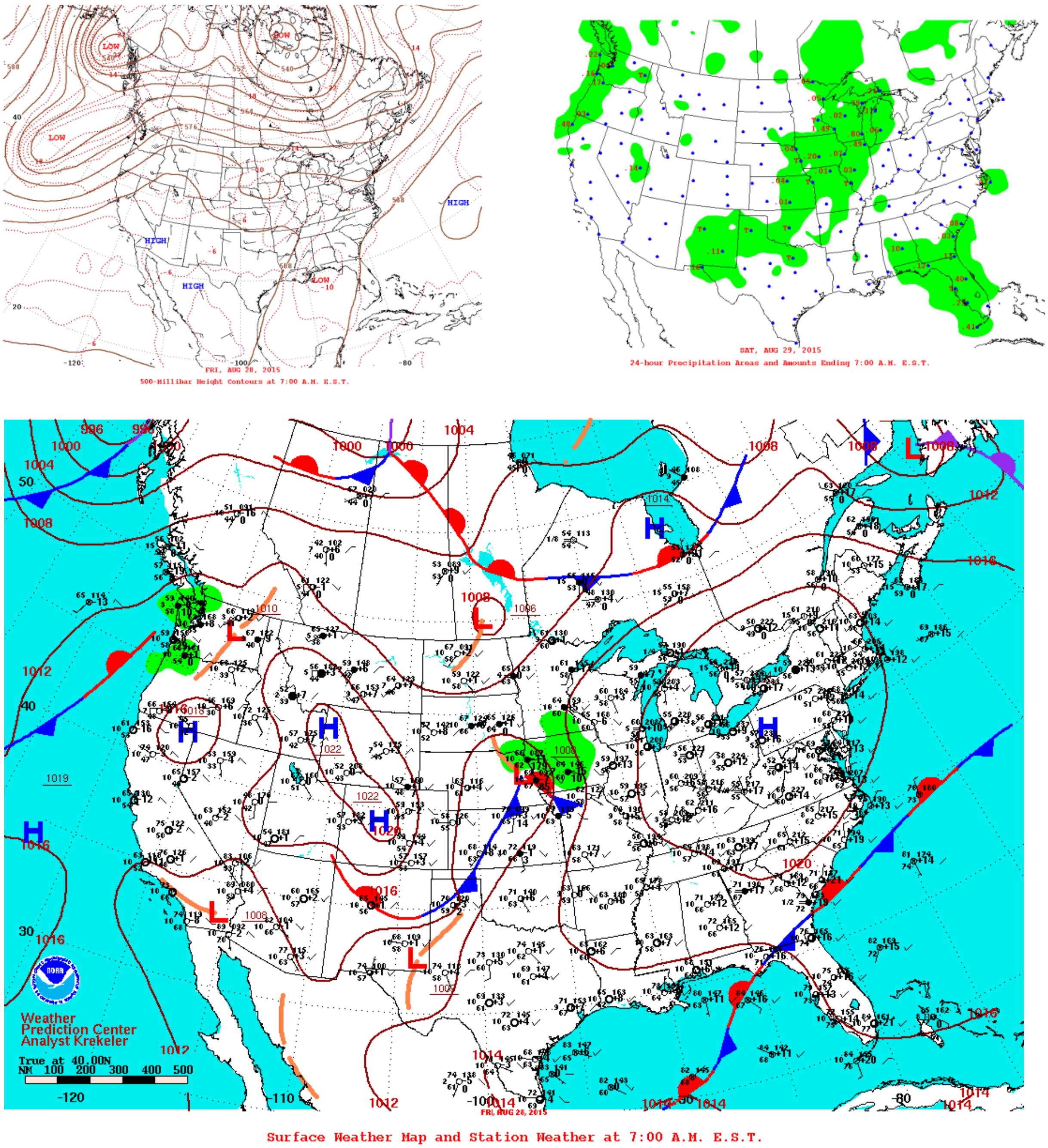

Figure 5-159. 500 hPa (top left), surface analysis (top right), and precipitation (bottom) for 15 August 2015.

Table 5-7. Comparisons of daily maximum 8-hour average ozone concentrations (MDA8) on episode days with concentrations on matching days. MDA8 values exceeding 70 ppb are shown in red type. Gray shading indicates MDA8 values for the episode days and blue shading indicates values for the matching days.

Aldine CAMS 8		Matching Day ->	8/14/2015	8/15/2015
		Matching Day MDA8 (ppb) ->	64	62
	Date	MDA8 (ppb)	MDA8 Difference (ppb): (EE Day - Matching Day)	
Episode days	7/27/2018	109	45	47
	7/28/2018	86	22	24
	8/24/2018	91	27	29

Bayland Park CAMS 53		Matching Day ->	8/14/2015	8/15/2015
		Matching Day MDA8 (ppb) ->	61	56
	Date	MDA8 (ppb)	MDA8 Difference (ppb): (EE Day - Matching Day)	
Episode days	7/26/2018	77	16	21
	8/23/2018	82	21	26

5.5.1 Statistical Regression Analysis

Dr. Dan Jaffe performed a generalized additive model (GAM) statistical regression analysis of weather- and air quality-related parameters and MDA8 ozone at Houston monitors and provided his analysis to the TCEQ. Because the regression equations were developed with ten years of data, they represent the relationship between air quality and meteorology under typical emission patterns.

Dr. Jaffe describes the method: "*In brief, the method develops a statistical prediction scheme for the MDA8 using meteorological predictors such as daily max temperature, wind speed, relative humidity, trajectory distance, etc. The model uses a training dataset to predict MDA8 ozone based on past years relationships. The residual (the unexplained portion of the variance) can identify days with unusual ozone levels, if the residual is sufficiently large* ". The GAM analysis quantified residuals suggesting that atypical conditions contributed ozone to the Aldine Park MDA8 on July 27 and on August 23-24. Dr. Jaffe concludes that evidence for unusual enhancement of the MDA8 ozone was weaker for July 26. July 28 was not analyzed. Using analyses complementary to the GAM, Dr. Jaffe infers that wildfire emissions contributed to the ozone residuals found by the GAM and therefore to the Houston ozone exceedances on July 26-27 and August 23-24. The complementary analyses considered that enhanced levels of $PM_{2.5}$ occurred in Houston during these periods and that hourly ground level $PM_{2.5}$ and ozone were correlated at Houston CAMS during the hours 10 am – 6 pm.

6.0 SUMMARY

6.1 July 26-28, 2018 Houston Ozone Episode

During July 2018, wildfires in Ontario, Canada and Louisiana generated ozone precursors that may have contributed to unusually high ozone concentrations at Bayland Park CAMS 53 on July 26 and at Aldine CAMS 8 on July 27 and July 28.

During the last week of July 2018, the Houston area and the surrounding region of East Texas experienced a multi-day period of high ozone. Houston ozone values rose between July 24-27 and then fell from July 27-July 30. Ozone monitors located in rural areas outside Houston show rising and falling trends similar to Aldine CAMS 8 and Bayland Park CAMS 53, consistent with a regional ozone episode influenced by the arrival of polluted continental air with high levels of background ozone.

July 27 had the highest value of MDA8 ozone measured at Aldine CAMS 8 during the previous five years. MDA8 values for July 27 exceeded the 99th percentile of values for the April-October for 2014-2018 period, while July 26 and July 28 were above the 98th percentile for Bayland Park CAMS 53 and Aldine CAMS 8, respectively. When the full year is considered, all three days exceeded the 99th percentile for their monitors for the 2014-2018 period.

For the Bayland Park monitor, MDA8 values for July 26 and August 23 exceeded the 98th percentile when compared against April-October 2014-2018 MDA8 values and exceeded the 99th percentile when the full year is considered. This analysis shows that ozone was unusually high at Aldine CAMS 8 and Bayland Park CAMS 53 during the July and August Houston ozone episodes and that MDA8 values were among the very highest values measured at these monitors during the preceding five years.

Meteorological conditions during the July episode were generally consistent with TCEQ’s conceptual model for non-event high ozone days in Houston. However, July 26 and 27 were unusual in that they had northeasterly afternoon winds that were favorable for transport of ozone and precursors from upwind fires in Louisiana and from more distant fires.

HYSPLIT trajectories using the NAM 12 km, EDAS 40 km and NARR 36 km meteorological analyses are consistent in showing a source-receptor relationship between the North Bay Wildfire Complex in eastern Ontario and the Houston area for emissions occurring through a deep layer of the lower atmosphere and at multiple times. Of the other large fire complexes burning during the week prior to July 26-28, only the Garner Complex and South Umpqua Complex in Oregon had forward trajectories that reached Houston, and this was only true for a small number of hours for NARR analysis trajectories initialized at 3,000 m. Therefore, evidence from the HYSPLIT trajectory analysis for transport from distant fires to Houston is strongest for the North Bay Complex. HYSPLIT trajectories using all three meteorological analyses also showed a source-receptor relationship between Louisiana fires occurring July 25-26 and the Houston area.

Satellite imagery from multiple platforms shows that the smoke plume from the North Bay Complex fires moved southward across the Midwest and Southeast US toward Louisiana between July 22-25. Between July 24 and July 25, the Canadian wildfire plume signal grew more diffuse and less intense until it merged with a broad area of smoke over Louisiana on July 25. By July 26, the NOAA HMS smoke field no longer covered a broad swath of Texas and Louisiana, as it did on July 25. By July 26, the area of dense, regional smoke was north of Oklahoma and Arkansas and the only smoke diagnosed by HMS over East Texas and Louisiana came from smaller fires, whose individual plumes were visible in the vicinity of the fires. During July 26-28, the HMS product shows only small smoke plumes from fires in Louisiana and Texas.

Although the NOAA HMS smoke product suggests transport of smoke from western wildfires to Houston was possible, we were not able to trace an AOD, CO or true color signal from western wildfires across the US to southeast Texas.

Multiple lines of evidence from surface and satellite-based monitoring systems indicate the presence of smoke in the Houston area aloft and at the surface. The widespread presence of smoke in the Houston area provides support for the hypothesis that wildfires influenced ground level ozone during July 26-28.

Photochemical modeling indicated small (<1 ppb) MDA8 ozone impacts from wildfire emissions at Bayland Park CAMS 53 and Aldine CAMS 8 during the July 26-28 episode. However, matching day and GAM analyses suggest that an atypical process or processes had a larger impact on Houston ozone during July 26-28. In this context “atypical” means that ozone was higher than expected given the weather conditions on the episode days. The matching day analysis and the GAM analysis do not provide information on the nature of the process or processes contributing to the ozone residuals on July 26-28.

6.2 August 23-24, 2018 Houston Ozone Episode

During August 2018, very large wildfires were burning in California, Oregon, Washington and in the Canadian Provinces of British Columbia. Wildfires in California, Oregon, Nevada and Louisiana generated ozone precursors that may have contributed to unusually high ozone concentrations at Bayland Park CAMS 53 on August 23 and at Aldine CAMS 8 on August 24.

During late August 2018, the Houston area experienced a multi-day period of high ozone. Ozone values rose between August 21-24 and then fell from August 24-29. Ozone monitors located in rural areas outside Houston show rising and falling trends similar to Aldine CAMS 8 and Bayland Park CAMS 53 monitors, consistent with a regional ozone episode influenced by the arrival of polluted continental air with high levels of background ozone. Meteorological conditions August episode were generally consistent with TCEQ’s conceptual model for non-event high ozone days in Houston.

On August 23, Bayland Park CAMS 53 monitored an MDA8 ozone value of 82 ppb and reached a peak 1-hour ozone value of 112 ppb. On August 24, the MDA8 at Aldine CAMS 8 was 91 ppb. This was the highest value of the MDA8 in the Houston area on August 24 and the peak 1-hour average ozone at Aldine was 106 ppb. August 23 and 24 exceeded the 99th percentile of values for CAMS 53 and CAMS 8, respectively for 2014-2018 for both the full year and April-October periods. By August 25, the Houston ozone episode had begun to subside.

HYSPLIT trajectories using the NAM 12 km, EDAS 40 km and NARR 36 km meteorological analyses are consistent in showing source-receptor relationships between the Houston area and the Mendocino Complex (CA) the Carr Fire (CA) the South Sugarloaf Complex (NV) and the Klondike, Taylor Creek and Miles Fire Complexes (OR). HYSPLIT trajectories using all three meteorological analyses also showed a source-receptor relationship between Louisiana fires occurring August 22-23 and the Houston area.

Satellite imagery from multiple platforms shows extensive, thick plumes of smoke across Canada and the northern and central US emanating from fires in British Columbia and the western US during the week before the August 23-24 Houston ozone episode.

During the week leading up to August 23-24, the smoke plumes moved from California and Oregon southward and eastward toward Texas behind an advancing cold front associated with a low-pressure system moving eastward across the Midwest. The southeast movement of the smoke-influenced air is apparent in MODIS AOD and AIRS CO retrievals as well as the true color (visible) satellite images. The evolution of the NRTEEM photochemical model smoke tracer plume emanating from the FINN fire locations is consistent with the evolution of satellite-retrieved regions of high CO and AOD associated with the fire plumes as well as with the smoke plumes emanating from the western US/Canada fires simulated by the NOAA HRRR surface and vertically integrated smoke analyses.

As the cold front advanced southward across East Texas on August 20, new fires began burning in central and western Louisiana. The number of Louisiana fires grew with each passing day between August 20 and August 23. On August 22 and 23, the MODIS and GOES 16 AOD retrievals, the NRTEEM modeling smoke tracer and NOAA HRRR smoke product animations show that smoke from the plumes of the Louisiana fires merged with the smoke from the distant wildfires and was advected toward Houston as high pressure built over the southeast US and low-level winds developed an easterly component.

Multiple lines of evidence from surface and satellite-based monitoring systems indicate the presence of smoke in the Houston area aloft and at the surface. The widespread presence of smoke in the Houston area provides support for the hypothesis that wildfires influenced ground level ozone during August 23-24.

Photochemical modeling indicated MDA8 ozone impacts from wildfire emissions were less than 3 ppb at Bayland Park CAMS 53 and Aldine CAMS 8 during the August 23-24 episode. However, matching day and GAM analyses suggest that an atypical process or processes had a larger impact on Houston ozone during August 23-24. In this context “atypical” means that ozone was higher than expected given the weather conditions on the episode days. The matching day analysis and the GAM analysis do not provide information on the nature of the process or processes contributing to the ozone residuals on August 23-24.

7.0 REFERENCES

Baker, K. R., Woody, M. C., Tonnesen, G. S., Hutzell, W., Pye, H. O. T., Beaver, M. R., ... & Pierce, T. 2016. Contribution of regional-scale fire events to ozone and PM2. 5 air quality estimated by photochemical modeling approaches. Atmospheric Environment, 140, 539-554.Emery, C., E. Tai, G. Yarwood, and R. Morris, 2011. Investigation into approaches to reduce excessive vertical transport over complex terrain in a regional photochemical grid model. Atmospheric Environment. 45. 7341-7351. 10.1016/j.atmosenv.2011.07.052.

Baker, K. R., Woody, M. C., Valin, L., Szykman, J., Yates, E. L., Iraci, L. T., ... & Campuzano-Jost, P. 2018. Photochemical model evaluation of 2013 California wild fire air quality impacts using surface, aircraft, and satellite data. Science of The Total Environment, 637, 1137-1149.

Ek, M., Bill Lapenta, Geoff DiMego, Hendrik Tolman, John Derber, Yuejian Zhu, Vijay Tallapragada, Mark Iredell, Shrinivas Moorthi, Suru Saha. 2014. The NOAA Operational Numerical Guidance System. 29th Session of the World Weather/Climate Research Programme (WWRP/WCRP) Working Group on Numerical Experimentation (WGNE-29) Bureau of Meteorology, Melbourne, Australia, 10-14 March 2014.

Emery, C., E. Tai, and G. Yarwood, 2001. "Enhanced Meteorological Modeling and Performance Evaluation for Two Texas Ozone Episodes." Prepared for the Texas Natural Resource Conservation Commission, prepared by ENVIRON.

ENVIRON and Alpine. 2012. Western Regional Air Partnership (WRAP) West-wide Jump-start Air Quality Modeling Study (WestJumpAQMS) – WRF Application/Evaluation. ENVIRON International Corporation, Novato, California. Alpine Geophysics, LLC. University of North Carolina. February 29. (http://www.wrapair2.org/pdf/WestJumpAQMS_2008_Annual_WRF_Final_Report_February29_2012.pdf).

Giles, D. M., Sinyuk, A., Sorokin, M. G., Schafer, J. S., Smirnov, A., Slutsker, I., Eck, T. F., Holben, B. N., Lewis, J. R., Campbell, J. R., Welton, E. J., Korkin, S. V., and Lyapustin, A. I. (2019): Advancements in the Aerosol Robotic Network (AERONET) Version 3 database – automated near-real-time quality control algorithm with improved cloud screening for Sun photometer aerosol optical depth (AOD) measurements, Atmos. Meas. Tech., 12, 169-209, https://doi.org/10.5194/amt-12-169-2019.

Guenther, A., Karl, T., Harley, P., Wiedinmyer, C., Palmer, Geron, C. 2006. Estimates of global terrestrial isoprene emissions using MEGAN (Model of Emissions of Gases and Aerosols from Nature), Atmos. Chem Phys., 6, 3181-3210.

Johnson, J., E. Tai, P. Karamchandani, G. Wilson, and G. Yarwood. 2013. TCEQ Ozone Forecasting System. Prepared for Mark Estes, TCEQ. November.

Johnson, J., G. Wilson, D.J. Rasmussen, G. Yarwood. 2015. "Daily Near Real-Time Ozone Modeling for Texas." Prepared for Texas Commission on Environmental Quality, Austin, TX. January.

Johnson, J., G. Wilson, D.J. Rasmussen, G. Yarwood. 2016a. "Daily Near Real-Time Ozone Modeling for Texas." Prepared for Texas Commission on Environmental Quality, Austin, TX. January.

Johnson, J., G. Wilson, A. Wentland, W. -C. Hsieh, and G. Yarwood. 2016b. "Daily Near Real-Time Ozone Modeling for Texas." Prepared for Texas Commission on Environmental Quality (TCEQ), TX. December.

Johnson, J., G. Wilson, M. Jimenez, T. Shah, R. Beardsley and G. Yarwood. 2017. "Fire Impact Modeling with CAMx." Prepared for Texas Commission on Environmental Quality (TCEQ), TX. July.

Johnson, J., G. Wilson, J. Bandoro, K. Richman, L. Huang, R. Beardsley and G. Yarwood, 2018. Near-Real Time Exceptional Event Modeling. Prepared for Mark Estes, TCEQ. August 2018.

Kota, S. H., G. Schade, M. Estes, D. Boyer, Q. Ying. 2015. Evaluation of MEGAN predicted biogenic isoprene emissions at urban locations in Southeast Texas, Atmos. Environ., 110, 54-64. doi:10.1016/j.atmosenv.2015.03.027.

McDonald-Buller, E., Y. Kimura, C. Wiedinmyer, C. Emery, Z. Liu and G. Yarwood. 2015. Targeted Improvements in the Fire INventory from NCAR (FINN) Model for Texas Air Quality Planning. Prepared for David Sullivan, Texas Air Quality Research Program and The University of Texas at Austin. August.

McNally, D. E., 2009. "12km MM5 Performance Goals." Presentation to the Ad-Hoc Meteorology Group. 25-June. (http://www.epa.gov/scram001/adhoc/mcnally2009.pdf).

Ramboll, 2017. The User's Guide to the Comprehensive Air Quality Model with Extensions Version 6.40. Available from Ramboll, 773 San Marin Drive, Novato, CA. 94998 and at http://www.camx.com.

Shah, T., L. Parker, J. Grant and Greg Yarwood. 2018. "Modeling Inventories for Mexico and Caribbean Countries to Support Quantitative Analysis of International Transport Impacts on Ozone Design Values and Regional Haze." Prepared for Texas Commission on Environmental Quality (TCEQ), TX. June.

Skamarock, W.C., J.B. Klemp, J. Dudhia, D.O. Gill, D.M. Barker, M.G. Duda, X-Y Huang, W. Wang, J.G. Powers. 2008. "A Description of the Advanced Research WRF Version 3." NCAR Technical Note, NCAR/TN-45+STR (June 2008). http://www.mmm.ucar.edu/wrf/users/.

Stoeckenius, T.E., Emery, C.A., Shah, T.P., Johnson, J.R., Parker, L.K., Pollack, A.K., 2009. Air Quality Modeling Study for the Four Corners Region. Prepared for the New Mexico Environment Department, Air Quality Bureau, Santa Fe, NM. ENVIRON International Corporation, Novato, CA.

Sullivan, D. 2009. Effects of Meteorology on Pollutant Trends. Final Report to TCEQ. Grant Activities No. 582-5-86245-FY08-01. Prepared by Dave Sullivan, University of Texas at Austin Center for Energy and Environmental Resources, Prepared for Kasey Savanich, for the Texas Commission on Environmental Quality, March 16, 2009.

TCEQ (2009). Houston-Galveston-Brazoria Nonattainment Area Ozone Conceptual Model. The TCEQ Data Analysis Team. Texas Commission on Environmental Quality. May.

Wiedinmyer, C., Akagi, S. K., Yokelson, R. J., Emmons, L. K., Al-Saadi, J. A., Orlando, J. J., and Soja, A. J.: The Fire INventory from NCAR (FINN): a high resolution global model to estimate the emissions from open burning, Geosci. Model Dev., 4, 625-641, doi:10.5194/gmd-4-625-2011, 2011.

Wesely, M. L.: Parameterization of surface resistances to gaseous dry deposition in regional-scale numerical models, Atmos. Environ., 23, 1293–1304, 1989.

Wu, Z., Schwede, D.B., Vet, R., Walker, J.T., Shaw, M., Staebler, R. and Zhang, L., 2018. Evaluation and intercomparison of five North American dry deposition algorithms at a mixed forest site. Journal of Advances in Modeling Earth Systems. doi: 10.1029/2017MS001231.

Yu, H., A. Guenther, C. Warneke, J. de Gouw, S. Kemball-Cook, J. Jung, J. Johnson, Z. Liu, and G. Yarwood, 2015. "Improved Land Cover and Emission Factor Inputs for Estimating Biogenic Isoprene and Monoterpene Emissions for Texas Air Quality Simulations". Prepared for Texas Air Quality Research Program. (AQRP Project 14-016, September 2015).

Appendix A

NRTEEM Ozone Model Performance Evaluation

Appendix A NRTEEM Ozone Model Performance Evaluation

In this Appendix, we present model performance statistics (NMB, NMB and correlation coefficient) charts for 1-hour ozone for July 20-28, 2018 and August 18-24, 2018.

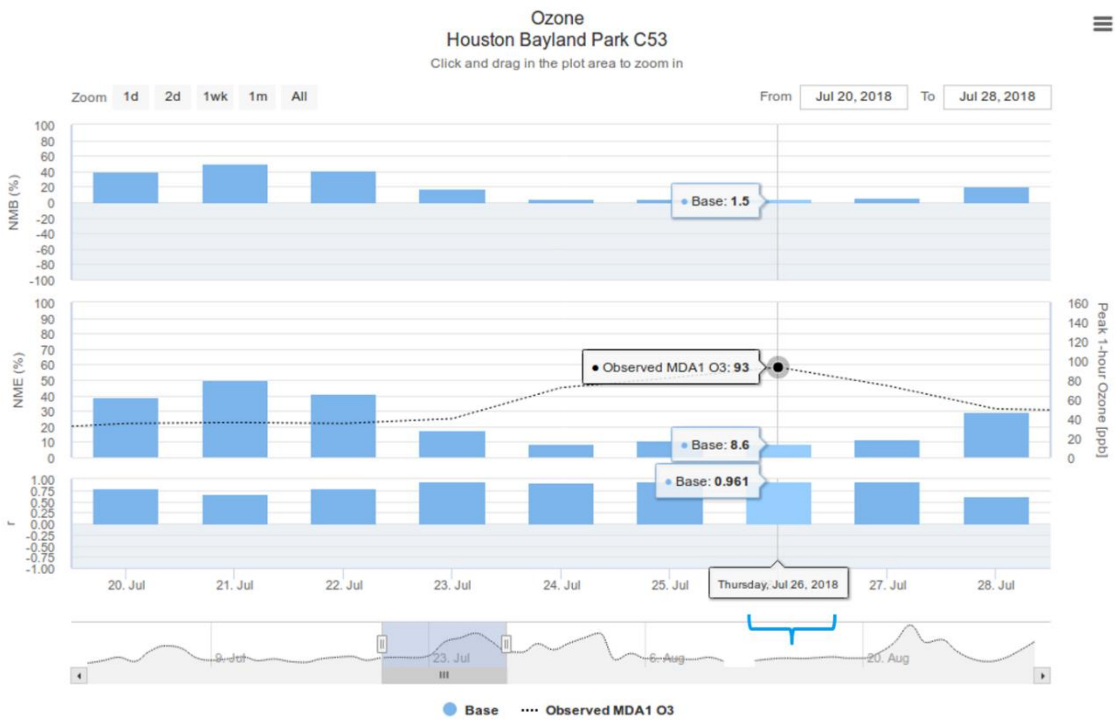

Figure A-1. NRTEEM model performance statistics for daily 1-hour ozone (20 ppb cutoff) at Bayland Park C53 for July 20-28, 2018. Statistics shown for July 26.

Figure A-2. NRTEEM model performance statistics for daily 1-hour ozone (20 ppb cutoff) at Aldine C8 for July 20-28, 2018. Statistics shown for July 27.

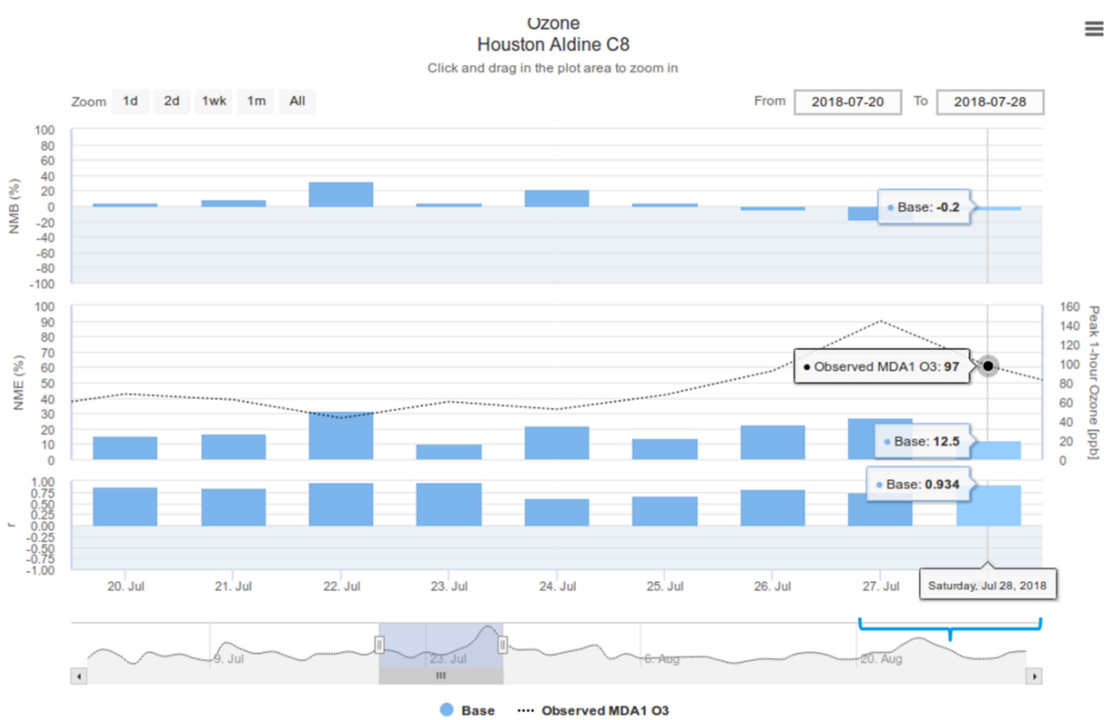

Figure A-3. NRTEEM model performance statistics for daily 1-hour ozone (20 ppb cutoff) at Aldine C8 for July 20-28, 2018. Statistics shown for July 28.

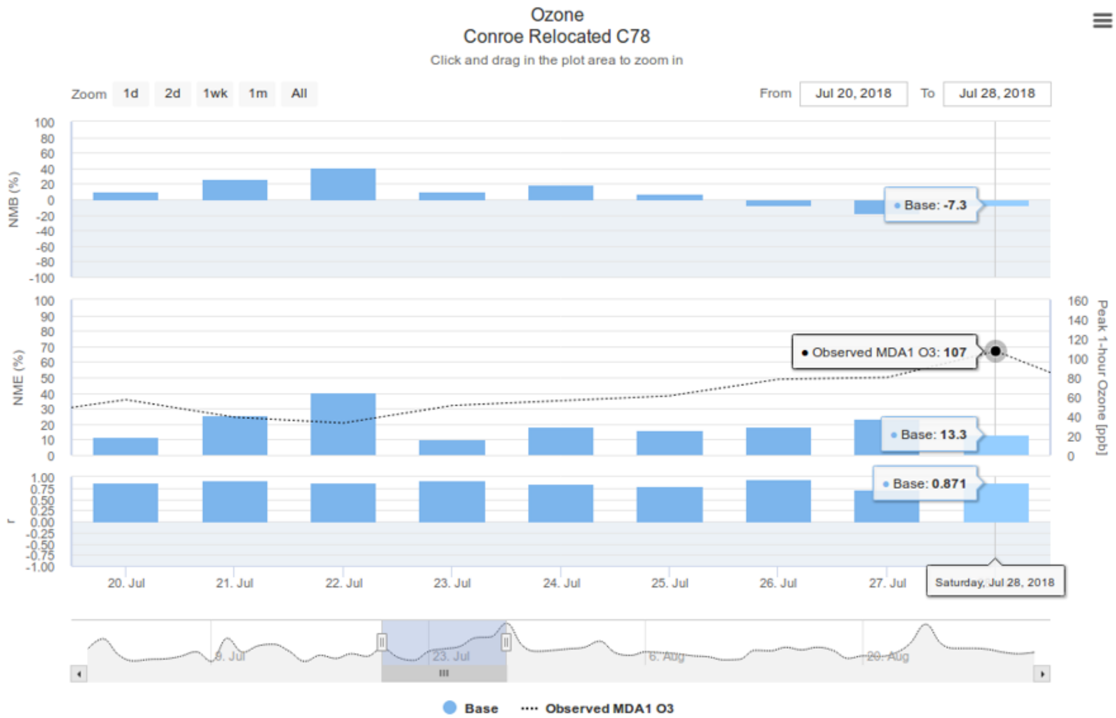

Figure A-4. NRTEEM model performance statistics for daily 1-hour ozone (20 ppb cutoff) at Conroe Relocated C78 for July 20-28, 2018. Statistics shown for July 28.

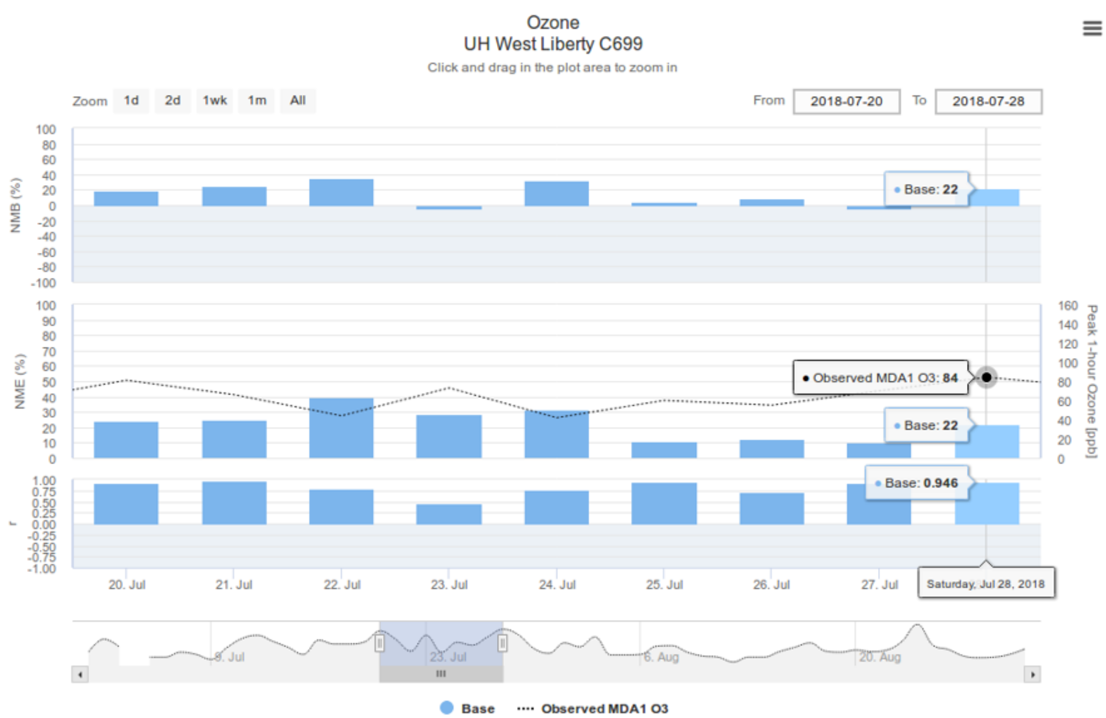

Figure A-5. NRTEEM model performance statistics for daily 1-hour ozone (20 ppb cutoff) at UH West Liberty C699 for July 20-28, 2018. Statistics shown for July 28.

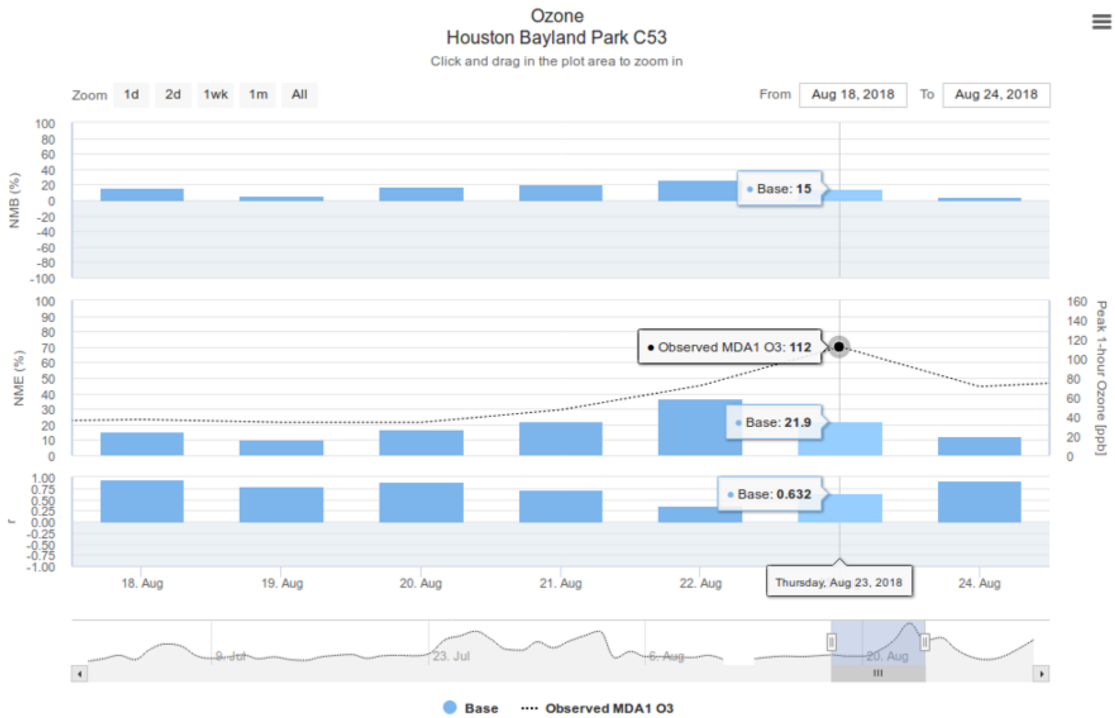

Figure A-6. NRTEEM model performance statistics for daily 1-hour ozone (20 ppb cutoff) at Bayland Park C53 for August 18-24, 2018. Statistics shown for August 23.

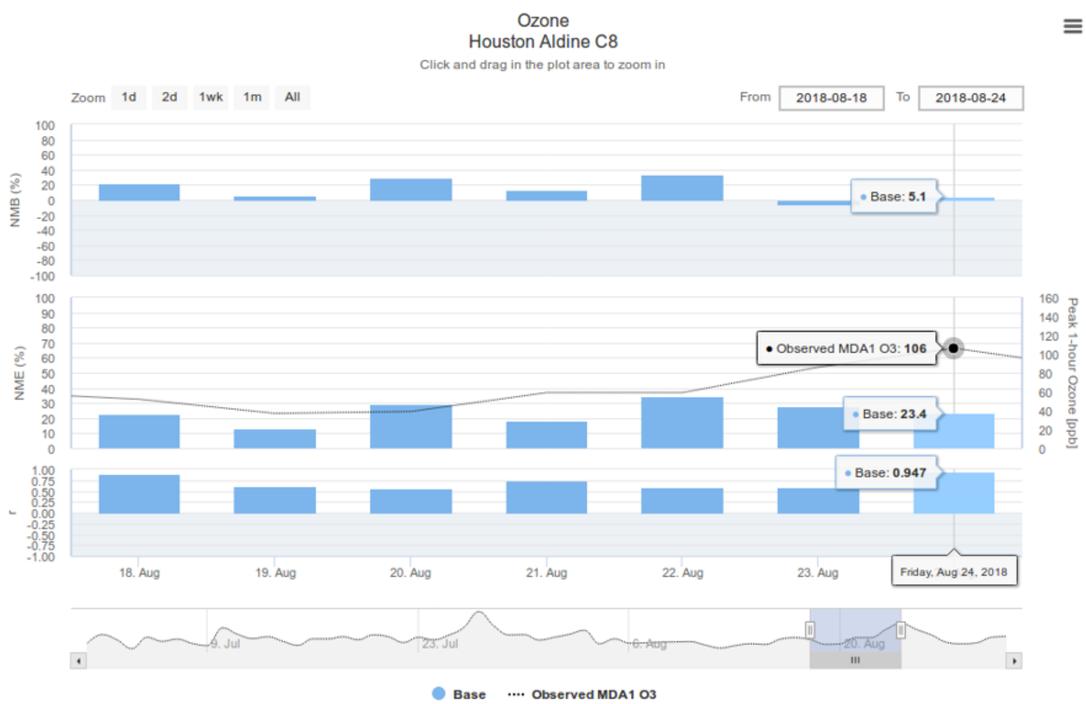

Figure A-7. NRTEEM model performance statistics for daily 1-hour ozone (20 ppb cutoff) at Aldine C8 for August 18-24, 2018. Statistics shown for August 24.

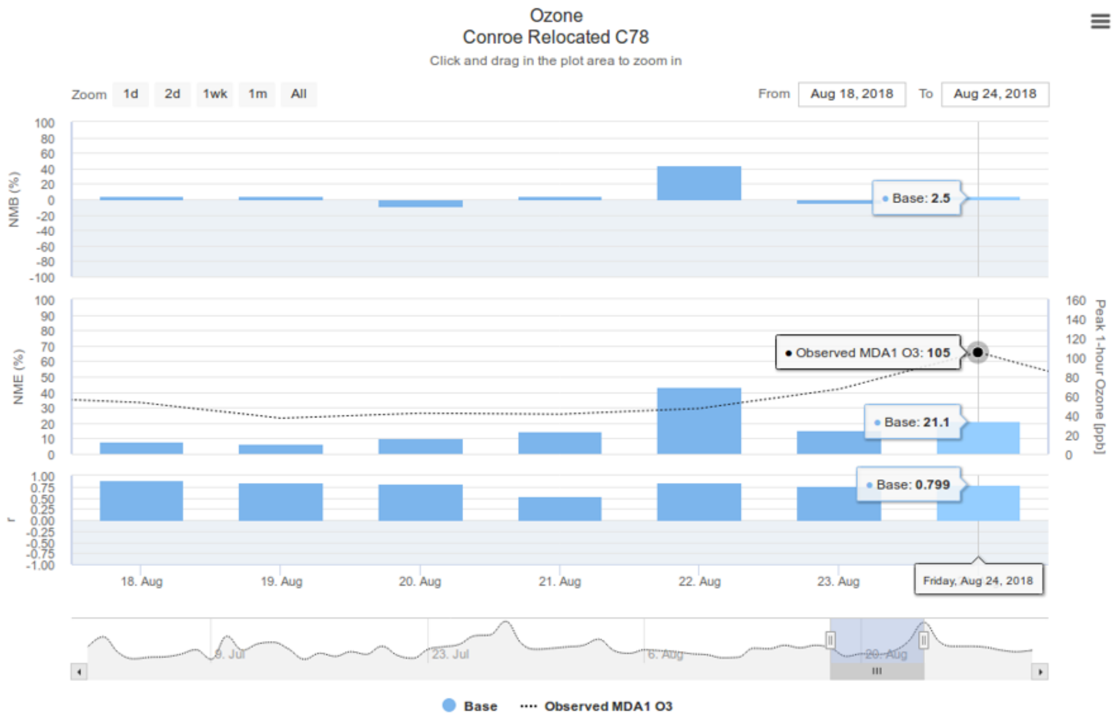

Figure A-8. NRTEEM model performance statistics for daily 1-hour ozone (20 ppb cutoff) at Conroe Relocated C78 for August 18-24, 2018. Statistics shown for August 24.

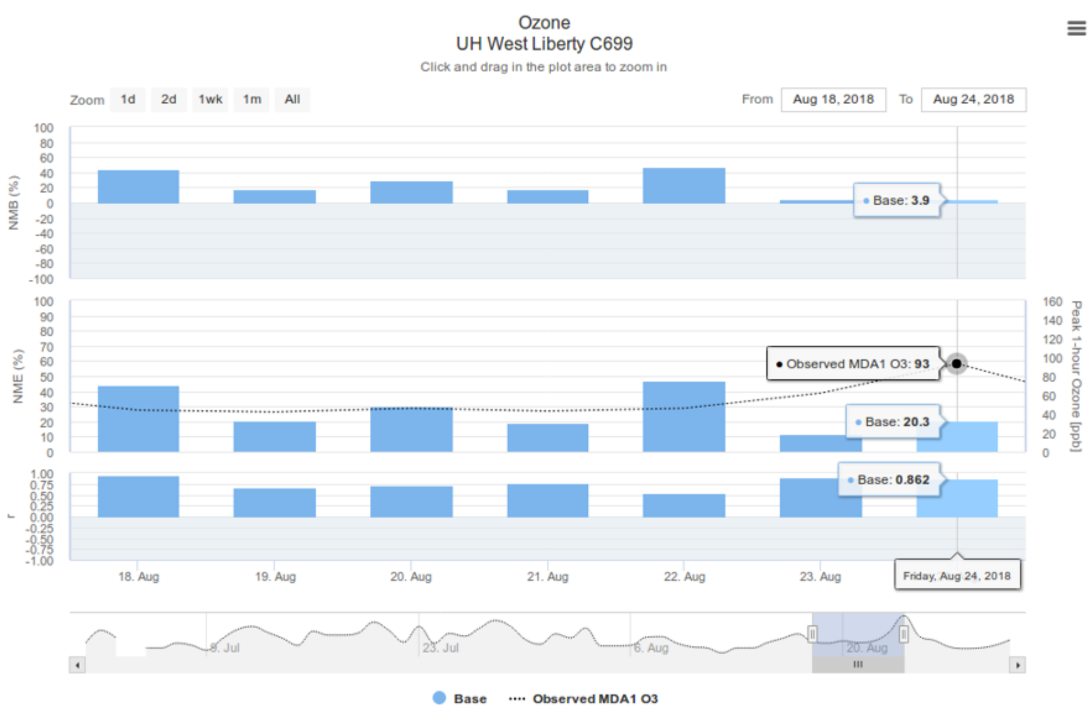

Figure A-9. NRTEEM model performance statistics for daily 1-hour ozone (20 ppb cutoff) at UH West Liberty C699 for August 18-24, 2018. Statistics shown for August 24.